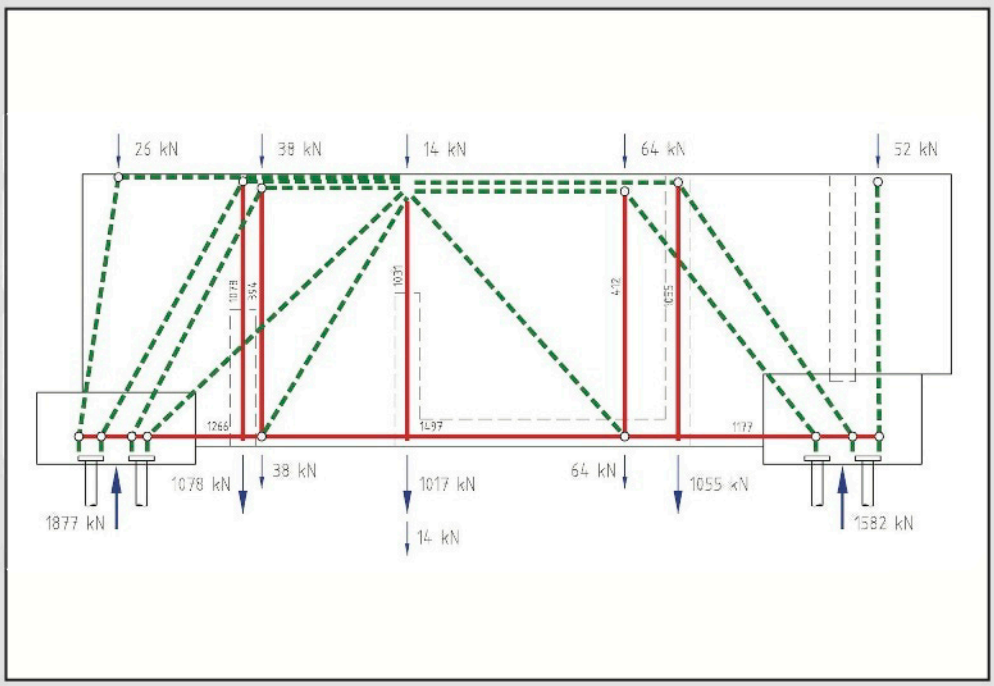
This document is the intellectual property of the fib – International Federation for Structural Concrete. All rights reserved.
This PDF of fib Bulletin 61 is intended for use and/or distribution solely within fib National Member Groups.

bulletin 61

technical report



Design examples for strut-and-tie models

This document is the intellectual property of the fib – International Federation for Structural Concrete. All rights reserved.
This PDF of fib Bulletin 61 is intended for use and/or distribution solely within fib National Member Groups.

Design examples for strut-and-tie models

Technical Report prepared by
Working Party 1.1-3
in *fib* Task Group 1.1, *Design Applications*

September 2011

This document is the intellectual property of the fib – International Federation for Structural Concrete. All rights reserved.
This PDF of fib Bulletin 61 is intended for use and/or distribution solely within fib National Member Groups.

Subject to priorities defined by the Technical Council and the Presidium, the results of ***fib***'s work in Commissions and Task Groups are published in a continuously numbered series of technical publications called 'Bulletins'. The following categories are used:

category	minimum approval procedure required prior to publication
Technical Report	approved by a Task Group and the Chairpersons of the Commission
State-of-Art Report	approved by a Commission
Manual, Guide (to good practice) or Recommendation	approved by the Technical Council of ***fib***
Model Code	approved by the General Assembly of ***fib***

Any publication not having met the above requirements will be clearly identified as preliminary draft.

This Bulletin N° 61 was approved as a "Technical Report" by Task Group 1.1 in January 2011.

This report was written by Working Party 1.1.3, Design examples for the application of strut-and-tie models, in *fib* Task Group 1.1, Design Applications. The Working Party consisted of the following members:

Karl-Heinz Reineck (Convenor; Univ. of Stuttgart, Germany)

Jõao F. Almeida (JSJ Consultoria e Projectos Lda, Portugal), Carlos Bajo (Ferrovial Agromán SA, Spain), Sebastian Dieste Ballestrino (FHECOR Ingenieros Consultores, Spain), Stathis N. Bousias (Univ. of Patras, Greece), Jose M. Camara (Inst. Superior Tecnico, Portugal), Hugo Corres Peiretti (ETS de Ingenieros de Caminos, Spain), Ľudovít Fillo (Slovak Technical Univ., Slovakia), Stein Atle Haugerud (Dr. techn. Olav Olsen a.s., Norway), Toshio Ichihashi (Taisei Corporation, Japan), Milan Kalny (Pontex s.r.o., Czech Republic), Dan Kuchma (Univ. of Illinois, USA), Miguel Lourenço (JSJ Consultoria e Projectos Lda, Portugal), Duc Thanh Nguyen (Danang City, Vietnam), Fabrizio Palmisano (PPV Consulting, Italy), Santiago Pérez-Fadon (Ferrovial - Agromán, Spain), Hiroshi Shiratani (Taisei Corporation, Japan), Jean-Marc Voumard (VSL, Switzerland)

Short biographical summaries for the authors are given on pages 217-219.

Contact information for Task Group members can be found in the ***fib*** Directory or through the online services on the ***fib*** website, www.fib-international.org.

Cover image: see Example 3

© fédération internationale du béton (***fib***), 2011

Although the International Federation for Structural Concrete ***fib*** – fédération internationale du béton – does its best to ensure that any information given is accurate, no liability or responsibility of any kind (including liability for negligence) is accepted in this respect by the organisation, its members, servants or agents.

All rights reserved. No part of this publication may be reproduced, modified, translated, stored in a retrieval system, or transmitted in any form or by any means, electronic, mechanical, photocopying, recording, or otherwise, without prior written permission.

First published in 2011 by the International Federation for Structural Concrete (*fib*)
Postal address: Case Postale 88, CH-1015 Lausanne, Switzerland
Street address: Federal Institute of Technology Lausanne – EPFL, Section Génie Civil
Tel +41 21 693 2747 • Fax +41 21 693 6245
fib@epfl.ch • www.fib-international.org

ISSN 1562-3610
ISBN 978-2-88394-101-4

Printed by DCC Document Competence Center Siegmar Kästl e.K., Germany

This document is the intellectual property of the fib – International Federation for Structural Concrete. All rights reserved.
This PDF of fib Bulletin 61 is intended for use and/or distribution solely within fib National Member Groups.

Preface

fib Bulletin 61 is a continuation of the *fib* Bulletin 16 (2002), and again the main objective is to demonstrate the application of the FIP Recommendations "Practical Design of Structural Concrete", and especially to illustrate the use of strut-and-tie models to design discontinuity regions (D-regions) in concrete structures.

Most of the 14 examples are existing structures built in the last years. Although some of the presented structures can be considered as quite important or some also as complex, the chosen examples are not intended to be exceptional. The main aim is to treat particular design aspects, by selecting D-regions of the presented structures that are designed and detailed following the proposed design principles and specifications for the use of strut-and-tie models.

Additionally 2 papers are presented in the end. Paper 15 deals with the role of concrete tension fields in modelling with strut-and-tie models. Paper 16 aims at summarizing the experiences the Working Group gained in applying strut-and-tie models for the examples presented in this Bulletin.

It is hoped that this document will be of interest to those engaged in the design of structural concrete, supporting the use of more consistent design and detailing tools like strut-and-tie models.

We acknowledge the contributions of all members of the Working Group, and especially the tremendous work of the authors and their co-authors in preparing these examples. The editor also wants to thank Ms. Elfriede Schnee, ILEK, University of Stuttgart for providing some of the drawings. In addition, the work by Laura Thommen-Vidale, *fib* secretariat, on the final editing this Bulletin is greatly appreciated.

Stein Atle Haugerud
Convenor of TG 1.1

Karl-Heinz Reineck
Convenor of WP 1.1.3
and editor of this Bulletin

Gordon Clark
Chair of *fib* Commission 1

This document is the intellectual property of the fib – International Federation for Structural Concrete. All rights reserved.
This PDF of fib Bulletin 61 is intended for use and/or distribution solely within fib National Member Groups.

Contents

Preface iii

Examples

1 Solving structural design problems with strut-and-tie models 1
Sebastián Dieste Ballestrino, José Romo Martín, Eduardo García Díaz, Hugo Corres Peiretti

The strut-and-tie method has been demonstrated to be a powerful tool for the modelling and design of structural concrete. In the conceptual and the structural design stage, the method allows study of different resistant models and evaluation of the most suitable one. In the analysis stage, this method enables the stresses in the structure to be adequately evaluated, allowing calculation of the amount of reinforcement and verification of the stress level of concrete. Additionally, it is especially useful in identifying the critical zones and organizing the reinforcement layout.

This Example 1 provides a set of application examples for the strut-and-tie method that allows us to understand the creation of the models and the verification of the elements, struts, ties and nodes. Simple structural elements have been chosen, as they are usually designed according to certain traditional rules that are often applied without clear justification. These examples are: Example 1–1: Footing under uniaxial bending; Example 1–2: Footing under biaxial bending; Example 1–3: Pile cap for precast concrete piles; Example 1–4: Diaphragm of a box girder bridge.

For those facing the design with strut-and-tie models for the first time these examples are intended to be a guide and a reference for similar cases. For those with more experience in structural design, some refinements and possible difficulties in applying the method are discussed.

2 Precast corbels fitted to columns 31
Jean-Marc Voumard

In a repair work new corbels had to be fitted to existing columns with post-tensioned bars. The new corbels are made of two precast "C"-shaped concrete elements. A simple and a more refined strut–and–tie model is presented, and a check performed of the transfer of forces by friction across the interface between corbel and column.

3 Lift shaft substructure 37
Stein Atle Haugerud, Karolin Reineck

The example demonstrates the application of strut-and-tie model approach for the design of a lift shaft substructure in a 7-story office building. The design with the aid of strut-and-tie models, widely based on the FIP Recommendations (1999), is presented in detail for a deep beam subjected to concentrated loads from intersecting members. The example deals with issues related to concentrated loads near support and detailing aspects of indirect supports. The development of the strut-and-tie model is outlined followed by capacity checks and consequent detailing of critical anchorage zones.

4 Continuous deep beam 45
Miguel S. Lourenço, João F. Almeida, Rui Boia

This example shows the application of strut-and-tie models to the design and detailing of a continuous deep beam in an office building. It is a simple model, although some special aspects are worth mentioned, namely the support stiffness, minimum reinforcement disposals and detailing in node regions. A strut-and-tie model is developed for the whole region and the node regions are checked. Finally, the detailing is presented following closely the developed strut-and-tie model.

5 Shear wall in office building 53
Ľudovít Fillo, Vladimír Benko

A twenty-storey office building was designed for Vienna, Austria. This 76 m tall structure has plan dimensions of 17 m (30 m) 54 m. A transverse shear wall of varying dimensions was designed with strut-and-tie models for a combination of seismic, permanent and imposed loads.

6 Deep beam with an opening 67
Tjen Tjhin, Sukit Yindeesuk, Daniel Kuchma

A large load transfer beam is designed to support a heavy concentrated load and a lighter distributed loading. This storey deep beam is simply supported at its left edge, while the right side frames into a shear wall. The design is complicated by the presence of a rectangular opening between the concentrated load and the shear wall.

This document is the intellectual property of the fib – International Federation for Structural Concrete. All rights reserved.
This PDF of fib Bulletin 61 is intended for use and/or distribution solely within fib National Member Groups.

7 Anchorage block for external prestressing tendon – comparison with test results 77
Toshio Ichihashi, Hiroshi Shiratani

An anchorage block on a concrete bridge deck, arranged on the thin slab or web and subjected to prestressing force of external tendons, is a typical D-region problem for concrete structures. In this example, a three-dimensional strut-and-tie model is applied to an actually implemented loading test using a 1/2 size model of an anchorage block. The anchorage block was analysed according to FIP Recommendations (1999) in order to estimate its capacity. The calculated capacity has been compared with the test result. It was concluded that the strut-and-tie model has proved to be useful for estimating the anchorage capacity.

8 Suspended precast RC member 85
Ľudovít Fillo, Jaroslav Halvoník

The bridge links two parts of the shopping centre "Avion" divided by busy street in Bratislava, Slovakia. Heavy traffic forced authorities to keep opened the street during construction works. Contractor was forced to offer a semi-precast solution that allowed building bridge without significant disturbances of the traffic. This was reason to use suspended precast reinforced concrete members. Special shape, support and loads of this prefabricated shell offer the possibility for analysis by strut and tie models.

9 Connection between prefabricated beams 95
Miguel S. Lourenço, José N. Camara

This example shows the application of strut-and-tie models for the design of the connection between prefabricated beams of a viaduct. Two different models were developed for the de-sign, considering both construction and service loads. The nodal regions close to the prestress anchorage zones were checked and the detailing is presented following the performed design models.

10 Clamped support of large prefabricated T-girder 103
Hannes Ludescher

In the example, the clamped support of a large T-girder in a connection composed of shear panels is illustrated. The beam with a span of about 35 m is placed as prefabricated girder and consecutively integrated into the structure in order to establish a clamped support. In the operational phase, the connection has to resist to large closing and minor opening moments. The example illustrates the design for the closing moment, starting with the definition of section forces and qualitative modelling. As a result, tendon layout is amended and main reinforcement intensities are outlined.

11 Abutment shear wall of Viaduct 1 on Algarve Highway 117
Miguel S. Lourenço, João F. Almeida

This example shows the application of strut-and-tie models for the design of a viaduct fixed abutments shear walls subject to seismic and permanent loads. Seismic actions conduce to several load conditions, though different strut-and-tie models were performed. Concrete stresses at node regions were checked assuming simplified considerations for the compression strength subject to reverse and cyclic loads. Local third plane models were developed to improve the detailing of critical anchorage zones and load support regions.

12 Designing D-regions of the Enmedio stream bridge 133
Santiago Perez-Fadón Martínez, Carlos J. Bajo Pavía

This example presents the design of five discontinuity regions (D-regions) of the Enmedio Stream Bridge using strut-and-tie models. It is shown that even or especially for very complex D-regions the strut-and-tie models are an appropriate and excellent design tool, which explains the flow of forces and thus leads to a better understanding of the structure.

13 D-regions of the pylons of a cable-stayed bridge 155
Duc Thanh Nguyen

In this example the check of two typical D-regions in Pylons of a cable-stayed bridge using strut-and-tie models are presented. These are the regions where the loads from the stiffening beam are transferred to the pylons and to their cross beams. It shows that strut-and-tie models can follow clearly the flow of forces and, therefore, are excellent tools for the check and de-tailing of such complicated D-regions.

This document is the intellectual property of the fib – International Federation for Structural Concrete. All rights reserved.
This PDF of fib Bulletin 61 is intended for use and/or distribution solely within fib National Member Groups.

14 Design of T-connections in an offshore terminal 163
Hannes Ludescher, Stein Atle Haugerud

The design of off-shore terminals is characterised by a high number of loading situations. They result from various load phases, starting with construction including post-tensioning, assembling, transportation, installation, operation and accidental situations. In order to cover all critical situations in every section of the structure, a systematic and highly automated de-sign process has been developed. Modern computers enable to verify structural safety and serviceability for hundreds of design combinations in all sections. Contrary to sectional design of B-regions, design of D-regions cannot be automated. Engineering judgement is required to identify and delimit these regions, establish design criteria for the various elements and develop models that allow verification of these criteria. This article presents the design process adopted for the design of connections in an off-shore terminal, mainly of T-shaped connections.

Papers

15 Strut-and-tie models utilizing concrete tension fields 185
Karl-Heinz Reineck

In codes the utilization of the concrete tensile strength has often been denied and explicitly been ruled out. Yet, the bond and anchorage of reinforcement in concrete members cannot be explained without the action of the concrete tensile strength. However, this is covered by using shear stresses for the bond strength. Likewise, the ultimate capacity of members without shear reinforcement has been defined in terms of shear stresses, for which empirically derived formulae are given. However, such equations do not give any insight in the structural behav-iour and the flow of the forces within the member.

This paper describes the shear transfer in members without shear reinforcement and derives a simple truss model with inclined concrete ties. However, the ultimate capacity cannot be explained by the concrete ties attaining the concrete tensile strength but it is determined by the limited capacity of the friction along the cracks and the dowel action. This model also explains the transition from B- to D-regions in members without shear reinforcement and enables the design of the D-regions, as demonstrated by an example.

16 Gaining experience with strut-and-tie models for the design of concrete structures 197
Karl-Heinz Reineck, Miguel S. Lourenço, João F. Almeida, Stein Atle Haugerud

Author information 217

Editorial Comments

In the drawings of strut-and-tie models the following well known convention is used:

for struts: dashed lines and for ties: solid lines.

The notation follows that of the CEB-FIP Model Code 1990 respectively that of the FIP Recommendations 1999 “Practical design of structural concrete.

For the spacing of reinforcing bars various symbols were used in the examples according to the different traditions in the various countries:

á @ at c s = / // - #

In the calculations the decimal symbol is a comma (,), and for the thousands separator a point (.) is used. However, due to different conventions in CAD programs, in some figures the decimal point used instead of a comma; in such cases a note has been added the relevant figure caption.

This document is the intellectual property of the fib – International Federation for Structural Concrete. All rights reserved.
This PDF of fib Bulletin 61 is intended for use and/or distribution solely within fib National Member Groups.

Example 1: Solving structural design problems with strut-and-tie models

Sebastián Dieste Ballestrino, José Romo Martín, Eduardo García Díaz, Hugo Corres Peiretti

Example 1–1: Footing under uniaxial bending

1 Description of design task

1.1 The structure

In this example, a complete study of a spread footing under axial force and bending moment, using the strut-and-tie method, is made. A three-dimensional strut-and-tie model is proposed, giving a clear proposal for the path of loads. There are no clear recommendations to model this type of structure, which could be used to solve other similar problems. In this case it is particularly important to resolve efficiently the anchorage of the tensile bars of the columns, which need to have a continuity with the ties at the bottom of the foundation.

1.2 Geometry and loads

The geometry of the footing and the design loads are shown in Fig. 1.1-1 and Fig. 1.1-2.

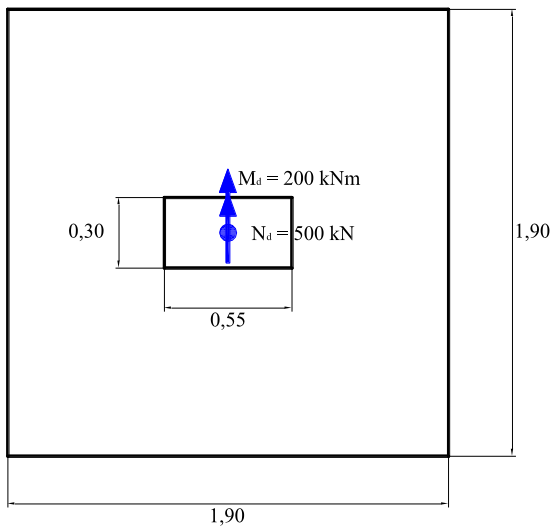


Fig. 1.1-1: Geometry and loads, plan view

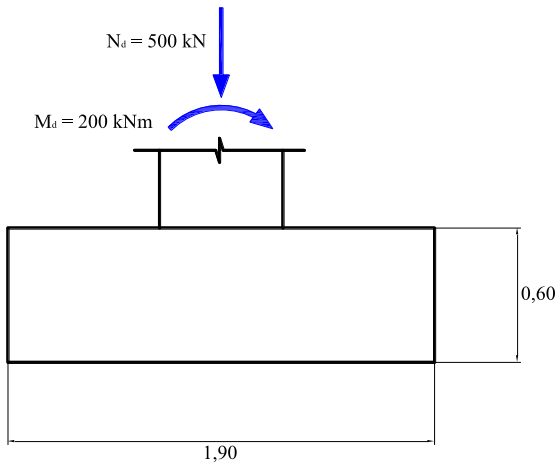


Fig. 1.1-2: Geometry and loads, front view (dimensions in m)

This document is the intellectual property of the fib – International Federation for Structural Concrete. All rights reserved.
This PDF of fib Bulletin 61 is intended for use and/or distribution solely within fib National Member Groups.

1.3 Design values for materials

Concrete: $f_{ck} = 25{,}0\ \text{MPa}$

$f_{1cd} = 0{,}85 \cdot f_{ck}/1{,}5 = 0{,}85 \cdot 25/1{,}5 = 14{,}17\ \text{MPa}$

Reinforcement: $f_{yk} = 500\ \text{MPa}; \quad f_{yd} = \dfrac{f_{yk}}{1{,}15} = \dfrac{500}{1{,}15} = 435\ \text{MPa}$

2 Design procedure

The design procedure includes the following steps:

- Step 1: Determination of the equilibrium of external forces.
- Step 2: Creation of a strut-and-tie model that resists the internal force flow.
- Step 3: Determination of amount of reinforcement.
- Step 4: Design of nodes and check of nodal pressure.
- Step 5: Arrangement of reinforcement.

3 Design calculations

3.1 Step 1: Determination of the equilibrium of external forces

The usual hypothesis of considering the footing as a rigid body is adopted. The footing's equilibrium is obtained calculating the truss chord forces in the column and the soil reaction acting on the footing. In this case, self-weight of the footing need not to be considered.

The truss chord forces in the column base are derived from a cross-sectional analysis as shown in Fig. 1.1-3:

$C_d = 788\ \text{kN}; \qquad T_d = 288\ \text{kN}$

The equilibrium of external forces is shown in Fig. 1.1-4, and the eccentricity of the resultant load is $e = \dfrac{M_d}{N_d} = \dfrac{200}{500} = 0{,}40\ \text{m}$

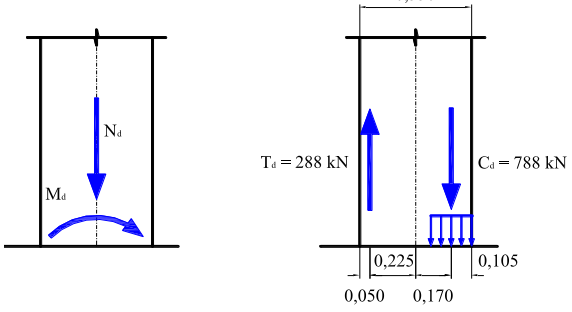


Fig. 1.1-3: Equivalent column forces

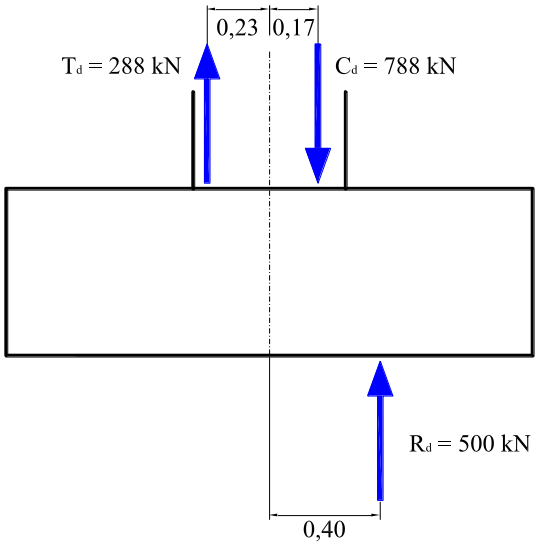


Fig. 1.1-4: Equilibrium of external forces (dimensions in m)

This document is the intellectual property of the fib – International Federation for Structural Concrete. All rights reserved.
This PDF of fib Bulletin 61 is intended for use and/or distribution solely within fib National Member Groups.

3.2 Step 2: Creation of a strut-and-tie model

The three-dimensional strut-and-tie model initially developed to idealize the force transfer through the footing is shown in Fig. 1.1-5 and Fig. 1.1-6.

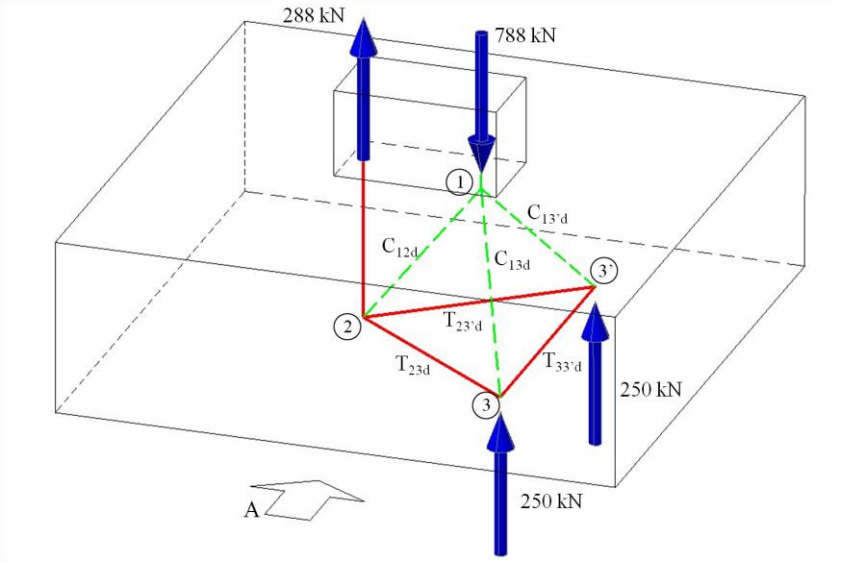


Fig. 1.1-5: Initial three-dimensional strut-and-tie model (isometric view)

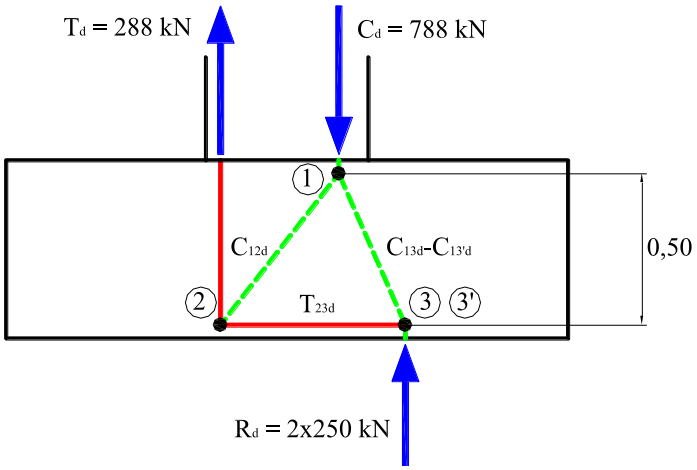


Fig. 1.1-6: View A with two-dimensional idealization of the three-dimensional model (dimensions in m)

The model in Fig. 1.1-5 represents the most efficient and logical force flow, as ties T_{23d} and $T_{23'd}$ would require only that amount of reinforcement needed to satisfy the equilibrium. Nevertheless, the triangular ties disposition would require a very specific and not practical reinforcement. To solve this problem, a new three-dimensional model has been assumed model, as shown in Fig. 1.1-7. This new model can be easily constructed with a perpendicular arrangement of reinforcement, built with bars set up in parallel to the external faces of the footing. The new nodes 4 and 4' are positioned in the middle of half of the footing, the reinforcement of which is considered for tie T_{44d}. At node 2 the tie is bent (see Fig. 1.1-11) and the reinforcement is anchored behind the bend at node 2´ with the anchorage length $l_{b,net}$ = 450 mm (see section 3.4). This starts from the end of the bend, so that node 2´ in the middle of the anchorage length is in a distance of 225 mm from the end of the bend.

This document is the intellectual property of the fib – International Federation for Structural Concrete. All rights reserved.
This PDF of fib Bulletin 61 is intended for use and/or distribution solely within fib National Member Groups.

For simplicity, the truss forces are determined from idealized planar models. The first one is obtained from the plan view of the model in Fig. 1.1-8, where q_{4h} = 40° and q_{3h} = 64°. The second model corresponds to the view A of the three-dimensional model in Fig. 1.1-9, where $\theta_2 = 52°$ and $\theta_2 = 65°$. Finally, a third, totally symmetrical planar model has been created in Fig. 1.1-10, corresponding to the view B of the three-dimensional model.

The calculation of the forces in the strut-and-tie model starts from equilibrium of node 3, see Fig. 1.1-9:

$$T_{34'd} = 250 \cdot 0{,}230/\ 0{,}50 = 115 \text{ kN}$$

The reinforcement required in the transverse direction for tie $T_{33'd}$ can be calculated from the idealized two-dimensional truss model in Fig. 1.1-10:

$$\frac{T_{33'd}}{250} = \frac{0{,}48}{0{,}50} \Rightarrow T_{33'd} = 240 \text{ kN}$$

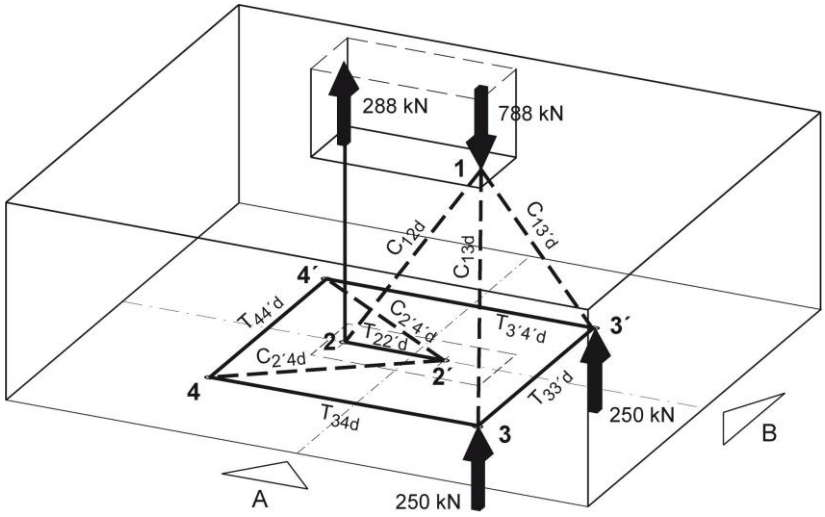


Fig. 1.1-7: Second three-dimensional strut-and-tie model (isometric view)

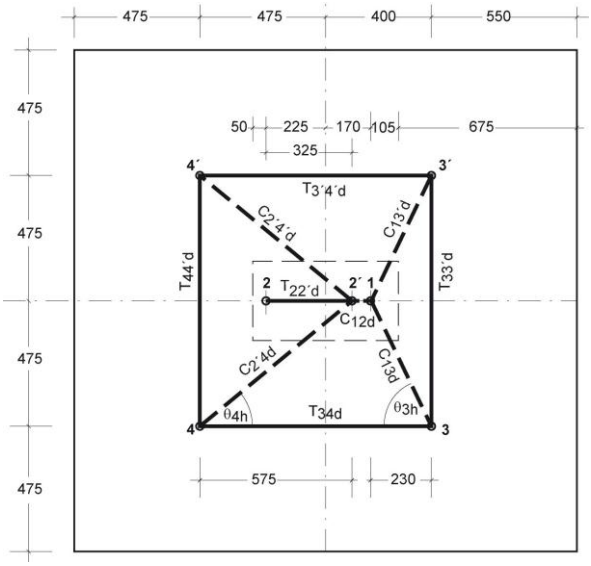


Fig. 1.1-8: Plan view of the 3D model (dimensions in m)

This document is the intellectual property of the fib – International Federation for Structural Concrete. All rights reserved.
This PDF of fib Bulletin 61 is intended for use and/or distribution solely within fib National Member Groups.

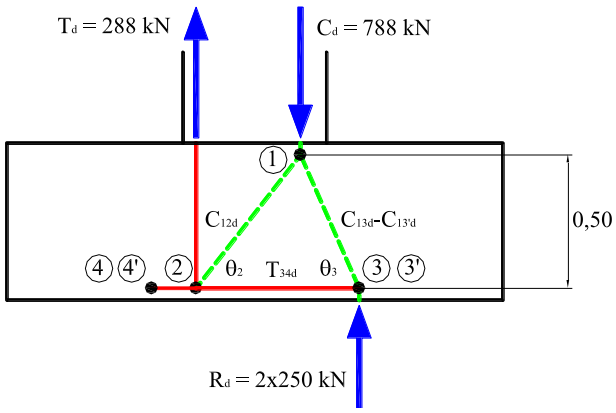


Fig. 1.1-9: View A with two-dimensional idealization of the 3D model (dimensions in m)

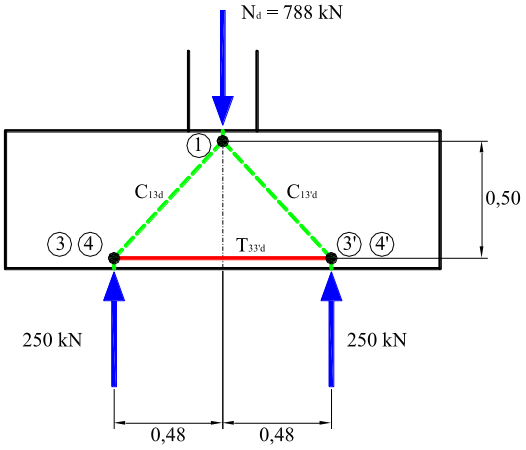


Fig. 1.1-10: View B with two-dimensional idealization of the 3D model

It can be observed in the plan view, Fig. 1.1-8, that the C_{13d} must be in equilibrium with the T_{34d} and $T_{33'd}$ ties, hence, they must be joined in a unique force, T_{3d}, contained in the same vertical plane containing the C_{13d} strut and the soil reaction, $R_d/2$. Therefore:

$$T_{3d} = \sqrt{T_{34d}^{\,2} + T_{33'd}^{\,2}} = \sqrt{115^2 + 240^2} = 266 \text{ kN}$$

$$C_{13d} = \sqrt{\left(R_d / 2\right)^2 + T_{3d}^{\,2}} = \sqrt{250^2 + 266^2} = 365 \text{ kN}$$

From vertical equilibrium of Node 2 (Fig. 1.1-9):

$$C_{12d} = \frac{288}{\sin(\theta_2)} = 367 \text{ kN}$$

The following step consists in calculating the horizontal equilibrium. It must be seen that struts C_{24d} and $C_{24'd}$ are symmetrical and, therefore, the horizontal resultant of the calculated C_{12d} must be divided by two (Fig. 1.1-8).

$$C_{24d} = C_{24'd} = (C_{12d}/2)\cos\theta_2 / \cos\theta_{4h} = 151 \text{ kN}$$

Finally, the equilibrium of Node 4 gives the force resisted by the tie $T_{44'd}$:

$$T_{44'd} = C_{24d} \cdot \sin\theta_{4h} = 97 \text{ kN}$$

3.3 Step 3: Determination of amount of reinforcement

The total longitudinal reinforcement, obtained from the previous calculations, is:

$$A_{34s} = T_{34d} / f_{yd} = 115.000 / 435 = 264 \text{ mm}^2$$

$$A_{33's} = T_{33'd} / f_{yd} = 240.000 / 435 = 551 \text{ mm}^2$$

$$A_{44's} = T_{44'd} / f_{yd} = 95.000 / 435 = 218 \text{ mm}^2$$

Assuming that each tie has an influence width of half the width of the foundation b = 0,95 m, the $A_{33's}$ area is adopted as the highest one:

$$A_{33's} = 551 / 0{,}95 = 580 \text{ mm}^2/\text{m} \quad \rightarrow \quad \text{Ø } 16 / 0{,}20 \text{ is adopted.}$$

This document is the intellectual property of the fib – International Federation for Structural Concrete. All rights reserved.
This PDF of fib Bulletin 61 is intended for use and/or distribution solely within fib National Member Groups.

3.4 Step 4: Design of nodes and check of nodal pressure

A design check of the nodal zones is performed only for the governing nodes 1 and 2. Nodes 3 and 4 are the result of the model simplification, nevertheless, they are not real nodes because no concentration of stresses exist upon them.

Node 1: Node 1 is a three-dimensional multi-compressed node, but it can be considered, in a simplified way, as a planar multi-compressed node (CCC) after projecting the spatial node on the symmetry plane (Fig. 1.1-10). According to FIP Recommendations (1999*)*:

$$f_{cd,eff} = \nu_2 \cdot f_{1\,cd} = 1{,}20 \cdot 14{,}17 = 17{,}00 \text{ MPa}$$

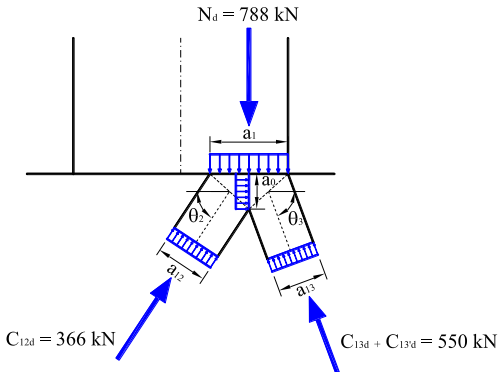


Fig. 1.1-10: Node 1

The geometry of the previous node is defined by the following dimensions:

$a_0 = 0{,}09$ m ; $a_1 = 0{,}20$ m (from the sectional analysis of the column)

$\theta_2 = 52°$; $\theta_3 = 65°$

$$a_{12} = a_1 \cdot \left(\frac{\tan(\theta_2)}{\tan(\theta_2) + \tan(\theta_3)} \right) \cdot \sin(\theta_2) + a_0 \cdot \cos(\theta_2) = 0{,}11 \text{ m}$$

$$a_{13} = a_1 \cdot \left(\frac{\tan(\theta_3)}{\tan(\theta_2) + \tan(\theta_3)} \right) \cdot \sin(\theta_3) + a_0 \cdot \cos(\theta_3) = 0{,}15 \text{ m}$$

Assuming that the width of the node is equal to the column width b = 0,30 m:

$$\sigma_{1\,cd} = \frac{N_d}{b \cdot a_1} = \frac{788}{0{,}30 \cdot 0{,}20} = 13.133 \text{ kN/m}^2 = 13{,}13 \text{ MPa} < f_{cd,eff}$$

$$\sigma_{12\,cd} = \frac{C_{12d}}{b \cdot a_{12}} = \frac{366}{0{,}30 \cdot 0{,}11} = 11.090 \text{ kN/m}^2 = 11{,}09 \text{ MPa} < f_{cd,eff}$$

$$\sigma_{13\,cd} = \frac{C_{13d} + C_{13'd}}{b \cdot a_{13}} = \frac{550}{0{,}30 \cdot 0{,}15} = 12.220 \text{ kN/m}^2 = 12{,}22 \text{ MPa} < f_{cd,eff}$$

Node 2: Node 2 originally is a TTC-node (see Fig. 1.1-5 and 6), but according to the model in Fig. 1.1-7 it is a CCT-node, and Fig. 1.1-11 shows the node after projecting the spatial node on the symmetry plane. The anchorage of the column reinforcement is developed in this node according to the FIP Recommendations (1999), 5.6.3 as follows:

This document is the intellectual property of the fib – International Federation for Structural Concrete. All rights reserved.
This PDF of fib Bulletin 61 is intended for use and/or distribution solely within fib National Member Groups.

$d_b = 10\phi$ see FIP Recommendations (1999), Table 5.2

$d_b = 10 \cdot 0,016 = 0,16\,\text{m} \Rightarrow d_b = 0,20\,\text{m}$ is adopted.

$a_{12} = d_b \cdot \cos(\theta_2) = 0,20 \cdot \cos(52) = 0,12\,\text{m}$

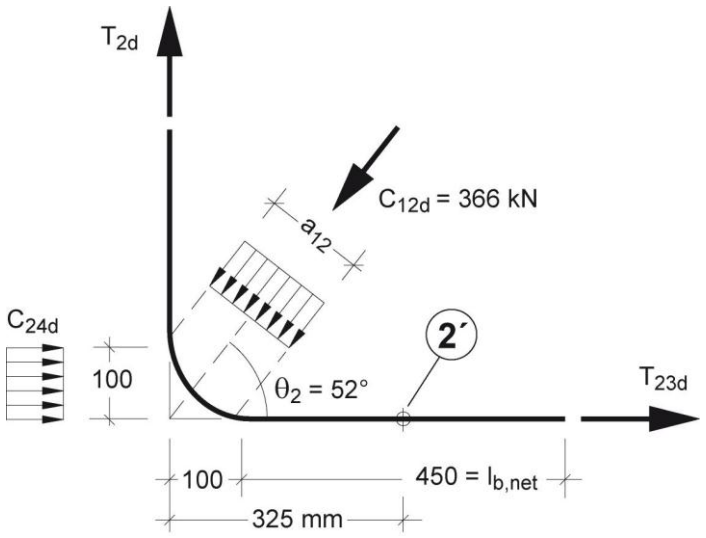


Fig. 1.1-11: Node 2 (dimensions in mm)

As the reinforcement is anchored at the node, the effective concrete compressive strength is determined as following, according to FIP Recommendations (1999):

$f_{cd,eff} = \nu_2 \cdot f_{1\,cd} = 0,85 \cdot 14,17 = 12,04\,\text{MPa}$

Assuming that the width of the node is equal to the column width $\Rightarrow b = 0,30\,\text{m}$ gives:

$$\sigma_{c12\,d} = \frac{C_{12d}}{b \cdot a_{12}} = \frac{366}{0,30 \cdot 0,12} = 10.167\,\text{kN/m}^2 = 10,17\,\text{MPa} < f_{cd,eff}$$

Compressive stress due to the horizontal C_{24d} strut must also be determined. Therefore, the inclined C_{12d} strut has to be projected on the horizontal axis in order to obtain the total stress exerted upon the node. Compressive strength is obtained assuming that the height of the node is equal to 0,10 m and its width is equal to the column width, $b = 0,30\,\text{m}$.

$$\sigma_{c24\,d} = \frac{C_{12d} \cdot \cos(\theta_2)}{b \cdot a} = \frac{366 \cdot \cos(52)}{0,30 \cdot 0,10} = 7.511\,\text{kN/m}^2 = 7,51\,\text{MPa} < f_{cd,eff}$$

The anchorage length of the column reinforcement is determined according to FIP Recommendations (1999), Table 2.5 and Fig.5.11:

$l_b = 40,3 \cdot 0,016 = 0,65\,\text{m}$

$l_{b,net} = 0,7 \cdot l_b = 0,7 \cdot 0,65 = 0,45\,\text{m}$

The anchorage length $l_{b,net}$ starts from the end of the bend, so that node 2´ in the middle of the anchorage length is in a distance of 225 mm from the end of the bend (see Fig. 1.1-11).

This document is the intellectual property of the fib – International Federation for Structural Concrete. All rights reserved.
This PDF of fib Bulletin 61 is intended for use and/or distribution solely within fib National Member Groups.

3.5 Step 5: Arrangement of reinforcement

The footing reinforcement is shown in Fig. 1.1-12 and Fig. 1.1-13.

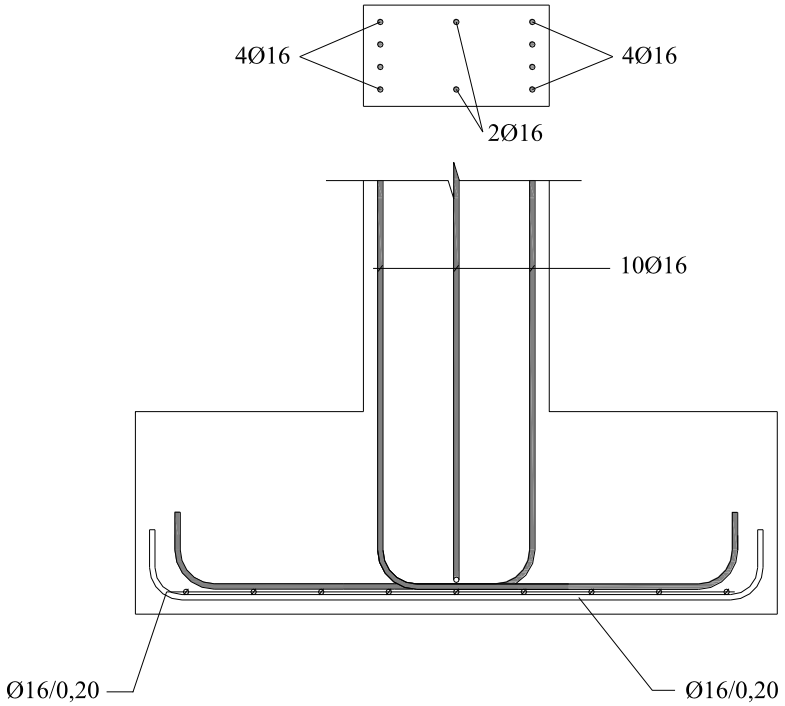


Fig. 1.1-12: Arrangement of reinforcement, front view

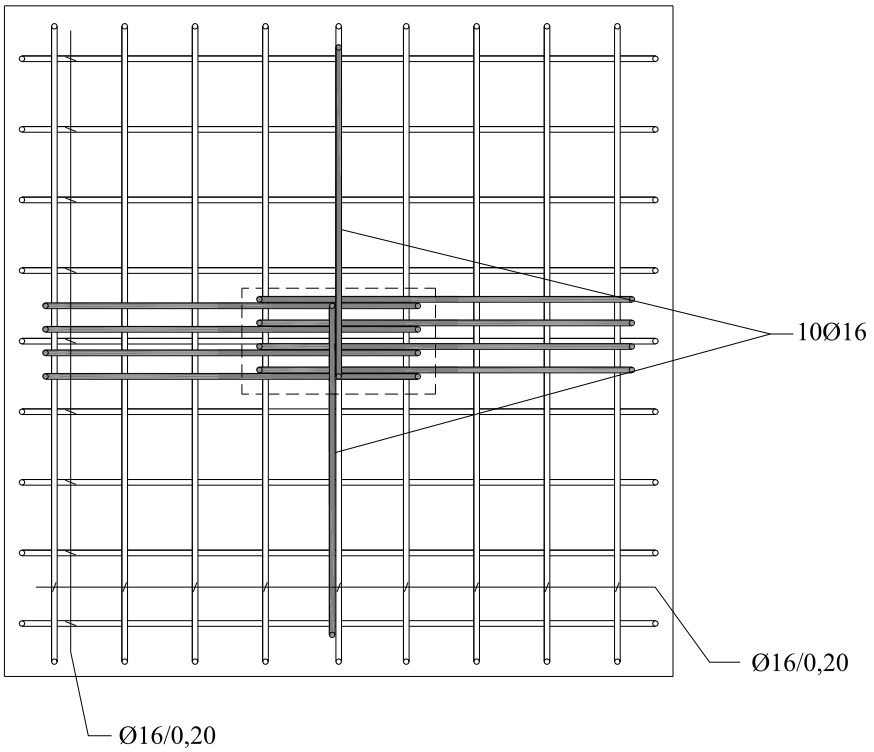


Fig. 1.1-13: Arrangement of reinforcement, plan view

This document is the intellectual property of the fib – International Federation for Structural Concrete. All rights reserved.
This PDF of fib Bulletin 61 is intended for use and/or distribution solely within fib National Member Groups.

Example 1–2: Footing under biaxial bending

1 Description of design task

1.1 The structure

In this example, the design of a footing under an axial load and biaxial bending moments is presented. As the applied bending moment is not orthogonal to the footing faces, it is necessary to develop a more complex model than that proposed for the previous example, although the design approach is similar. Some difficulties are discussed which arise when using three-dimensional models and some ways to solve them are proposed.

These types of structural members are usually designed with simple rules, e.g. by calculating the bending moment in the axis of the column. Even though these proceedings are correct and useful for practical design, they are not clear in relation to the real force flow and they do not give precise information for developing the arrangement of the reinforcement.

1.2 Geometry and loads

The geometry of the footing and the design loads are shown in Fig. 1.2-1 and Fig. 1.2-2, where:

N_d = 12.500 kN; M_{xd} = 4.000 kNm; M_{yd} = 10.000 kNm

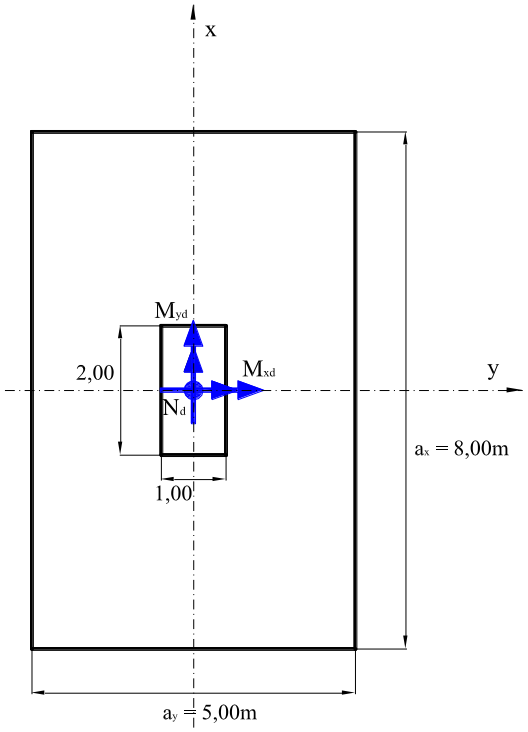


Fig. 1.2-1: Geometry and loads, plan view

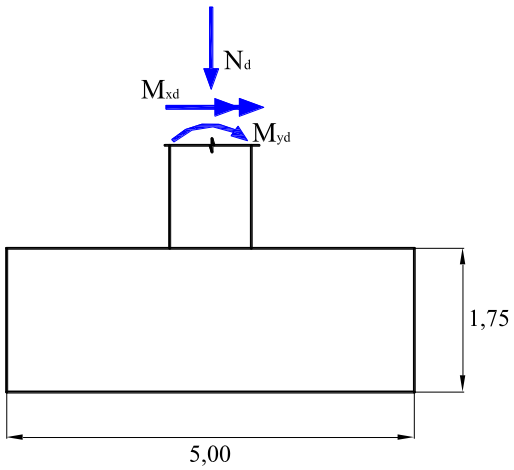


Fig. 1.2-2: Geometry and loads, front view (dimensions in m)

This document is the intellectual property of the fib – International Federation for Structural Concrete. All rights reserved.
This PDF of fib Bulletin 61 is intended for use and/or distribution solely within fib National Member Groups.

1.3 Design values for materials

Concrete: $f_{ck} = 25{,}0\ \text{MPa}$

$f_{1cd} = 0{,}85 \cdot f_{ck}/1{,}5 = 0{,}85 \cdot 25/1{,}5 = 14{,}17\ \text{MPa}$

Reinforcement: $f_{yk} = 500\ \text{MPa}; \quad f_{yd} = \dfrac{f_{yk}}{1{,}15} = \dfrac{500}{1{,}15} = 435\ \text{MPa}$

2 Design procedure

The design procedure includes the following steps:

- Step 1: Determination of the equilibrium of external forces.
- Step 2: Creation of a strut-and-tie model that resists the internal force flow.
- Step 3: Determination of amount of reinforcement.
- Step 4: Design of nodes and check of nodal pressure.
- Step 5: Arrangement of reinforcement.

3 Design calculations

3.1 Step 1: Determination of the equilibrium of external forces

The usual hypothesis of considering the footing as a rigid body is adopted. Column forces and soil pressure acting on the footing are first calculated. The eccentricities of the loads are:

$$e_x = \frac{M_{yd}}{N_d} = \frac{10.000}{12.500} = 0{,}80 \le \frac{a_x}{6} = 1{,}33\ \text{m}; \quad e_y = \frac{M_{xd}}{N_d} = \frac{4.000}{12.500} = 0{,}32 \le \frac{a_y}{6} = 0{,}83\ \text{m}$$

The above values show that all the soil under the footing is compressed. In order to calculate the soil reaction and its distribution, the footing is divided in four quadrants. Soil reactions are assumed to be positioned at the centre of each quadrant (Fig. 1.2-3).

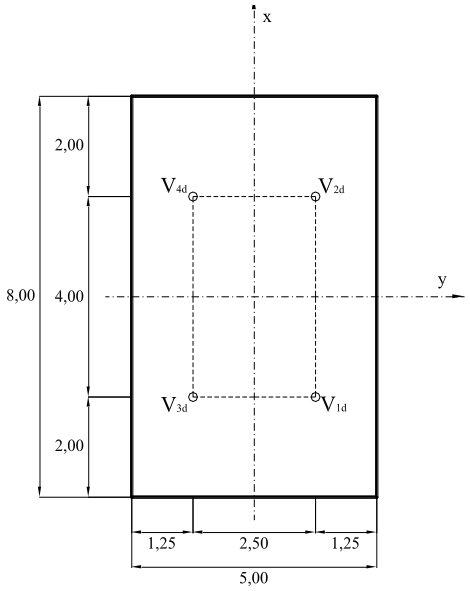


Fig. 1.2-3: Soil reactions (dimensions in m)

This document is the intellectual property of the fib – International Federation for Structural Concrete. All rights reserved.
This PDF of fib Bulletin 61 is intended for use and/or distribution solely within fib National Member Groups.

The four concentrated soil reactions can then be calculated as follows:

$$V_{1d} = \frac{N_d}{4} + \frac{M_{xd}}{2,5}\cdot\frac{1}{2} + \frac{M_{yd}}{4,0}\cdot\frac{1}{2} = \frac{12.500}{4} + \frac{4.000}{2,5}\cdot\frac{1}{2} + \frac{10.000}{4,0}\cdot\frac{1}{2} = 5.175\,\text{kN}$$

$$V_{2d} = \frac{N_d}{4} + \frac{M_{xd}}{2,5}\cdot\frac{1}{2} - \frac{M_{yd}}{4,0}\cdot\frac{1}{2} = \frac{12.500}{4} + \frac{4.000}{2,5}\cdot\frac{1}{2} - \frac{10.000}{4,0}\cdot\frac{1}{2} = 2.675\,\text{kN}$$

$$V_{3d} = \frac{N_d}{4} - \frac{M_{xd}}{2,5}\cdot\frac{1}{2} + \frac{M_{yd}}{4,0}\cdot\frac{1}{2} = \frac{12.500}{4} - \frac{4.000}{2,5}\cdot\frac{1}{2} + \frac{10.000}{4,0}\cdot\frac{1}{2} = 3.575\,\text{kN}$$

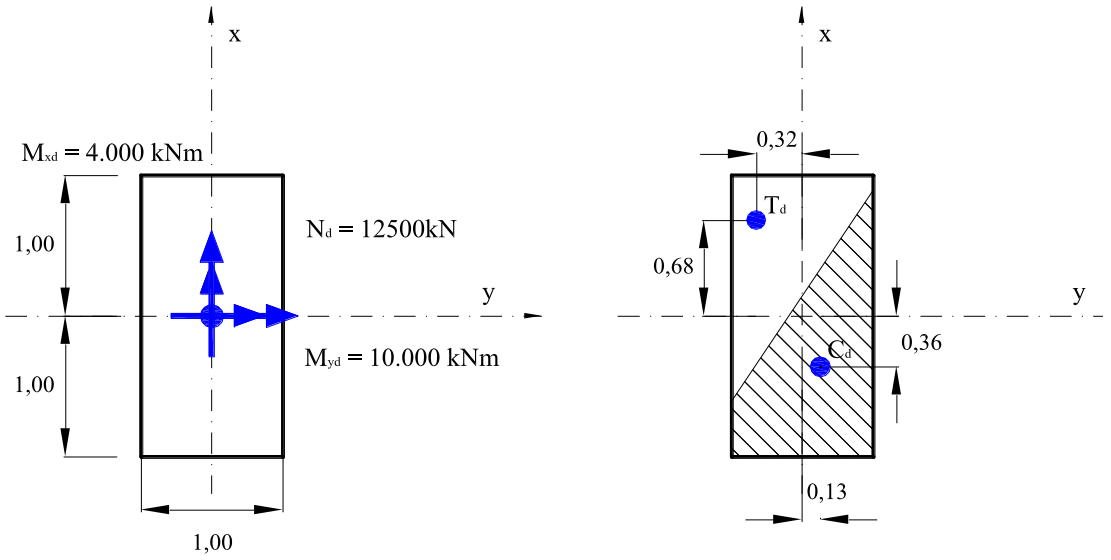
$$V_{4d} = \frac{N_d}{4} - \frac{M_{xd}}{2,5}\cdot\frac{1}{2} - \frac{M_{yd}}{4,0}\cdot\frac{1}{2} = \frac{12.500}{4} - \frac{4.000}{2,5}\cdot\frac{1}{2} - \frac{10.000}{4,0}\cdot\frac{1}{2} = 1.075\,\text{kN}$$

From the above given section effects at the base of the column the equivalent compressive force C_d and the tensile force T_d can be derived from a section analysis of the base of the column, see Fig. 1.2-4:

$T_d = 5.300\ \text{kN}$ $\quad d_{tx} = 0,68\ \text{m}$ $\quad d_{ty} = 0,32\ \text{m}$

$C_d = 17.800\ \text{kN}$ $\quad d_{cx} = 0,36\ \text{m}$ $\quad d_{ty} = 0,13\ \text{m}$

All the external forces applied on the footing, by the column and the soil reaction, have, therefore, been calculated.



a) section effects *b) reaction forces*

Fig. 1.2-4: Equivalent column forces (dimensions in m)

3.2 Step 2: Creation of a strut-and-tie model

A three-dimensional strut-and-tie model representing the internal force flow is proposed as shown in Fig. 1.2-5. A lateral and a plan view of the 3-d model are also shown in Fig. 1.2-6 and Fig. 1.2-7. The model has firstly been considered as a planar model, shown in Fig. 1.2-6, and then a three-dimensional model has been developed, see Fig. 1.2-5, which shows the force flow through the footing in a clear way.

This document is the intellectual property of the fib – International Federation for Structural Concrete. All rights reserved.
This PDF of fib Bulletin 61 is intended for use and/or distribution solely within fib National Member Groups.

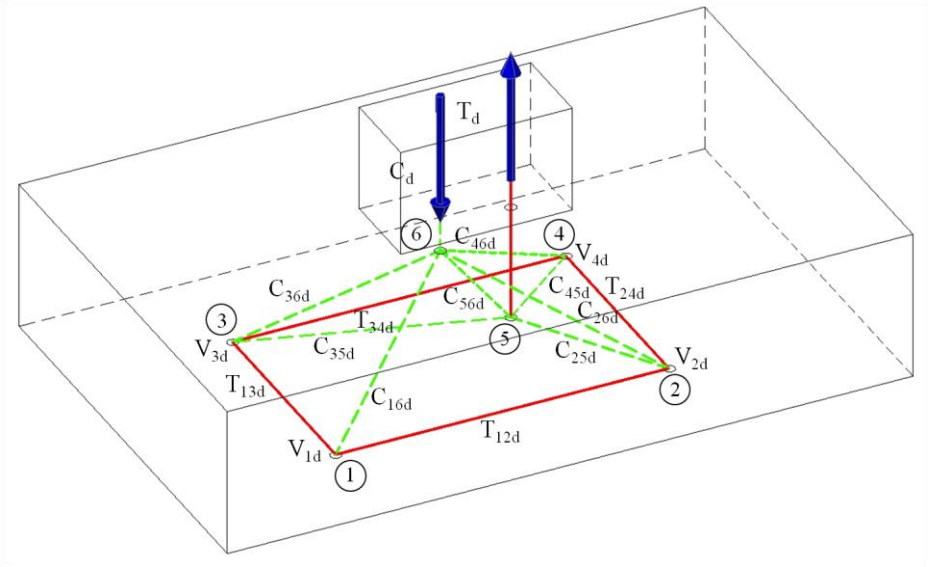


Fig. 1.2-5: Three-dimensional strut-and-tie model (isometric view)

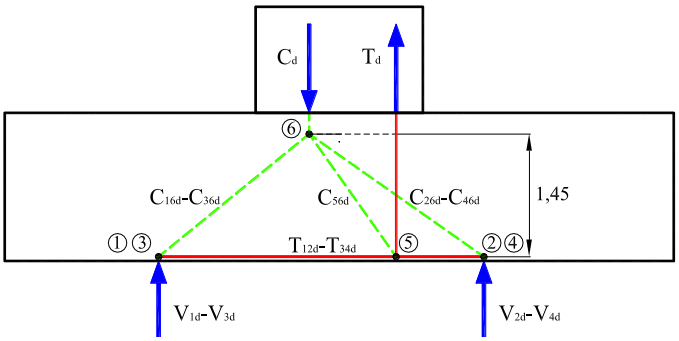


Fig. 1.2-6: Lateral view of the strut-and-tie model (dimensions in m)

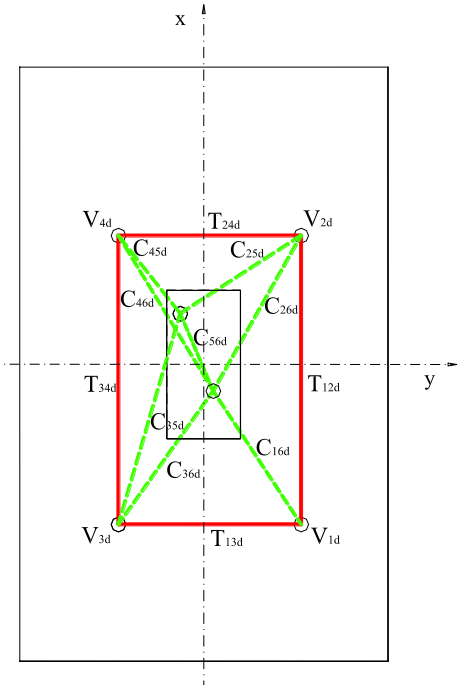


Fig. 1.2-7: Plan view of the strut-and-tie model

This document is the intellectual property of the fib – International Federation for Structural Concrete. All rights reserved.
This PDF of fib Bulletin 61 is intended for use and/or distribution solely within fib National Member Groups.

In order to calculate the forces of the strut-and-tie model, the inner lever arm has to be estimated, and a value of z = 1,45 m has been assumed (see Fig. 1.2-6). The forces in the struts and ties are found by simple equilibrium considerations. The self-weight of the footing does not need to be considered. The results are shown in Table 1.2-1.

Table 1.2-1: Forces in ties and struts

Ties	**Force (kN)**	**Struts**	**Force (kN)**
T_{12d}	5.853	C_{16d}	8.776
T_{13d}	3.997	C_{26d}	5.520
T_{34d}	5.753	C_{36d}	6.386
T_{24d}	3.845	C_{46d}	2.279
T_{d}	5.300	C_{56d}	6.727
		C_{25d}	2.320
		C_{45d}	4.911
		C_{35d}	1.806

3.3 Step 3: Determination of amount of reinforcement

Reinforcement in x-direction corresponds to the tie T_{12d} with the highest tension:

$$T_{xd} = T_{12d} = 5.853\,\text{kN} \qquad A^{i}_{sx} = \frac{T_{xd}}{f_{yd}} = \frac{5.853.000}{435} = 13.500\,\text{mm}^2$$

The influence zone of the tie T_{12d} is 2,5 m, then:

$$A^{i}_{sx} = \frac{13.500\,\text{mm}^2}{2,5\,\text{m}} = 5.400\,\text{mm}^2/\text{m} \Rightarrow 1\phi 32/0,20 + 1\phi 20/0,20 \quad \text{is adopted.}$$

Reinforcement in y-direction corresponds to the tie T_{13d} with the highest tension:

$$T_{yd} = T_{13d} = 3.997\,\text{kN} \qquad A_{sy} = \frac{T_{yd}}{f_{yd}} = \frac{3.997.000}{435} = 9.200\,\text{mm}^2$$

The influence zone of the tie T_{13d} is 4,0 m, hence:

$$A_{sy} = \frac{9.200\,\text{mm}^2}{4,0\,\text{m}} = 2.300\,\text{mm}^2/\text{m} \Rightarrow \phi 25/0,20$$

3.4 Step 4: Design of nodes and check of nodal pressure

Stress concentration is produced only at node 6 of the three-dimensional model. Guidance and information to check this kind of nodes are rarely found. Instead of making a geometrical definition of this node to check the stresses on its faces, it is proposed to calculate the minimum required area for the strut, C_{16d} with the highest force:

$$C_{16d} = 8.772\,\text{kN}$$

This document is the intellectual property of the fib – International Federation for Structural Concrete. All rights reserved.
This PDF of fib Bulletin 61 is intended for use and/or distribution solely within fib National Member Groups.

According to FIP Recommendations (1999), for triaxial compression nodes, the triaxial hydrostatic compressive strength of the concrete may be used:

$$f_{3cd} = 3,88 \cdot f_{1cd} = 54,98 \text{ MPa}$$

Hence:

$$A_{req} = \frac{C_{16d}}{f_{3cd}} = \frac{8.776}{54,98} = 0,16 \text{ m}^2 \Rightarrow A_{req} = 0,40 \times 0,40 \text{ m}^2$$

In this case it can be clearly seen (Fig. 1.2-4) that the required area is available, because the contact zone between the C_{16d} strut and the column is larger than A_{req}.

The anchorage of the column bars at node 5 can be solved in the same way as for node 2 of the previous Example 1-1. The anchorage length of the column bar is calculated, according to FIP Recommendations (1999), Table 2.5 and Fig. 1.2-5.11, as follows:

$$l_b = 40,3 \cdot 0,025 = 1,01 \text{m}$$

$$l_{b,net} = 0,7 \cdot l_b = 0,7 \cdot 1,01 = 0,70 \text{ m}$$

3.5 Step 5: Arrangement of reinforcement

Ties must be anchored from the point of application of the soil reactions. In the x-direction, the minimum distance between the point of application of the soil reaction and the nearest edge of the footing is:

$$L_x = 4,00 - 2,00 = 2,00 \text{ m} \text{ (see Fig. 1.2-3)}$$

According to FIP Recommendations (1999), Table 2.5, the anchorage length is:

$$l_b = 40,3 \cdot 32 = 1.290 \text{ mm} = 1,29 \text{ m} \leq L_x$$

In the y-direction, the minimum distance between the point of application of the soil reaction and the nearest edge of the footing is:

$$L_y = 2,50 - 1,25 = 1,25 \text{ m} \text{ (see Fig. 1.2-3)}$$

According to FIP Recommendations (1999), Table 2.5, the anchorage length is:

$$l_b = 40,3 \cdot 25 = 1.008 \text{ mm} = 1,01 \text{ m} \leq L_y$$

Extending the reinforcement to the edge of the footing would be enough, nevertheless as usual in footings of these dimensions, the reinforcement is also bent and extended along the lateral face, as shown in Fig. 1.2-8.

This document is the intellectual property of the fib – International Federation for Structural Concrete. All rights reserved.
This PDF of fib Bulletin 61 is intended for use and/or distribution solely within fib National Member Groups.

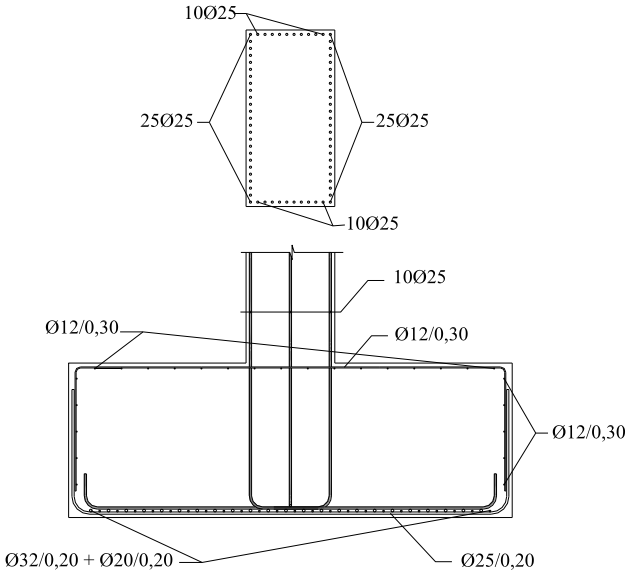


Fig. 1.2-8: Arrangement of reinforcement, front view

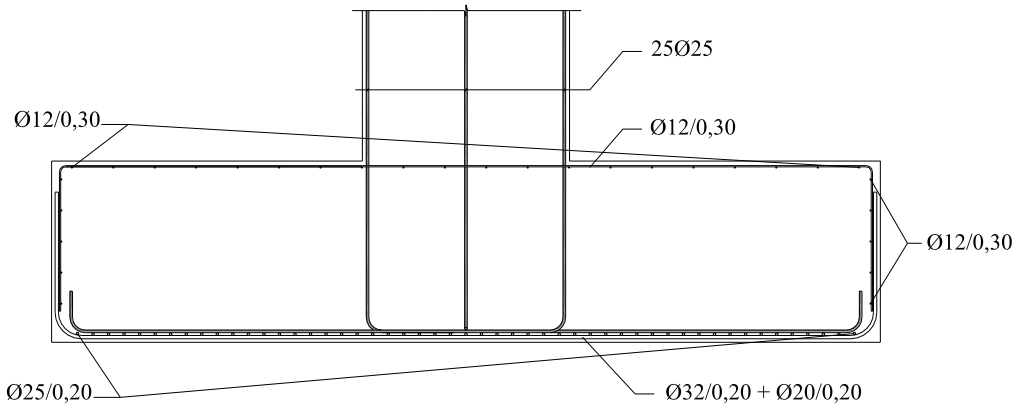


Fig. 1.2-9: Arrangement of reinforcement, lateral view

This document is the intellectual property of the fib – International Federation for Structural Concrete. All rights reserved.
This PDF of fib Bulletin 61 is intended for use and/or distribution solely within fib National Member Groups.

Example 1–3: Pile cap for precast concrete piles

1 Description of design task

1.1 The structure

A pile cap over prefabricated piles is usually designed with strut-and-tie models. Experimental results have shown that the strut-and-tie method correctly predicts the behaviour of pile caps, as they are a particular example of a three-dimensional D-region. This example identifies typical design issues met when designing highly loaded pile caps, and shows the means to solve them. The transfer of forces from the column to the pile cap is analyzed considering the force flow in concrete and in rebars separately, using different strut-and-tie models.

Precast piles can transmit a service stress of about 12 MPa. In such cases, it becomes difficult to comply with the low compressive stresses allowed for nodes, since according to FIP Recommendations (1999) this should be less than $f_{cd,eff} = 0{,}85 \cdot f_{1cd}$. The example here presented is taken from real design cases provided by pile manufacturers. The piles with a rectangular cross section of $0{,}35 \cdot 0{,}35\,\text{m}$ have an ultimate axial capacity of 2.150 kN.

1.2 Geometry and loads

The geometry of the pile cap and the design loads are shown in Figs. 1.3-1 and 1.3-2.

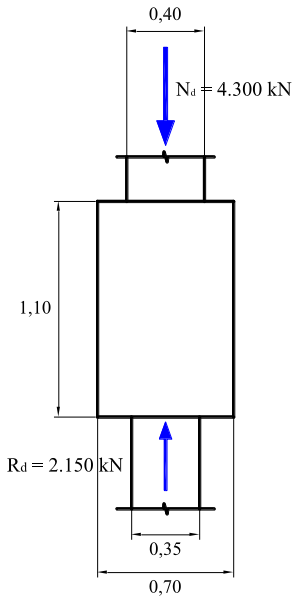


Fig. 1.3-1: Geometry and loads, lateral view

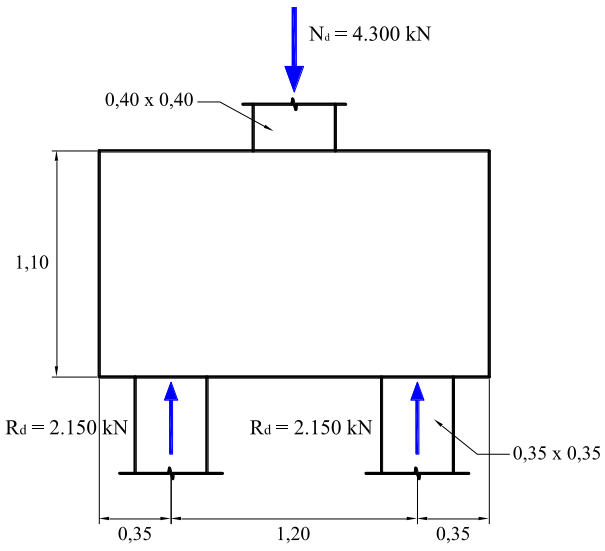


Fig. 1.3-2: Geometry and loads, front view (dimensions in m)

This document is the intellectual property of the fib – International Federation for Structural Concrete. All rights reserved.
This PDF of fib Bulletin 61 is intended for use and/or distribution solely within fib National Member Groups.

1.3 Design values for materials

Concrete:

- column and cap: f_{ck} = 30 MPa
  $f_{1cd} = 0{,}85 \cdot f_{ck} / 1{,}5 = 0{,}85 \cdot 30 / 1{,}5 = 17{,}0$ MPa
- piles: f_{ck} = 50 MPa
  $f_{1cd} = 0{,}85 \cdot f_{ck} / 1{,}5 = 0{,}85 \cdot 50 / 1{,}5 = 28{,}3$ MPa

Reinforcement: $f_{yk} = 500$ MPa; $f_{yd} = \frac{f_{yk}}{1{,}15} = \frac{500}{1{,}15} = 435$ MPa

2 Design procedure

The design procedure includes the following steps:

- Step 1: Creation of a strut-and-tie model following the flow of stresses.
- Step 2: Determination of amount of reinforcement.
- Step 3: Node design and check of nodal pressure.
- Step 4: Arrangement of reinforcement.

3 Design calculations

3.1 Step 1: Creation of a strut-and-tie model following the flow of stresses

Two different models A and B are proposed. Model A (Fig. 1.3-3) is a simple model usually used to design pile caps. The self-weight of the footing needs not to be considered.

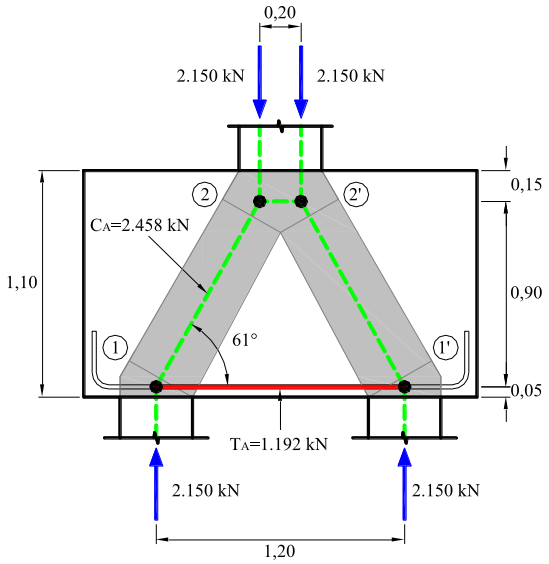


Fig. 1.3-3: Model A (dimensions in m)

In order to start the calculations of the forces, the inner lever arm must be defined, and as frequently assumed in practice for such members the following value of z = 0,90 m has been assumed (see Fig. 1.3-3).

This document is the intellectual property of the fib – International Federation for Structural Concrete. All rights reserved.
This PDF of fib Bulletin 61 is intended for use and/or distribution solely within fib National Member Groups.

A check of nodal pressure has to be done in this model in order to estimate its validity. Node 2, then, is a CCC node, as shown in Fig. 1.3-4a. According to FIP Recommendations (1999), the effective strength of concrete in CCC nodes is:

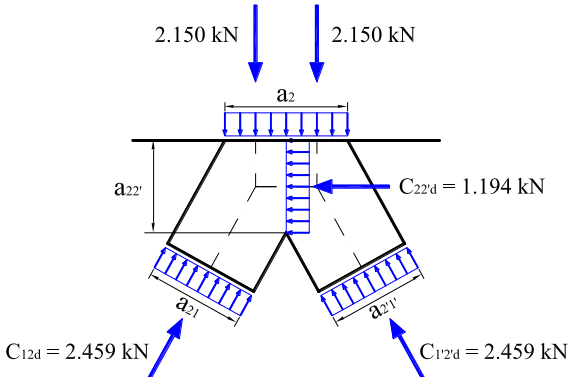
$$f_{2cd} = 1{,}20 \cdot f_{1\,cd} = 1{,}20 \cdot 17{,}0 = 20{,}4\ \text{MPa}$$

The node dimensions b and a_2 are defined by the sides of the column $b = 0{,}40$ m = width of the node and $a_2 = 0{,}40$ m, giving:

$$a_{22'} = 2 \cdot (1{,}10 - 0{,}05 - 0{,}90) = 0{,}30\text{m};$$

$$a_{21} = \frac{0{,}40}{2} \cdot \sin(61) + 0{,}30 \cdot \cos(61) = 0{,}32\ \text{m}$$

The stresses are calculated in Fig. 1.3-4b, and it can be seen that node stresses are higher than the effective strength of concrete in the interface between the column and the pile cap.



$$\sigma_{2d} = \frac{N_d}{b \cdot a_2} = \frac{4.300}{0{,}40 \cdot 0{,}40} = 26{,}88\ \text{MPa} > f_{2cd}$$

$$\sigma_{21d} = \frac{C_{12d}}{b \cdot a_{21}} = \frac{2.459}{0{,}40 \cdot 0{,}32} = 19{,}21\ \text{MPa} < f_{2cd}$$

$$\sigma_{22'd} = \frac{C_{22'd}}{b \cdot a_{22'}} = \frac{1.194}{0{,}40 \cdot 0{,}30} = 9{,}95\ \text{MPa} < f_{2cd}$$

a) geometry and forces *b) stresses*

Fig. 1.3-4: Nodes 2 and 2'

The model A does not correctly evaluate the introduction of forces from column to pile cap because forces in the column reinforcement loads are transferred by bonding to the cap along the anchorage length, whereas concrete forces in the column are transferred directly by bearing stresses to the cap's concrete. This effect can mainly be relevant for highly reinforced columns, when a very important part of axial load is carried by the reinforcement.

The second model B (Fig. 1.3-7) is developed by superposition of two models that consider separately concrete and reinforcement forces (Fig. 1.3-5 and Fig. 1.3-6). The self-weight of the footing does not need to be considered. Performing a sectional analysis of the column, the compressive forces N_{sd} in the rebars and N_{cd} in the concrete can be determined:

N_{sd} = 2.650 kN N_{cd} = 1.650 kN

Model B1, used for compressive forces of concrete in column analysis, is obtained in the same way as Model A. Model B2, used for compressive forces of column reinforcement analysis, is obtained similarly to Model A, but it is assumed that the force in the bars is applied at a distance $l_b/2$ measured from the top face of the pile cap, being l_b the anchorage length of the bars, determined by the use of the FIP Recommendations (1999), Table 2.5:

$l_b = 36{,}2 \cdot 0{,}025 = 0{,}90$ m (C30, S500)

This document is the intellectual property of the fib – International Federation for Structural Concrete. All rights reserved.
This PDF of fib Bulletin 61 is intended for use and/or distribution solely within fib National Member Groups.

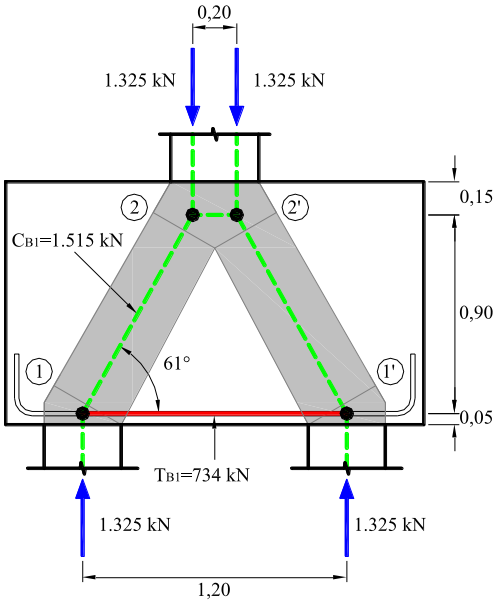


Fig. 1.3-5: Model B1: compressive forces of concrete in column (dimensions in m)

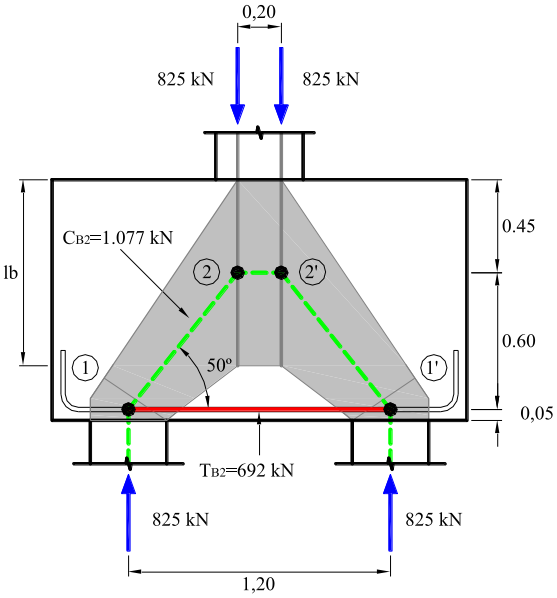


Fig. 1.3-6: Model B2: compressive forces of column reinforcement (dimensions in m)

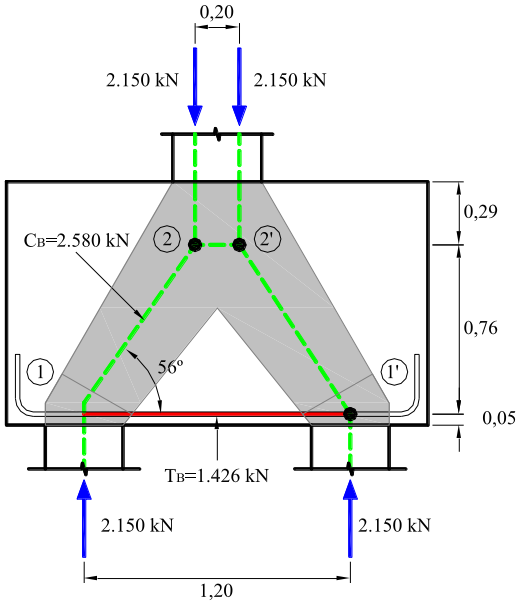


Fig. 1.3-7: Model B. Superposition of models B1 and B2 (dimensions in m)

Forces in the struts and ties of model B (see Fig. 1.3-7) result from the vectorial sum of forces of models B1 and B2:

$$\mathbf{T_B = T_{B1} + T_{B2}} \quad \text{and} \quad \mathbf{C_B = C_{B1} + C_{B2}}$$

$$T_B = T_{B1} + T_{B2} = 734 + 692 = 1.426 \text{kN}$$

$$C_B = \sqrt{2150^2 + 1426^2} = 2.580 \text{kN}$$

$$\alpha = \text{a tan}\left(\frac{2150}{1426}\right) = 56^o$$

This document is the intellectual property of the fib – International Federation for Structural Concrete. All rights reserved.
This PDF of fib Bulletin 61 is intended for use and/or distribution solely within fib National Member Groups.

3.2 Step 2: Determination of amount of reinforcement

Principal reinforcement is obtained dimensioning tie 1-1'in model B:

$$A_{s\,11'} = \frac{T_B}{f_{yd}} = \frac{1.426.000}{435} = 3.280\ \text{mm}^2 \Rightarrow 7\phi 25 \quad \text{are adopted.}$$

Notice that model A underestimates the tensile force over tie 1-1':

$$\frac{T_{\text{model B}}}{T_{\text{model A}}} = \frac{1.426}{1.192} = 1{,}20$$

This difference is especially relevant when the column is highly reinforced and big diameter bars are used, which is a common situation in building columns, where sectional dimensions usually have to be as small as possible due to architectural reasons.

3.3 Step 3: Node design and check of nodal pressure

Node 1: Node 1 is a C-C-T-node. According to the FIP Recommendations (1999) the effective concrete strength is $f_{cd,eff} = 0{,}85 \cdot f_{1\,cd} = 0{,}85 \cdot 17{,}00 = 14{,}45\ \text{MPa}$.

Node geometry is defined by:

$b = 0{,}35$ m = node width; $a_1 = 0{,}35$ m; u = 2 · 0,05 = 0,10 m

$$a_{12} = 0{,}35 \cdot \sin(56) + 0{,}10 \cdot \cos(56) = 0{,}35\ \text{m}$$

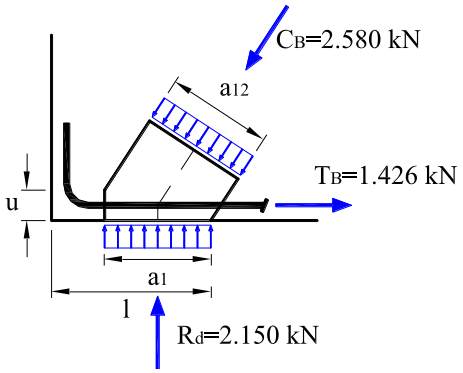


Fig. 1.3-8: Node 1

Check of the anchorage length, according to FIP Recommendations (1999):

$$l_{b,net} = (36{,}2 \cdot 0{,}02) \cdot 0{,}7 \cdot \frac{2}{3} = 0{,}34\,\text{m} < l$$

$$l = 0{,}35 + \frac{0{,}35}{2} - 0{,}05 = 0{,}48\,\text{m}$$

Then: $\sigma_{1d} = \dfrac{R_d}{b \cdot a_1} = \dfrac{2.150}{0{,}35 \cdot 0{,}35} = 17{,}55\ \text{MPa} > f_{cd,eff}$

$$\sigma_{12d} = \frac{C_B}{b \cdot a_{12}} = \frac{2.580}{0{,}35 \cdot 0{,}35} = 21{,}06\ \text{MPa} > f_{cd,eff}$$

The concrete stresses are higher than $f_{cd,eff}$.

This document is the intellectual property of the fib – International Federation for Structural Concrete. All rights reserved.
This PDF of fib Bulletin 61 is intended for use and/or distribution solely within fib National Member Groups.

To solve this problem, a transversal model is proposed (Fig. 1.3-9) considering the transversal dispersion of stresses.

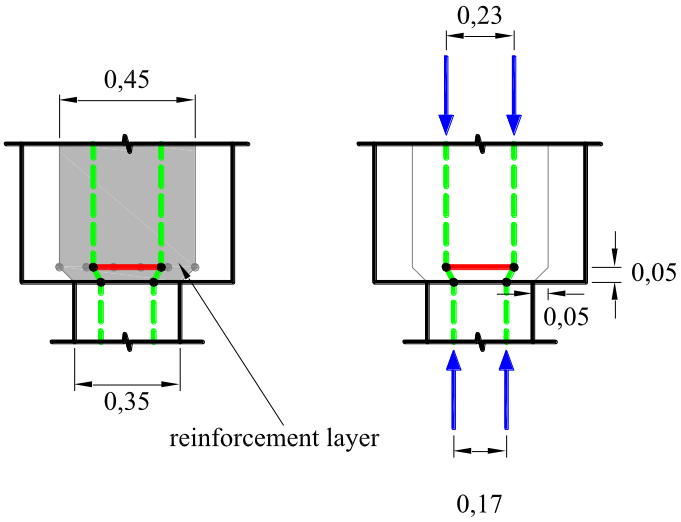


Fig. 1.3-9: Transversal model (dimensions in m)

Concrete stresses are now checked considering a node width, b = 0,45m:

$$\sigma_{1d} = \frac{R_d}{b \cdot a_1} = \frac{2.150}{0{,}45 \cdot 0{,}35} = 13{,}65\ \text{MPa} < f_{cd,eff}$$

$$\sigma_{12d} = \frac{C_B}{b \cdot a_{12}} = \frac{2.580}{0{,}45 \cdot 0{,}35} = 16{,}38\ \text{MPa} > f_{cd,eff}$$

As $\sigma_{12d} > f_{cd,eff}$, a configuration of reinforcement with three layers is adopted in order to spread the concrete stresses in node 1 (Fig. 1.3-10 and Fig. 1.3-11). Reinforcement consists of 3×4ϕ20. With the new reinforcement disposition, geometry and forces of the elements of the model are slightly modified. Nevertheless, as these changes are small, analysis result does not change.

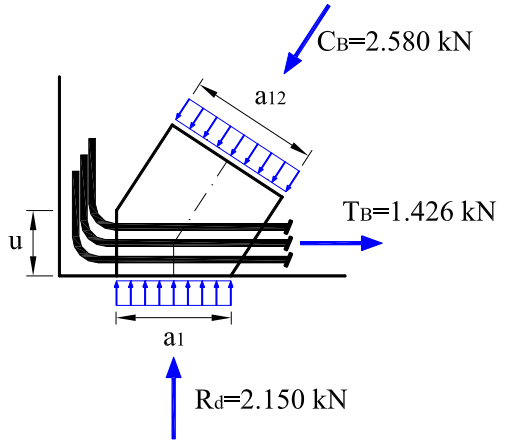


Fig. 1.3-10: Node 1 with 3 bar layers

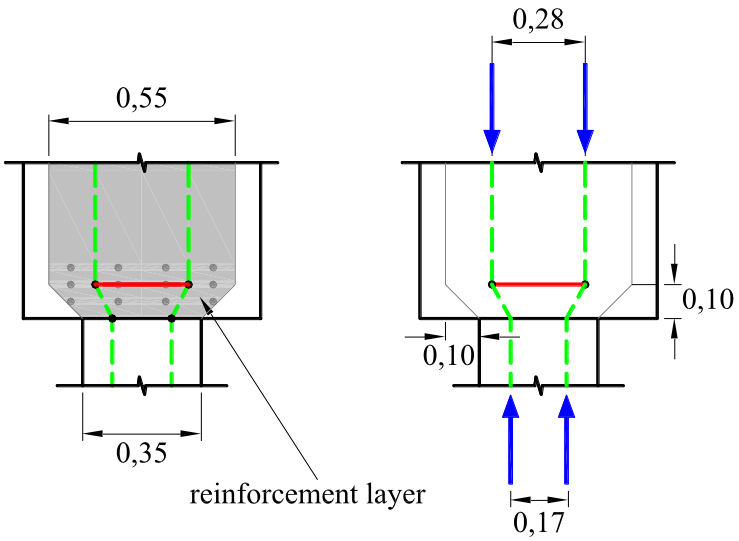


Fig. 1.3-11: Transversal model with 3 bar layers (dimensions in m)

This document is the intellectual property of the fib – International Federation for Structural Concrete. All rights reserved.
This PDF of fib Bulletin 61 is intended for use and/or distribution solely within fib National Member Groups.

The new node geometry is determined and stresses are checked:

$$u = 0{,}20\ \text{m}; \qquad a_{12} = 0{,}35 \cdot \sin(56) + 0{,}20 \cdot \cos(56) = 0{,}40\ \text{m}$$

$$\sigma_{12d} = \frac{C_B}{b \cdot a_{12}} = \frac{2.580}{0{,}55 \cdot 0{,}40} = 11{,}73\ \text{MPa} < f_{cd,eff}$$

It is necessary to materialize the amount of reinforcement needed to resist the stresses of the new tie appearing in the transversal model. This reinforcement is determined as follows:

$$T_d = \left(\frac{0{,}55}{4} - \frac{0{,}35}{4}\right) \cdot \frac{1}{0{,}10} \frac{2.150}{2} = 538\ \text{kN};$$

$$A_s = \frac{538.000}{435} = 1.240\ \text{mm}^2 \Rightarrow 3\text{x}6\ \phi 10$$

Node 2: Interface between column and cap remains the critical section. Concrete stresses are evaluated in model B1.

$$\sigma_{2d} = \frac{N_{d\ (\text{model B1})}}{b \cdot a_2} = \frac{2.650}{0{,}40 \cdot 0{,}40} = 16{,}56\ \text{MPa} < f_{2cd}$$

Notice that column and cap's concrete has the same resistance, therefore it is not necessary to check stresses in node 2, because it has already been checked when dimensioning the column.

3.4 Step 4: Arrangement of reinforcement

The detailing of the reinforcement is shown in Fig. 1.3-12 and Fig. 1.3-13.

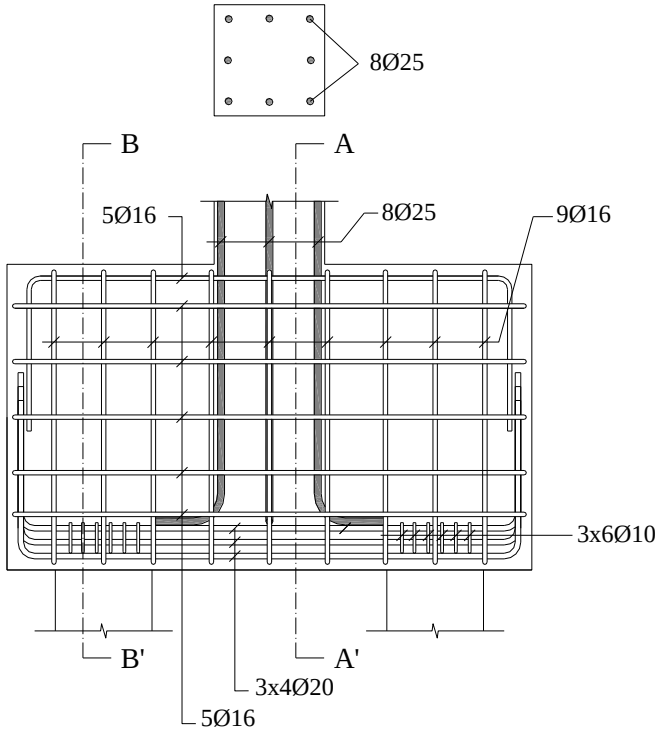


Fig. 1.3-12: Arrangement of reinforcement, front view (dimensions in m)

This document is the intellectual property of the fib – International Federation for Structural Concrete. All rights reserved.
This PDF of fib Bulletin 61 is intended for use and/or distribution solely within fib National Member Groups.

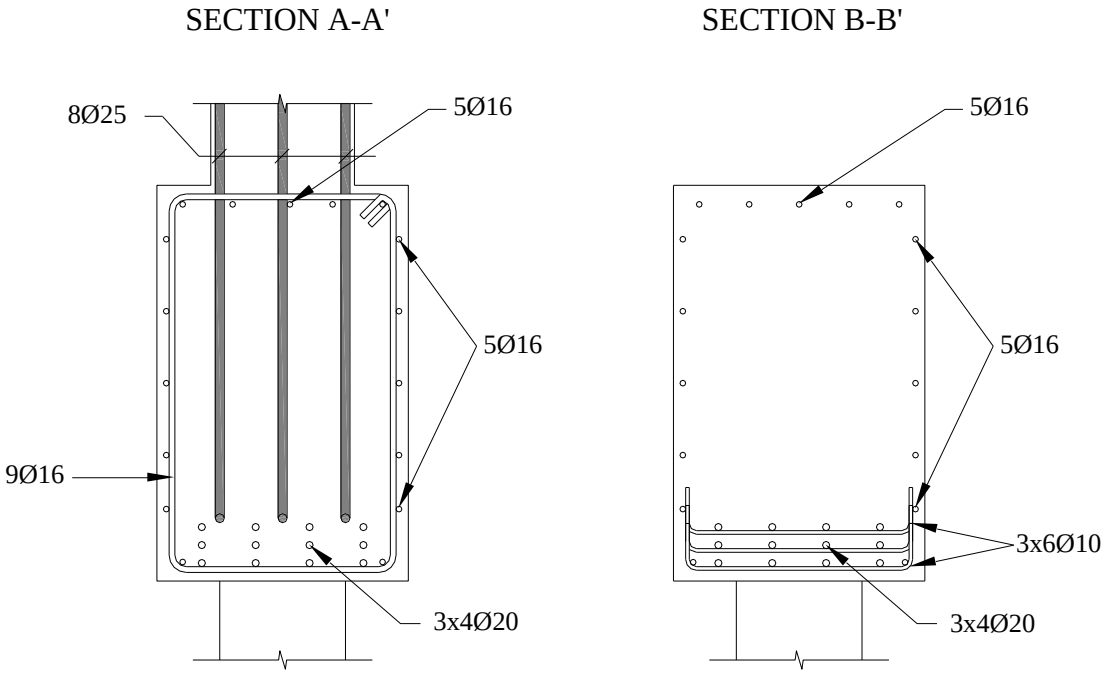


Fig. 1.3-13: Arrangement of reinforcement in sections A-A' and B-B'

This document is the intellectual property of the fib – International Federation for Structural Concrete. All rights reserved.
This PDF of fib Bulletin 61 is intended for use and/or distribution solely within fib National Member Groups.

Example 1–4: Bridge diaphragm

1 Description of design task

1.1 The structure

The diaphragm of a box girder bridge is an example of a typical D-region for such bridges. It is simply solved with the strut and tie method. Thereby it is assumed that the shear forces in the box girder are transmitted through the webs and from there to the load bearing plates. Once the model is established, the set of loads in equilibrium is imposed and the forces in the model solved.

1.2 Geometry and loads

The geometry of a box girder bridge and the design loads are shown in Figs. 1.4-1 and 1.4-2.

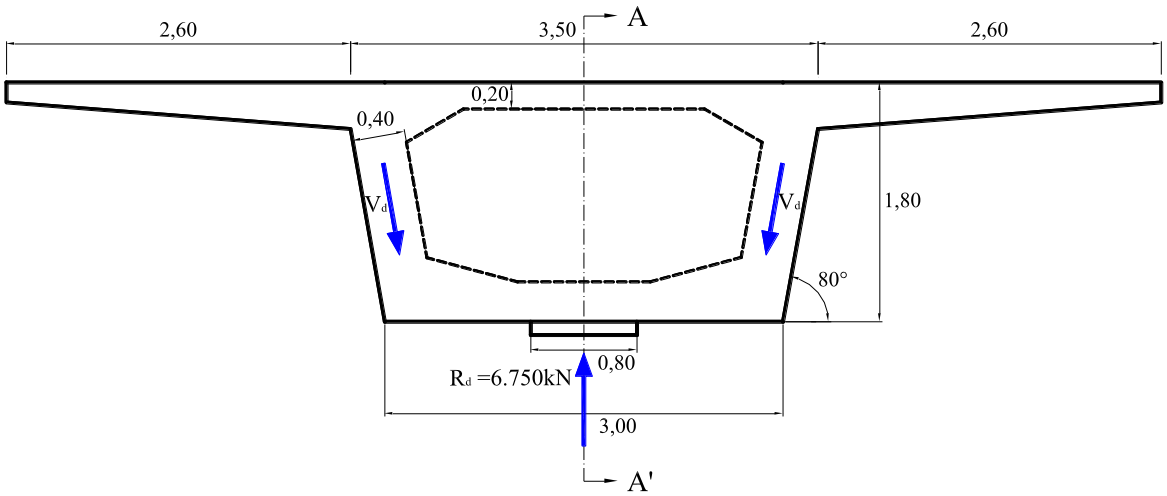


Fig. 1.4-1: Cross-section with geometry and loads (dimensions in m)

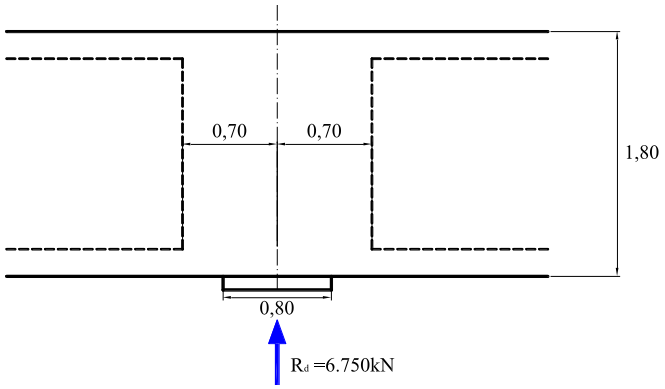


Fig. 1.4-2: Section A-A with geometry and loads (dimensions in m)

This document is the intellectual property of the fib – International Federation for Structural Concrete. All rights reserved.
This PDF of fib Bulletin 61 is intended for use and/or distribution solely within fib National Member Groups.

1.3 Design values for materials

Concrete: $f_{ck} = 35$ MPa

Concrete: $f_{1cd} = 0{,}85 \cdot f_{ck} / 1{,}5 = 0{,}85 \cdot 35/1{,}5 = 19{,}8$ MPa

Reinforcement: $f_{yk} = 500$ MPa; $f_{yd} = \frac{f_{yk}}{1{,}15} = \frac{500}{1{,}15} = 435$ MPa

2 Design procedure

The design procedure contains the following steps:

- Step 1: Creation of a strut-and-tie model.
- Step 2: Determination of amount of reinforcement.
- Step 3: Design of nodes and check of nodal pressure.
- Step 4: Arrangement of reinforcement.

3 Design calculations

3.1 Step 1: Creation of a strut-and-tie model

The shear of the box girder is transmitted by the webs to the column through the diaphragm, which works as a so-called "indirect support", see FIP Recommendations (1999), 6.5.2.2. A three-dimensional strut-and-tie model is proposed to explain the global behaviour as shown in Fig. 1.4-3. Additionally a two-dimensional linear elastic finite element model has been used as an aid to develop the diaphragm model, and the results are shown in Fig. 1.4-4.

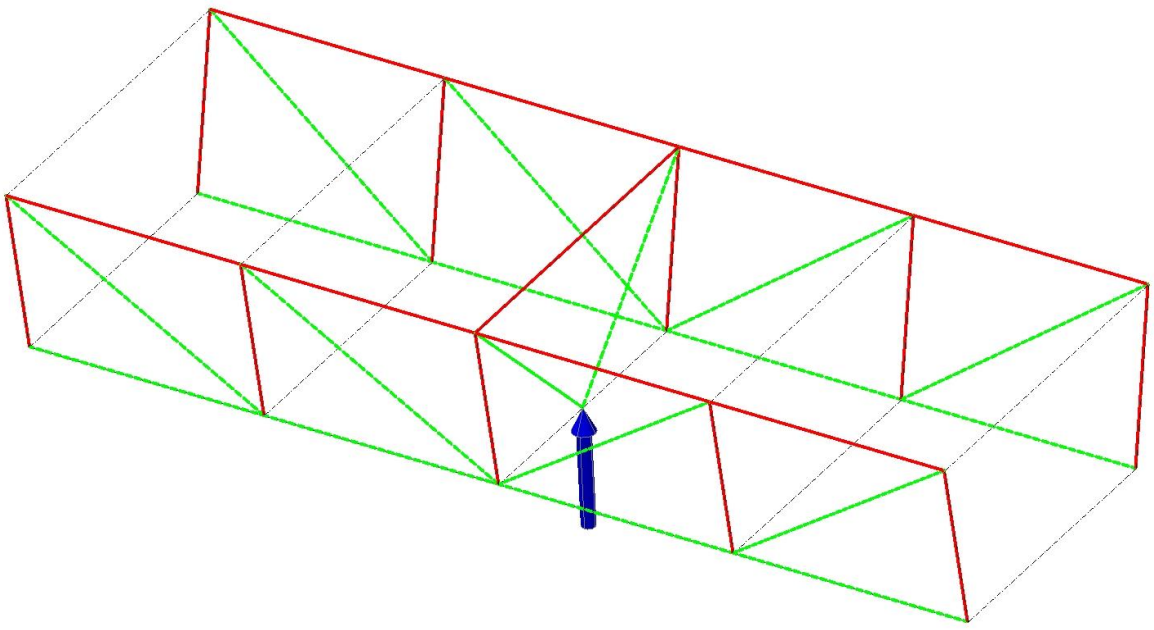


Fig. 1.4-3: The three-dimensional model of the box girder

This document is the intellectual property of the fib – International Federation for Structural Concrete. All rights reserved.
This PDF of fib Bulletin 61 is intended for use and/or distribution solely within fib National Member Groups.

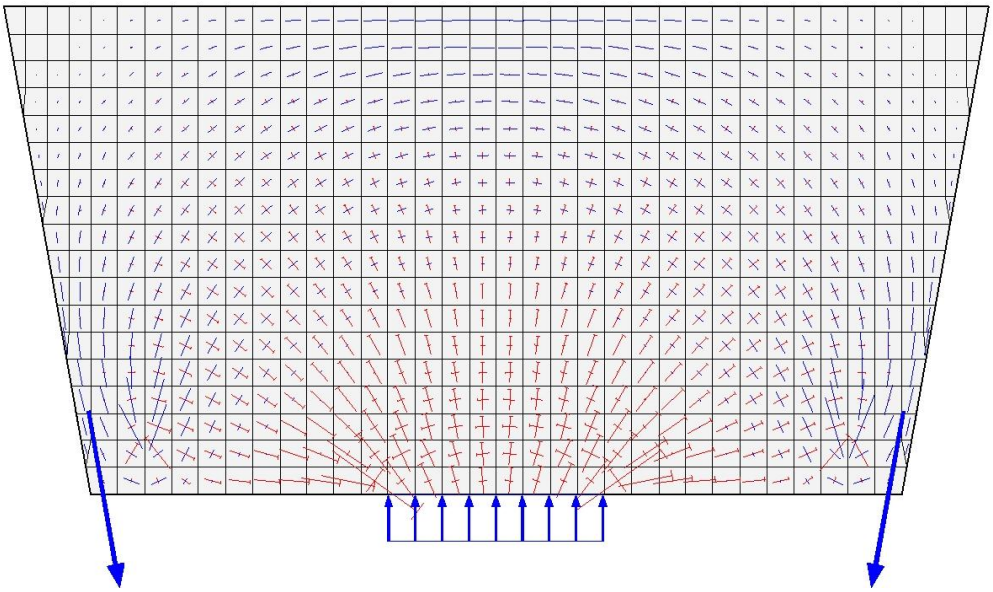


Fig. 1.4-4: The two-dimensional finite element model

There are several possible strut-and-tie models. A simple and clear one is the model presented in Fig. 1.4-5, whereby for the inner lever arm a value of z = 1,45 m is adopted.

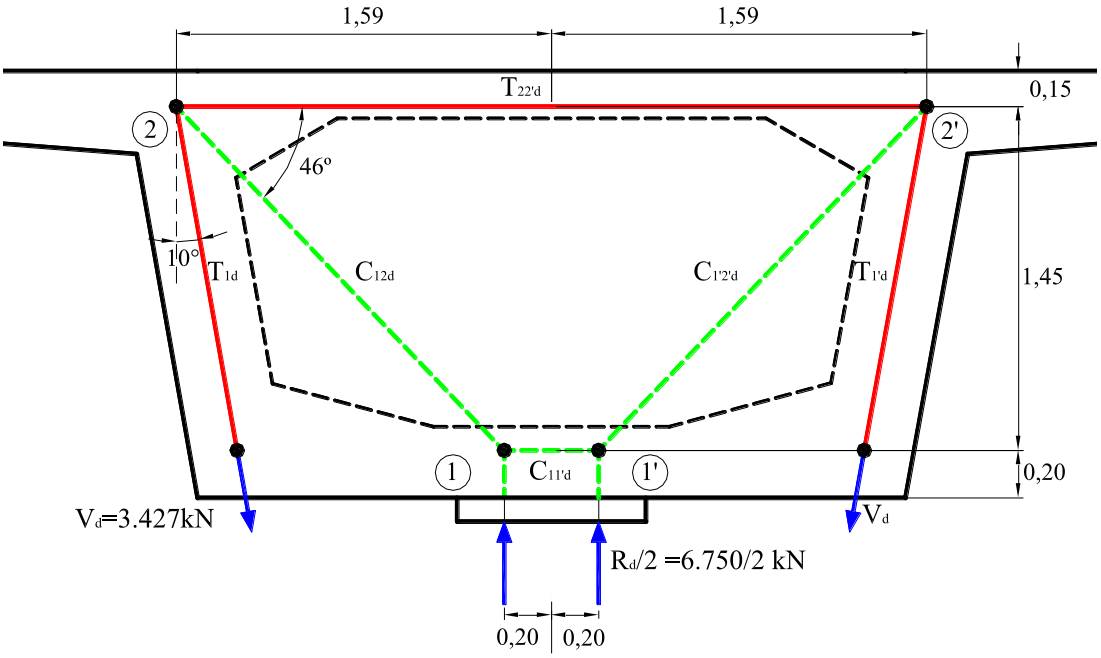


Fig. 1.4-5: Strut-and-tie model for the diaphragm (dimensions in m)

The design reaction is $R_d = 6.750\ \text{kN}$, so that:

$$V_d = \frac{6.750}{2 \cdot \cos(10)} = 3.427\ \text{kN}$$

This document is the intellectual property of the fib – International Federation for Structural Concrete. All rights reserved.
This PDF of fib Bulletin 61 is intended for use and/or distribution solely within fib National Member Groups.

It is assumed that the shear transmitted by the webs is applied on the bottom corners of the diaphragms (see Fig. 1.4-4), so it is necessary to hang up these load nns with the T_{1d} and $T_{1'd}$ ties.

Element forces are determined with simple equilibrium considerations:

- equilibrium of node 1: $C_{12d} = \dfrac{6.750/2}{\sin(46)} = 4.692\ \text{kN}$; $C_{11'd} = C_{12d} \cdot \cos(46) = 3.259\ \text{kN}$

- equilibrium of node 2: $T_{22'd} = C_{12d} \cdot \cos(46) - V_d \cdot \sin(10) = 2.664\ \text{kN}$

3.2 Step 2: Determination of amount of reinforcement

Firstly, the reinforcement to be disposed at the top of cross section has to be defined.

$$A_{s22'} = \frac{T_{22'}}{f_{yd}} = \frac{2.664.000}{435} = 6.124\ \text{mm}^2 \Rightarrow 20\phi 20$$

In addition, the total support force has to be transferred to the top of the diaphragm by means of a *hanging-up* reinforcement within the width of the diaphragm. This reinforcement is calculated as follows:

$$A_{svd} = \frac{V_d}{f_{yd}} = \frac{3.427.000}{435} = 7.878\ \text{mm}^2 \Rightarrow \quad \text{stirrups: } 20\phi 16 \text{ are adopted.}$$

3.3 Step 3: Design of nodes and check of nodal pressure

Node 1: Node 1 connects only struts and could be considered as a planar C-C-C-node, as shown in Fig. 1.4-6.

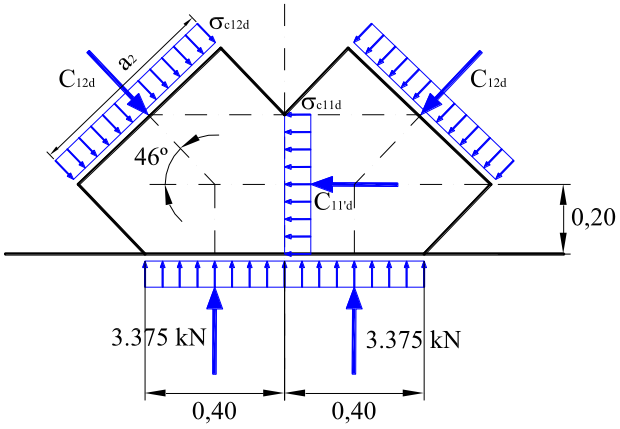


Fig. 1.4-6: Node 1 (dimensions in m)

This document is the intellectual property of the fib – International Federation for Structural Concrete. All rights reserved.
This PDF of fib Bulletin 61 is intended for use and/or distribution solely within fib National Member Groups.

According to FIP Recommendations (1999): $f_{2cd} = 1,20 \cdot f_{1cd} = 1,20 \cdot 19,83 = 23,80$ MPa

The width of the node is equal to the width of the load bearing plate:

$$b_1 = 2 \cdot 0,40 = 0,80 \text{ m} ; \qquad a_1 = 0,40 \cdot \sin(46) + 2 \cdot 0,20 \cdot \cos(46) = 0,57 \text{ m}$$

$$\sigma_{c12d} = \frac{C_{12d}}{b_1 \cdot a_1} = \frac{4.692}{0,80 \cdot 0,57} = 10.289 \text{ kN/m}^2 = 10,29 \text{ MPa} < f_{2cd}$$

$$\sigma_{c11'd} = \frac{C_{11'd}}{b_1 \cdot 2 \cdot 0,20} = \frac{3.259}{0,80 \cdot 2 \cdot 0,20} = 10.184 \text{ kN/m}^2 = 10,18 \text{ MPa} < f_{2cd}$$

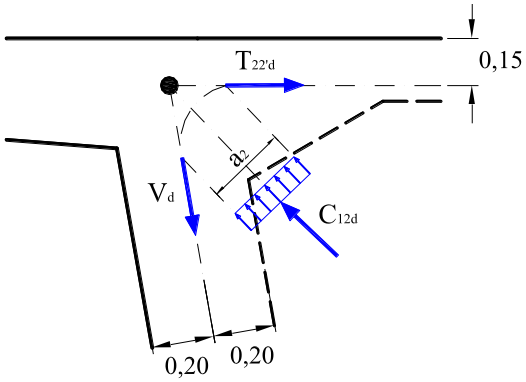


Fig. 1.4-7: Node 2

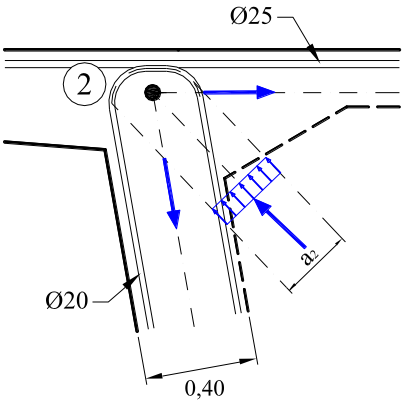


Fig. 1.4-8: Node 2 with stirrup disposition (dimensions in m)

Node 2: Node 2 is a C-T-T-node, as shown in Fig. 1.4-7 and Fig. 1.4-8.

As the reinforcement is anchored in the node, the effective concrete compression stress is determined as following, according to FIP Recommendations (1999):

$$f_{cd,eff} = \nu_2 \cdot f_{1cd} = 0,85 \cdot 19,83 = 16,86 \text{ MPa}$$

The width of the node is equal to the diaphragm width:

$$b_2 = 2 \cdot 0,70 = 1,40 \text{ m} \qquad a_2 = 2 \cdot 0,13 = 0,26 \text{ m}$$

$$\sigma_{c12d} = \frac{C_{12d}}{b_2 \cdot a_2} = \frac{4.692}{1,40 \cdot 0,26} = 12.890 \text{ kN/m}^2 = 12,89 \text{ MPa} < f_{2cd}$$

3.4 Step 4: Arrangement of reinforcement

The principal reinforcement is obtained dimensioning the model ties as shown is Step 2 and the reinforcement layout is shown in Fig. 1.4-9 and Fig. 1.4-10. A reinforcement mesh is necessary to control cracking and to ensure enough ductility to the diaphragm. According to FIP Recommendations (1999), 8.6 (3), for deep beams, a mesh of orthogonal reinforcement with a minimum area of 0,1% of the cross-section in each direction should be provided at each face:

$$A_{s\,M} = \frac{0,10}{100} \cdot 1.000 \cdot 1.400 = 1.400 \text{ mm}^2 \Rightarrow \#\,\phi 20 / 0,15 \quad \text{is adopted.}$$

This document is the intellectual property of the fib – International Federation for Structural Concrete. All rights reserved.
This PDF of fib Bulletin 61 is intended for use and/or distribution solely within fib National Member Groups.

In the bottom flange of the diaphragm the reinforcement is calculated as 1/3 of the principal reinforcement: $A_s = \frac{1}{3} \cdot (6.124) = 2.041\,\text{mm}^2 \rightarrow 7\ \text{Ø}20$ is adopted.

The anchorage length of the top reinforcement rebars is calculated according to FIP Recommendations (1999), Table 2.5.

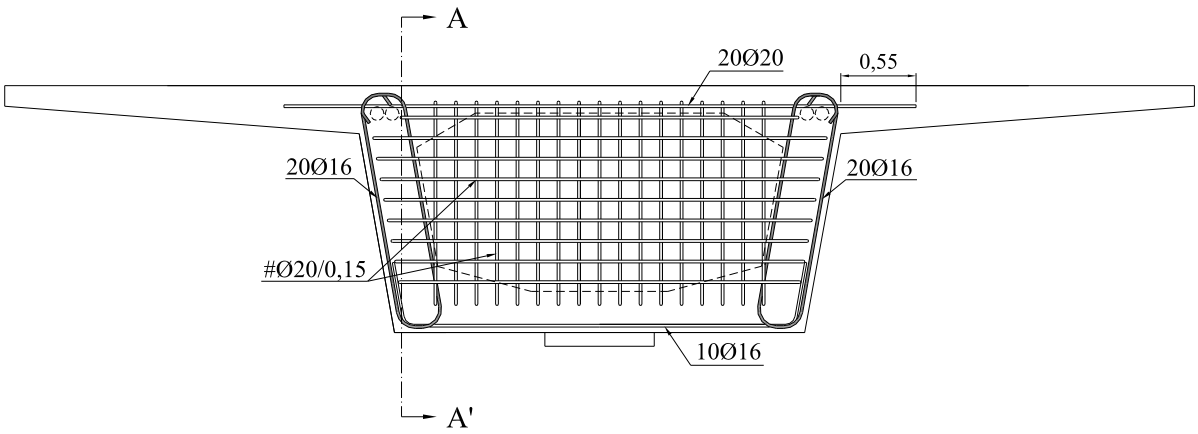


Fig. 1.4-9: Arrangement of reinforcement, cross-section

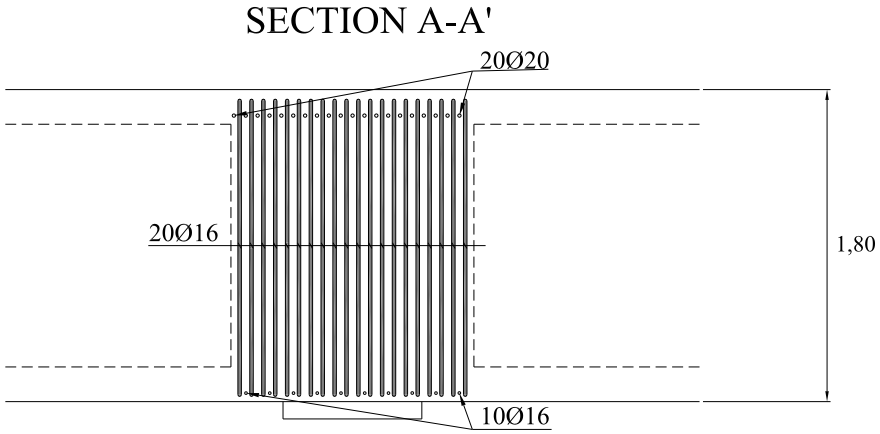


Fig. 1.4-10: Longitudinal section A-A with arrangement of reinforcement

This document is the intellectual property of the fib – International Federation for Structural Concrete. All rights reserved.
This PDF of fib Bulletin 61 is intended for use and/or distribution solely within fib National Member Groups.

1-5 Summary and conclusions for Examples 1-1 to 1-4

The examples presented in this chapter try to show, in a clear and didactic way, the application strut-and-tie models for solving and dimensioning several structural members.

Structures with a three-dimensional behaviour are solved in Examples 1-1 and 1-2. It is necessary to use several simplifications in order to fulfill the nodes verification, since there are not clear instructions or recommendations for these cases.

Example 1-3 shows the importance of considering in a separated way the loads transmitted by steel and concrete from the column to the pile cap. Different ways are shown to solve the problem of highly stressed nodes.

Finally, in Example 1-4 a typical case of an indirect support applied to a bridge diaphragm is presented.

After solving these examples, the following conclusions can be stated:

1: The application of the strut-and-tie method, even for relatively simple structural members, obliges the design engineer to clearly understand the force flow inside the member and its critical zones, generally its nodes.

2: This method might be not very efficient when solving simple structural members for which there already exist rules of simpler application that guarantee a correct dimensioning. Nevertheless, the strut-and-tie model provides a deep insight into the structural behaviour of the members, from which the mentioned rules are obtained.

3: There exist difficulties when applying the strut-and-tie method to the nodes verification of three-dimensional models. This problem can be solved by assimilating the global model to two-dimensional projections.

References

FIP Recommendations (1999): Practical Design of Structural Concrete. FIP-Commission 3 "Practical Design", Sept. 1996. Publ.: SETO, London, Sept. 1999. (distributed by: *fib*, Lausanne. Web http://www.fib-international.org)

This document is the intellectual property of the fib – International Federation for Structural Concrete. All rights reserved.
This PDF of fib Bulletin 61 is intended for use and/or distribution solely within fib National Member Groups.

Example 2: Precast corbels fitted to columns

Jean-Marc Voumard

1 Introduction and design task

For the car park underneath the Auchan Shopping Centre in Warsaw, the existing support structure of the beams does not allow for sufficient dilatation. The solution allows the horizontal slab movement by means of creating a gap between beams and columns and installing bearing pads under the newly corbel-supported beams. The load is transferred from existing corbels to temporary supports equipped with jacking units. The existing corbels are then sawed and removed in order to provide a 10-mm gap between beams and columns. The new corbels, made of two precast "C"-shaped concrete elements, are fitted to the column with post-tensioned bars, followed by installation of the bearing pads (Fig. 2-1a). The load is then re-transferred from temporary supports to the columns (Fig. 2-1b).

These works, which encompass repairs to 57 columns, were completed by the end of November 2002. In this particular case, the repair works were executed with PT bars.

The purpose of the example hereafter is to show the design procedure using strut-and-tie models and to verify the feasibility of a solution without post-tensioning, in particular with regard to safety against sliding. For clarity, the actual 3D- system has been simplified to a 2D-model that does not take into account the lateral forces.



a) view of corbel *b) load transfer on the corbel*

Fig. 2-1: Precast corbel with post-tensioning bars

This document is the intellectual property of the fib – International Federation for Structural Concrete. All rights reserved.
This PDF of fib Bulletin 61 is intended for use and/or distribution solely within fib National Member Groups.

2 Materials and loads

Concrete C30/37: $f_{ck,cyl}$ = 30 MPa; f_{cd} = 17 MPa

f_{ctm} = 2,9 MPa**;** $f_{ctk} = 0{,}7 \cdot f_{ctm} = 0{,}7 \cdot 2{,}9 = 2{,}03$ MPa

f_{ctd} = design value of concrete tensile strength = f_{ctk} / γ_{ct} with γ_{ct} = 1,8 for ULS

$f_{ctd} = f_{ctk} / 1{,}8 = 2{,}03 / 1{,}8 = 1{,}13$ MPa

Reinforcement S400: f_{yd} = 350 MPa

Prestressing bars ∅36 mm: $P_{residual}$ = 500 kN

The geometry of the corbel is shown in Fig. 2-2. The applied factored loads are as follows:

F_v = 1.050 kN at a_c = 400 mm

F_h = 210 kN

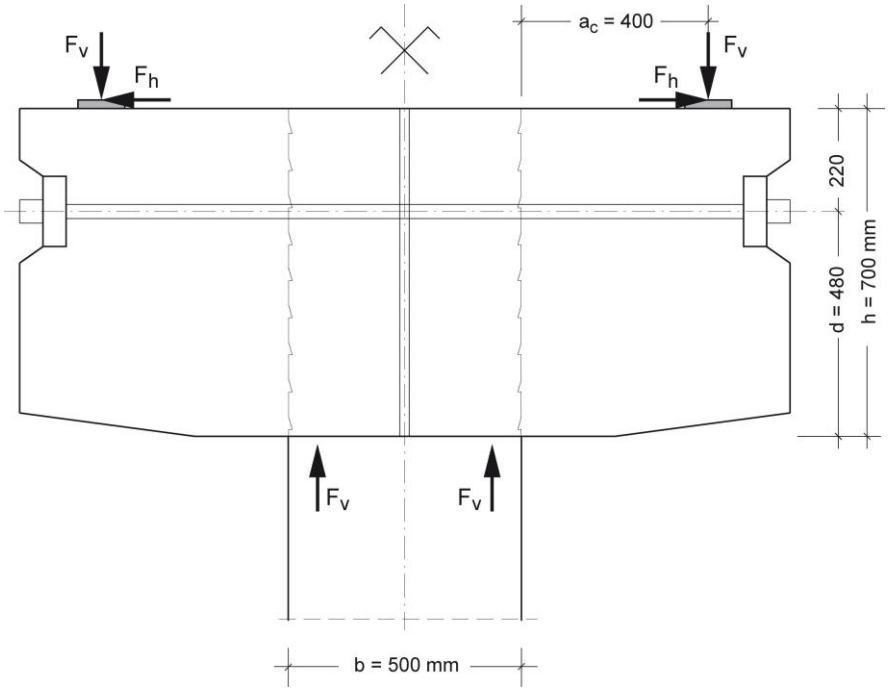


Fig. 2-2: Geometry of the corbel

3 Design of the corbel with a strut-and-tie model

The strut-and-tie model is shown in Fig. 2-3, whereby two cases are shown on the left and right side. These models follow the FIP Recommendations (1999), sect. 6.5.2.3. In Fig. 2-3a the simple model is shown, where the load is directly transferred to the column. The model in Fig. 2-3b applies for the slender cases with distances of $0{,}5\ z \leq a \leq 2z$.

This document is the intellectual property of the fib – International Federation for Structural Concrete. All rights reserved.
This PDF of fib Bulletin 61 is intended for use and/or distribution solely within fib National Member Groups.

The design of the models follows sections 6.5.2 and 6.5.3 of the FIP Recommendations (1999), where in Fig. 6.15 detailed rules are given for the design in subsequent steps.
Step 1: $a_1 = F_v / (b \cdot f_{cd,eff})$

where: $f_{cd,eff} = \nu_1 \cdot f_{1cd}$ and $\nu_1 = 1 - f_{ck}/250 = 1 - 30/250 = 0{,}88$

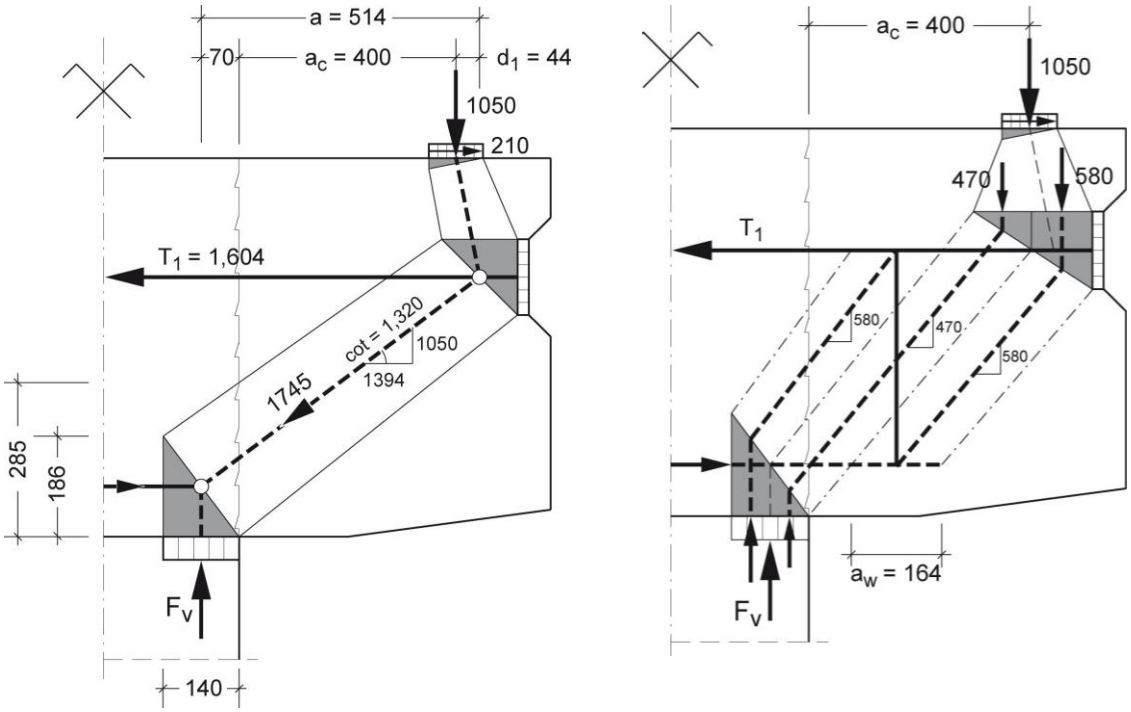
$f_{cd,eff} = 0{,}88 \cdot 17 = 15{,}0$ MPa

$a_1 = 1.050 \cdot 10^3 / (500 \cdot 15{,}0) = 140$ mm

When calculating the distance a, the transfer of the loads by an inclined strut must be considered, which increases a by a distance d_1:

$$d_1 = (h-d) \cdot Fh/Fv = (700-480) \cdot 210/1050 = 44\,\text{mm}$$

$$a = a_c + \frac{a_1}{2} + d_1 = 400 + \frac{140}{2} + 44 = 514\ \text{mm}$$



a) simple model *b) refined model for 0,5 z ≤ a ≤ 2z*

Fig. 2-3: Strut-and-tie models for the corbel

Step 2: $a_2 = d - \sqrt{d^2 - 2 \cdot a \cdot a_1} = 480 - \sqrt{480^2 - 2 \cdot 514 \cdot 140} = 186$ mm

$$z = d - \frac{a_2}{2} = 480 - \frac{186}{2} = 387\ \text{mm}$$

Step 3: $\cot\theta = a / z = 514 / 387 = 1{,}328 \rightarrow \theta = 37°$

Step 4: $T_1 = F_v \cdot \cot\theta + F_h = 1.050 \cdot 1{,}328 + 210 = 1.604$ kN

$A_{s1} = 1.604 \cdot 10^3 / 350 = 4.583$ mm^2

Step 5: For the anchorage of tie T_1 anchor plates are provided.

This document is the intellectual property of the fib – International Federation for Structural Concrete. All rights reserved.
This PDF of fib Bulletin 61 is intended for use and/or distribution solely within fib National Member Groups.

These different steps were developed for the simple model in Fig. 2-3a. Since this corbel is relatively slender with a/z = 1,328 the model of Fig. 6.14 and Eq.(6.34) of the FIP Recommendations (1999) applies:

$$F_1 = F_v \cdot (2 \cdot a/z - 1)/3 = 1.050\ (2 \cdot 1{,}328 - 1)/3 = 1.050 \cdot 0{,}552 = 580 \text{ kN}$$

$$A_{sw} = \frac{F_1}{f_{yd}} = \frac{580 \cdot 10^3}{350} = 1.657 \text{ mm}^2$$

The required stirrups may be distributed over a length of about a_w = 164 mm, as the model with the stress fields shows in Fig. 2-3b. In the FIP Recommendations (1999) an estimate of this value is given of $a_w = 0{,}85 \cdot a - z/4 = 0{,}85 \cdot 514 - 387/4 = 342$ mm, which was obviously derived for cases with different geometries than here.

4 Transfer of forces across interface between corbel and column for the prestressed corbel

The check of safety against sliding at the interface between the column and the corbel is performed according to section 5.5 in the FIP Recommendations (1999).

$$\tau_{fd} = \beta \cdot f_{ctd} + \mu \cdot \sigma_{fd} \leq 0.25 \cdot f_{1cd} \qquad (1)$$

where:

β = coefficient from Table 5.1

σ_{fd} = normal stress on interface

μ = friction coefficient from Table 5.1

f_{ctd} = design value of concrete tensile strength = 1,13 MPa

The interface between the column and the corbel is regarded as smooth, and from Table 5.1 the following values apply:

β = 0,2 and μ = 0,6

The tie force T_1 = 1.604 is taken by prestressing bars, and the number of bars required is:

n = 1.604 / 500 = 3,2 bars → 4 bars ∅36 mm selected

The prestressing force is $P = 4 \cdot 500 = 2.000$ kN and thus is far greater than T_1 = 1.604 kN. This means that according to the model there will be no tension in the tie and the interface can be regarded as uncracked over the full depth.

If for comparison the stresses according to the bending theory are calculated, then a small tension stress of + 0,60 MPa occurs at the top fibre due to prestressing and loading. This is about half the design value of the concrete tensile strength of 1,13 MPa, so that no cracking is to be expected.

Therefore, the contact area is $A_{cont} = 500 \cdot 700$ mm^2, and the stress σ_{fd} in Eq.(1) is:

$$\sigma_{fd} = P / A_{cont} = 2.000 \cdot 10^3 / (500 \cdot 700) = 5{,}7 \text{ MPa}$$

This document is the intellectual property of the fib – International Federation for Structural Concrete. All rights reserved.
This PDF of fib Bulletin 61 is intended for use and/or distribution solely within fib National Member Groups.

The shear-friction capacity acc. to Eq.(1) then is:

$$\tau_{fd} = 0{,}2 \cdot 1{,}13 + 0{,}6 \cdot 5{,}7 = 0{,}23 + 3{,}42 = 3{,}65 \text{ MPa} < 0{,}25 \cdot 17{,}0 = 4{,}25 \text{ MPa}$$

The corresponding resisisting friction force transferable over the interface is:

$$F_{Rfd} = \tau_{fd} \cdot A_{cont} = 3{,}65 \cdot 500 \cdot 700 \cdot 10^{-3} = 1.278 \text{ kN}$$

The applied force is: $F_{Ed} = F_v = 1.050$ kN, so that $F_{Rfd} > F_{Ed}$, and the smooth interface can transfer the applied load.

5 Feasibility study of a solution with reinforcing bars

For comparison purposes a solution of corbels with reinforcing bars is presented instead of the prestressing bars.

For the required tie force of $T_1 = 1.604$ kN the following reinforcement is required:

$$A_{s1} = T_1 / f_{yd} = 1.604 \cdot 10^{-3} / 350 = 4.583 \text{ mm}^2$$

In this case the interface is cracked and so only the compression zone can be relied on for the transfer of the vertical force. For assessing the depth of the compression zone, the simple model of Fig. 2-3a is used, and this gives a length of the compressed interface of 285 mm, so that the contact area is $A_{cont} = 500 \cdot 285$ mm^2.

The normal force on this contact area is defined by the horizontal component of the inclined strut, and this is according to step 3 of section 3:

$$C_h = F_v \cdot \cot\theta = 1.050 \cdot 1{,}328 = 1.394 \text{ kN}$$

The normal stress of the interface is then:

$$\sigma_{fd} = C_h / A_{cont} = 1.394 \cdot 10^3 / (500 \cdot 285) = 9{,}8 \text{ MPa}$$

The shear-friction capacity acc. to Eq.(1) then is:

$$\tau_{fd} = 0{,}2 \cdot 1{,}13 + 0{,}6 \cdot 9{,}8 = 0{,}23 + 5{,}87 = 6{,}1 \text{ MPa} > 0{,}25 \cdot 17{,}0 = 4{,}25 \text{ MPa}$$

With the upper limit of $\tau_{fd} = 4{,}25$ MPa the resisting friction force transferable over the interface then is:

$$F_{Rfd} = \tau_{fd} \cdot A_{cont} = 4{,}25 \cdot 500 \cdot 285 \cdot 10^{-3} = 606 \text{ kN}$$

The applied force is: $F_{Ed} = F_v = 1.050$ kN $>> F_{Rfd}$, so that the smooth interface cannot transfer the applied load. Even a rough interface cannot transfer the load, because the upper limit for τ_{fd} applies.

Even if the more refined model in Fig. 2-3b would be used to determine the length of the compressed interface, the slight increase of the contact area would not suffice to bridge the large gap between F_{Rfd} and F_{Ed}.

So it must be concluded that a solution with reinforcing bars is not feasible.

This document is the intellectual property of the fib – International Federation for Structural Concrete. All rights reserved.
This PDF of fib Bulletin 61 is intended for use and/or distribution solely within fib National Member Groups.

6 Conclusions

This Example 2 shows that it is important to mobilize a sufficient contact area of the concrete in order to transfer the forces across the interface between the column and the corbel fitted to it. With a reasonable amount of prestressing, the entire concrete section is under compression at factored load and can therefore be mobilized for the shear transfer.

The study of a solution with reinforcing bars shows, that most of the interface is subjected to tension, respectively cracked, and therefore inactive for shear transfer. The remaining small depth of the compression zone is too small as contact area to transfer the force even if a rough interface is assumed, because the shear stress across the joint is limited to a maximum value according to the FIP Recommendations (1999). This would also be valid for a solution with partial prestressing.

References

FIP Recommendations (1999): Practical Design of Structural Concrete. FIP-Commission 3 "Practical Design", Sept. 1996. Publ.: SETO, London, Sept. 1999 (Distributed by: *fib*, Lausanne: Web http://www.fib-international.org)

This document is the intellectual property of the fib – International Federation for Structural Concrete. All rights reserved.
This PDF of fib Bulletin 61 is intended for use and/or distribution solely within fib National Member Groups.

Example 3: Lift shaft substructure

Stein Atle Haugerud, Karolin Reineck

1 Presentation of structure

1.1 General

The example demonstrates the application of strut-and-tie models for the design of a lift shaft substructure in a multi-story office building built in Oslo 2001 (Fig. 3-1). The 7-story structure is set on a sloping site and includes four levels of office space and three levels of parking. The building features an all-precast superstructure with floors of topped hollow-core slabs on steel beams and spliced concrete columns.

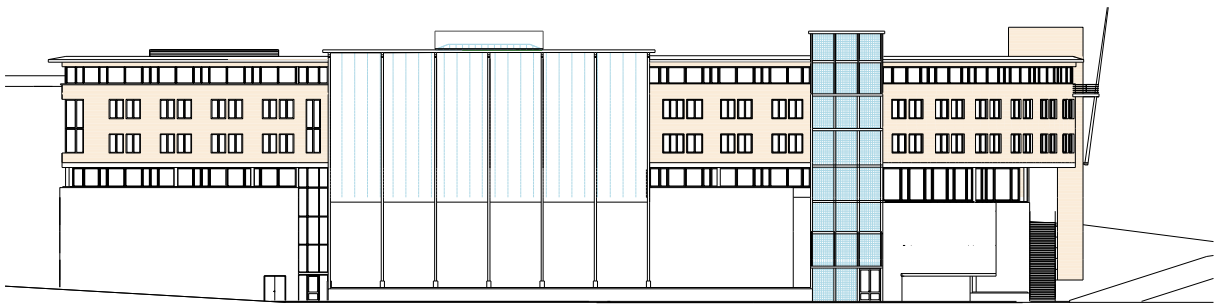


Fig. 3-1: Office complex Gulhaugveien 4 (Oslo), west facade

1.2 Description of structure

The lift shaft accommodates both elevator and a stairway and is built up by precast wall elements and glass panes. The shaft is supported by a beam grid structure (Fig. 3-2) consisting of two primary beams (① and ②) and four cross beams (③ - ⑥). The lift shaft substructure is founded on drilled steel core piles and is casted in-situ integrally with the pile caps.

This document is the intellectual property of the fib – International Federation for Structural Concrete. All rights reserved.
This PDF of fib Bulletin 61 is intended for use and/or distribution solely within fib National Member Groups.

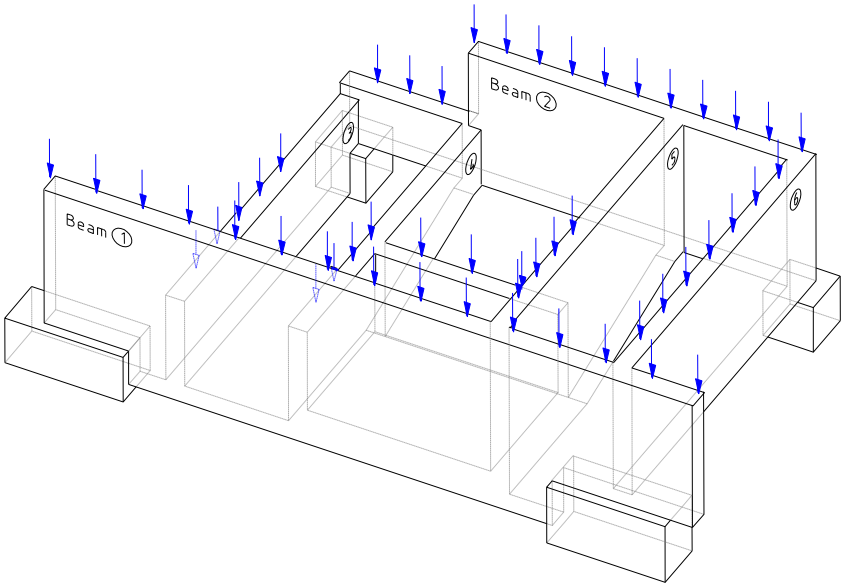


Fig. 3-2: Lift shaft substructure, isometric view

The beam grid consists of deep beams with slenderness ℓ_0 / h varying from 1,8 – 3,6. The low slenderness ratios and the presence of significant concentrated loads, advocates the application of a strut-and-tie modelling approach in the design of the individual beams. The design with the aid of strut-and-tie models is demonstrated in detail for one of the primary beams, i.e. beam ① as identified in Fig. 3-2 and 3-3.

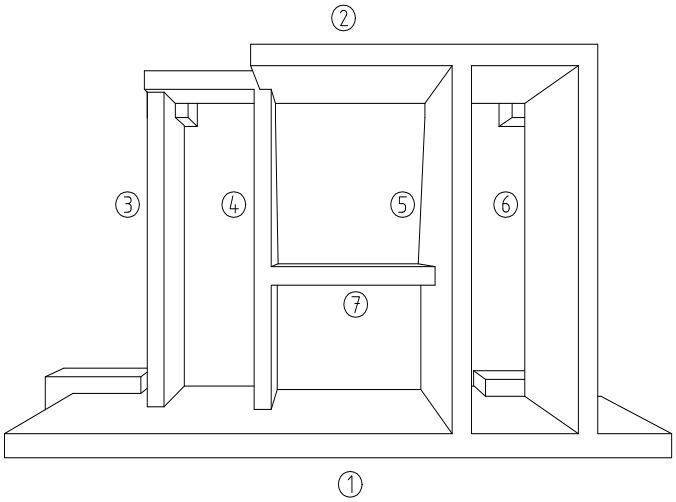


Fig. 3-3: Lift shaft substructure - beam notations

1.3 Description of design task

1.3.1 Geometry and loads

The dimensions and associated loading for beam ① is given in Fig. 3-4. In addition to dead load, beam ① must resist the suspended loads from the indirectly supported cross beams ③ - ⑤. Here the self-weight of the beam is set to act with one half at top and one half at the bottom of the beam (i.e. suspended load). Unless otherwise noted, all subsequent load effects are at ultimate.

This document is the intellectual property of the fib – International Federation for Structural Concrete. All rights reserved.
This PDF of fib Bulletin 61 is intended for use and/or distribution solely within fib National Member Groups.

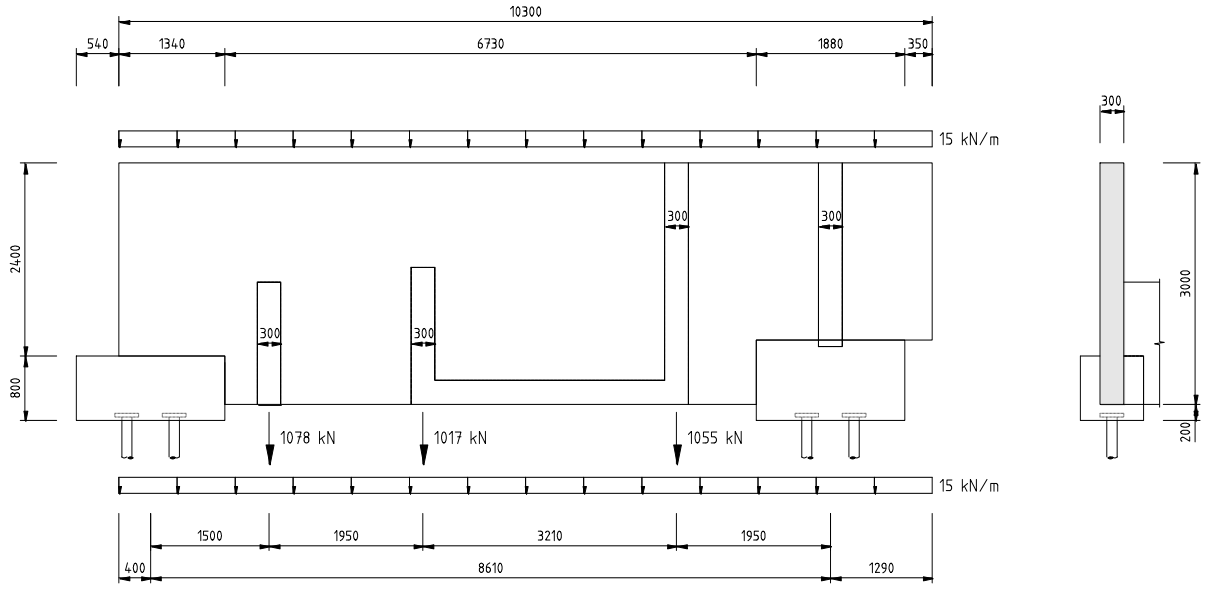


Fig. 3-4: Geometry and loads - beam ① (lengths in mm)

1.3.2 Design values for materials

The material design parameters in accordance with FIP Recommendations (1999):

- Concrete grade C35/45: f_{ck} = 35 MPa; f_{ctm} = 3,2MPa

  $f_{1cd} = \alpha f_{ck} / \gamma_c = 0{,}85 \cdot 35 / 1{,}5 = 19{,}8\text{MPa}$

- Reinforcement grade B500C: f_{yk} = 500 Pa

  $f_{yd} = f_{yk} / \gamma_s = 500 / 1{,}15 = 435$ MPa

1.3.3 Statement of design problem

Evidently from the intuitive truss model in Fig. 3-5, the entire beam can be considered as a D-region due to its aspect ratio and the singularities introduced by the concentrated loads from the supported cross beams. Whereas the tie reinforcement, adequate position and cross-sectional area, may be determined from a rather coarse model (e.g. from Fig. 3-5), the detailing of the indirect support will require more careful consideration. As will be shown, the anchorage for the suspension reinforcement as well as the anchorage of the main reinforcement from the supported beam is critical for the load bearing capacity.

2 Design procedure

The first design step consists of conceiving a strut-and-tie model. Although the model in Fig. 3-5 identifies the flow of the internal forces, a more refined model is developed to reflect direct support of concentrated loads in vicinity of the support and better predict the stress distribution in the critical zones. Subsequent steps include design of the principal reinforcement, checking the stresses in critical regions and consequent detailing.

This document is the intellectual property of the fib – International Federation for Structural Concrete. All rights reserved.
This PDF of fib Bulletin 61 is intended for use and/or distribution solely within fib National Member Groups.

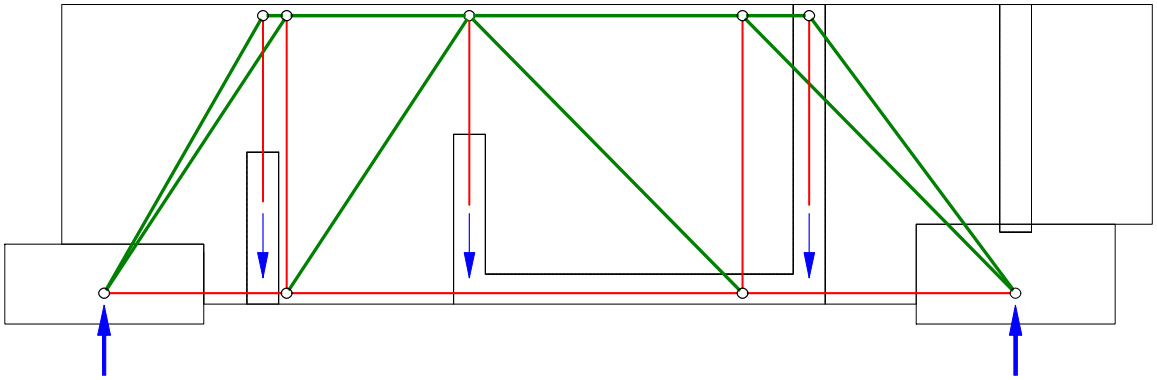


Fig. 3-5: Principal strut-and-tie model - beam ①.

3 Design calculations

3.1 Strut-and-tie model

The distance to the support of the outermost two cross beams (③ and ⑤) is sufficiently small to allow a direct support. The concentrated load resulting from beam ④, however, may only be supported partially by a direct strut to the left support. Notably, as the suspended load from beam ④ coincides with the point of zero shear (Fig. 3-6), only the *shear force* can be considered for the direct support and not the entire suspension force.

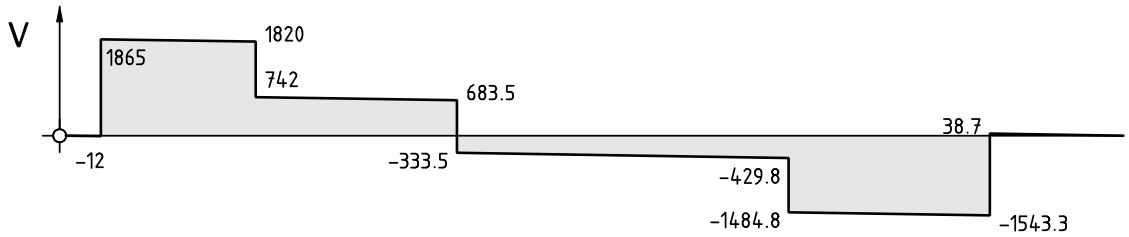
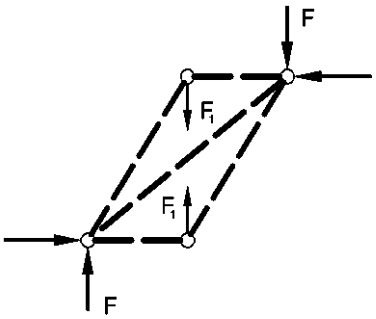


Fig. 3-6: Shear force diagram [kN] - beam ①

A direct transmission is assumed according to the FIP Recommendations (1999), Sect. 6.5.2.3 as shown in Fig. 3-7. The shear reinforcement is designed for the part $F_1$of the load.



$$F_1 = \frac{F}{3}\left(\frac{2\,a}{z} - 1\right)$$

$$= \frac{684}{3}\left(\frac{2 \cdot 3{,}45}{2{,}76} - 1\right) = \frac{684}{2{,}0} = 342 \;\; kN$$

Fig. 3-7: Model for load near a support according to the FIP Recommendations (1999)

This document is the intellectual property of the fib – International Federation for Structural Concrete. All rights reserved.
This PDF of fib Bulletin 61 is intended for use and/or distribution solely within fib National Member Groups.

With the redundant force F_1 determined, the strut-and-tie model can be developed only from equilibrium conditions. Starting with the compression node at the point of contra shear, the geometry of the node may be constructed from the allowable concrete stress (Fig. 3-8), and the assumption of the angle θ of the two inclined struts (fans).

The effective strength $f_{cd,eff}$ of the compression zone according to the FIP Recommendations (1999), Sect. 5.3.2 (2) is:

$$f_{cd,eff} = \nu_1 f_{1cd} = (1 - f_{ck}/250) f_{1cd} = (1 - 35/250) f_{1cd} = 0{,}86 f_{1cd} \quad (= 17{,}0 \text{ MPa})$$

The resulting model is shown in Fig. 3-9 and the associated stress fields in Fig. 3-10.

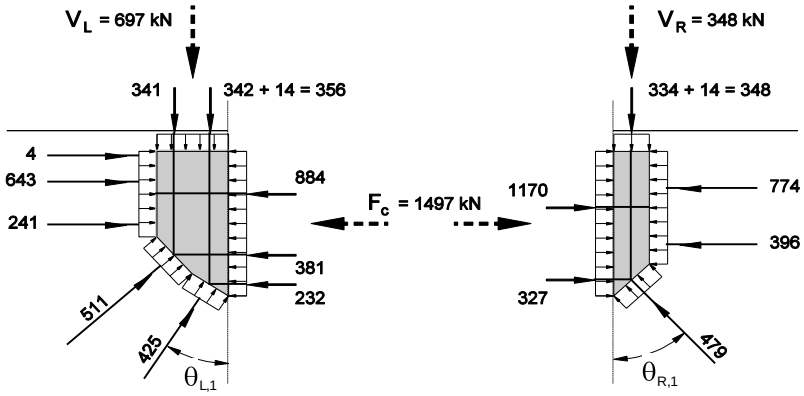


Fig. 3-8: Detail of compression node at contra shear - beam ①

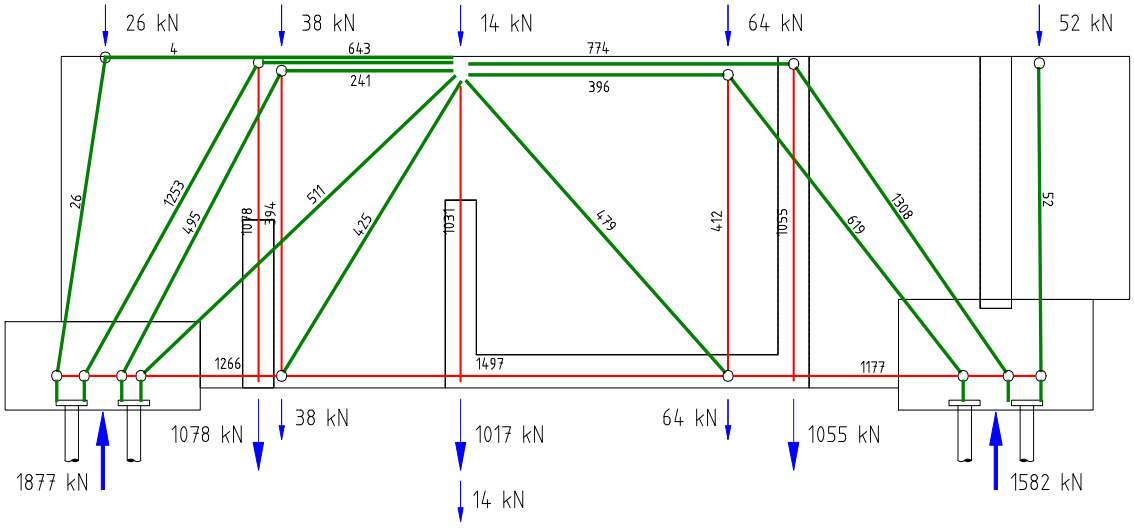


Fig. 3-9: Strut-and-tie model and resultants - beam ①

This document is the intellectual property of the fib – International Federation for Structural Concrete. All rights reserved.
This PDF of fib Bulletin 61 is intended for use and/or distribution solely within fib National Member Groups.

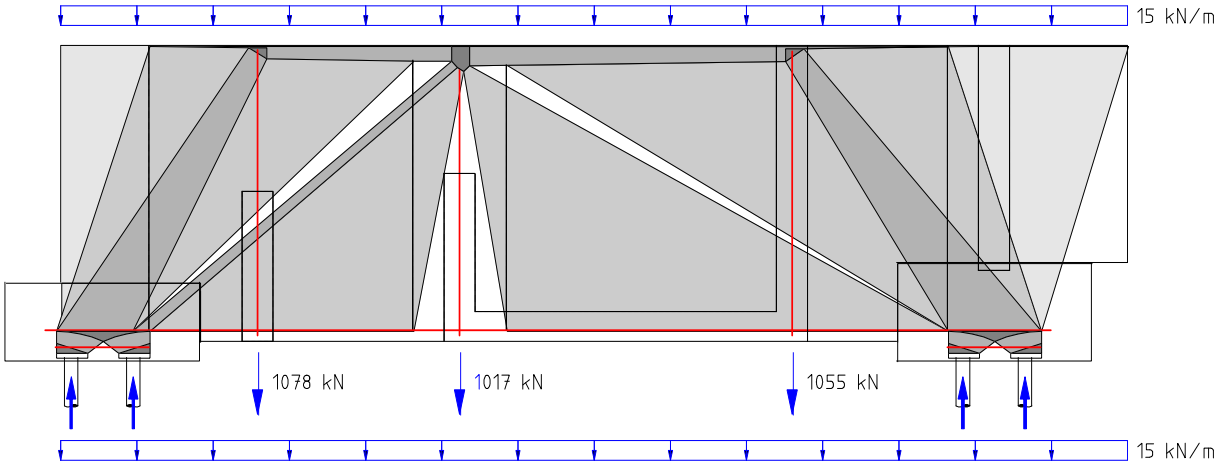


Fig. 3-10: Stress fields - beam ①

3.2 Design of reinforcement

Due to the dominating concentrated loads staggering of the principal reinforcement is not considered. Hence the required amount of tension reinforcement is found from the maximum tie force (Fig. 3-9):

$$\text{req. } A_s = F_s / f_{yd} = 1.497 \cdot 10^3 / 435 = 3.441 \text{ mm}^2 \quad \Rightarrow \quad \text{provided } 8Ø25 \ (3.926 \text{ mm}^2)$$

The suspension reinforcement is designed for the entire support reaction from the supported beams. The reinforcement will be provided as shear links enclosing the main reinforcement in the secondary beams, i.e. placed within the common intersection zone (Fig. 3-11):

$$\text{req. } A_{s,susp} = F_{s,susp} / f_{yd} = 1.078 \cdot 10^3 / 435 = 2.478 \text{ mm}^2$$

$$\Rightarrow \quad \text{provided } 5 \text{ links } Ø20 \ (3.141 \text{ mm}^2)$$

Despite of high shear forces, the need for shear reinforcement is marginal as a consequence of the extensive direct support. The calculated shear reinforcement will be covered by the minimum reinforcement corresponding to a shear ratio of ρ_w = 0,13 % (393 mm²/m) for the concrete grade used:

$$\text{req. } a_{sv,\,left} = F_{sv,\,left} / (f_{yd} \cdot l_{v,l}) = 394 \cdot 10^3 / (435 \cdot 2{,}55) = 355 \text{ mm}^2/\text{m}$$

$$\text{req. } a_{sv,\,right} = F_{sv,\,right} / (f_{yd} \cdot l_{v,r}) = 412 \cdot 10^3 / (435 \cdot 4{,}26) = 222 \text{ mm}^2/\text{m}$$

$$\Rightarrow \quad \text{provided links } Ø8 \text{ @ } 200 \text{ mm } (502 \text{ mm}^2/\text{m})$$

Notably the amount of shear reinforcement is generously chosen to compensate for the fact that, under service loads, some part of the suspension force is likely carried by bond along the stirrups legs rather than transferred to the top of the beam by hoop anchorage.

This document is the intellectual property of the fib – International Federation for Structural Concrete. All rights reserved.
This PDF of fib Bulletin 61 is intended for use and/or distribution solely within fib National Member Groups.

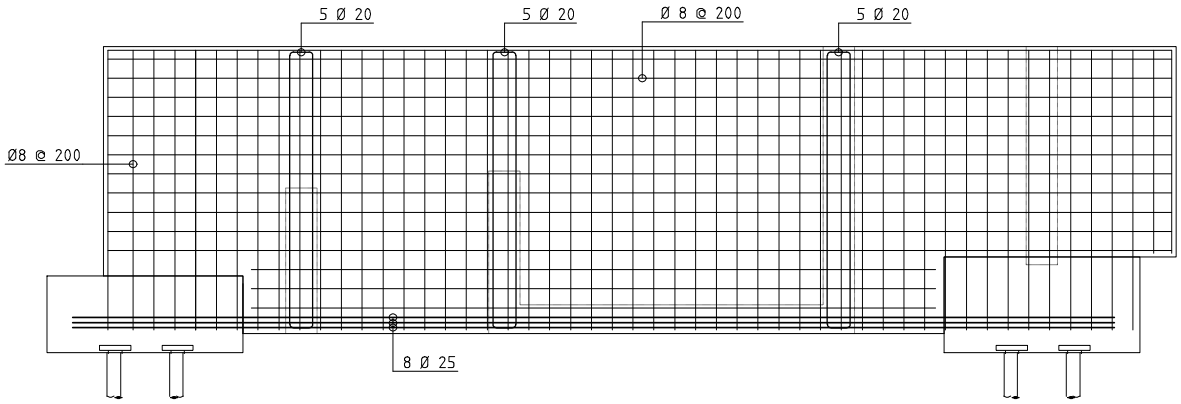


Fig. 3-11: Reinforcement configuration - beam ① (pile head reinforcement not shown).

3.3 Anchorage of reinforcement

3.3.1 Anchorage at supports

The pile cap geometry allows for a straight bar anchorage of the longitudinal tension reinforcement over the supports. Governing is the anchorage at the left support, for which the required basic anchorage length is calculated as follows:

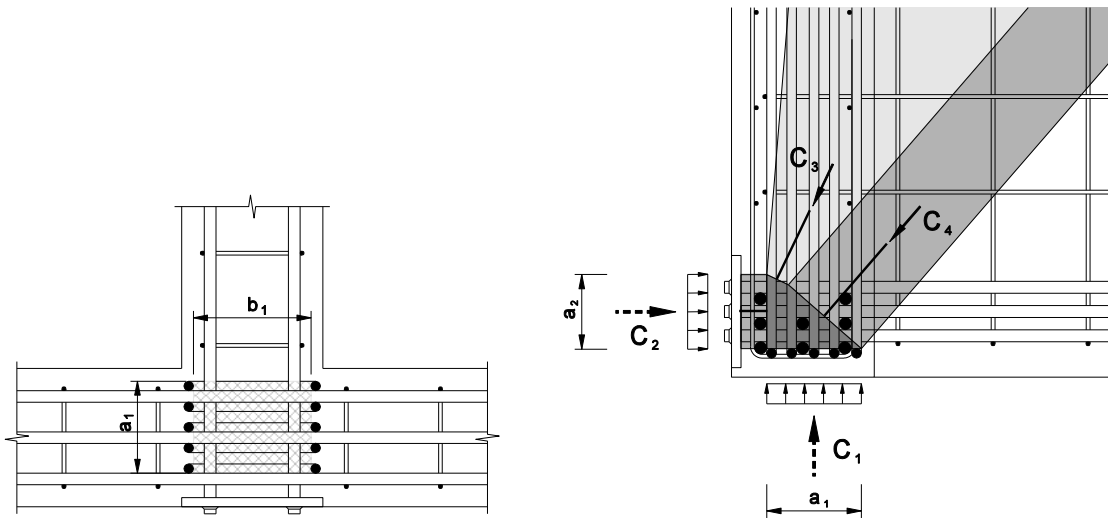
$$\text{req. } l_{b,\,left} = \alpha_a \, l_b \, (A_{s,\,req.} / A_{s,\,prov.}) =$$

$$= 1{,}0 \cdot 33{,}0 \cdot 25 \cdot (1.266 / 1.497) \cdot (3.441 / 3.926) = 611 \text{ mm}$$

As shown in Fig. 3-11, this is less than the available anchorage length l_a = 1.000 mm measured from the face of the pile cap support.

3.3.2 Anchorage at the indirect supports

Due to the limited width (300 mm) of the supporting beam, conventional anchorage of the main reinforcement by means of end hooks is not feasible. Hence an end plate anchorage as shown in Fig. 3-12a is adopted. The suspension reinforcement consists of links enclosing the main reinforcement, Fig. 3-12b. Their arrangement, i.e. distribution a_1 and net leg distance b_1, is determined from the allowable concrete stress σ_c .



a) anchorage of main reinforcement in supported beam *b) arrangement of the suspension bars*

Fig. 3-12: Indirect support of the cross beams

This document is the intellectual property of the fib – International Federation for Structural Concrete. All rights reserved.
This PDF of fib Bulletin 61 is intended for use and/or distribution solely within fib National Member Groups.

The node is regarded as a compression node (C-C-C-node) as the load in both ties are transferred to the strut(s) by bearing pressure. However, no benefit of the biaxial stress condition is taken due to prevailing lateral tension in the supporting beam. Hence the effective strength of the node is utilized to f_{1cd} (i.e. $\nu_2 = 1{,}0$):

$$_{req}\, b_1 = C_1 / (f_{cd,eff} \cdot a_1) = 1.078 \cdot 10^3 / (19{,}8 \cdot 200) = 272 \text{ mm}$$

4 Summary and conclusions

Design of a deep beam subjected to concentrated loads from intersecting members is presented. The beam design is based on the strut-and-tie model procedure in line with the FIP Recommendations (1999). The example deals with issues related to concentrated loads near support and detailing aspects of indirect supports. The example also covers the design and anchorage of the reinforcement, as well as capacity checks of nodal zones.

References

FIP Recommendations (1999): Practical Design of Structural Concrete. FIP-Commission 3 "Practical Design", Sept. 1996. Publ.: SETO, London, Sept. 1999. (Distributed by: *fib*, Lausanne. Web http://www.fib-international.org)

fib Bulletin 16 (2002): Design Examples for the FIP Recommendations "Practical design of structural concrete". *fib*, Lausanne. January 2002

This document is the intellectual property of the fib – International Federation for Structural Concrete. All rights reserved.
This PDF of fib Bulletin 61 is intended for use and/or distribution solely within fib National Member Groups.

Example 4: Continuous deep beam

Miguel S. Lourenço, João F. Almeida, Rui Boia

1 Description of the design task

1.1 Geometry and loads

The deep beam showed in Fig. 4-1 transfers distributed loads from the floors below and above to three supporting columns. The beam dead load was simulated by a uniform load equally distributed at the bottom and tonp of the deep beam.

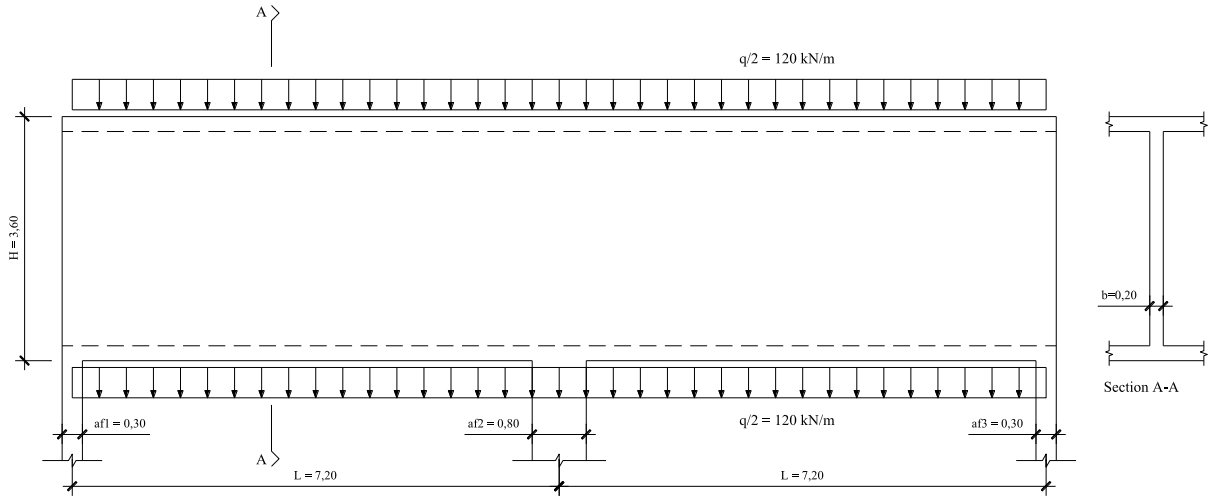


Fig. 4-1: Continuous deep beam geometry and loads

1.2 Design values for materials

The materials used for this design are:

Concrete: C30/37: f_{ck} = 30 MPa; f_{1cd} = 0,85 · 30 /1,5 = 17,0 MPa

Reinforcement A500NR: f_{yk} = 500 MPa; f_{yd} = 500 /1,15 = 435 MPa

1.3 Statement of design problem

The design strut-and-tie model for continuous deep beam presented in sect. 6.5.5 of the FIP Recommendations (1999) is defined assuming a certain distribution for the support reactions. However, the supports stiffness can influence the distribution of external reactions leading to different internal forces. In practice the support reactions are obtained from the global model of the structure in which the deep beam could be modelled by e.g. linear members considering the shear stiffness or by a finite element mesh.

In this case, the deep beam is incorporated in an office building, so the support reactions were directly obtained from the global model where the deep beam was modelled by a coarse finite element mesh and the columns by linear members.

This document is the intellectual property of the fib – International Federation for Structural Concrete. All rights reserved.
This PDF of fib Bulletin 61 is intended for use and/or distribution solely within fib National Member Groups.

The support reactions obtained are represented in Fig. 4-2 as well as the corresponding bending moment diagram obtained by the bending theory.

Applying the load path method for the development of the strut-and-tie model, it is easy to realize that the main support and span ties of the deep beam are associated with the external reactions. In the following a general procedure is presented for the continuous deep beam design according to the external reactions.

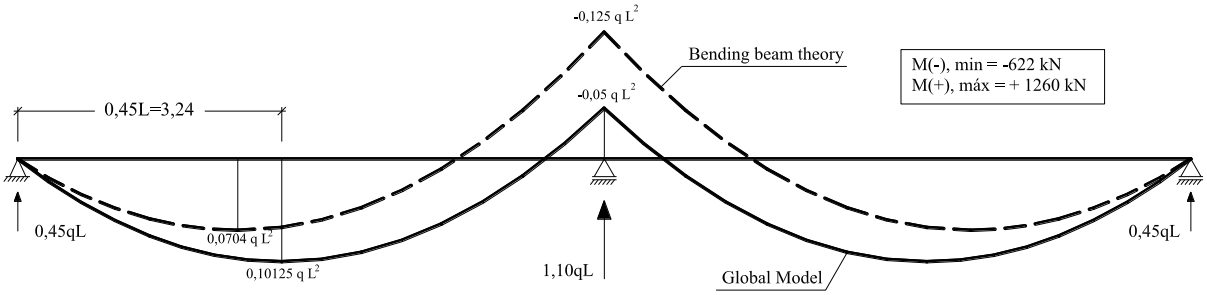


Fig. 4-2: Support reactions and bending moments

2 Design procedure

Fig. 4-3 shows a general model for the deep beam. The resultant angles θ_1 and θ_2 can be obtained by geometrical conditions given by the following equations:

$$\cot(\theta_1) = \frac{b_1 \cdot L}{2 \cdot z_1} \text{ and } \cot(\theta_2) = \frac{\left(\frac{b_2}{2} + b_3\right) \cdot L - a_{f2} + a'_{f2}}{z_1}$$

On the other hand, the internal equilibrium leads to the condition that the compression C_1 must be equal in the nodes A and B, resulting in the following equations:

$$C_1^A = C_1^B \Leftrightarrow b_1 \cdot L \cdot q \cdot \cot(\theta_1) = b_2 \cdot L \cdot q \cdot \cot(\theta_2) \Leftrightarrow b_1 \cdot \cot(\theta_1) = b_2 \cdot \cot(\theta_2)$$

with,

$$b_1+b_2+b_3 = 1 \quad \text{and} \quad a'_{F2} = \frac{b_2}{b_2 + b_3} \frac{a_{f2}}{4}$$

Knowing b_1, the variable b_2 is obtained by solving the nonlinear equation, $b_1 \cdot \cot(\theta_1) = b_2 \cdot \cot(\theta_2)$. For practical purposes, only one node may be assumed in the middle support, leading to the simplified equation:

$$b_1^2 + 2 \cdot b_1 b_2 + b_2^2 - 2 \cdot b_2 = 0$$

A more simple model is achieved by setting the inner level arm z_1 equal to z_2 to a value of approximately $0{,}7 \cdot L$, i.e. aligning the compression C_1 with the tie T_2. In this case, it should be better to consider only one resultant force ($b_2 \cdot L \cdot q + b_3 \cdot L \cdot q$) in the distributed loads.

This document is the intellectual property of the fib – International Federation for Structural Concrete. All rights reserved.
This PDF of fib Bulletin 61 is intended for use and/or distribution solely within fib National Member Groups.

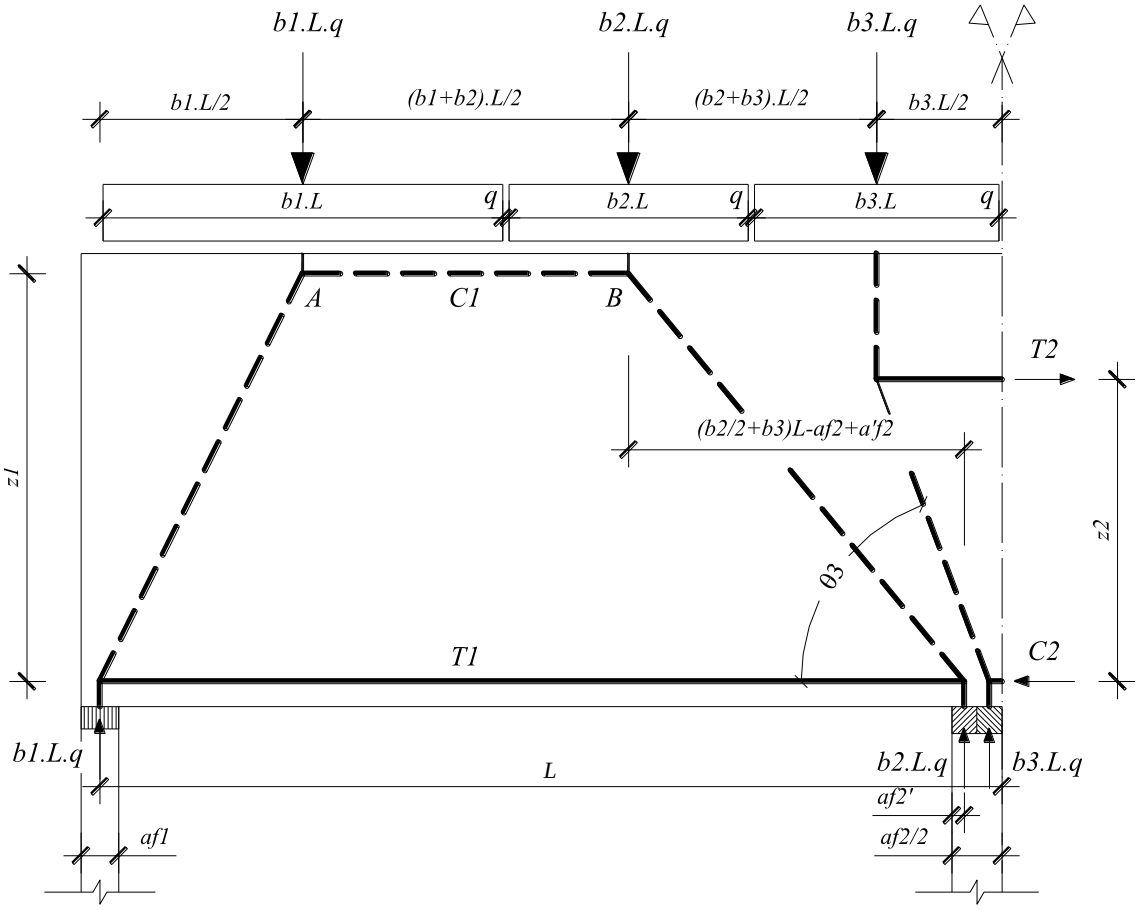


Fig. 4-3: Generic strut-and-tie model according to the load path method

In this particular case b_1=0,45; z_1=0,45L; z_2=0,33L; a_{f2}=0,80m and L=7,20m, resulting in b_2=0,272 and the strut-and-tie model shown in Fig. 4-4.

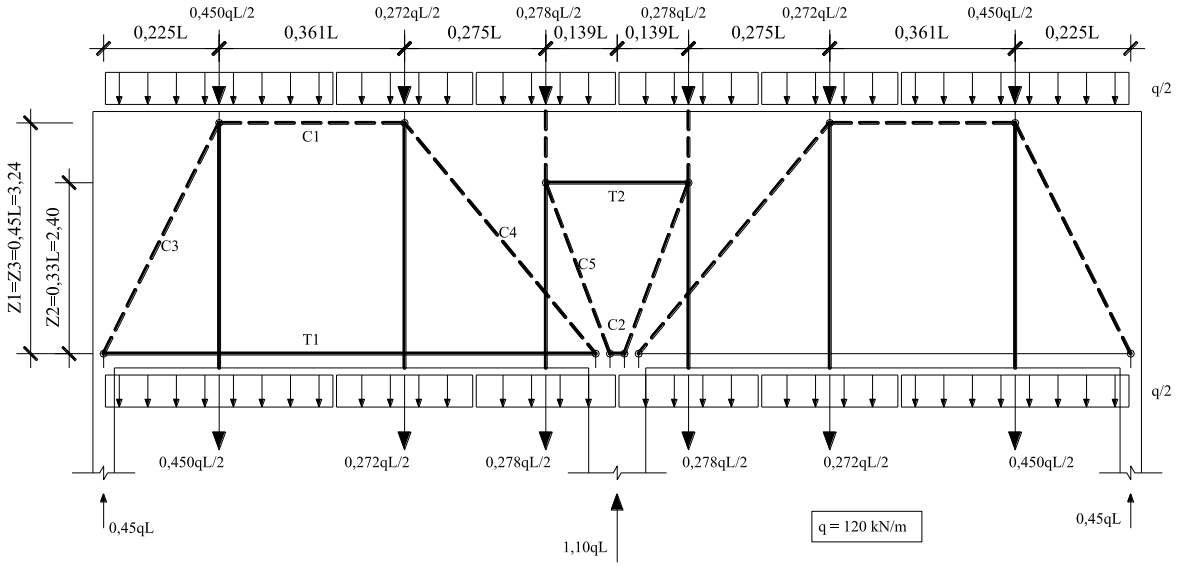


Fig. 4-4: Strut-and-tie model

This document is the intellectual property of the fib – International Federation for Structural Concrete. All rights reserved.
This PDF of fib Bulletin 61 is intended for use and/or distribution solely within fib National Member Groups.

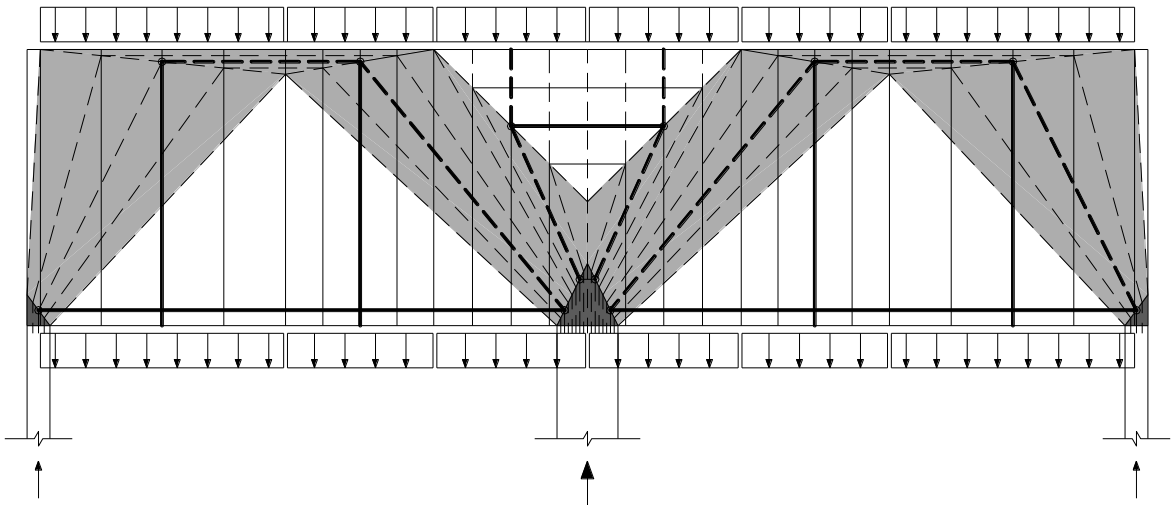


Fig. 4-5: Stress field model

3 Design calculations

3.1 Reinforcement

The required minimum reinforcement is given by $0{,}002 \cdot A_c = 400$ mm^2/m. Reinforcement meshes ϕ8//150 mm were provided on both surfaces ($A_{s,prov}$= 667 mm^2/m).

The ties T_1 and T_2, may be obtained by node equilibrium:

$T_1 = C_1 = 1260 / 3{,}24 = 389$ kN $\rightarrow A_{s,req} = 890$ mm^2 $\rightarrow$ 8 ϕ12 mm ($A_{s,prov}$=904 mm^2)

$T_2 = C_2 = 622 / 2{,}40 = 259$ kN $\rightarrow A_{s,req} = 600$ mm^2

The required reinforcement area for tie T_2 is less than the provided minimum reinforcement area of ϕ8 //150 mm, even if distributed over 1,0 m. However, the minimum reinforcement area for a tension element was adopted, in order to efficiently control cracking due to time dependent behaviour of concrete, temperature variations, imposed deformations induced by the top and bottom slabs or other not considered effects.

$A_{s,min} = h \cdot b \cdot f_{ctm}/f_{sy} = 200 \cdot 1.000 \cdot 2{,}9/435 = 1.330$ mm^2/m $\rightarrow 4 \times$ ϕ8 //150 mm

The required suspended reinforcement from the above floor:

$A_{s,req} = 240 / 0{,}435 = 276$ mm^2/m < 667 mm^2/m (2 × ϕ8 //150 mm)

3.2 Concrete stresses and node regions

3.2.1 Check of concrete stresses on strut C_1

The inner level arm z_1 was set in order to limit concrete stresses of strut C_1. According to sect. 5.3.2 of FIP Recommendations (1999) the concrete strength is:

$f_{cd,eff} = (1\text{-}f_{ck}/250)\, f_{1cd} = 15$ MPa

$$C_1 = 1.260\ kN \rightarrow \sigma_{C1} = \frac{1.260}{2 \cdot (3{,}6 - 3{,}24 - 0{,}4/2) \cdot 0{,}2} = 9.844\ \text{kN/m}^2 = 9{,}8\ \text{MPa} < f_{cd,eff}$$

This document is the intellectual property of the fib – International Federation for Structural Concrete. All rights reserved.
This PDF of fib Bulletin 61 is intended for use and/or distribution solely within fib National Member Groups.

3.2.2 End support node

In Fig. 4-6 is shown the end support node of the deep beam. It is a CCT node and according to sect. 5.6 of FIP Recommendations (1999) the concrete stresses must be limited to $f_{cd,eff}$= 0,85 f_{1cd} = 13,6 MPa.

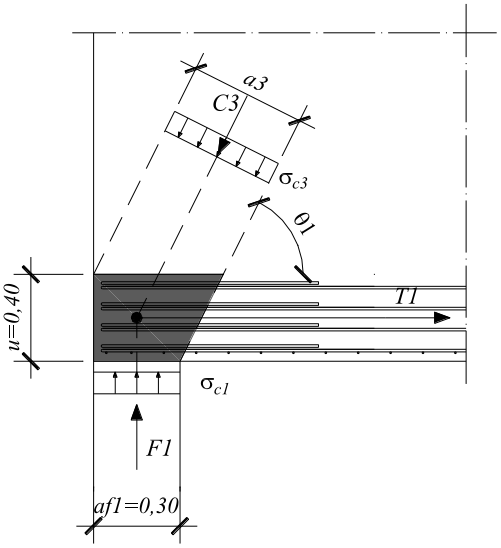


Fig. 4-6: End-support-node region of the deep beam

a) bearing pressure

$F_1 = 0{,}45 \cdot q \cdot L = 778\ kN \rightarrow \sigma_{c1} = 778/(0{,}3 \times 0{,}2) = 12.967\ \text{kN/m}^2 = 13{,}0\ \text{MPa} < f_{cd,eff}$

b) diagonal strut

$tan(\theta_1) = (0{,}45/0{,}33) \quad \Leftrightarrow \theta_1 = 63{,}43^o$

$C_3 = F_1 / sin(\theta_1) = 870\ \text{kN}$

$a_3 = a_{F1} \cdot sin(\theta_1) + u \cdot cos(\theta_1) = 0{,}30 \times sin\ (63{,}43^o) + 0{,}40 \times cos\ (63{,}43^o) = 0{,}45\ \text{m}$

σ_{c3}= 0,870/(0,45×0,2) = 9,7 MPa < $f_{cd,eff}$

c) reinforcement anchorage length

Assuming a reinforcement cover of 50 mm and some eventual lack of precision in placing the bottom reinforcement, the anchorage length considered for the straight bars is $l_{b,eff}$ = 220 mm. According to sect. 5.6.4 of FIP Recommendations (1999) the required anchorage length is:

$$l_b = \frac{2}{3}\frac{\phi \cdot f_{yd}}{4 \cdot f_{bd}} = \frac{2}{3}\frac{12 \cdot 435}{4 \cdot 3} = 290\,\text{mm}$$

The maximum bond force provided by the ϕ12 straight bars is:

$F_{bd,\phi 12} = n \cdot \pi \cdot \phi \cdot l_{b,eff} \cdot f_{bd} \cdot 1{,}5 = 8\pi \cdot 0{,}012 \cdot 0{,}22 \cdot 3000 \cdot 1{,}5 = 299\ \text{kN}$

Providing additional loop bars ϕ8, results the following bond force:

$F_{bd,\phi 8} = n \cdot \pi \cdot \phi \cdot l_{b,eff} \cdot f_{bd} \cdot 1{,}5/0{,}7 = 8 \cdot \pi \cdot 0{,}008 \cdot 0{,}22 \cdot 3000 \cdot 1{,}5/0{,}7 = 284\ \text{kN}$

$F_{bd,\phi 12} + F_{bd,\phi 8} = 583\ \text{kN} > T_1 = 389\ \text{kN}$

This document is the intellectual property of the fib – International Federation for Structural Concrete. All rights reserved.
This PDF of fib Bulletin 61 is intended for use and/or distribution solely within fib National Member Groups.

d) lap length of the loops

According to sect. 5.7.2 of FIP Recommendations (1999), the required lap length to transmit the forces from the loops to the main reinforcement (tie T1) is shown in Fig. 4-7, and obtained by:

$$l_0 = \alpha_s \cdot l_b = \alpha_s \cdot \varnothing \cdot f_{yd} / (4 \cdot f_{bd}) = 2 \cdot 8 \cdot 435 / (4 \cdot 3{,}0) = 580 \text{ mm}$$

Loops were provided with 2.0 m length, which results in $l_{0,prov}$= 900 mm.

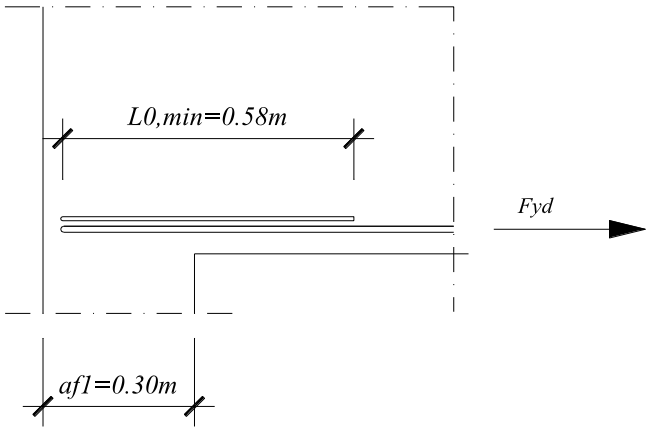


Fig. 4-7: Minimum lap length of the loops in the end-support-node region

3.2.3 Inner support node

In Fig. 4-8 is shown the inner-support node of the deep beam where, for simplification, the two diagonal struts from each span, are considered as one with the weighed average strut angle. This node is the combination of two CCT nodes so the concrete strength is given by $f_{cd,eff}$ = 0,85 f_{1cd} = 14,5 MPa.

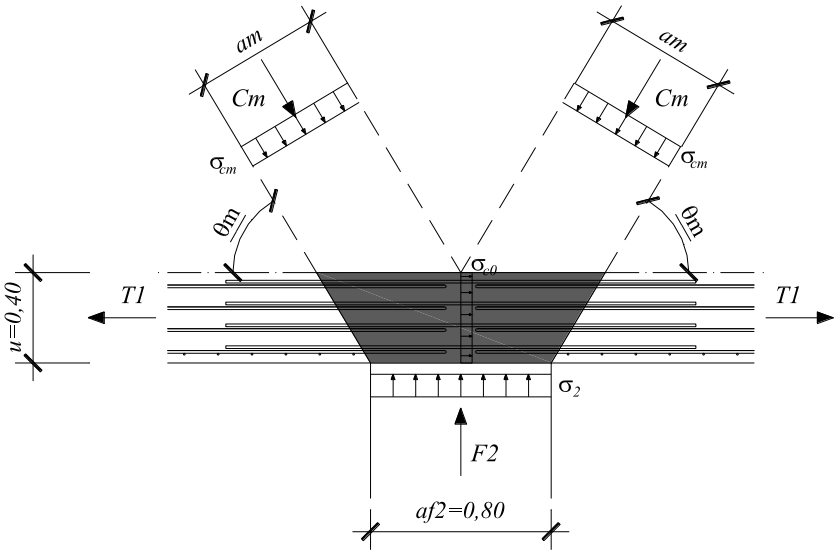


Fig. 4-8: Deep beam's inner-support-node region

This document is the intellectual property of the fib – International Federation for Structural Concrete. All rights reserved.
This PDF of fib Bulletin 61 is intended for use and/or distribution solely within fib National Member Groups.

a) bearing pressure

$F_2 = 1{,}10 \cdot q \cdot L = 1.900$ kN $\rightarrow \sigma_2 = 1.900/(0{,}8 \times 0{,}2) = 11{,}9$ MPa $< f_{cd,eff}$

b) diagonal struts

The weighted average strut angle is: $\theta_m = 59{,}1^o$.

$C_m = F_2 / (2 \cdot sin\ \theta_m) = 1.900 / (2 \cdot sin\ 59{,}1^o) = 1.107\ kN$

$a_m = a_2/2 \cdot sin\ \theta_m + u \cdot cos\ \theta_m = 0{,}80/2 \cdot sin(59{,}1^o) + 0{,}40 \times cos(59{,}1^o) = 0{,}55$ m

$\sigma_{cm} = 1{,}107/(0{,}55 \cdot 0{,}20) = 10{,}0$ MPa $< f_{cd,eff}$

c) horizontal node pressure $\sigma_{C,0}$

$C_2 = T_2 = 259\ kN$

$\sigma_{C,0} = C_2 / (u \cdot b) = 0{,}259/ (0{,}4 \cdot 0{,}2) = 3{,}2$ MPa $< f_{cd,eff}$

d) anchorage of reinforcement

According to sect. 5.6.4 of FIP Recommendations (1999) the anchorage length needed is:

$$l_b = \frac{2}{3}\frac{\phi \cdot f_{yd}}{4 \cdot f_{bd}} = \frac{2}{3}\frac{12 \cdot 435}{4 \cdot 3} = 290\,\text{mm} \quad < l_{b,prov} = 800/2 - 50 - 30 = 320 \text{ mm}$$

Although sufficient anchorage length is provided, additional steel bars were placed on the inner support to prevent local cracking in the node region, due to other effects besides the loads applied, that could influence the node strength considered in calculation.

4 Detailing

The reinforcement layout of the deep beam is shown in Fig. 4-9.

References

FIP Recommendations (1999): Practical Design of Structural Concrete.
FIP-Commission 3 "Practical Design", Sept. 1996. Publ.: SETO, London, Sept. 1999
(Distributed by: *fib*, Lausanne. Web http://www.fib-international.org)

This document is the intellectual property of the fib – International Federation for Structural Concrete. All rights reserved.
This PDF of fib Bulletin 61 is intended for use and/or distribution solely within fib National Member Groups.

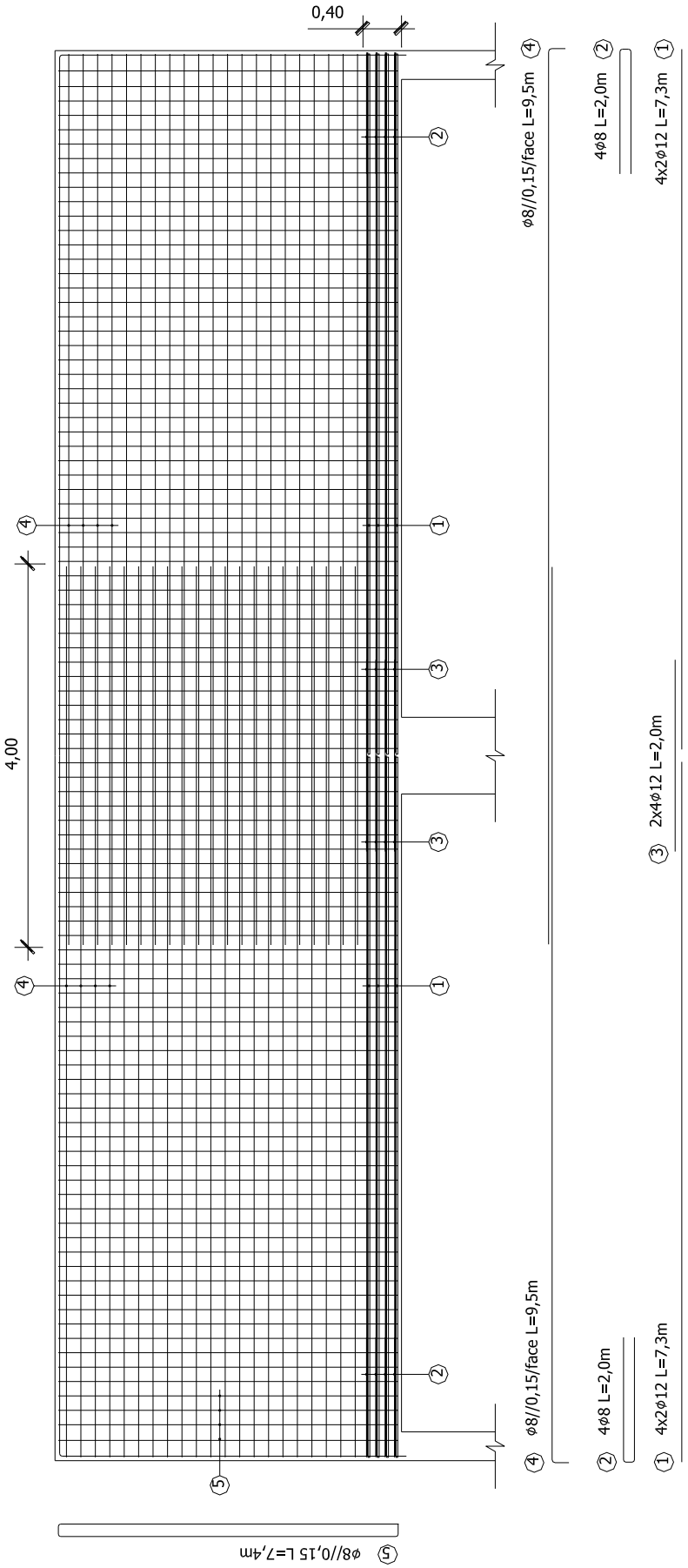


Fig. 4-9: Reinforcement layout of the deep beam

This document is the intellectual property of the fib – International Federation for Structural Concrete. All rights reserved.
This PDF of fib Bulletin 61 is intended for use and/or distribution solely within fib National Member Groups.

Example 5: Shear wall in office building

Ľudovít Fillo, Vladimír Benko

1 Structure

1.1 Description of the structure

A twenty-storey, 76 m tall, office building is presented in Fig. 5-1 in axonometric view with plan dimensions of 17 m (30 m) × 54 m. Its foundation is 10,3 m under the ground. The diaphragm walls and piles of 1200 mm diameter are designed with respect to geology and expected differential settlement. The composite concrete columns of 500 mm diameter resist vertical loads and reinforced concrete walls 350 mm and inner core should principally resist horizontal loads (wind, seismic and so on). The depth of reinforced concrete slabs varies from 220 to 260 mm.

In the following the shear wall shown in Fig. 5-1 is designed with strut-and-tie models.

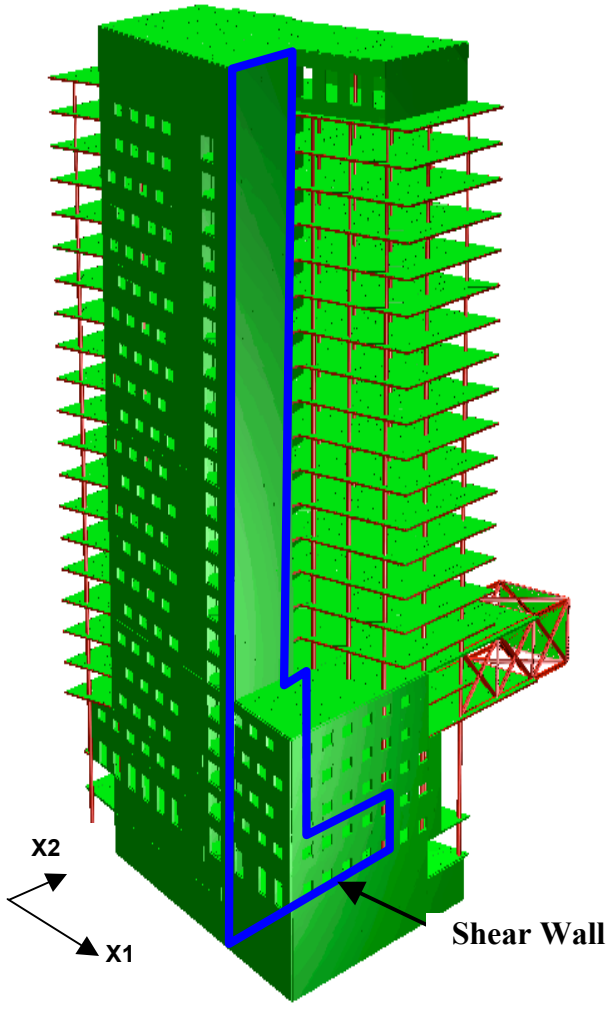


Fig. 5- 1: Axonometric view of the office building

This document is the intellectual property of the fib – International Federation for Structural Concrete. All rights reserved.
This PDF of fib Bulletin 61 is intended for use and/or distribution solely within fib National Member Groups.

1.2 Design problem

1.2.1 Geometry and loads

The STRAP software was used to analyze statically and dynamically this high-rise building. Total dead load of the structure is G_1 = 232 MN, another permanent load G_2 = 39,6 MN and variable load Q = 93,4 MN.

Vienna belongs to a region of seismic zone No 3, with effective horizontal acceleration of 0,80 m/s^2. The subsoil is Group II – dense sediments. The seismic analysis was based on multi-modal response spectrum.

Parameters:

$\alpha = 0{,}082$ ratio of the design ground acceleration to the acceleration of gravity

$\beta_0 = 2{,}5$ factor

$S = 1{,}0$ soil factor

$q = q_0\, k_D\, k_R\, k_w = 5 \cdot 0{,}5 \cdot 0{,}8 \cdot 1 = 2{,}0 \geq 1{,}5$ behavior factor

CQC (Complete Quadratic Combination) was used for the combination of mode shapes. The first 15 natural modes were determined by multi-modal analysis (Fig. 5-2).

Global masses included in dynamic analysis represented 299,6 MN.

$$P_{tot} = G_1 + G_2 + 0{,}3Q = 299{,}6\ MN$$

From the seismic combination comes the horizontal seismic load on the building 10,6 MN in the direction x_2 (Fig. 5-1). The shear wall was then subjected to horizontal load 2,122 MN and to vertical load of 18,0 MN plus 17,431 MN load from columns (Fig. 5-3). A part of vertical uniform load comes from slab on the floor levels.

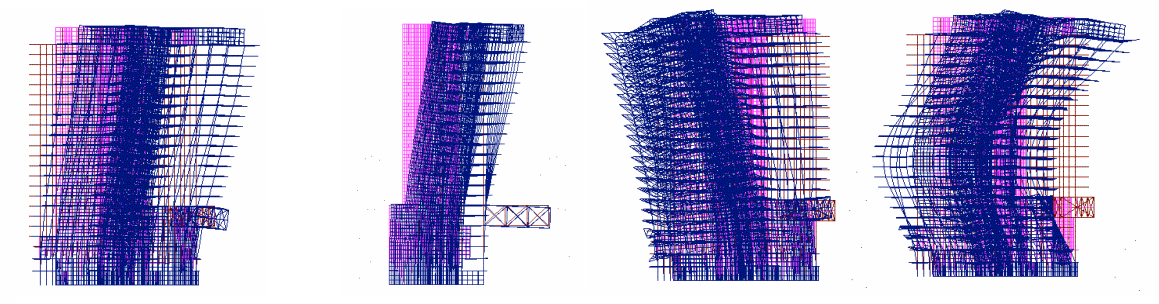


Fig. 5-2: Mode shapes 1-4 (f_1=0,43 Hz) (f_2=0,59 Hz) (f_3=1,22 Hz) (f_4=1,64)

1.2.2 Design values of materials

The material design parameters were selected in accordance with FIP Recommendations (1999) for seismic combination of loads.

- Concrete grade C40/50: f_{ck}=40 MPa f_{ctm}=3,5 MPa

$f_{1cd} = \alpha\, f_{ck} / \gamma_c = 0{,}85 \cdot 40 / 1{,}2 = 28{,}3$ MPa

- Reinforcement grade B500C:

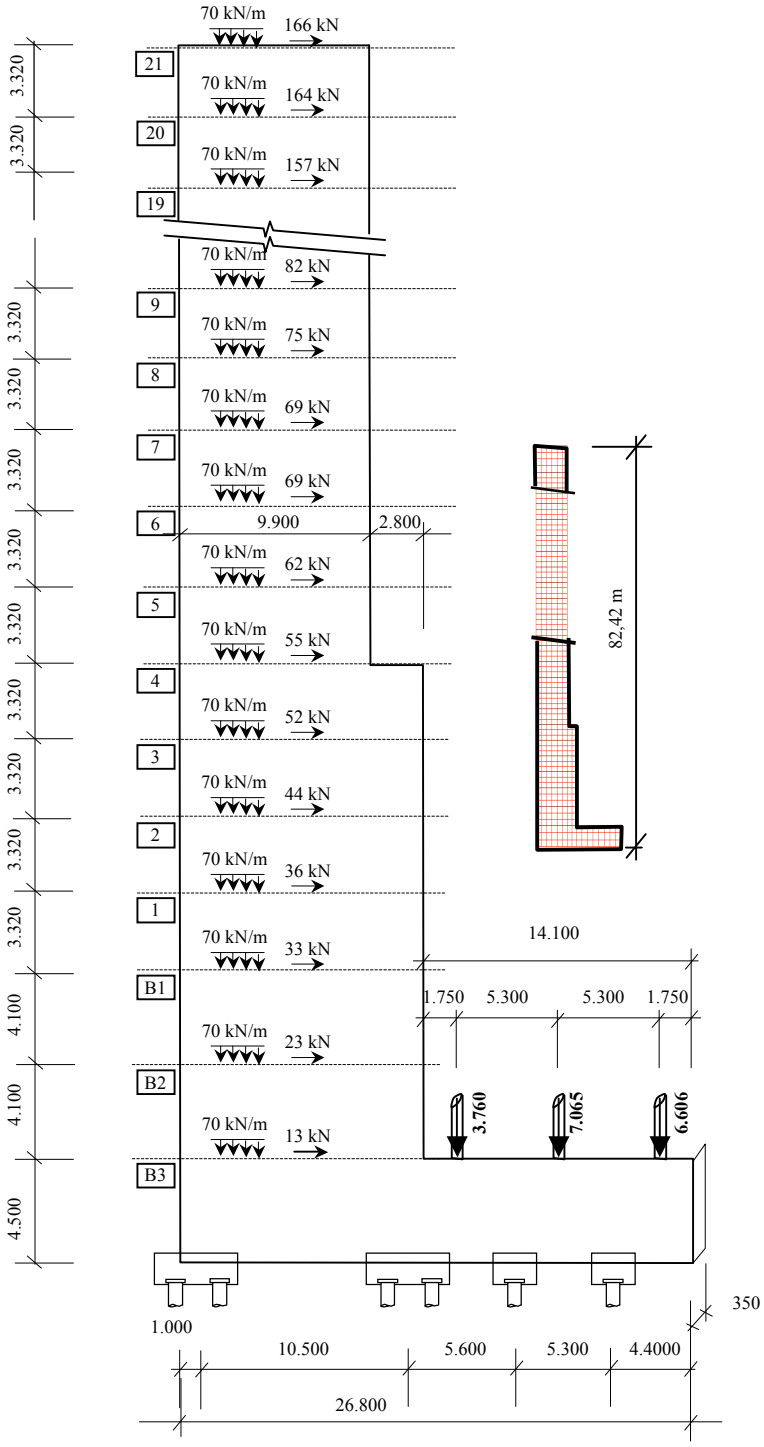
f_{yk} = 550 MPa; $f_{yd} = f_{yk} / \gamma_s = 550 / 1{,}0 = 550$ MPa

This document is the intellectual property of the fib – International Federation for Structural Concrete. All rights reserved.
This PDF of fib Bulletin 61 is intended for use and/or distribution solely within fib National Member Groups.

In a case of the compression chord of a beam with linear strain distribution, the rectangular stress block is used over full depth of the compression zone acc. to the FIP Recommendations (1999), sect. 5.3.2 (2):

$$f_{cd,eff} = \nu_1 \, f_{1cd} = 0{,}84 \cdot 28{,}3 = 23{,}8 \text{ MPa}$$

where: $\nu_1 = \left(1 - \frac{f_{ck}}{250}\right) = \left(1 - \frac{40}{250}\right) = 0{,}84$



floor	horizontal force
19	157 kN
18	137 kN
17	131 kN
16	125 kN
15	120 kN
14	114 kN
13	107 kN
12	101 kN
11	94 kN
10	88 kN
9	82 kN

Fig.5-3: Geometry and loads – shear wall – quasipermanent loads, seismic loads (dimensions in mm)

This document is the intellectual property of the fib – International Federation for Structural Concrete. All rights reserved.
This PDF of fib Bulletin 61 is intended for use and/or distribution solely within fib National Member Groups.

The capacity of struts with cracks parallel to the strut and bonded transverse reinforcement is:

$$f_{cd,eff} = \nu_2 \, f_{1cd} = 0{,}8 \cdot 28{,}3 = 22{,}7 \text{ MPa} = f_{cwd}$$

The strength of struts transferred across cracks with normal crack widths is:

$$f_{cd,eff} = \nu_2 \, f_{1cd} = 0{,}6 \cdot 28{,}3 = 17 \text{ MPa}$$

The compression stress capacity in nodes: $f_{cd,eff} = \nu_2 \, f_{1cd} = 0{,}85 \cdot 28{,}3 = 24$ MPa

For biaxial compression nodes the strength is according to Eq.(5.19a) of the FIP Recommendations (1999):

$$f_{2cd} = 1{,}2 \, f_{1cd} = 1{,}2 \cdot 28{,}3 = 34 \text{ MPa}$$

1.2.3 Description of the design problem

According to the definition of D-regions, parts under levels 4 and B3 of the shear wall (Fig. 5-3) comprise statically and geometrically regions of discontinuity due to the changing geometry and the singularities introduced by the concentrated loads from the columns under level B3, respectively.

1.3 Design procedures

First step was to perform shear and flexural design at the level 4 and B3 respectively, see Fig. 5-3. Subsequent steps include formulation of strut-and-tie models, designing of the principal reinforcement, verifying the stresses in critical regions and nodes with detailing.

2 Design calculations

2.1 Minimal vertical and horizontal reinforcement of the wall

The area of minimum vertical reinforcement: $A_{s,vert} = 0{,}004 \, A_c$ for both wall faces.

$A_{s,ver} = 0{,}002 \cdot 9{,}9 \cdot 0{,}35 = 0{,}00693 \text{ m}^2 \quad \rightarrow 752 \text{ mm}^2\text{/m}$, ∅12 á 150 mm at the each wall face.

The area of minimum horizontal reinforcement:

$A_{s,hor} = 0{,}3 \cdot A_{s,ver} = 0{,}3 \cdot 700 = 210 \text{ mm}^2 \quad \rightarrow 251 \text{ mm}^2\text{/m}$ ∅8 á 200 mm at the each face.

2.2 Flexural and shear design

2.2.1 Model A

In model A the horizontal forces act from left hand side at the **level 6** (Fig. 5-3).

The bending moment $M_{Edh} = 52{,}443$ MN.m and the axial force $N_{Ed} = 11{,}088$ MN are acting at the centre of gravity of the wall cross-section at **level 6**. After defining the average location of the reinforcement resultant - tie $a_t = 0{,}25$ m, the neutral axis depth x is obtained from equation of moments M_{Edh} (from horizontal forces) and moment from vertical forces to node 6t (Fig. 5-4):

$z_s = 0{,}5h_w - a_t = 0{,}5 \cdot 9{,}9 - 0{,}25 = 4{,}7 \text{ m}$ and $d = h_w - a_t = 9{,}9 - 0{,}25 = 9{,}65 \text{ m}$.

This document is the intellectual property of the fib – International Federation for Structural Concrete. All rights reserved.
This PDF of fib Bulletin 61 is intended for use and/or distribution solely within fib National Member Groups.

$$x = d - \sqrt{d^2 - \frac{M_{Ed} + N_{Ed}\, z_s}{0{,}5\, b_w\, f_{cd,eff}}} = 9{,}65 - \sqrt{9{,}65^2 - \frac{52{,}443 + 11{,}088 \cdot 4{,}7}{0{,}5 \cdot 0{,}35 \cdot 23{,}8}} = 1{,}403 \text{ m}$$

This gives the inner lever arm: $z = d - 0{,}5x = 9{,}65 - 0{,}5 \cdot 1{,}403 = 8{,}949$ m

The compression chord force is: $F_c = x b_w f_{cd,eff} = 1{,}403 \cdot 0{,}35 \cdot 23{,}8 = 11{,}687$ MN

At level 4 the bending moment M_{Edh} = 64,594 MNm and the axial force N_{Ed} = 11,088 MN are acting at the centre of gravity of the wall cross-section. With the strut position placed 0,70 m from the right face of the wall, the tension chord force is obtained from equation of above-mentioned moments to node 4c (Fig. 5-4):

$$F_t = \frac{M_{Ed} - N_{Ed}(0{,}5h_w - a_s)}{z} = \frac{64{,}594 - 11{,}088(4{,}95 - 0{,}7)}{8{,}949} = 1{,}954 \text{ MN}$$

At level B1 (Fig. 5-3) the bending moment M_{Edh} = 90,968 MN.m and the axial forces N_{Ed} = 12,474 MN and ΔN_{Ed} = 3,556 (the axial force between levels 4 and B1) are acting at the centre of gravity of the wall cross-section. After defining the average location of the reinforcement resultant - tie a_t = 0,25 m, neutral axis depth x is calculated from equation of z moments M_{Edh} (from horizontal forces) and moment from vertical forces to the node B1t (Fig. 5-4):

$$z_t = 0{,}5h_w - a_t = 0{,}5 \cdot 12{,}7 - 0{,}25 = 6{,}1 \text{ m} \quad \text{and} \quad d = h_w - a_t = 12{,}7 - 0{,}25 = 12{,}45 \text{ m}$$

$$x = d - \sqrt{d^2 - \frac{M_{Edh} + \sum N_{Ed}\, z_t}{0{,}5\, b_w\, f_{cd,eff}}} = 12{,}45 - \sqrt{12{,}45^2 - \frac{90{,}968 + 12{,}474 \cdot 4{,}7 + 3{,}556 \cdot 6{,}1}{0{,}5 \cdot 0{,}35 \cdot 23{,}8}} = 1{,}779 \text{ m}$$

$$z = d - 0{,}5x = 12{,}45 - 0{,}5 \cdot 1{,}779 = 11{,}561 \text{ m}$$

$$F_c = x b_w f_{cd,eff} = 1{,}779 \cdot 0{,}35 \cdot 23{,}8 = 14{,}819\ MN$$

At level B3 the bending moment M_{Edh} = 108,127 MN.m and the axial force N_{Ed} = 12,474 MN and ΔN_{Ed} = 3,556 (the axial force between levels 4 and B1) are acting at the centre of gravity of the wall cross-section. The tension chord force is obtained from equation of above-mentioned moments to node B3c (Fig. 5-4):

$$F_t = \frac{M_{Edh} - \sum N_{Ed} z_s}{z} = \frac{108{,}127 - 12{,}474 \cdot 6{,}86 - 3{,}556 \cdot 5{,}46}{11{,}561} = 0{,}271 \text{ MN}$$

2.2.2 Model B

In model B the horizontal forces act from the right hand side at level B1 (Fig. 5-5).

The shear and flexural design until level 4 is the same as in the previous model A. The different strut and tie model appears under level 4. At level B1 the bending moment M_{Edh} = 90,968 MN.m and the axial forces N_{Ed} = 12,474 MN and ΔN_{Ed} = 3,556 (the axial force between levels 4 and B1) are acting at the centre of gravity of the wall cross-section. After defining the average location of the reinforcement resultant as a_t = 0,25 m, the neutral axis depth x is calculated from equation of moments M_{Edh} (from horizontal forces) and moment from vertical forces to the node B1t (Fig. 5-5):

This document is the intellectual property of the fib – International Federation for Structural Concrete. All rights reserved.
This PDF of fib Bulletin 61 is intended for use and/or distribution solely within fib National Member Groups.

$$z_t = 0{,}5h_w - a_t = 0{,}5 \cdot 12{,}7 - 0{,}25 = 6{,}1\,\text{m} \quad \text{and} \quad d = h_w - a_t = 12{,}7 - 0{,}25 = 12{,}45\,\text{m}$$

$$x = d - \sqrt{d^2 - \frac{M_{Edh} + \sum N_{Ed}\, z_{st}}{0{,}5\, b_w\, f_{cd,eff}}} = 12{,}45 - \sqrt{12{,}45^2 - \frac{90{,}968 + 12{,}474 \cdot 7{,}5 + 3{,}556 \cdot 6{,}1}{0{,}5 \cdot 0{,}35 \cdot 23{,}8}} = 2{,}179$$

$$z = d - 0{,}5x = 12{,}45 - 0{,}5 \cdot 2{,}179 = 11{,}36\ \text{m}$$

$$F_c = x b_w f_{cdeff} = 2{,}179 \cdot 0{,}35 \cdot 23{,}8 = 18{,}151\,\text{MN}$$

The bending moment M_{Edh} = 108,127 MN.m and the axial force N_{Ed} = 12,474 MN and ΔN_{Ed} = 3,556 (the axial force between levels 4 and B3) are acting at the centre of gravity of the wall cross-section at level B3. The tension chord force is calculated from equation of above-mentioned moments to node B3c (Fig. 5-5):

$$F_t = \frac{M_{Edh} - \sum N_{Ed} z_{sc}}{z} = \frac{108{,}127 - 12{,}474 \cdot 3{,}86 - 3{,}556 \cdot 5{,}26}{11{,}36} = 3{,}633\,\text{MN}$$

2.2.3 Shear design

At level 4 the shear force is V_{Ed} = 1,861 MN and the normal force N_{Ed} = 11,78 MN.

The shear design is performed for a member in axial compression, see Eq.(6.9b) and (6.10b) of the FIP Recommendations (1999):

σ_{xd} = - 11,78 / (0,35 · 9,90) = - 4,94 MPa

$\cot\beta_r$ = 1,20 - 0,2 · σ_{xd} /f_{ctm} = 1,20 – 0,2 · (-4,94)/3,5 = 1,48

$V_{fd} = 0{,}10 \cdot (1 - \cot\beta_r/4) \cdot (b_w\, z\, f_{cwd}) = 0{,}10 \cdot (1 - 1{,}48/4) \cdot (0{,}35 \cdot 8{,}945 \cdot 22{,}7) =$
$= 0{,}0629 \cdot 71{,}2 = 4{,}48$ MN

Therefore, V_{Ed} = 1,861 << V_{fd} = 4,48 MN and so only minimum shear reinforcement is required, see section 2.1. The angle θ of the inclined struts in the web will therefore be low with an angle of around 20°. This means that the assumed angle of 45° is far too conservative for B-regions. It should also be noted that in this case Eq. (6.11) of the FIP Recommendations (1999) does not apply.

2.3 Strut-and-tie models

The stresses of the structure are plotted and visualized in the form of trajectories for left hand side seismic horizontal forces. They are here taken as the basis for the development of strut-and-tie models.

Model A (Fig.5-4) reflects the principal paths of forces when the seismic horizontal forces act from left and illustrates the load bearing behaviour of the structure in the B and D regions. In section 2.1 the location of the ties and struts was decided from the flexural design at specific levels of the shear wall for two possible directions of horizontal seismic forces at all storey levels.

Similarly model B (Fig.5-5) was developed for the seismic horizontal forces acting from right.

This document is the intellectual property of the fib – International Federation for Structural Concrete. All rights reserved.
This PDF of fib Bulletin 61 is intended for use and/or distribution solely within fib National Member Groups.

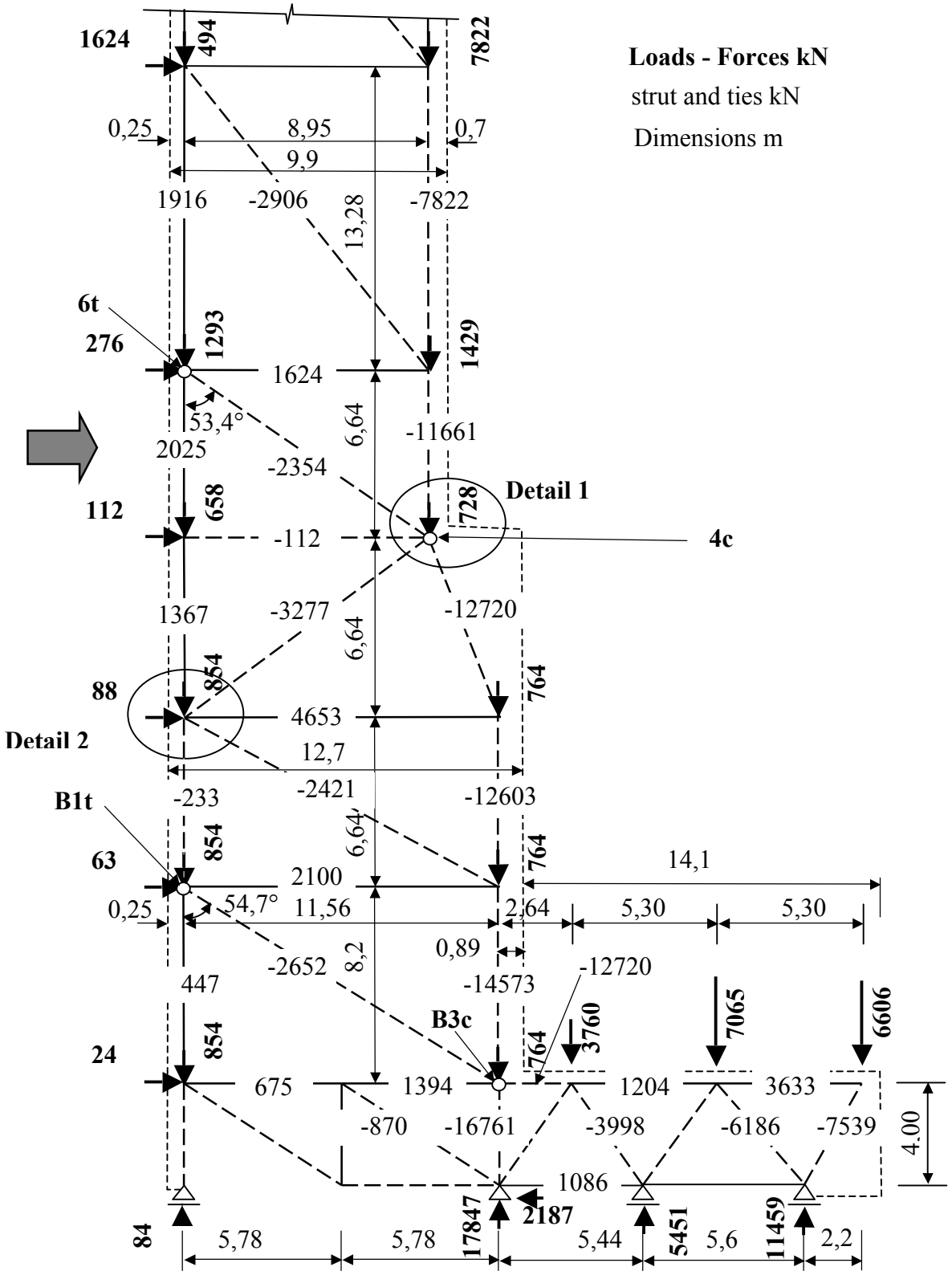


Fig. 5-4: Strut-and-tie model A for seismic horizontal forces from left

This document is the intellectual property of the fib – International Federation for Structural Concrete. All rights reserved.
This PDF of fib Bulletin 61 is intended for use and/or distribution solely within fib National Member Groups.

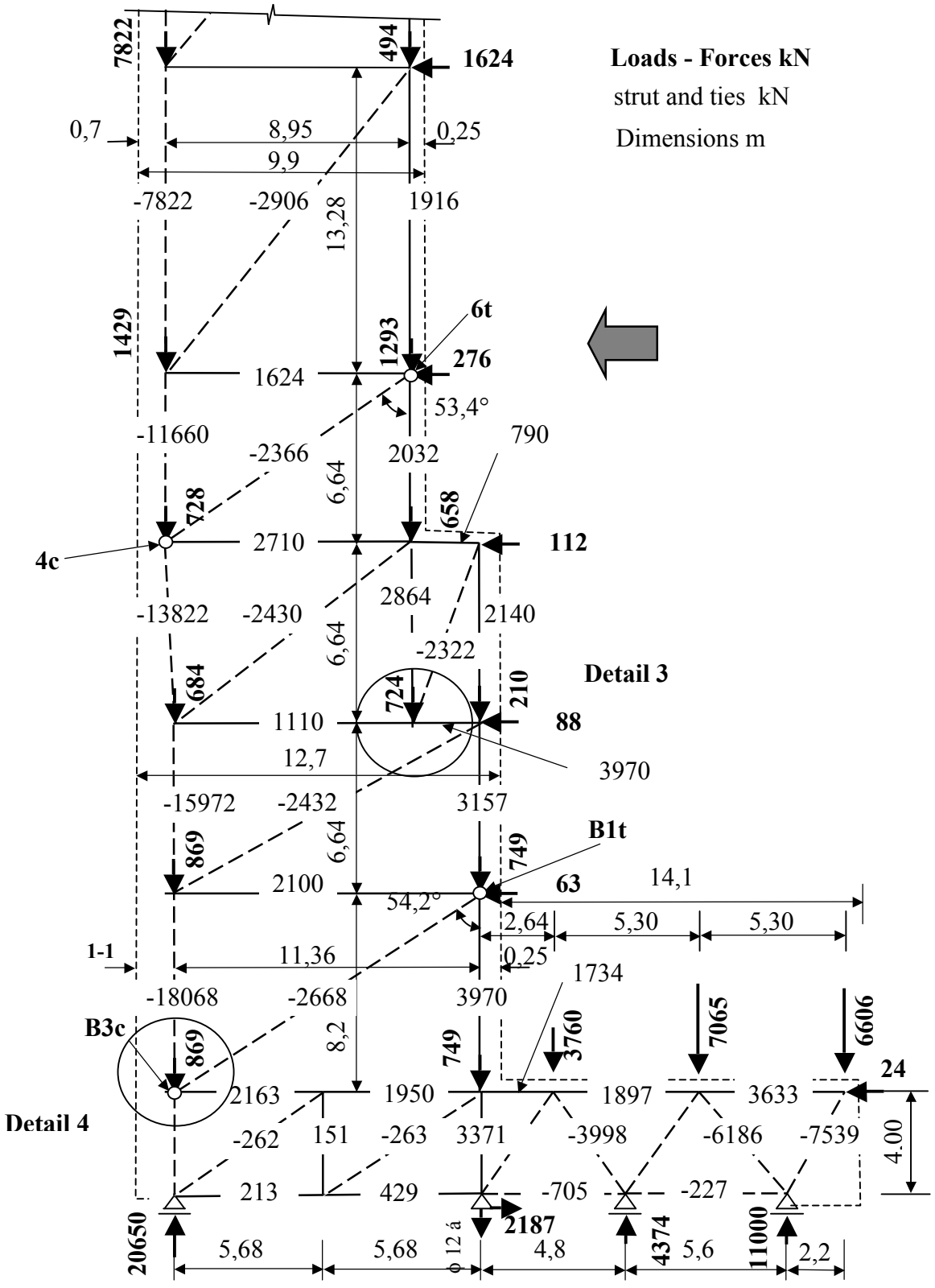


Fig. 5-5: Strut-and-tie model B for seismic horizontal forces from right

This document is the intellectual property of the fib – International Federation for Structural Concrete. All rights reserved.
This PDF of fib Bulletin 61 is intended for use and/or distribution solely within fib National Member Groups.

2.3 Dimensioning of struts and ties

2.3.1 Model A (Fig.5-4)

At level 6 the vertical tension chord force 2,025 MN requires tension reinforcement area:

$$A_s = \frac{F_t}{f_{yd}} = \frac{2{,}025 \cdot 10^6}{550} = 3.682 \text{ mm}^2 \rightarrow 8\varphi 25 \left(3.927\right)$$

For the vertical compression chord 11,661 MN the compression stress $f_{cd,eff}$ = 23,8 MPa results in a strut width of x = 11,661/ (23,8 · 0,35) = 1,40 m.

The stresses in the inclined struts need not to be checked because the shear force is very low, see section 2.2.3.

At level B1 (Fig. 5-4) the force in the vertical tension chord is 0,447 MN, and the required reinforcement area is: $A_s = 0{,}447 \cdot 10^6 / 550 = 813 \text{ mm}^2 \rightarrow 2\varnothing 25$ mm (982 mm^2)

2.3.2 Model B (Fig. 5-5)

At level B1 the force in the vertical tension chord is 3,970 MN, and the required reinforcement area is: $A_s = 3{,}970 \cdot 10^6 / 550 = 7.218 \text{ mm}^2 \rightarrow 16\varnothing 25$ mm (7.856 mm^2)

For the vertical compression chord force of 18,068 MN the max strut width x is:

x = 18,068 / (23,8 · 0,350) = 2,169 m

2.4 Nodes

2.4.1 Detail 1 – Model A

Detail 1 of model A (see Fig. 5-4), shown in Fig. 5-6, presents a CCC-node with 5 forces.

For the compressive force of 12,389 MN, the maximum strut width x is:

x = 12,389 / (22,7 ·0,350) = 1,560 m

For other forces the following values are calculated:

- force 12,720 MN: x = 12,720/ (22,7·0,350) = 1,600 m;
- force 2,354 MN: x = 2,354 / (22,7·0,350) = 0,296 m;
- force of diagonal 3,277 MN: strut width x = 3,277 /(22,7·0,350) = 0,412 m.

2.4.2 Detail 2 – Model A

Three struts and two ties converge in the node shown in Fig. 5-7.

The anchorage geometry on the Fig. 5-7 allows a straight bar anchorage of the longitudinal vertical reinforcement. The required basic development length is:

$$f_{\text{bd}} = 1{,}05 \cdot f_{ctm} = 1{,}05 \cdot 3{,}5 = 3{,}7 \text{ MPa - good conditions } \left(\text{C40/50}\right)$$

This document is the intellectual property of the fib – International Federation for Structural Concrete. All rights reserved.
This PDF of fib Bulletin 61 is intended for use and/or distribution solely within fib National Member Groups.

$$l_b = \frac{f_{yd}}{4 f_{bd}} \varphi = \frac{550}{4 \cdot 3{,}7} \varphi = 37 \cdot \varphi$$

For the vertical tension force of 1,367 MN, the required reinforcement area is:

$$\text{req}A_s = F_{td} / f_{yd} = 1{,}367 \cdot 10^6 / 550 = 2.485 \text{ mm}^2 \Rightarrow 8\ \phi\ 20\ (2.512 \text{ mm}^2)$$

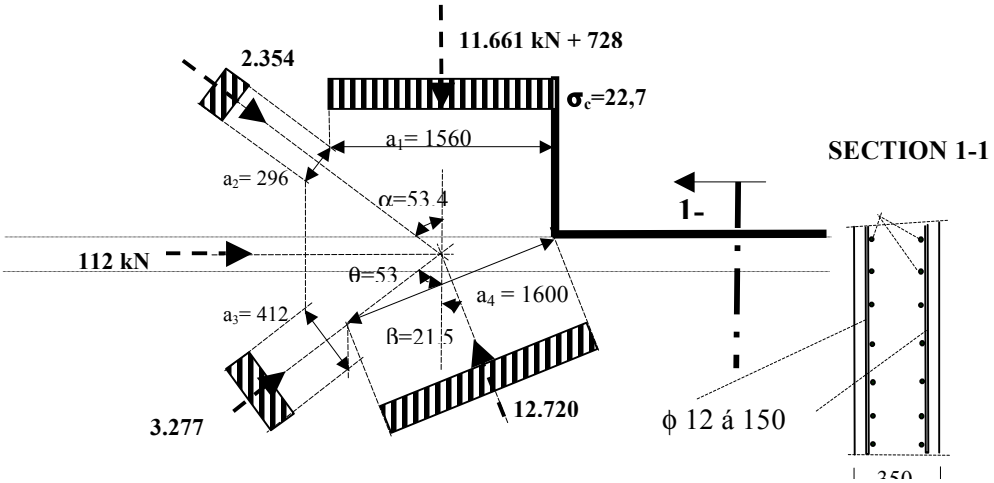


Fig. 5-6: Detail 1

$$\text{req}\ell_b = \alpha_a \ell_b \left(\frac{A_{s,req}}{A_{s,prov}} \right) = 1{,}0 \cdot 37 \cdot 20 \left(\frac{2.485}{2.512} \right) = 732 \text{ mm} \quad \text{vertical}$$

For the compressive force of diagonal 3,277 MN, the maximum strut width x is:

$$x = 3{,}277 / (22{,}7 \cdot 0{,}350) = 0{,}412 \text{ m}$$

For the horizontal tensile force of 4,653 MN, the required reinforcement area is

$$\text{req}A_s = F_{td} / f_{yd} = 4{,}653 \cdot 10^6 / 550 = 8.460 \text{ mm}^2 \Rightarrow 18\ \phi\ 25\ (8.838 \text{ mm}^2)$$

$$\text{req}\ell_b = \alpha_a \ell_b \left(\frac{A_{s,req}}{A_{s,prov}} \right) = 0{,}7 \cdot 37 \cdot 25 \left(\frac{8.460}{8.838} \right) = 620 \text{ mm} \quad \text{horizontal loops}$$

For the diagonal compressive force 2,421 MN, the strut width a_1 = 342 mm follows from the geometry of the node, and this results in a stress of σ_c = 2,421/ (0,342 ·0,350) = 20,2 MPa.

This document is the intellectual property of the fib – International Federation for Structural Concrete. All rights reserved.
This PDF of fib Bulletin 61 is intended for use and/or distribution solely within fib National Member Groups.

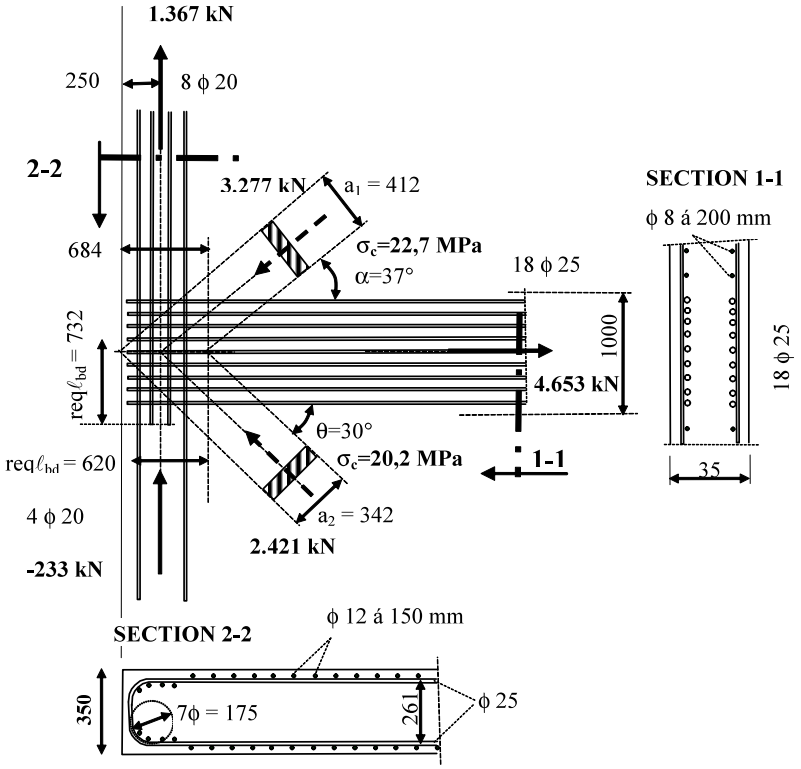


Fig. 5-7: Detail 2

2.4.3 Detail 3 – Model B (Fig. 5-5)

Detail 3 of model B (see Fig. 5-5) is shown in Fig. 5-8.

For the horizontal tensile force of 3,970 MN, the required tension reinforcement area is

$$\text{req}A_s = F_{td} / f_{yd} = 3{,}970 \cdot 10^6 / 550 = 7.218 \text{ mm}^2 \Rightarrow 16\ \phi\ 25\ (7.856 \text{ mm}^2)$$

$$\text{req}\ell_b = \alpha_a \ell_b \left(\frac{A_{s,req}}{A_{s,prov}} \right) = 1{,}0 \cdot 37 \cdot 25 \left(\frac{7.218}{7.856} \right) = 849 \text{ mm} \text{ horizontally}$$

For the compressive force of diagonal 2,322 MN, the strut width a_1 = 1094 mm results from the geometry of the node, so that σ_c = 2,322/ (1,094 ·0,350) = 6,1 MPa

For the vertical tensile force of 2,864 MN, the required reinforcement area is

$$\text{req}A_s = F_{td} / f_{yd} = 2{,}864 \cdot 10^6 / 550 = 5.207 \text{ mm}^2 \Rightarrow 12\ \phi\ 25\ (5.892 \text{ mm}^2)$$

$$\text{req}\ell_b = \alpha_a \ell_b \left(\frac{A_{s,req}}{A_{s,prov}} \right) = 0{,}7 \cdot 37 \cdot 25 \left(\frac{5.207}{5.892} \right) = 572 \text{ mm} \text{ vertical loops}$$

For the horizontal tensile force of 1,110 MN, the required reinforcement area is

$$\text{req}A_s = F_{td} / f_{yd} = 1{,}110 \cdot 10^6 / 550 = 2.019 \text{ mm}^2 \Rightarrow 6\ \phi\ 22\ (2.946 \text{ mm}^2)$$

This document is the intellectual property of the fib – International Federation for Structural Concrete. All rights reserved.
This PDF of fib Bulletin 61 is intended for use and/or distribution solely within fib National Member Groups.

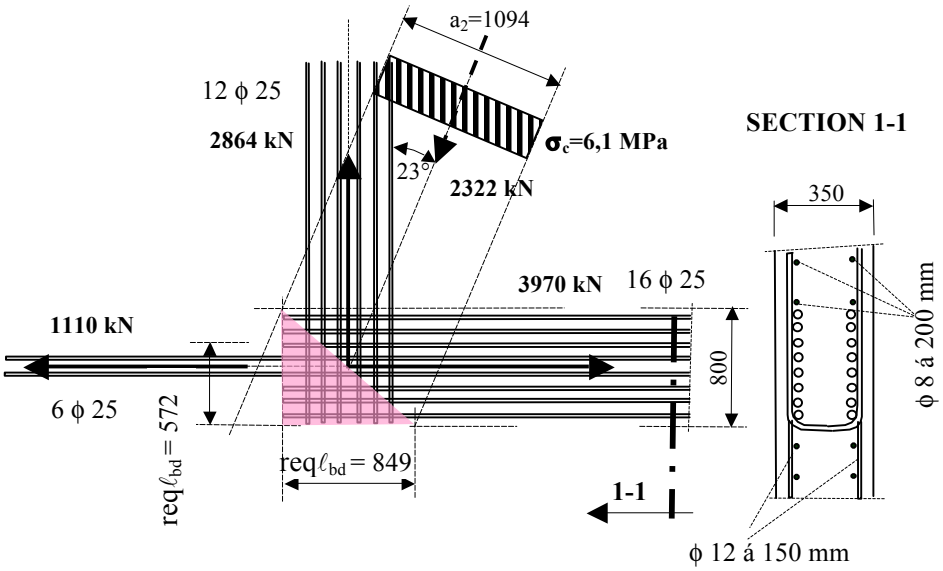


Fig. 5-8: Detail 3 with a TTC-node

2.4.4 Detail 4 – Model B (Fig. 5-5)

Detail 4 of model B (see Fig. 5-5) is a TCC-node and it is shown in Fig. 5-9.

For the compressive force 18,937 MN, the strut width is x = 18,937/(23,8 ·0,350) = 2,273 m.

For the horizontal tensile force of 2,163 MN, the required reinforcement area is

$$\text{req}A_s = F_{td} / f_{yd} = 2.163 / 550 = 3.933 \text{ mm}^2 \Rightarrow 12\ \phi\ 20 + 2\ \phi\ 16\ (4.170 \text{ mm}^2)$$

$$\text{req}\ell_b = \alpha_a \ell_b \left(\frac{A_{s,req}}{A_{s,prov}} \right) = 0{,}7 \cdot 37 \cdot 20 \left(\frac{3.933}{4.170} \right) = 489 \text{ mm horizontally}$$

For the compressive force 1,562 MN, the strut width is x = 1,562/(23,8 ·0,350) = 0,188 m.

For the diagonal compressive force of 2,668 MN, the strut width a_1 = 595 mm results from the geometry of the node, and this gives: σ_c = 2,668/ (0,595 ·0,350) = 12,8 MPa

This document is the intellectual property of the fib – International Federation for Structural Concrete. All rights reserved.
This PDF of fib Bulletin 61 is intended for use and/or distribution solely within fib National Member Groups.

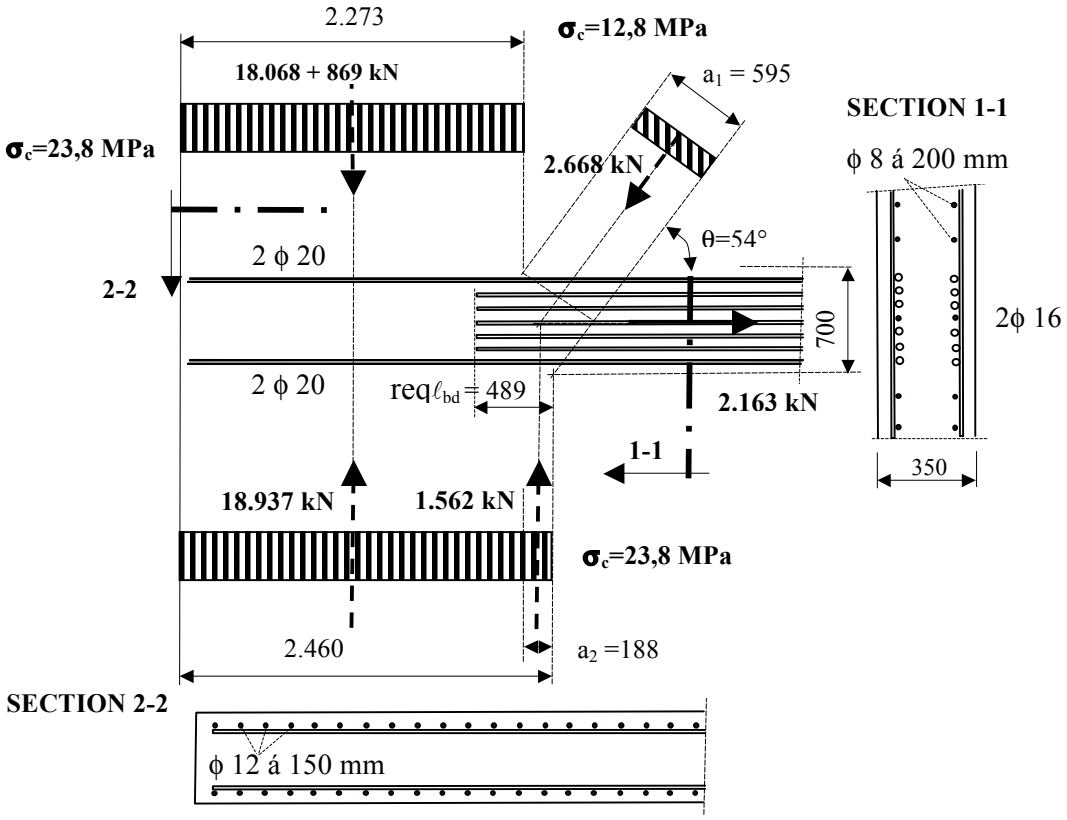


Fig. 5-11: Detail 4

3 Summary and conclusions

The shear wall of 76 m tall office building was designed using strut-and-tie models. The seismic, permanent and imposed loads were taken into account for different design situations. Based on vertical stresses and trajectories of principal stresses, appropriate strut-and-tie models were developed (Fig. 5-4 and Fig.5-5) yielding the tie forces used for the design of the reinforcement.

References

FIP Recommendations (1999): Practical Design of Structural Concrete.
FIP-Commission 3 "Practical Design", Sept. 1996. Publ.: SETO, London, Sept. 1999.
(Distributed by: *fib*, Lausanne. Web http://www.fib-international.org)

fib Bulletin 16 (2002): Design Examples for the FIP Recommendations "Practical design of structural concrete". *fib*, Lausanne. January 2002

Schlaich, J.; Schäfer, K; Jennewein, M. (1987): Toward a consistent design for structural concrete. PCI-Journ. V.32 (1987), No.3, 75-150

This document is the intellectual property of the fib – International Federation for Structural Concrete. All rights reserved.
This PDF of fib Bulletin 61 is intended for use and/or distribution solely within fib National Member Groups.

This document is the intellectual property of the fib – International Federation for Structural Concrete. All rights reserved.
This PDF of fib Bulletin 61 is intended for use and/or distribution solely within fib National Member Groups.

Example 6: Deep beam with an opening

Tjen Tjhin, Sukit Yindeesuk, Daniel Kuchma

1 Introduction and design task

A deep beam with an opening, as shown in Fig. 6-1, is designed using the strut-and-tie model (STM) approach. The beam supports a factored load from a column, P, of 5000 kN and a factored uniformly distributed load, q, of 120 kN/m. The distributed load includes the self-weight of the beam. The out-of-plane dimension of the beam is 600 mm. The compressive strength of the concrete is f_{ck} = 30 MPa and the yield strength of the steel reinforcement is f_{yk} = 420 MPa. This example is not from a real structure but draws from challenges in the design of deep load transfer members.

The deep beam is statically indeterminate to the first degree, as schematically shown in Fig. 6-2 in which the left support restrains the beam from vertical movement while the right supports restrains both vertical movement and rotation. For simplicity, and in consideration of the shape of the selected strut-and-tie model, the distributed load was lumped at four locations over the length of beam as also shown in Fig. 6-2.

The two reaction forces and one reaction moment were determined using four approaches, one linear elastic two-dimensional finite element analysis and three types of beam analyses. Table 6-1 illustrates that the vertical reaction force at end A, V_A, is not very sensitive to the analysis conducted. In the subsequent design, the value of V_A is taken as equal to 3000 kN and is treated as an additional external load acting on the structure, thus removing the external redundancy. This approach implicitly assumes that the structure possesses sufficient ductility, allowing internal force redistribution to occur to handle any deviation in the distribution of actual reaction forces.

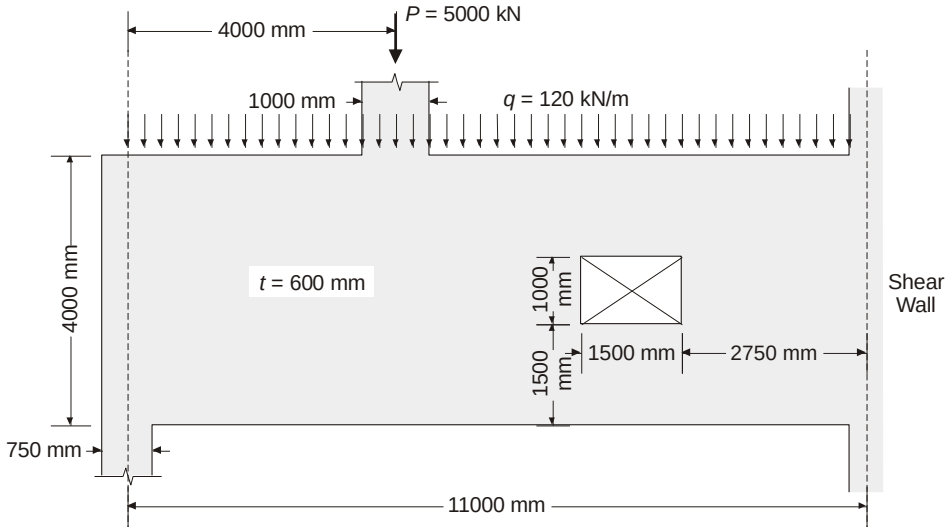


Fig. 6-1: Dimensions and loading conditions

This document is the intellectual property of the fib – International Federation for Structural Concrete. All rights reserved.
This PDF of fib Bulletin 61 is intended for use and/or distribution solely within fib National Member Groups.

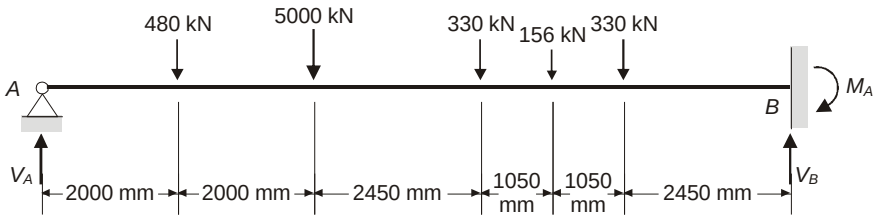


Fig. 6-2: Magnitude and location of the lumped uniformly distribution loading

Table 6-1: Reaction forces from four different analyses

Model	Reaction Force		
	V_A (kN)	V_B (kN)	M_A (kN-m)
Linear Finite (Quadrilateral) Element	3.000	3.310	9.430
Beam (Flexure Deformation Only, Uniform Stiffness)	2.890	3.420	10.530
Beam (Flexure Deformation Only, Considering Opening)	2.930	3.380	10.000
Beam (Flexure and Shear Deformations, Uniform Stiffness)	2.970	3.340	9.620

2 Selection of strut-and-tie model

The linear elastic principal stresses trajectories for this deep beam are shown in Fig. 6-3. They illustrate that the optimum directions for reinforcement at mid-depth and around the opening is close to 45 degrees from the longitudinal axis. However, the directions of the ties were taken to lie only in longitudinal or transverse directions for ease of construction. Fig. 6-4 presents the selected strut-and-tie model that will be used in the design of this member.

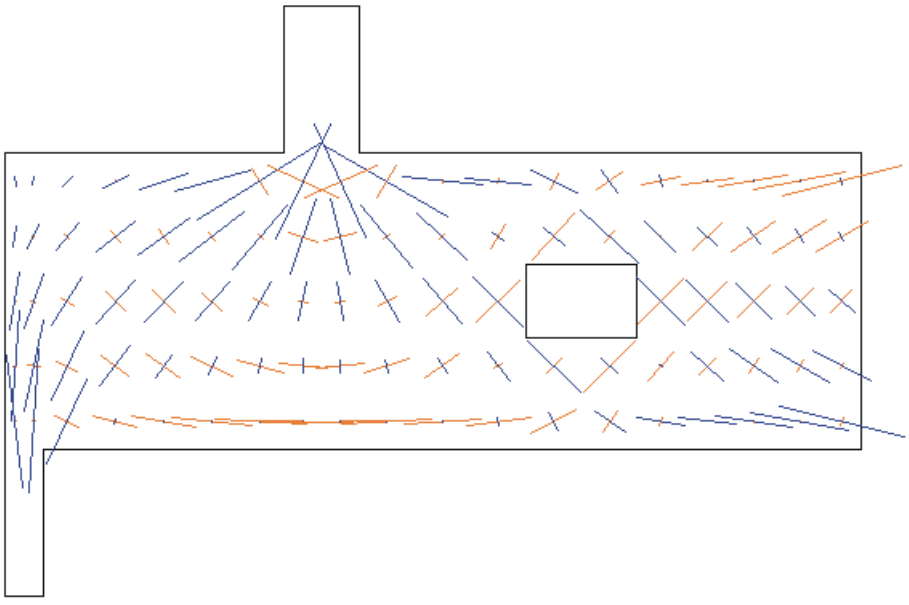


Fig. 6-3: Plot of principal stresses obtained from the FE analysis

This document is the intellectual property of the fib – International Federation for Structural Concrete. All rights reserved.
This PDF of fib Bulletin 61 is intended for use and/or distribution solely within fib National Member Groups.

In the selected model, the force transfer from the column loading to the left support is provided by a direct strut *BG* and by an indirect path in which the force in strut *BH* is lifted up by vertical tie *AH* and then down strut *AG* to the rigid support at *G* (see Fig. 6-4). The main force transfer on the right side of the column force is provided by two truss systems, one above and one below the opening. The truss system around the opening is shown in greater detail in Fig. 6-5.

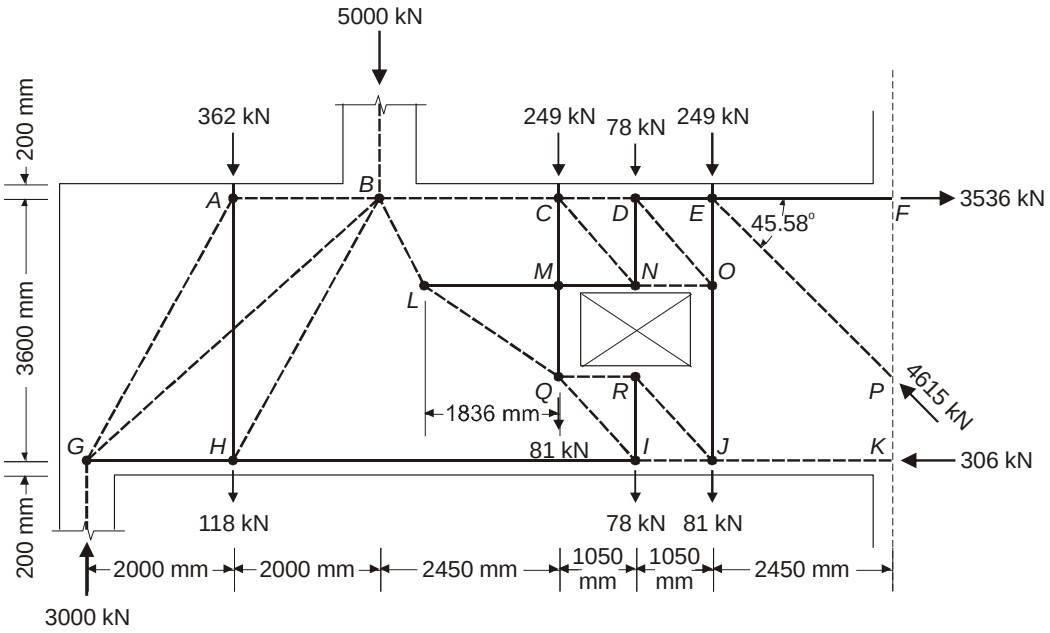


Fig. 6-4: Strut-and-tie model

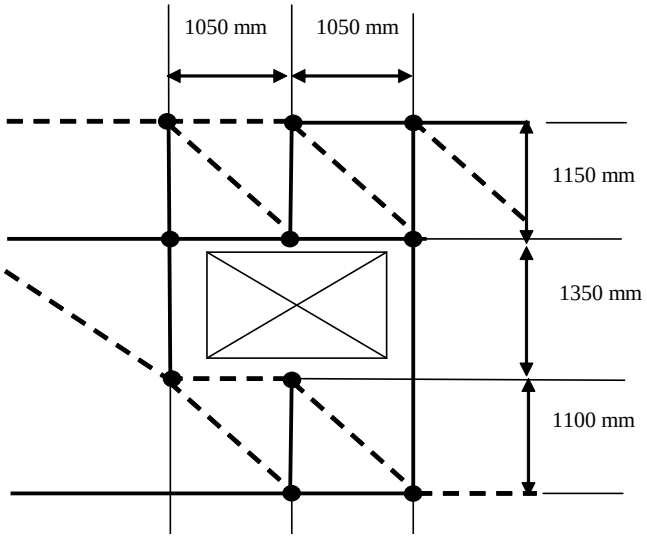


Fig. 6-5: Detailed strut-and-tie model around opening

Fig. 6-6 presents the distribution of the forces in the strut-and-tie model. A positive value indicates tension, and a negative value denotes compression. The strut-and-tie design program CAST, by Tjen et al. (2007b) was used to determine the forces in the members of the truss and to produce this image. Not all force values are clearly presented, but they are given in Tables 6-2 and 6-3 that follow in section 3.

This document is the intellectual property of the fib – International Federation for Structural Concrete. All rights reserved.
This PDF of fib Bulletin 61 is intended for use and/or distribution solely within fib National Member Groups.

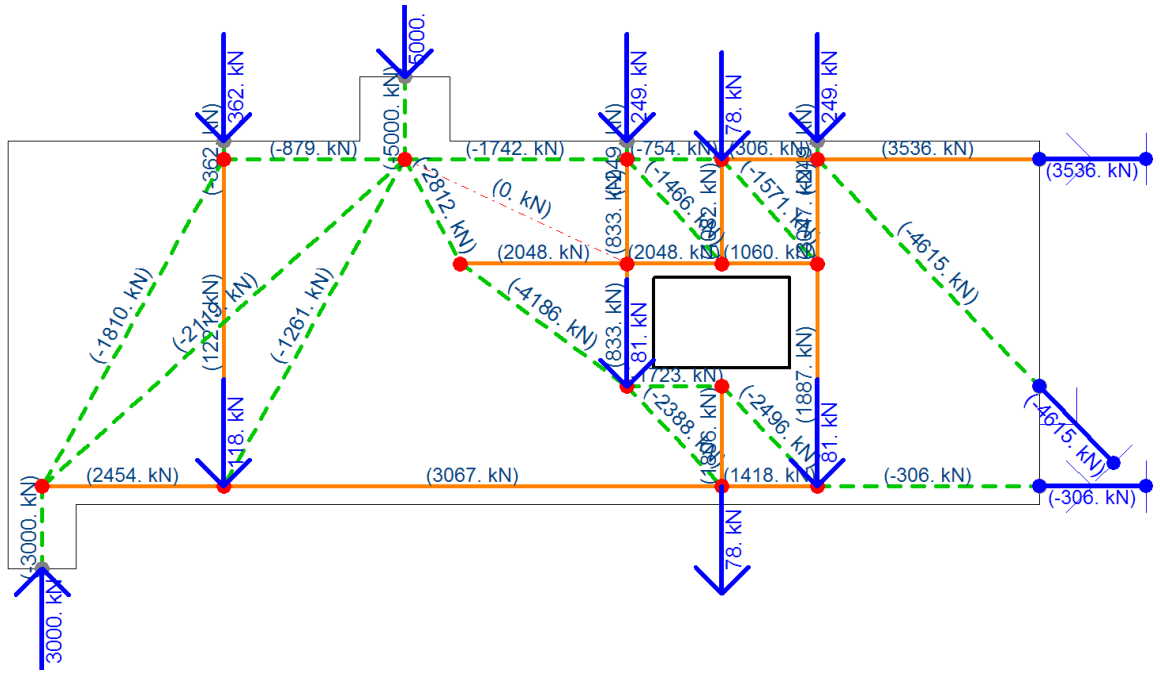


Fig. 6-6: Force distribution in the struts and ties

3 Design of member to satisfy code requirements

The design of this member requires that the struts have adequate capacity to support the compressive forces, that sufficient and properly anchored reinforcement is provided to carry the tie forces, and that these forces can be transmitted through nodal zones. Fig. 6-7 presents the widths of members that are approaching the maximum limit for what were considered to fit within the available space. If the associated capacity is calculated to be inadequate then a refined assessment of member widths would be needed to determine if a design solution is achievable using this strut-and-tie model.

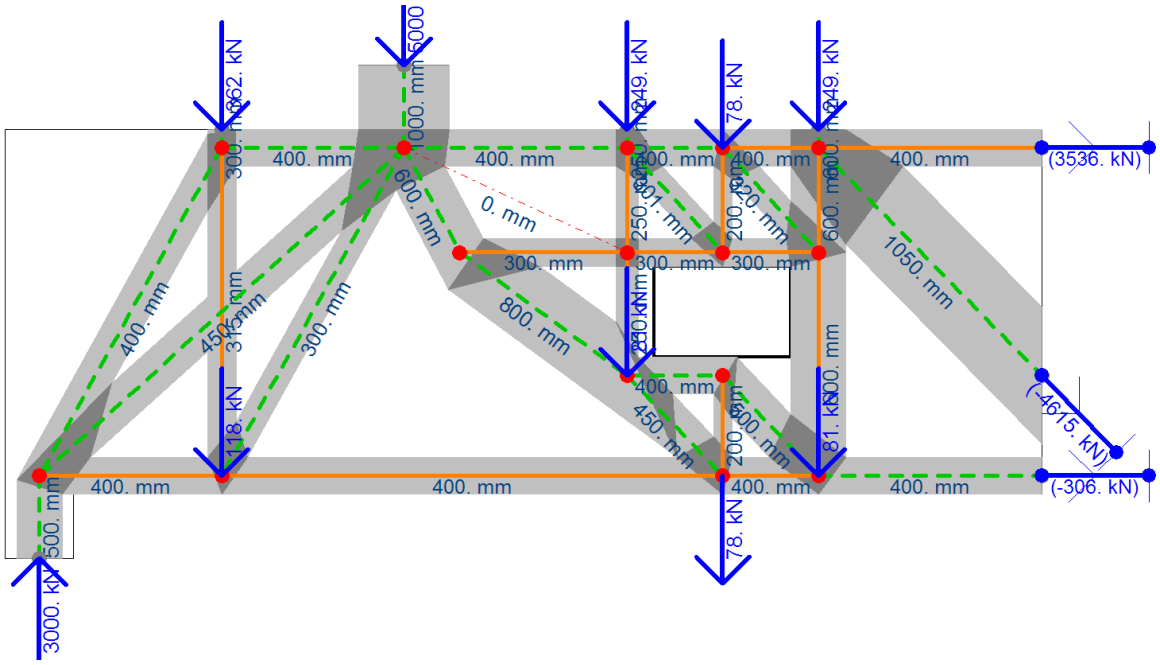


Fig. 6-7: Selected widths of struts and ties

This document is the intellectual property of the fib – International Federation for Structural Concrete. All rights reserved.
This PDF of fib Bulletin 61 is intended for use and/or distribution solely within fib National Member Groups.

In accordance to the compressive strength of struts presented in the FIP Recommendations (1999) for the "Practical Design of Structural Concrete", the strengths of the struts is equal to a stress limit $f_{cd,eff}$ times the area of the strut where for this design:

$f_{cd,eff} = \nu \cdot f_{1cd}$ where $f_{1cd} = \alpha \cdot f_{ck} / \gamma_c = 0{,}85 \cdot 30/1{,}5 = 17$ MPa

In this example, three types of struts are identified. The stress capacity for each of these three types of struts is given below:

- uncracked prismatic struts, for which

  $f_{cd,eff} = \nu_1 f_{1cd}$

  where $\nu_1 = (1 - f_{ck}/250) = (1 - 30/250) = 0{,}88 \rightarrow f_{cd,eff} = \nu_1 f_{1cd} = 0{,}88 \cdot 17 = 14{,}96$ MPa

- cracked struts in which the cracks are parallel to the direction of struts, for which $\nu_2 = 0{,}8$ and therefore $f_{cd,eff} = \nu_2 f_{1cd} = 0{,}8 \cdot 17 = 13{,}6$ MPa

- cracked struts in which the cracks are not parallel to the direction of struts, for which $\nu_2 = 0{,}6$ and therefore $f_{cd,eff} = \nu_2 f_{1cd} = 0{,}6 \cdot 17 = 10{,}2$ MPa

Table 6-2 tabulates the demands in struts, selected effective widths, strength reduction parameters, stress limits, and the ratio of demand to capacity. As shown, the demand is less than the provided capacity for all struts. The strut with the highest utilization (ratio of Demand/Capacity) is *QI* at 0,87 which is the strut beneath the bottom left corner of the opening. The strut with the second highest utilization is *DO* at 0,80 which is that above the top right corner of the opening. This is consistent with what would be expected.

Table 6-2: Strut force demands, selected widths, and force capacities

	Force Demand (kN)	**Selected Width (mm)**	**Value of ν_1 or ν_2**	**Stress Limit (MPa)**	**Force Capacity (kN)**	**Utilization (Demand / Capacity)**
JK	-306	400	0,88	14,96	-3.590	0,08
BC	-1.742	400	0,88	14,96	-3.590	0,49
AB	-879	400	0,88	14,96	-3.590	0,25
AG	-1.810	400	0,60	10,2	-2.448	0,74
BH	-1.261	300	0,60	10,2	-1.836	0,69
BL	-2.812	600	0,80	13,6	-4.896	0,57
EP	-4.615	1.050	0,80	13,6	-8.568	0,54
E'E	-249	600	0,88	14,96	-5.385	0,05
C'C	-249	250	0,88	14,96	-2.244	0,11
B'B	-5.000	1.000	0,88	14,96	-8.976	0,56
A'A	-362	300	0,88	14,96	-2.693	0,13
QI	-2.388	450	0,60	10,2	-2.754	0,87
LQ	-4.186	800	0,80	13,6	-6.528	0,64
DO	-1.571	320	0,60	10,2	-1.958	0,80
QR	-1.723	400	0,88	14,96	-3.590	0,48
RJ	-2.496	500	0,60	10,2	-3.060	0,82

Table 6-3 summarizes the tie demands, required reinforcement areas, selected reinforcement areas, and capacity of the ties. The utilization ratio (Demand / Capacity) is also provided in this table. The stress capacity of the reinforcement was taken as

$f_{yd} = f_{yk} / \gamma_s = 420 / 1{,}15 = 365$ MPa

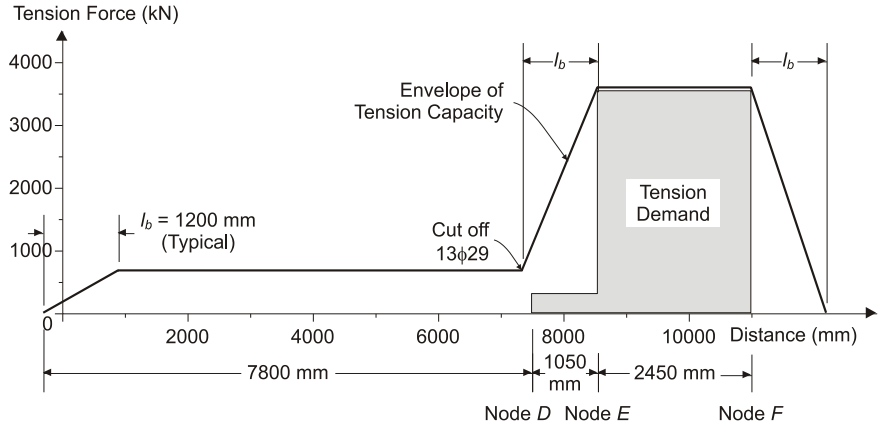
This document is the intellectual property of the fib – International Federation for Structural Concrete. All rights reserved.
This PDF of fib Bulletin 61 is intended for use and/or distribution solely within fib National Member Groups.

Table 6-3: Tie force demands, reinforcement areas, and force capacities

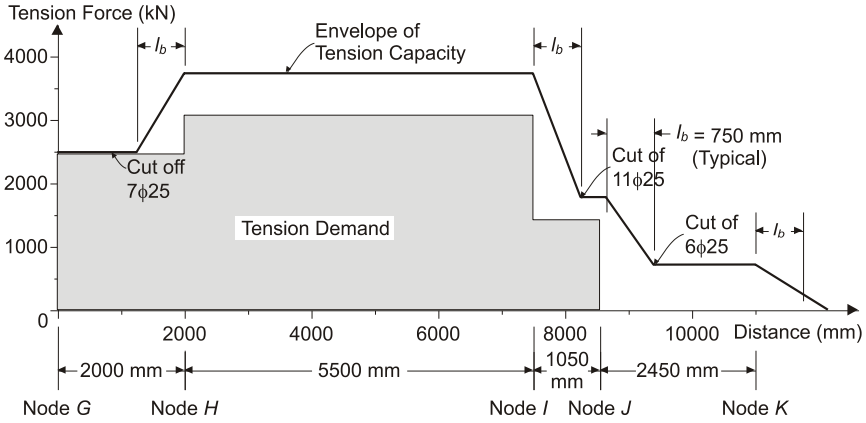
Tie ID	Force Demand (kN)	Required Steel Area (mm²)	Provided Steel Configuration	Area (mm²)	Force Capacity (kN)	Utilization (Demand / Capacity)
HI	3.067	8.397	2 Layers of 7 ϕ 25 +1 Layer of 5 ϕ 25	9.690	3.539	0,87
GH	2.454	6.720	2 Layers of 7 ϕ 25	7.140	2.608	0,94
EF	3.536	9.682	2 Layers of 6 ϕ 29 + 1 Layer of 4 ϕ 29	10.320	3.769	0,94
HA	1.220	3.342	14 Two-Legged Stirrups ϕ 13 @ 200 mm	3.612	1.319	0,93
JO	1.886	5.165	7 Layers of 2 ϕ 29	9.030	3.298	0,57
IR	1.806	4.944	14 Two-Legged Stirrups ϕ 16 @ 100 mm	5.572	2.035	0,89
NO	1.060	2.901	2 Layer of 5 ϕ 29	6.450	2.356	0,45
ND	1.082	2.964	14 Two-Legged Stirrups ϕ 16 @ 100 mm	5.572	2.035	0,53
MQ	834	2.282	5 Layer of 2 ϕ 19	2.840	1.037	0,80
LM	2.048	5.607	2 Layer of 5 ϕ 29	6.450	2.356	0,87
DE	306	837	2 Layers of 6 ϕ 29+ 1 Layer of 4 ϕ 29	10.320	3.769	0,08
IJ	1.418	3.882	2 Layer of 7 ϕ 25	7.140	2.608	054
MN	2.048	5.607	2 Layer of 5 ϕ 29	6.450	2.356	0,87
CM	834	2.282	5 Layer of 2 ϕ 19	2.840	1.037	0,80
OE	3.047	8.343	7 Layer of 2 ϕ 29	9.030	3.298	0,92

Fig. 6-8 illustrates the selection of cutoff points of the top chord and bottom chord bars, respectively. The available development length of the bars, l_b, is assumed to start at the nodes connecting longitudinal ties. The developed tension capacity of a given layer of bars along the development length is assumed to vary linearly from zero at the cutoff point to the full capacity at the development length. The required development length is a function of several factors. For concrete with a f_{ck} = 30 MPa with bars that have a diameter of 29 mm or less, the required development length for straight bars is equal to 30,4 d_b for bottom bars and 43,5 d_b for top bars in accordance to the FIP Recommendations (1999). In addition, the development length may be reduced in proportion to the ratio of required to the provided area of reinforcement. Considering these factors, the basic development length for 29 mm diameter top bars is approximately 1.200 mm as shown in Fig. 6-8(a). The basic development length for the 25 mm diameter bottom bars is 760 mm as shown in Fig. 6-8(b). The standard 90° hook is used to anchor tie *GH*. This reduces the required development length by 30% to 530 mm. This is smaller than the available anchorage length which is 750 –2(25) – 30 = 670 mm.

This document is the intellectual property of the fib – International Federation for Structural Concrete. All rights reserved.
This PDF of fib Bulletin 61 is intended for use and/or distribution solely within fib National Member Groups.



a) top chord



b) bottom chord

Fig. 6-8: Tension force demands and capacities of top and bottom chord

4 Checking capacity of complex nodal zones

The condition at nodes seldom governs a design in which the requirements for struts and ties have been satisfied. While this example is no exemption, it is interesting to examine the stress conditions in complex nodal zones. Consider nodal zone *B* which is a 6-sided CCC node. This nodal zone can be divided into $2(6)-4=8$ constant stress triangles in which the strength capacity for each of these is checked using a modified Mohr-Coulomb yield condition. Figure 6-9 shows the geometry, numbering, principal stress directions, and stress ratios of the triangles. Table 6-4 presents the triangle biaxial stress demands described in both the *x-y* coordinate system and principal directions. As in the sign convention of forces, a positive normal stress value indicates tension, and a negative value denotes compression. Table 6-5 lists the concrete contribution in carrying the biaxial stress demands, the available biaxial stress capacities, and the corresponding stress ratios. As shown and expected, the demands are well less than the available capacities. Additional information on making these types of checks is given by Tjen et al. (2007a).

Nodal zone *G* is a 4-sided CCT node. Thus, this nodal zone may be divided into $2(4)-4=4$ constant stress triangles. The strength of nodal zone G was also checked for adequacy according to the modified Mohr-Coulomb yield condition. The stress demand and capacity of the longitudinal reinforcing steel entering nodal zone *G* are 344 MPa and 348 MPa, respectively. Fig.6-10 shows a Mohr's circle representation of the stress state of nodal zone *G*.

This document is the intellectual property of the fib – International Federation for Structural Concrete. All rights reserved.
This PDF of fib Bulletin 61 is intended for use and/or distribution solely within fib National Member Groups.

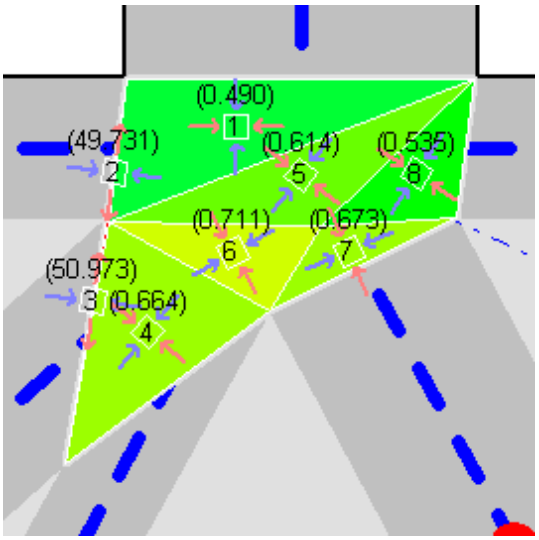


Fig. 6-9: Geometry, principal stress directions, and stress ratios of constant stress triangles of nodal zone B (decimal point instead of comma; see Editorial Comments on p. vi)

Table 6-4: Stress demands of nodal zone B

Triangle	*x-y*-Direction Stresses			Principal Stresses		
ID	*x*-Direction (MPa)	*y*-Direction (MPa)	Shear (MPa)	Maximum (MPa)	Minimum (MPa)	Principal Direction (degrees)
1	-3,50	-8,33	0	-3,50	-8,33	0
4	-4,70	-7,09	-5,27	-0,49	-11,30	-38,6
5	-8,13	-9,04	-1,81	-6,72	-10,45	-38,0
6	-11,1	-9,04	-1,74	-8,05	-12,09	-60,3
7	-10,86	-8,38	-1,34	-7,79	-11,45	-66,3
8	-7,41	-8,37	-1,11	-6,68	-9,10	-33,3

Table 6-5: Concrete biaxial stress demands, biaxial stress capacities, and stress ratios of constant stress triangles of nodal zone B

Triangle	Concrete Stress Demand (MPa)			Concrete Stress Capacity (MPa)			
ID	*x*-direction	*y*-direction	Shear	*x*-direction	*y*-direction	Shear	Stress ratio
1	-3,5	-8,33	0	-7,14	-17,01	0	0,49
4	-4,7	-7,09	-5,27	-7,08	-10,67	-7,94	0,664
5	-8,13	-9,04	-1,81	-13,24	-14,72	-2,94	0,614
6	-11,1	-9,04	-1,74	-15,61	-12,72	-2,45	0,711
7	-10,86	-8,38	-1,34	-16,14	-12,46	-1,99	0,673
8	-7,41	-8,37	-1,11	-13,85	-15,65	-2,08	0,535

While the nodal analyses presented in Figs. 6-9 and 6-10 as well as Tables 6-4 and 6-5 are not required by any code of practice, they provide an assessment methodology for determining the capacity of complex nodal zones.

To increase ductility capacity in the beam, as well as for the control of cracking, distributed reinforcement equal to 0,22% of the cross sectional area is provided in the horizontal direction. The final reinforcing details are presented in Fig. 6-11.

This document is the intellectual property of the fib – International Federation for Structural Concrete. All rights reserved.
This PDF of fib Bulletin 61 is intended for use and/or distribution solely within fib National Member Groups.

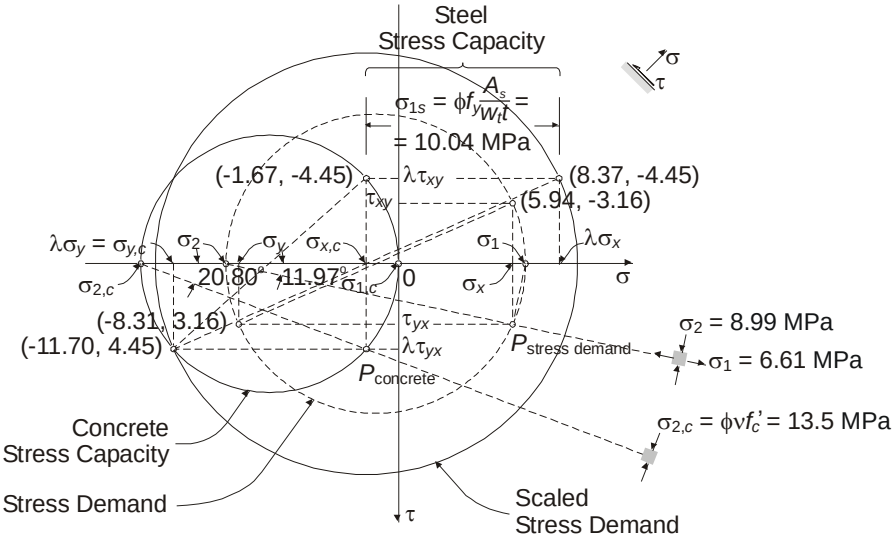


Fig. 6-10: Mohr's circle representation of the stress state of nodal zone G (decimal point instead of comma; see Editorial Comments on p. vi)

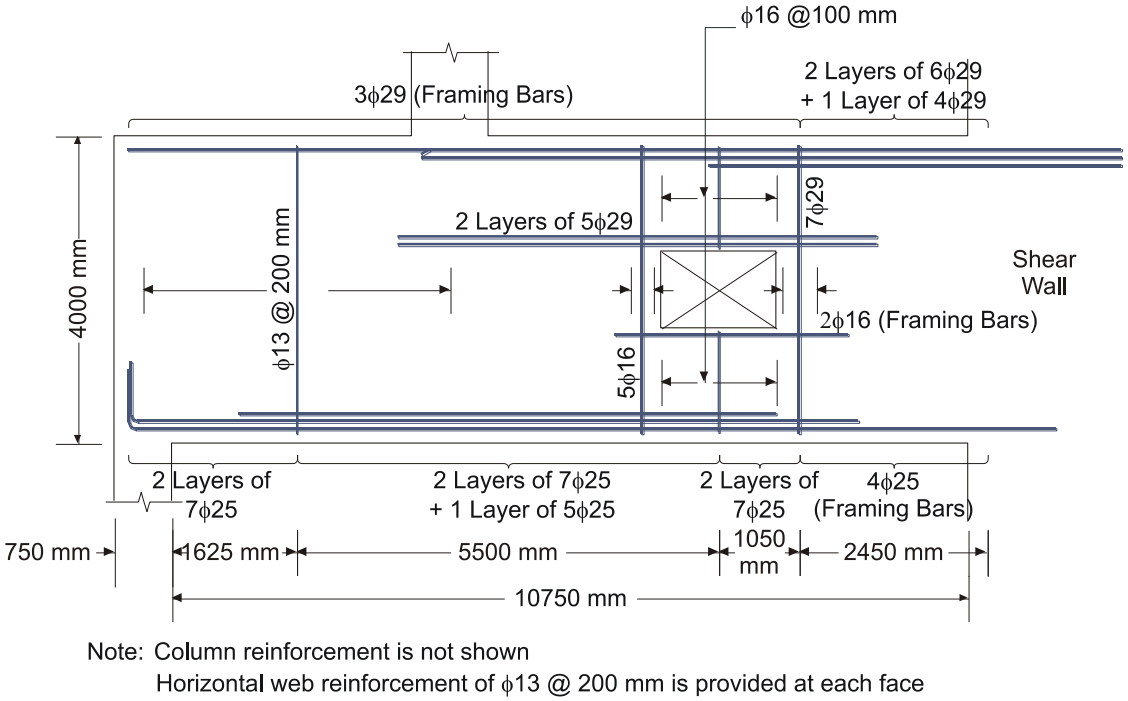


Fig. 6-11: Reinforcing details

5 References

FIP Recommendations (1999): Practical Design of Structural Concrete. FIP-Commission 3 "Practical Design", Sept. 1996. Publ.: SETO, London, Sept. 1999. (Distributed by: *fib*, Lausanne. Web: http://www.fib-international.org)

Tjhin, T. N.; Kuchma, D. A. (2007a): Limit State Assessment of Nodal Zone Capacity in Strut-and-Tie Models. Journal of Computers and Concrete, Vol. 4 (2007), No. 4 August, 3042-3052

Tjhin, T. N.; Kuchma, D. A. (2007b): Integrated Analysis and Design Tool for the Strut-and-Tie Method. Journal of Engineering Structures, Vol. 29 (2007), No.11 November, 3042-3052

This document is the intellectual property of the fib – International Federation for Structural Concrete. All rights reserved.
This PDF of fib Bulletin 61 is intended for use and/or distribution solely within fib National Member Groups.

This document is the intellectual property of the fib – International Federation for Structural Concrete. All rights reserved.
This PDF of fib Bulletin 61 is intended for use and/or distribution solely within fib National Member Groups.

Example 7: Anchorage block for external prestressing tendon - Comparison with test results

Toshio Ichihashi, Hiroshi Shiratani

1 Presentation of structure

This example demonstrates the application of a three-dimensional strut-and-tie model to a concrete anchorage block, which is constructed on a thin slab of a box-girder and subjected to the prestressing force of an external tendon. The analytical study was supplemented by testing a scaled model of the anchorage to examine its performance and capacity. The results obtained from the strut-and-tie model and those from testing are compared in this example. The loading test was conducted by the Japan Ministry of Land, Infrastructure, and Transport, and the Japan Prestressed Concrete Contractors Association (2001).

Fig. 7-1 shows the loading test model. A box girder of typical size for a two-lane bridge is assumed for this model. The scale is about 1/2 and the top slab is omitted for simplicity. The anchorage for the external prestressing tendon is applied at the bottom slab. Since this model is symmetric about the center line, only half side is shown in Fig.7-1. In this loading test, the prestressing tendons were anchored at the anchorage block and the end wall. The tendons were tensioned from the side of the end wall. The design strength of the concrete f_{ck} = 40 MPa (actual strength was 49 MPa), and the actual yield stress of the reinforcing bars was about 380MPa (Fig. 7-6).

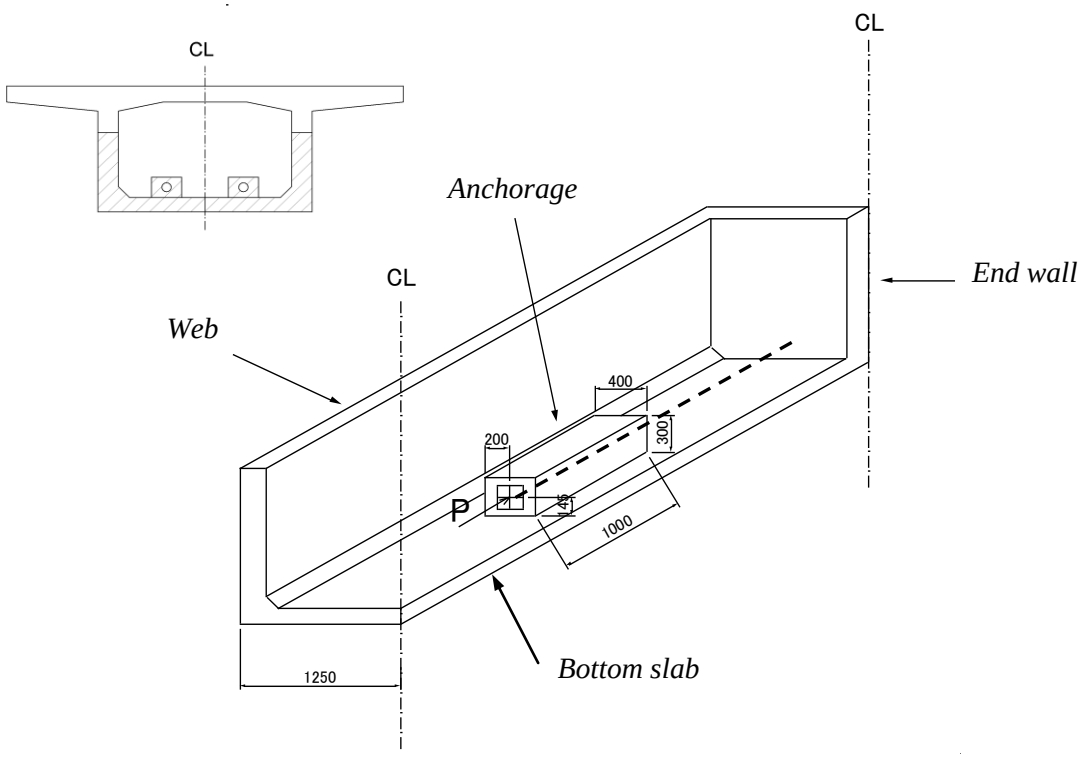


Fig. 7-1: Test model (dimensions in mm)

This document is the intellectual property of the fib – International Federation for Structural Concrete. All rights reserved.
This PDF of fib Bulletin 61 is intended for use and/or distribution solely within fib National Member Groups.

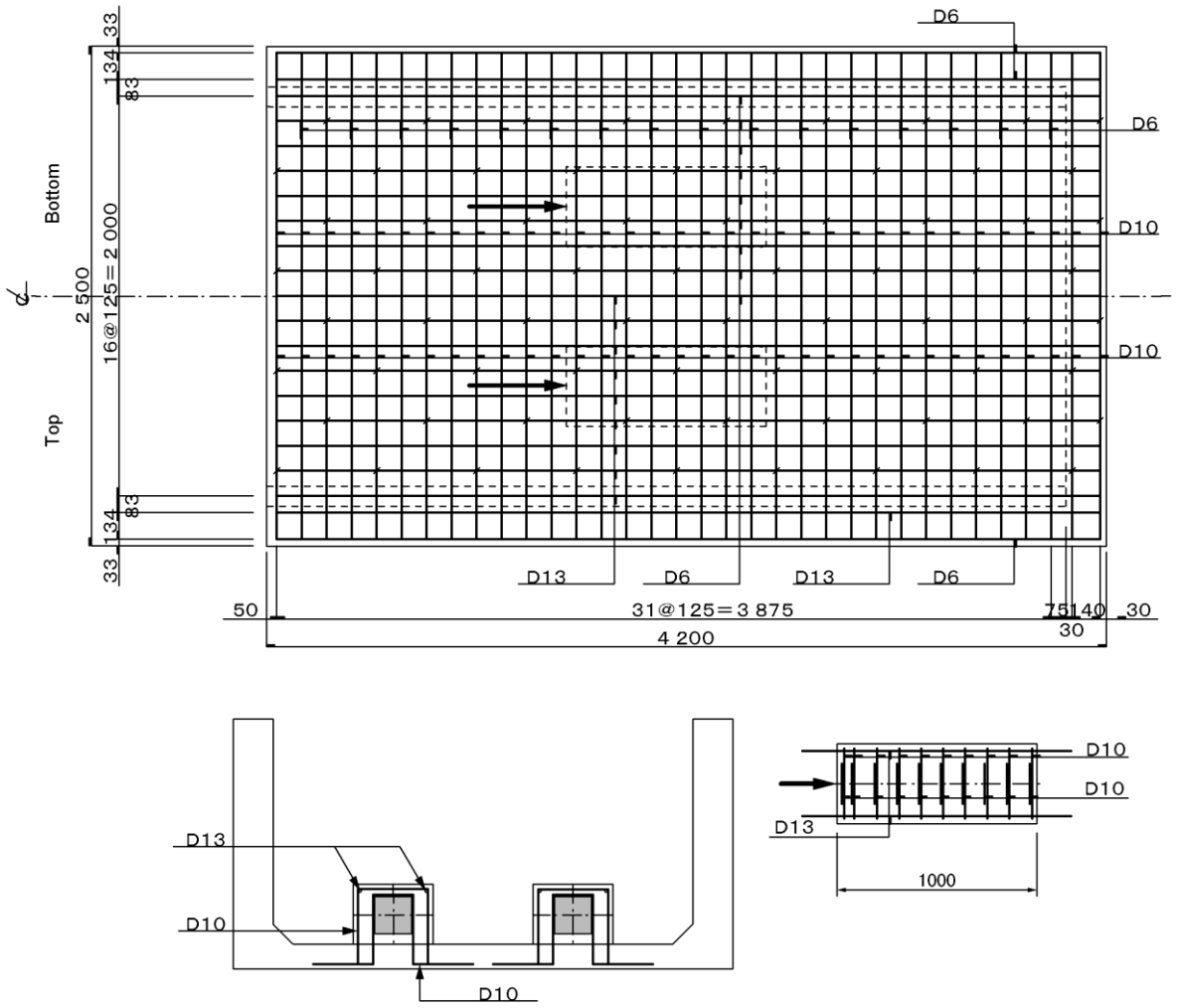


Fig. 7-2: Reinforcing bars in the test model (dimensions in mm)

Incidentally, another case of the loading test was also conducted: in this test model the anchorage blocks were arranged at the corner of the web and the bottom slab. The test result of this case was that the failure mode appeared to be the crushing of the concrete just behind the bearing plate of the tendon, although the capacity was so high that the test was finished without observing obvious failure. On the other hand, in the case of the model shown in Fig. 7- 1, failure was caused by yielding of the reinforcing bars in the bottom slab. Thus, from the viewpoint of studying the applicability of the strut-and-tie model to anchorage blocks on box-girders, the case shown in Fig.7-1 is more suitable as the object of this study. However, the arrangement of anchorages at the corner would certainly be recommended in real bridges.

The arrangement of the reinforcing bars in the anchorage and the bottom slab is indicated in Fig. 7-2.

2 Strut-and-tie model

The strut-and-tie model adopted in this example is shown in Fig. 7-3. This is a linear three-dimensional frame model. The solid lines represent ties (tension members), and the dashed lines represent struts (compression members). The sectional properties of the strut and tie members are set based on the areas of the slab concrete or reinforcing bars.

This document is the intellectual property of the fib – International Federation for Structural Concrete. All rights reserved.
This PDF of fib Bulletin 61 is intended for use and/or distribution solely within fib National Member Groups.

In this model the web and the end wall are omitted. The support condition is also indicated in Fig. 7-3. The support at the end wall line is fixed in the vertical and horizontal directions. The support line under the web is fixed in the vertical direction. In the preliminary study, the two cases of calculations, with the support under the web vertically fixed and free, were compared. As a result, although the sectional forces near the web were somewhat different, the sectional forces of the critical members (around the anchorage) were similar even with the change of these support conditions. Therefore, the web can be considered to have little influence on the capacity of the anchorage. Consequently, the web was omitted in the model for simplicity, and vertically fixed support condition under the web was assumed in this example.

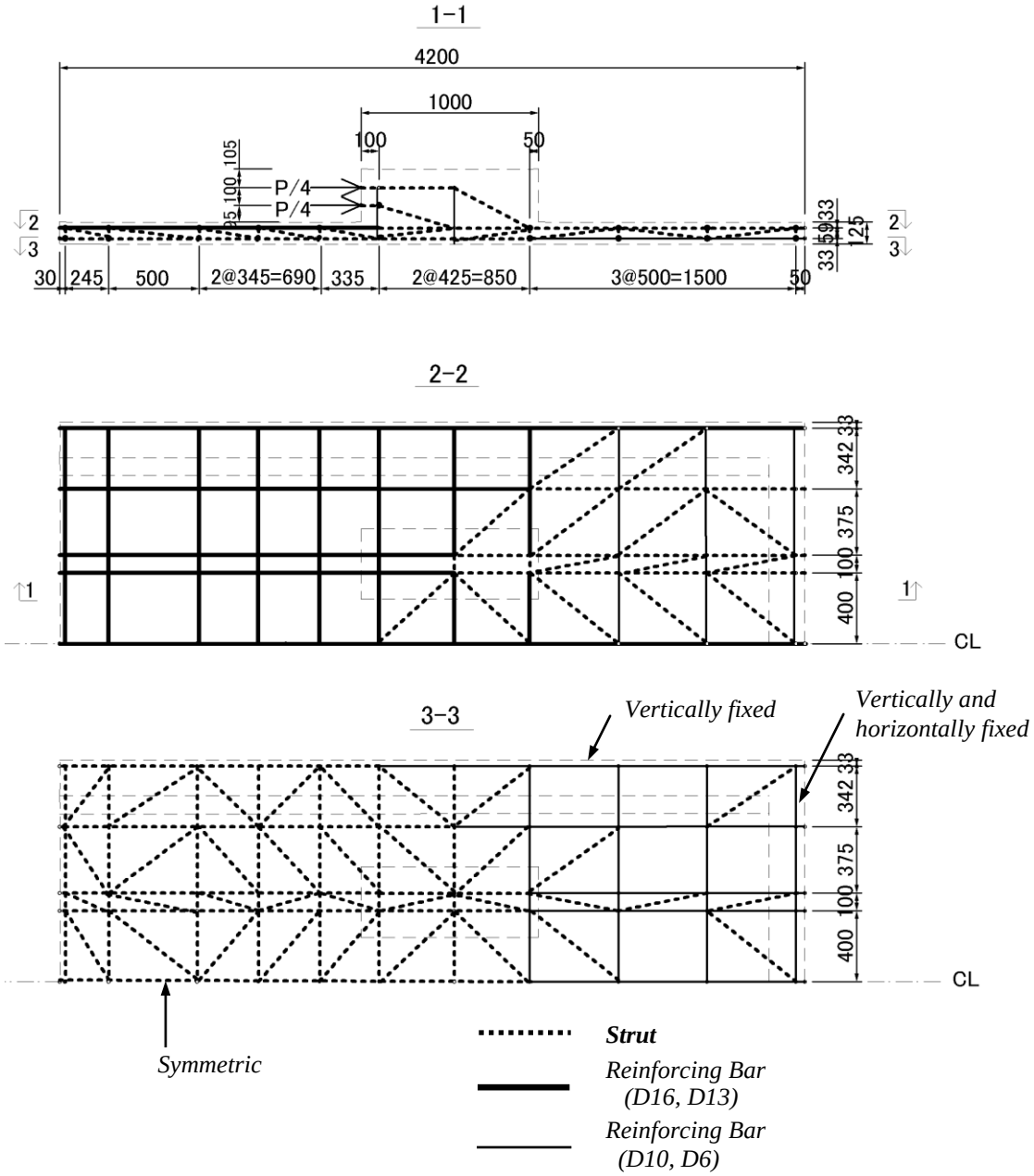


Fig. 7-3: Analytical model (dimensions in mm)

This document is the intellectual property of the fib – International Federation for Structural Concrete. All rights reserved.
This PDF of fib Bulletin 61 is intended for use and/or distribution solely within fib National Member Groups.

Since this frame analysis is linear, a concentrated unit load (P=1.000 kN) was applied at the anchorage. Then the stresses of all the members were examined. The capacity of the anchorage was obtained as the minimum load when the stress in one of the tie members reaches the yield stress.

Instead of analysing only the discontinuity region (i.e. the anchorage block) by using STM, a global strut-and-tie model is presented in this example. This unusual approach is the direct consequence of the unusual conditions of loading and restraints.

In this case the anchorage load produces two different effects in the bottom slab.

The first one is the horizontal action that can find equilibrium only in the end wall that is the only element horizontally restrained.

The second one is the bending moment caused by the eccentricity of the anchorage load. Differently from corbels in frames in which this moment is equilibrated by the columns, in this case it can find equilibrium thanks to the vertical reactions in the lateral web and in the end wall. This means that the forces produced by this moment have to travel in two directions and have to activate the slab behaviour to find equilibrium. This is the peculiar aspect that makes this case unusual and this is the reason why a global STM has been proposed.

As a principle of the strut-and-tie models, the ties should be arranged only in the same directions as the reinforcing bars. Therefore, all the diagonals of the frame model should be compressive members. As a first step, the frame model was made with diagonal members arranged in all the grids of the bottom slab. Then, the final frame model shown in Fig. 7-3 was obtained after some trials of eliminating the tensile diagonals.

3 Analytical results

The eccentricity of the applied load causes bending moments and shear forces in the slab (see Fig. 7-7), and Fig. 7-4 indicates the location where relatively severe tensions occur (note that the reaction forces acting on the slab are not shown in Fig. 7-4). The severe tensile stresses are longitudinally at the rear upper side (“A”) and the front lower side (“B”) of the bottom slab, and the vertical stress at the rear surface of the anchorage just below the bearing plate (“C”).

The calculated capacities are listed in Table 7-1. The capacity load is defined as the minimum among the yield loads of the individual tie members, P_y (= P· f_y /σ), where f_y = 380 MPa and σ = calculated stress for the unit load, *P* = 1.000 kN. The reinforcing bars in area “A” reach the yield stress first for the applied load of 720 kN.

It should be noted that the stresses in all the compression struts are much smaller than the design strength of the concrete strut, $f_{cd,eff}$, defined in FIP Recommendations(1999):

$$f_{cd,eff} = \nu_2 f_{1cd}$$

Thereby f_{1cd} is the design value for the uniaxial compressive strength of concrete and the factor ν_2 = 0,80. Therefore the check for the struts has been omitted in this example.

This document is the intellectual property of the fib – International Federation for Structural Concrete. All rights reserved.
This PDF of fib Bulletin 61 is intended for use and/or distribution solely within fib National Member Groups.

4 Comparison with loading test result

The loading test result is shown in Fig. 7-5, in which the applied forced is given with respect to the strain measured at the two reinforcing bars within area "A" (defined in Fig. 7-4). In the test, cracks occurred first within area "A". Subsequently strain at the reinforcing bars reached the yield strain (about 1.900×10^{-6}) at a load of about 1.000 kN. Since the increase of the applied load seized after the strain exceeded the yield strain, it can be considered that yielding of the reinforcing bars at area "A" was critical for the anchorage. At failure, many cracks were observed within areas "A" and "B". Therefore the calculated failure mode was similar to that of the test.

The yield load estimated by the strut-and-tie model (720 kN) is about 70% of the measured yield load. In the calculation, both longitudinal and transversal tension occurred in the members at the area "A" and "B". As shown in Fig. 7-6, in the loading test longitudinal, transverse and diagonal cracks were observed at area "A"; this indicates that also in the test the longitudinal and transverse tension occurred at area "A". However, while in the test effects like shear transmission along the cracks and the tension-stiffening, would somewhat contribute to inhibit rapid increase of tensile forces in the reinforcing bars, these effects cannot be taken into account in the strut-and-tie model because tensile concrete ties are not employed in principle. This may be the main reason that the calculated tensile stresses of the reinforcing bars were higher than the test results.

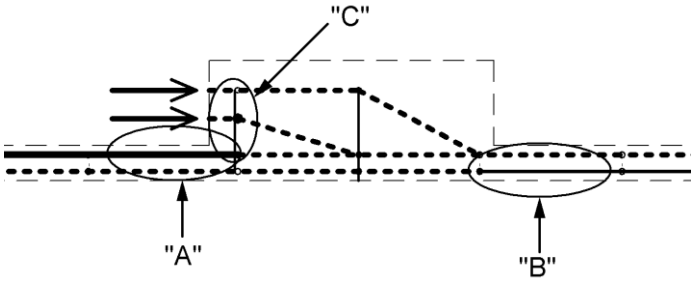


Fig. 7-4: Location of severe tension

Table 7-1: Estimated capacity

Location	Stress of reinforcing bar for P=1.000kN (MPa)	Yield load of reinforcing bar Py（kN）
"A"	***528***	***720***
"B"	502	756
"C"	269	1.413

This document is the intellectual property of the fib – International Federation for Structural Concrete. All rights reserved.
This PDF of fib Bulletin 61 is intended for use and/or distribution solely within fib National Member Groups.

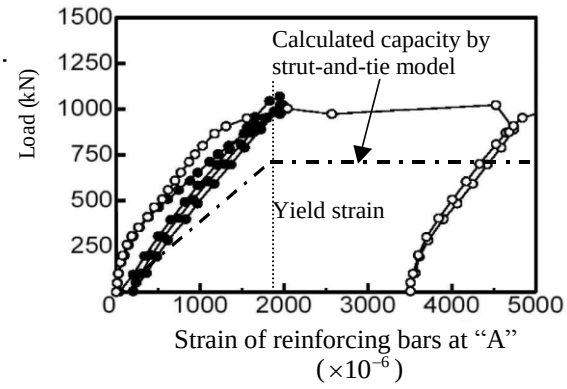


Fig. 7-5: Test result and comparison with calculation result

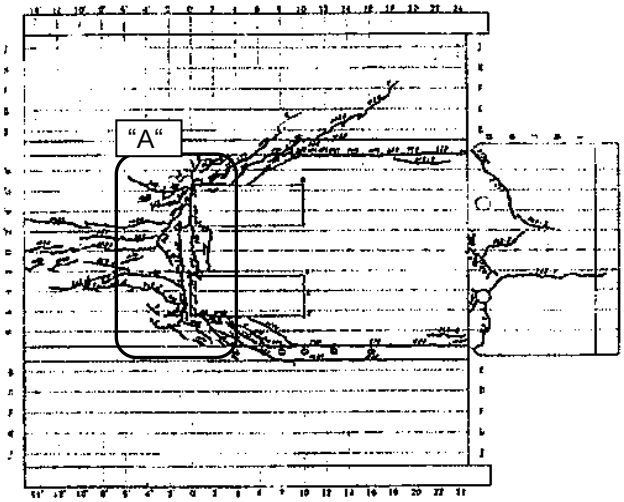


Fig. 7-6: Cracks at upper surface of bottom slab

5 Check of shear in slab

In the truss model shown in Fig. 7-3, vertical members and diagonals are arranged in the slab. However, stirrups were not arranged in the slab of the loading test model, so that these members should be concrete ties. For checking the capacity of the slab a check of the slab for punching is carried out, in accordance with CEB-FIP MC90. The punching force on the slab is induced by the eccentric loading of the horizontal prestressing force, as illustrated in Fig. 7-7.

The result of the check, for the prestressing load of 1.000 kN, is summarized in Table 7-2.

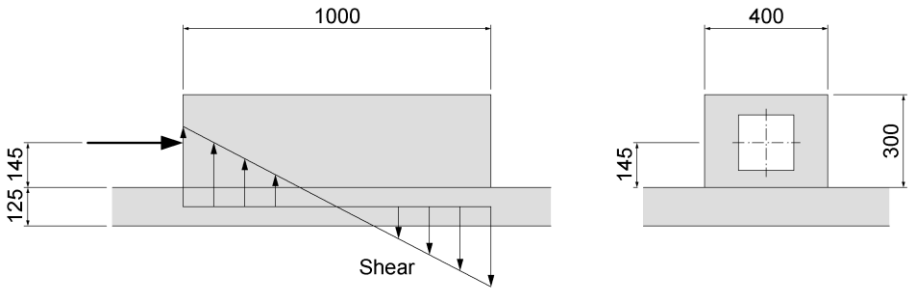


Fig. 7-7: Punching force (dimensions in mm)

This document is the intellectual property of the fib – International Federation for Structural Concrete. All rights reserved.
This PDF of fib Bulletin 61 is intended for use and/or distribution solely within fib National Member Groups.

Table 7-2: Check of slab for punching

Overturning moment : $M_{sd} = P_{sd} \cdot e$	M_{sd} = 1.000 × 0,145 = 145 kNm
Size of anchorage block: c_1, c_2 Effective depth of reinforcing bar: d	c_1 =1,0 *m* c_2 =0,4 *m* d =0,092 *m* (Longitudinal direction)
Parameter of control perimeter : $W_1 = \frac{c_1^2}{2} + c_1 c_2 + 4c_2 d + 16d^2 + 2\pi d c_1$	$W_1 = \frac{1{,}0^2}{2} + 1{,}0 \times 0{,}4 + 4 \times 0{,}4 \times 0{,}092 + 16 \times 0{,}092^2 + 2\pi \times 0{,}092 \times 1{,}0$ = 1,761 m^2
Coefficient for block dimension: K	0,75 (c_1 / c_2 = 2,5)
Shear stress : $\tau_{sd} = \frac{KM_{sd}}{W_1 d}$	$\tau_{sd} = \frac{0{,}75 \times 145}{1{,}761 \times 0{,}092}$ = 671 *kN/m²* = 0,67 MPa
Reinforcement ratio: ρ (Longitudinal direction)	0,68 %
Resistant shear stress $\tau_{rd} = 0{,}12\xi(100\rho f_{ck})^{1/3}$ where $\xi = 1 + \sqrt{200/d}$ ($\leq 2{,}0$)	$\xi = 1 + \sqrt{200/92}$ = 2,47 $\rightarrow$ 2,0 $\tau_{rd} = 0{,}12 \times (100 \times 0{,}0068 \times 49)^{1/3}$ = 0,77 *MPa*

The shear stress, τ_{sd}, for the prestressing load of 1.000 kN is smaller than the resistant shear stress, τ_{rd}. In estimating the resistant shear stress in the above check, the reinforcing bars only in the direction are taken into account. However, these longitudinal reinforcing bars have to resist the longitudinal tension as well as this punching. Therefore, it can be considered that the yield of the reinforcing bars in the area "A" caused a complex failure of the slab, due to the punching and axial tension, in the loading test. It is considered that the three-dimensional strut-and-tie model adopted in this example could predict this complex failure mode.

6 Supplementary remarks

As mentioned in Section 1, the experimental study carried out by the Japan Ministry of Land, Infrastructure, and Transport, and Japan Prestressed Concrete Contractors Association included a test case with the anchorage blocks arranged at the corner of the bottom slab and web. An elastic finite element analysis was carried out in the design of this test model. Based on this analysis, the reinforcing bars in and around the anchorage block were arranged so that the stresses of the reinforcing bars, assuming to carry all the tensions, do not exceed 180 MPa for the prestressing load of 868 kN (= 0,7·P_u). In the loading test of this case, the anchorage withstood the prestressing load of 1.350 kN without serious damages. The reinforcing bar arrangement of the test model taken in this example (anchorage block arranged on the bottom slab) is almost same as the above-mentioned test model (arranged at the corner). These test results indicate that the anchorage blocks arranged at the corner can provide higher capacities. Although the test model with anchorage blocks at the corner has not been taken in this example, a design example of the strut-and-tie model for an anchorage block at the corner has been presented in *fib* Bulletin 16 (2002).

This document is the intellectual property of the fib – International Federation for Structural Concrete. All rights reserved.
This PDF of fib Bulletin 61 is intended for use and/or distribution solely within fib National Member Groups.

Negative reaction (uplift) occurs at the rear side of the line support under the web, in this calculation for the prestressing load. The dead load of the test model is not taken into account in this calculation. Actually, in the loading test, the positive reaction due to the dead load would cancel the uplift due to the prestressing, although this fact has not been confirmed because detailed information for the reaction in the loading test is not available.

In this calculation, the total tension at the rear side of the anchorage block (area "A") was 20% of the total prestressing load. According to Section 6.5.7.3 of the FIP Recommendations (1999), the tension at the rear side of an anchorage can be estimated as about 25% of the prestressing load. In this example, the end of the slab at the rear side is assumed free in the horizontal direction. It may be the main reason that the calculated tension in this example is slightly smaller than estimated from the FIP Recommendations.

7 Conclusions

In this example the three-dimensional strut-and-tie model was applied to an anchorage block for a prestressing tendon arranged on the bottom slab of a box-girder. The analytical result was compared with the loading test result. In this study, the failure mode of the anchorage predicted by the strut-and-tie model was similar with the observed failure mode in the loading test result. Although the calculated capacity does not satisfactorily predict the loading test result, this example has proved that the strut-and-tie model would be useful for evaluating the capacities of anchorages for external prestressing tendons appropriately on the safe side. More precise estimation of the capacity may be possible with further study and modification of the model.

References

FIP Recommendations (1999): Practical Design of Structural Concrete.
FIP-Commission 3 "Practical Design", Sept. 1996. Publ.: SETO, London, Sept. 1999.
(Distributed by: *fib*, Lausanne. Web http://www.fib-international.org)

Nishikawa *et.al* (2001) : Study for Shape and Arrangement of Bar about Bracket of External Tendons, 11th Symposium for Developments of Prestressed Concrete, Japan Prestressed Concrete Engineering Association, 2001. (In Japanese)

CEB-FIP MC 90 (1993): Design of concrete structures. CEB-FIP-Model-Code 1990.
Thomas Telford, 1993

fib Bulletin 16 (2002): Design Examples for the FIP Recommendations "Practical design of structural concrete". *fib*, Lausanne. January 2002

This document is the intellectual property of the fib – International Federation for Structural Concrete. All rights reserved.
This PDF of fib Bulletin 61 is intended for use and/or distribution solely within fib National Member Groups.

Example 8: Suspended precast RC member

Ľudovít Fillo, Jaroslav Halvoník

1 Description of structure and design task

1.1 General

A three-span bridge with field lengths of 14,5 m +24,0 m +14,5 m (Fig. 8-1) has a prismatic cross-section composed of three precast beams connected with cast-in-situ concrete. The main precast beams, three inverted T-shaped pre-tensioned beams with a length of 23,2 m and 13,6 m, respectively, with a depth of 1,1 m (Fig. 8-2), support precast RC members, which are horizontally suspended steel ties anchored over the central main precast beams, serving as moulds for casting. The casting of the bridge was divided into two stages. In the first the space between the webs of the main precast beams was filled with concrete. After hardening of concrete, four 13-strand tendons located among the main beams were stressed. As a result three simply supported beams changed into a continuous system. In the next stage the area over the suspended RC members was cast and the other four 13-strand tendons among the main beam were stressed.

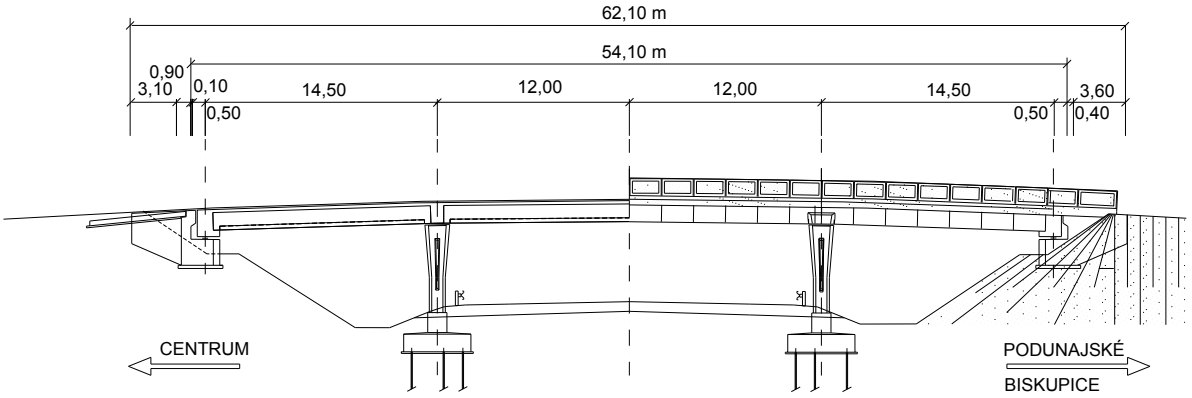


Fig. 8-1: Side section of the bridge

1.2 Geometry and loads

The suspended RC members serve two major functions in the structure (Fig. 8-2). The first is to offer a permanent mould for casting of the bridge during construction. The second is the architectural component, which provides the structure-required shape and the surface-required texture of the wood - an image of the cast-in-place concrete structure (Fig. 8-3 and 8-4). The suspended RC members have the width of 2 m and they are stiffened by two ribs.

This document is the intellectual property of the fib – International Federation for Structural Concrete. All rights reserved.
This PDF of fib Bulletin 61 is intended for use and/or distribution solely within fib National Member Groups.

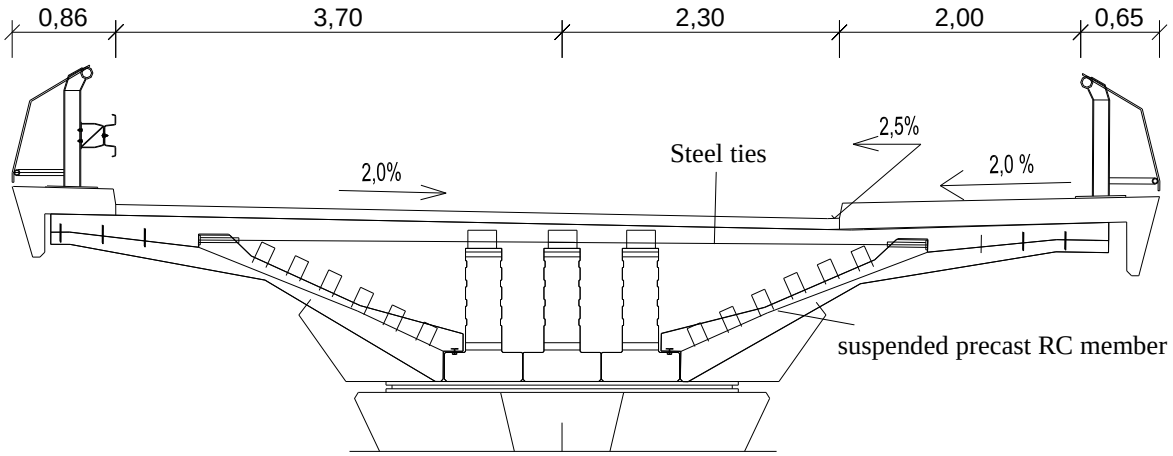


Fig. 8-2: Cross-section of the bridge



Fig. 8-3: Suspended precast RC member



Fig. 8-4: Stored precast RC members

This document is the intellectual property of the fib – International Federation for Structural Concrete. All rights reserved.
This PDF of fib Bulletin 61 is intended for use and/or distribution solely within fib National Member Groups.

The minimum depth of the slab is 100 mm and of the ribs 150 mm, respectively (Fig. 8-5). The suspended RC members were supported on the lower flange of the main precast beam via short corbels (Fig. 8-2). The gap between a web of the precast beam and the head of the corbel was filled by mortar, in order to provide the joint with the capacity to transmit compressive force. The precise geometry of the suspended RC member is presented in Fig. 8-5.

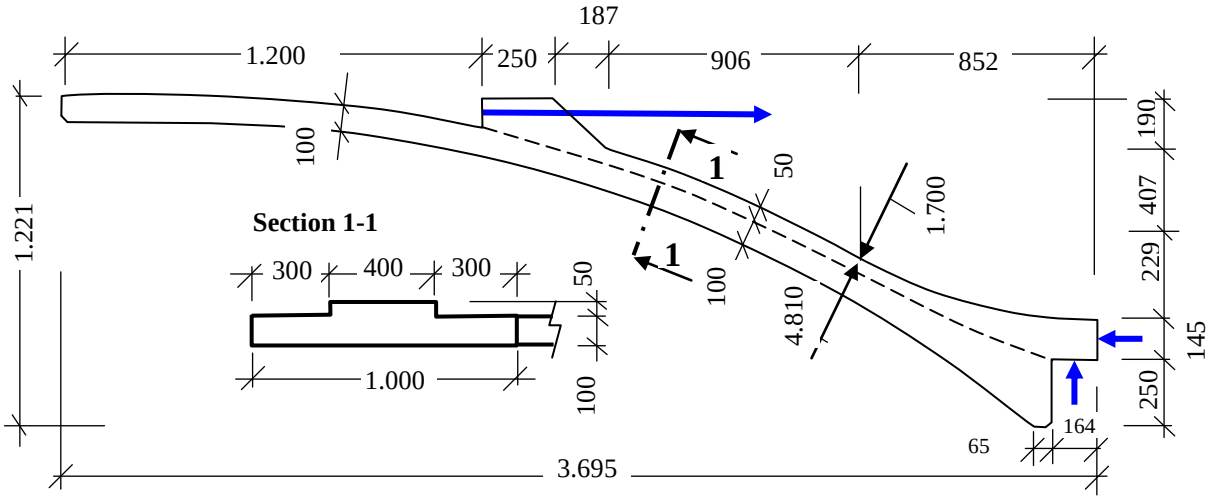


Fig. 8-5: Geometry and support conditions for suspended RC member (dimensions in mm, and m with decimal point; decimal is point instead of comma – see Editorial Comments on page vi.)

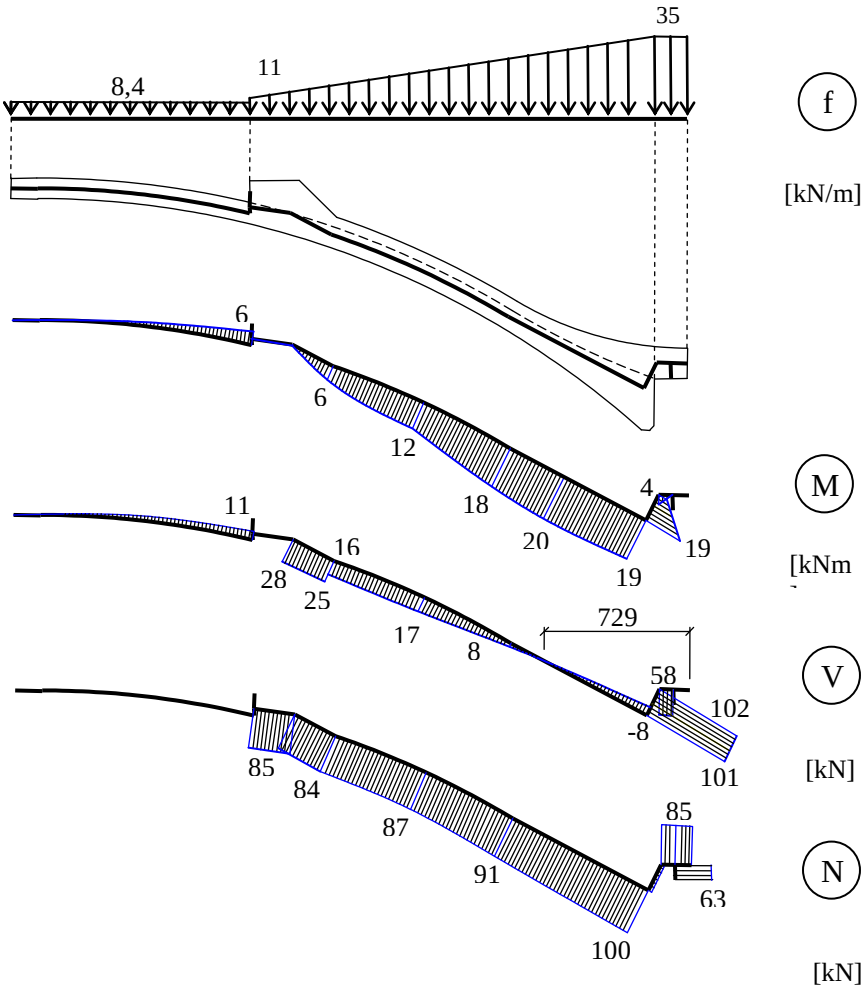


Fig. 8-6: Internal forces M,V,N

This document is the intellectual property of the fib – International Federation for Structural Concrete. All rights reserved.
This PDF of fib Bulletin 61 is intended for use and/or distribution solely within fib National Member Groups.

The suspended RC members have to bear their self-weight and the hydrostatic pressure of fresh concrete during casting. The maximum height of the fresh concrete was 1,06 m and the minimum 0,15 m at the end of the slab. Density of the fresh concrete was assumed 26 kN/m^3. The design dead and permanent loads acting on half of the suspended RC member are shown in Fig. 8-6.

1.3 Design values for materials

Concrete: C35/45 f_{ck}= 35 MPa

The capacity of a parallel compression field of a strut-and-tie model is reduced to an effective strength $f_{cd,eff}$. In the case of a compression chord in a beam with a linear strain distribution a rectangular stress block is used over the full depth of the compression zone $f_{cd,eff}$ is:

$$f_{cd,eff} = \nu_1 f_{1cd} = \left(1 - \frac{f_{ck}}{250}\right)\alpha \frac{f_{ck}}{\gamma_c} = \left(1 - \frac{35}{250}\right) 0{,}85 \frac{35}{1{,}5} = 17{,}1 \text{ MPa}$$

The capacity of struts transferring compression stress across cracks with normal width, e.g. in a web of a beam:

$$f_{cd,eff} = \nu_2 f_{1cd} = 0{,}6 \cdot 0{,}85 \frac{35}{1{,}5} = 11{,}9 \text{ MPa}$$

$$f_{1ct,d} = \frac{f_{ctm}}{\gamma_{ct}} = \frac{3{,}2}{1{,}8} = 1{,}8 \; MPa$$

Reinforcing steel B 500B (10505 -R)

f_{yk} = 500 MPa f_{yd}= f_{yk} / γ_s = 500 /1,15 = 435 MPa

1.4 Statement of design problem

The present example presents the design of a suspended RC member employing the strut-and-tie model approach. Two D-regions are analysed, one near the top support in the vicinity of suspension rod anchorage (Detail A in Fig. 8-7) and another corbel type D-region at the lower support (Detail B in Fig. 8-7).

2 Design procedure

2.1 Trajectories of principal stresses

Trajectories of principal stresses were calculated and depicted for the two above defined D-regions in Fig. 8-8 for detail A, and Fig. 8-9 for detail B. By tracing the trajectories, strut-and-tie models were prepared for design.

2.2 Strut-and-tie model

Due to the low magnitude of the shear force and the existence of normal force, the minimal inclination of diagonals in the lover beam part of the suspended RC member reinforced with stirrups was assumed at 23°.

The inclination of the struts in the cantilever slab without shear reinforcement – upper part of the member – was assumed at 30° and the ties are perpendicular to it, according to the model for members without shear reinforcement, see Fig. 6.40 in the FIP Recommendations (1999).

This document is the intellectual property of the fib – International Federation for Structural Concrete. All rights reserved.
This PDF of fib Bulletin 61 is intended for use and/or distribution solely within fib National Member Groups.

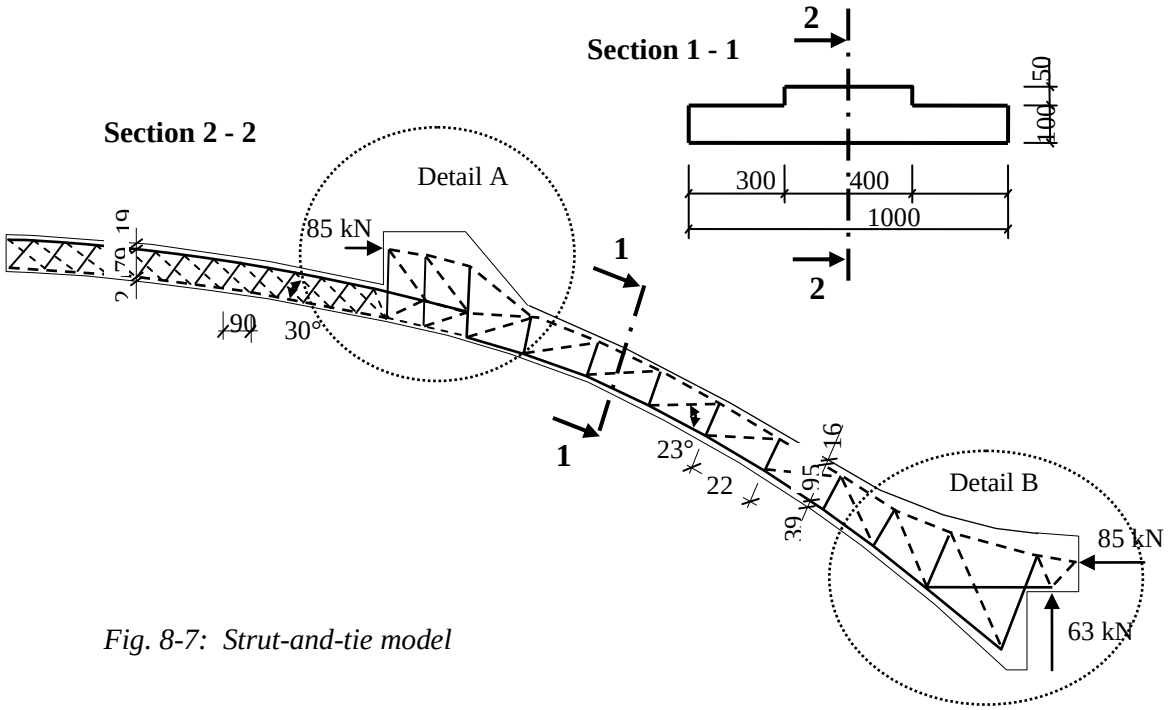


Fig. 8-7: Strut-and-tie model

2.3 Design

2.3.1 Design of slab – detail A

One-way spanning slab without transverse reinforcement with a biaxial tension – compression chord (Fig. 8-7 and 8-8).

- Compression chord F_{cd} = 68 kN

$$x = \frac{F_{cd}}{b_w f_{cd,eff}} = \frac{0{,}068}{1{,}0 \cdot 17{,}1} = 0{,}0040 \text{ m}$$

- Tension chord F_{sd} = 78 kN

$A_{s1} = F_{td} / f_{yd} = 0,\ 078 / 435 = 0{,}000\ 179\ m^2$ (∅8 – á150) → 330 mm^2

- Design shear capacity assessed by empirical formula:

$$d = h - a = 100 - 19 = 81 \text{ mm};\quad \kappa = 1 + \sqrt{\frac{200}{d}} = 2{,}57 \rightarrow 2;$$

$\rho_l = A_s/b_w d = 330/1000 \cdot 81 = 0{,}0041$

$$V_{Rd} = \left(0{,}10\ \kappa\ \sqrt[3]{100\rho_1 f_{ck}}\right) b_w d = \left(0{,}10 \cdot 2\sqrt[3]{100 \cdot 0{,}0041 \cdot 35}\right) 1 \cdot 0{,}081 = 0{,}039 \text{ MN} > V_{Ed} = 0{,}011 \text{ MN}$$

2.3.2 Design of T-beam – detail B

Concrete T-beam with transverse reinforcement and tension – compression chord (Fig. 8-8- and 8-9).

- Compression chord F_{cd} = 227 kN $\quad x = \frac{F_{cd}}{b_w f_{cd,eff}} = \frac{0{,}227}{0{,}4 \cdot 17{,}1} = 0{,}033 \text{ m}$

$$z = h - a - 0{,}5x = 150 - 39 - 0{,}5 \cdot 0{,}033 = 95 \text{ mm}$$

This document is the intellectual property of the fib – International Federation for Structural Concrete. All rights reserved.
This PDF of fib Bulletin 61 is intended for use and/or distribution solely within fib National Member Groups.

- Tension chord $F_{td} = 140$ kN

$A_{s1} = F_{td} / f_{yd} = 0{,}140 / 435 = 0{,}000\,322$ m^2 (4∅8 + ∅6 á 150) → 391 mm^2

- Diagonal strut $F_{cd} = 58$ kN

$$\sigma_{cd} = \frac{F_{cd}}{b_w z \cos\theta} = \frac{0{,}058}{0{,}4 \cdot 0{,}095 \cdot \cos 23^\circ} = 1{,}7 \text{ MPa} < f_{cd,eff} = 11{,}9 \text{ MPa}$$

- Stirrups – vertical ties $F_{td} = 25$ kN

$s_{max} = 0{,}75d = 0{,}75 \cdot 111 = 83$ mm s = 80 mm

$A_{sw} = F_{td}\, s / (z\, f_{yd}) = 0{,}025 \cdot 0{,}08 / (0{,}095 \cdot 435) = 0{,}000\,048$ m^2 (4∅6) → 113 mm^2

- Steel ties $F_{td} = 44$ kN

$A_s = F_{td} / f_{yd} = 0{,}044 / 435 = 0{,}000101$ m^2 (4∅6) → 113 mm^2

- Diagonal strut $F_{cd} = 83$ kN

$$\sigma_{cd} \approx \frac{F_{cd}}{b_w z \cos\theta} = \frac{0{,}083}{0{,}4 \cdot 0{,}095 \cdot \cos 23^\circ} = 2{,}4 \text{ MPa} < f_{cd,eff} = 11{,}9 \text{ MPa}$$

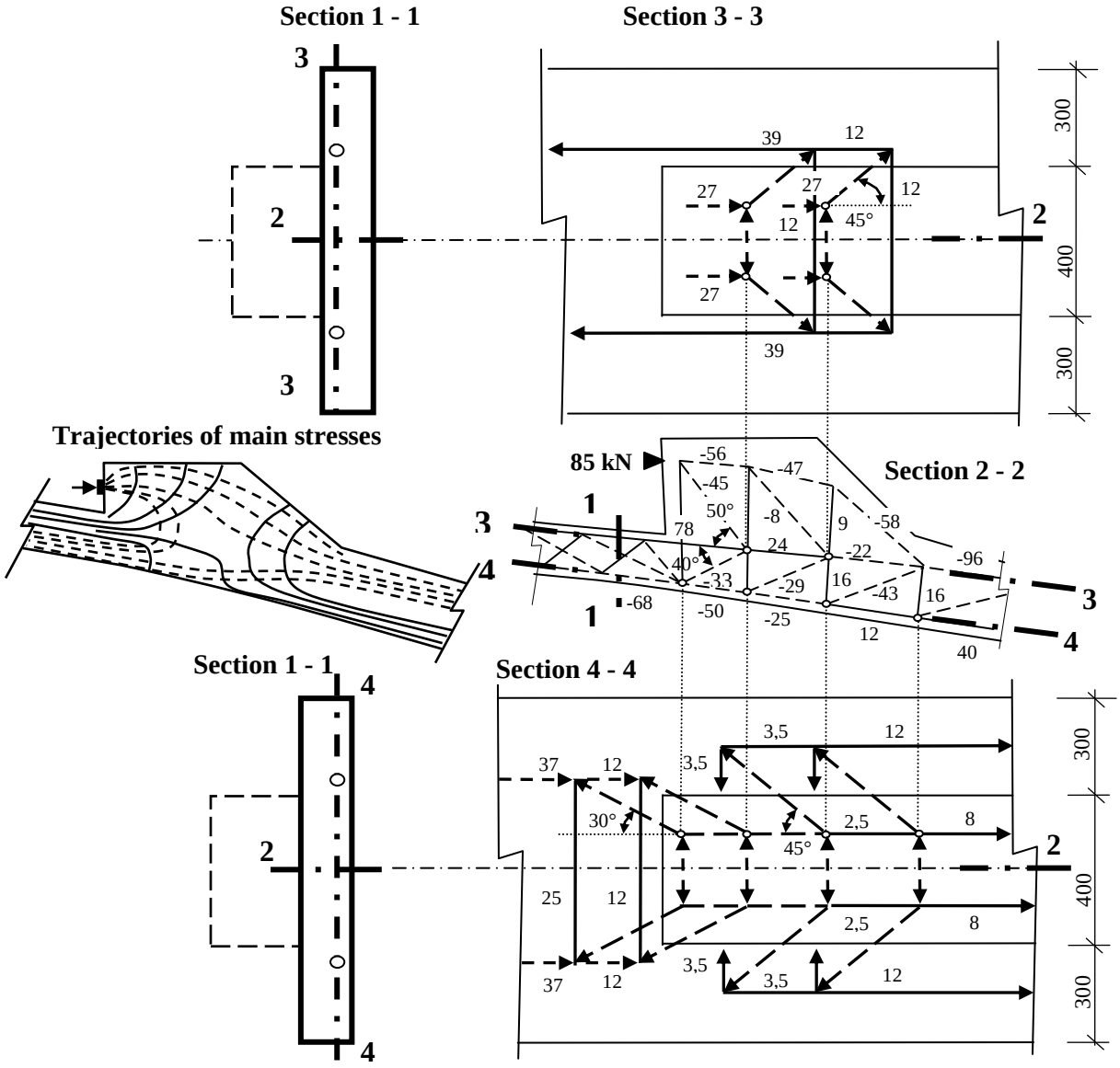


Fig. 8-8: Strut-and-tie models (detail A) –three sections- trajectories

This document is the intellectual property of the fib – International Federation for Structural Concrete. All rights reserved.
This PDF of fib Bulletin 61 is intended for use and/or distribution solely within fib National Member Groups.

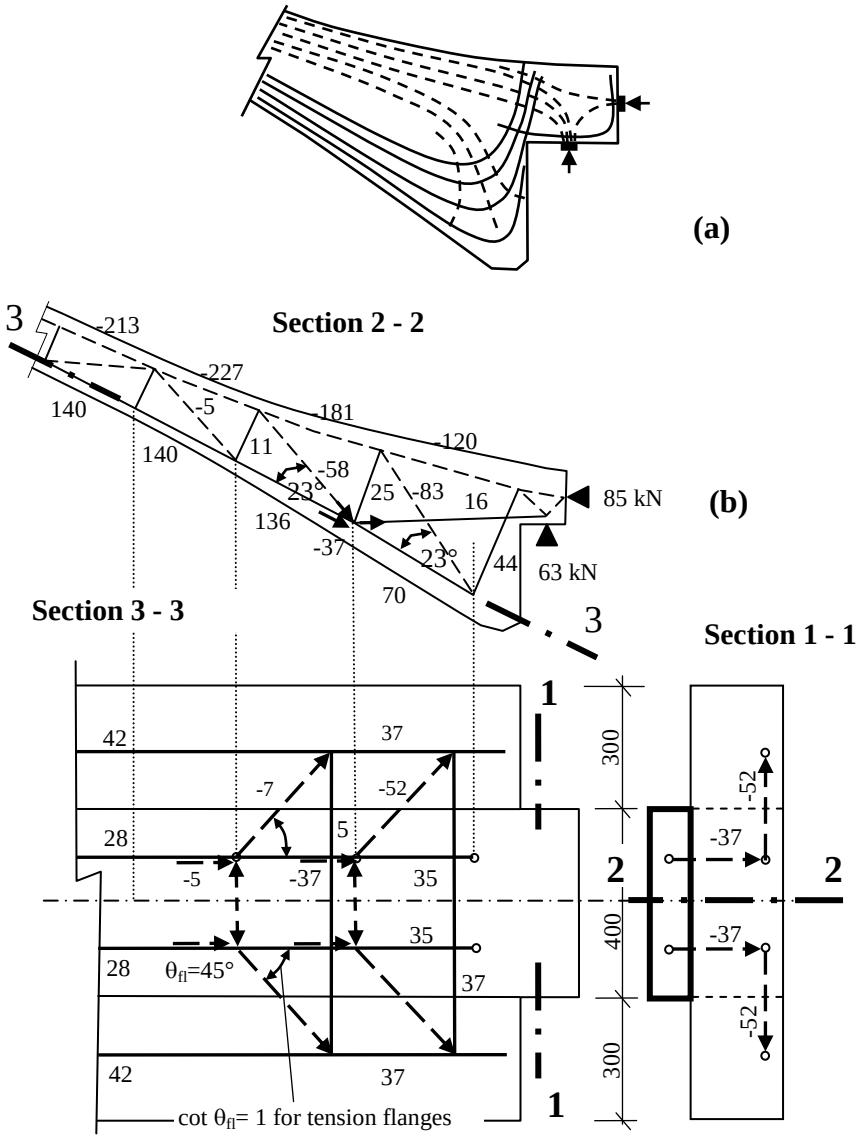


Fig. 8-9: Detail B: a) trajectories of main stresses
b) strut-and-tie model -slab forces

2.4 Detailing

The reinforcement layout is shown in Fig. 8-10.

This document is the intellectual property of the fib – International Federation for Structural Concrete. All rights reserved.
This PDF of fib Bulletin 61 is intended for use and/or distribution solely within fib National Member Groups.

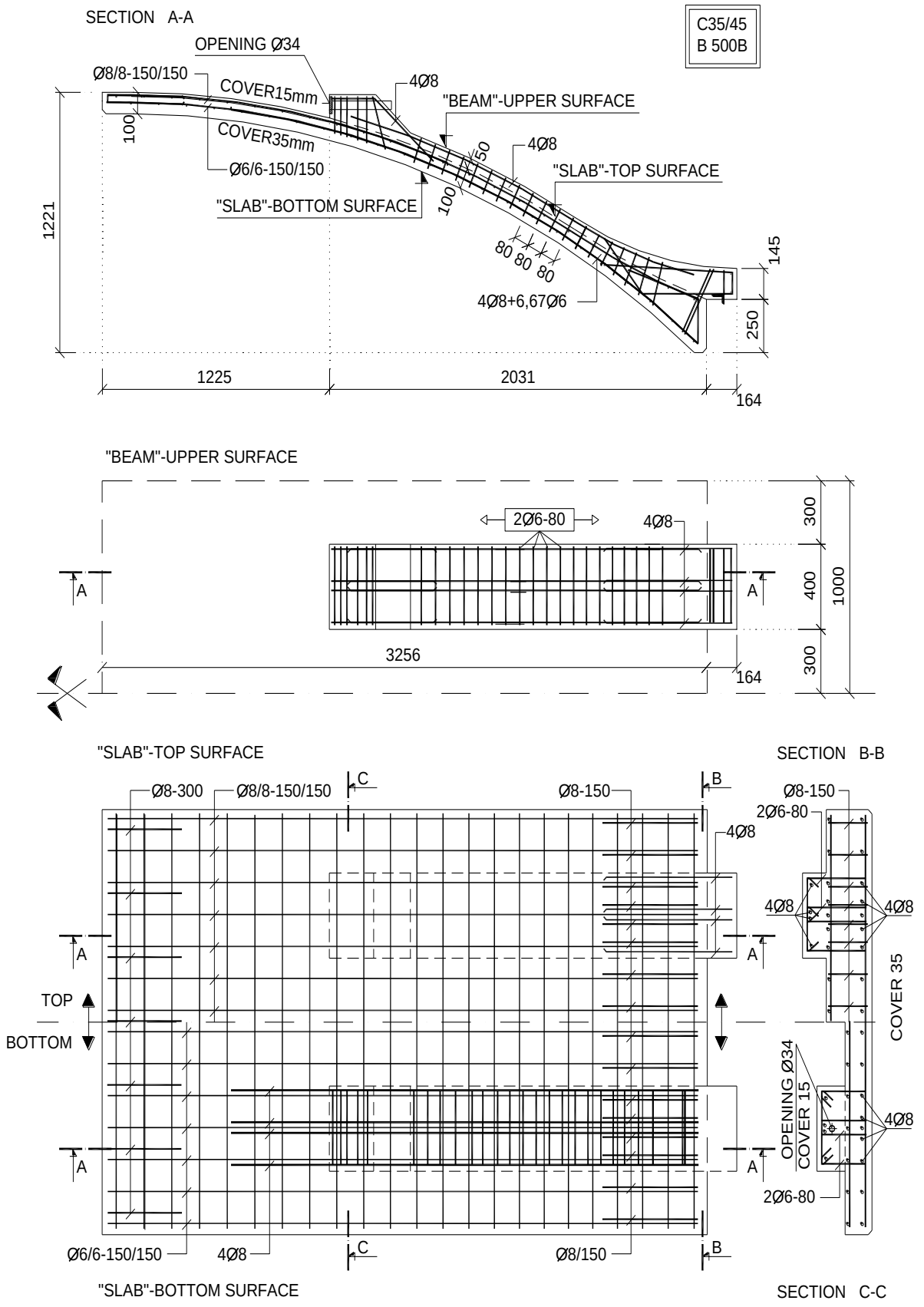


Fig. 8-10: Slab reinforcement configuration

This document is the intellectual property of the fib – International Federation for Structural Concrete. All rights reserved.
This PDF of fib Bulletin 61 is intended for use and/or distribution solely within fib National Member Groups.

3 Summary and conclusions

A suspended precast RC member of special shape was designed by strut-and-tie models. The simplified strut-and-tie model of the whole suspended RC member is presented in detail for two discontinuity-regions for which the resulting reinforcement layout is also provided.

Notation

f_{ck} = characteristic cylinder strength

f_{1cd} = the uniaxial design strength of concrete

$f_{cd,eff}$ = the effective concrete strength in a compression chord of a beam = $\nu_1 f_{1cd}$

$f_{cd,eff}$ = the effective concrete strength for struts transferred across cracks = 0,6 f_{1cd}

$f_{1ct,d}$ = the design value for uniaxial tensile strength of concrete

References

fib Bulletin 16 (2002): Design Examples for the FIP Recommendations "Practical design of structural concrete". *fib*, Lausanne. January 2002

FIP Recommendations (1999): Practical Design of Structural Concrete. FIP-Commission 3 "Practical Design", Sept. 1996. Publ.: SETO, London, Sept. 1999. (Distributed by: *fib*, Lausanne. Web http://www.fib-international.org)

Reineck, K.-H. (2002): (Editor): Examples for the Design of Structural Concrete with Strut-and-Tie Models. ACI SP-208 (2002), ACI, Farmington Hills, MI

Schlaich, J.; Schäfer, K; Jennewein, M. (1987): Toward a consistent design for structural concrete. PCI-Journ. V.32 (1987), No.3, 75-150

This document is the intellectual property of the fib – International Federation for Structural Concrete. All rights reserved.
This PDF of fib Bulletin 61 is intended for use and/or distribution solely within fib National Member Groups.

This document is the intellectual property of the fib – International Federation for Structural Concrete. All rights reserved.
This PDF of fib Bulletin 61 is intended for use and/or distribution solely within fib National Member Groups.

Example 9: Connection Between Prefabricated Beams

Miguel S. Lourenço, José N. Camara

1 Presentation of the structure

1.1 Description of the structure

The SATU (Automated System of Urban Transportation) project was developed for a new concept of urban transport. It is a fully automated vehicle grips within a moving cable, having the power source in one end of the system. In order to avoid obstruction with other infrastructure systems, it runs over a viaduct. The first phase of the development has a total extension of 1.200 m, with three stations and two connecting viaducts. One of the viaducts, connecting two main stations, has an extension of 337,5 m, with current spans of 30,0 m and 35,0 m (see Fig. 9-1) with significant plan curvature.

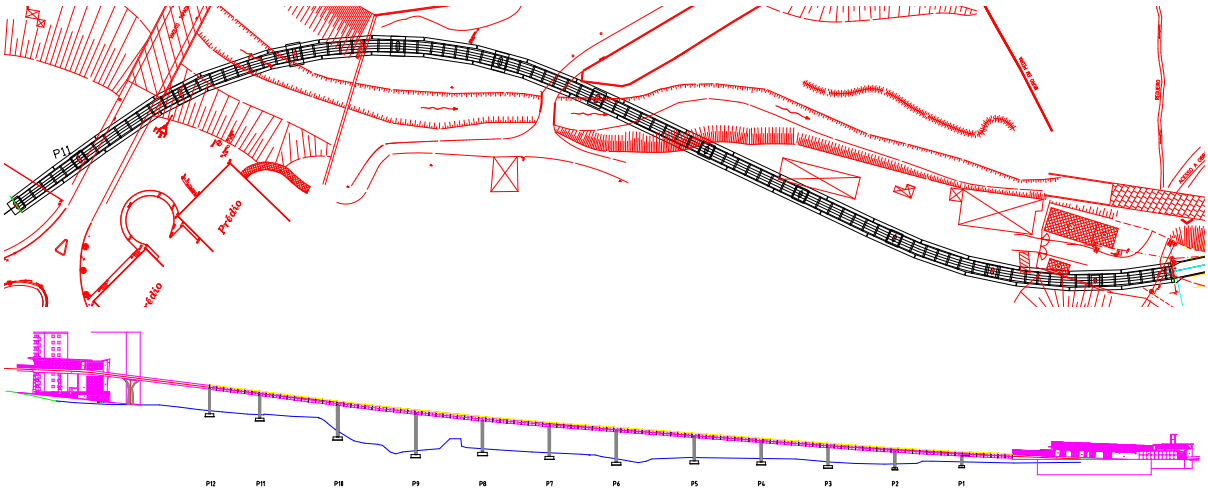


Fig. 9-1: Plan and elevation of viaduct 1

The viaducts superstructure (see Fig. 9-2) is characterized by two parallel prefabricated beams, connected at the bottom by a 0,25 m thick slab. The beams have an "I" cross section with a height of 1,70 m, a 1,00 m width flange and 0,25 m thick web. Transversally they are 4,45 m spaced apart and directly supported at the piers on "pot" type bearings.

The superstructure is fully continuous on its total length. Structural continuity was ensured, in general, by cast-in-situ joints between the pre-fabricated beams, over the supports. In the zones with higher plan curvatures, post-tensioned bars connecting the longitudinal beams were adopted at approximately 1/5 of the main spans. The connection geometry is shown in Figs. 3 to 5.

This document is the intellectual property of the fib – International Federation for Structural Concrete. All rights reserved.
This PDF of fib Bulletin 61 is intended for use and/or distribution solely within fib National Member Groups.

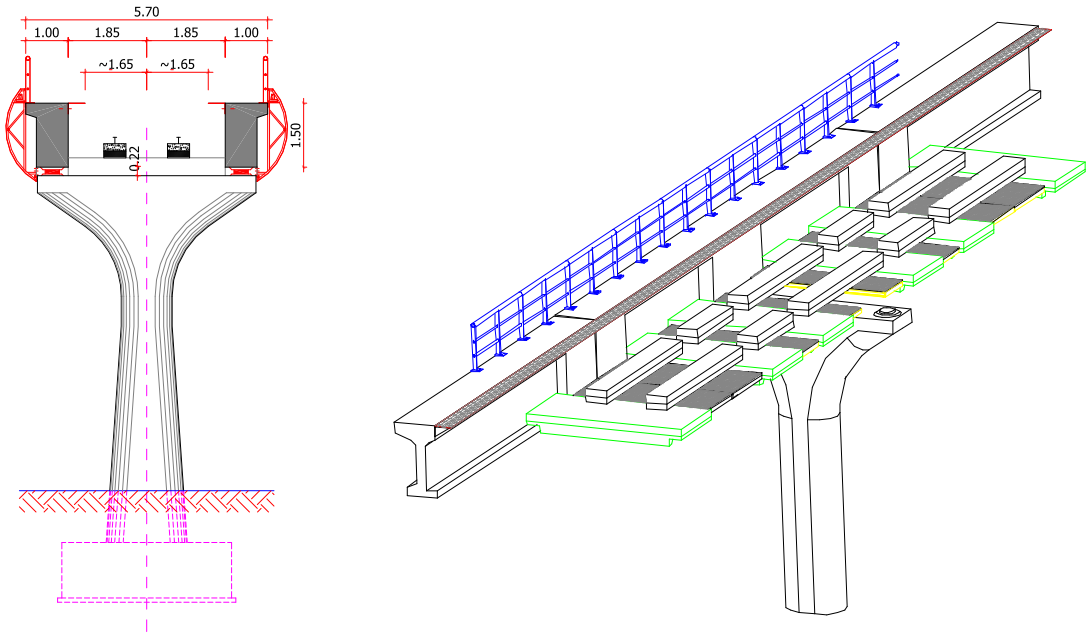


Fig. 9-2: Deck section and 3D view
(decimal point instead of comma; see Editorial Comments on p. vi)

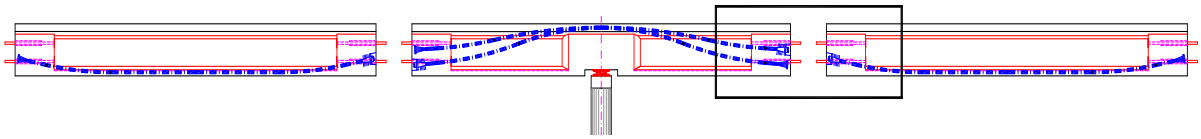


Fig. 9-3: Prestressing layout

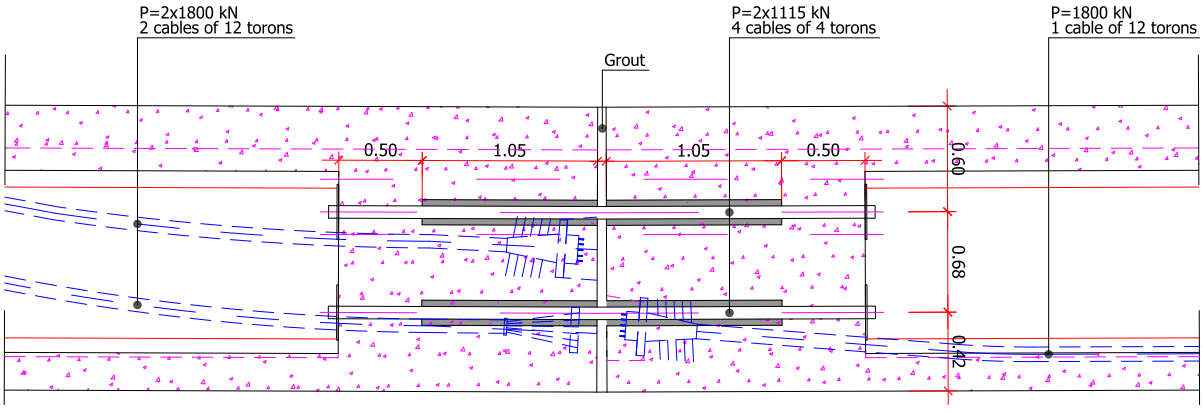
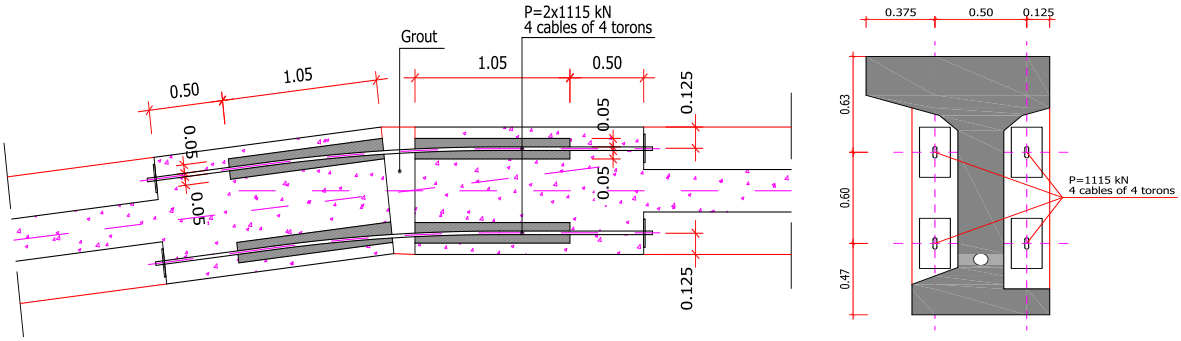


Fig. 9-4: Side view of connection
(decimal point instead of comma; see Editorial Comments on p. vi)

This document is the intellectual property of the fib – International Federation for Structural Concrete. All rights reserved.
This PDF of fib Bulletin 61 is intended for use and/or distribution solely within fib National Member Groups.



a) plan view of the connection *b) cross-section of beams*

Fig. 9-5: Plan view of connection between prefabricated beams and cross-section of beams (decimal point instead of comma; see Editorial Comments on p. vi)

1.2 Description of the design task

1.2.1 Loads for the construction phase and ultimate limit state

The loads for the construction phase are shown in Fig. 9-6. For the construction phase, temporary columns were placed near the connection, thus only equivalent loads from prestressing cables must be considered.

For the ultimate limit state, the shear and bending due to vehicle and self weight of the deck must be considered. The B-region analysis leaded to the loads presented in Fig. 9-6 in the cross sections adjacent to the D-region. Note that, close to 1/5 of the span, the bending moments are low and changes sign from the left side to the right side.

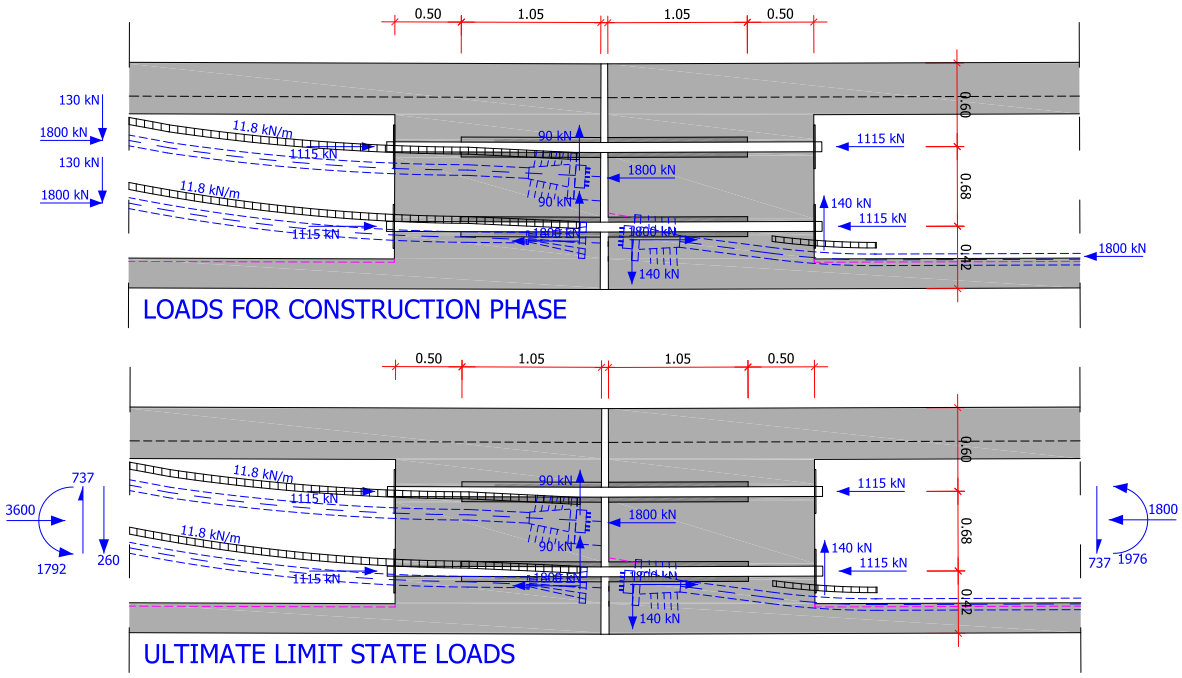


Fig. 9-6: Loads and stresses for both construction and ULS phases (decimal point instead of comma; see Editorial Comments on p. vi)

This document is the intellectual property of the fib – International Federation for Structural Concrete. All rights reserved.
This PDF of fib Bulletin 61 is intended for use and/or distribution solely within fib National Member Groups.

1.2.2 Design values for materials

Concrete: C45/55 $f_{cd} = \frac{f_{ck}}{\gamma_c} = \frac{45}{1,5} = 30\,\text{MPa}$; $f_{1cd} = 0,85 \times f_{cd} = 25,5\,\text{MPa}$

Steel reinforcement: A500NR f_{syk}=500 *MPa;* $f_{syd} = \frac{f_{syk}}{\gamma_s} = \frac{500}{1,15} = 435\,\text{MPa}$

2 Design procedure

2.1 Strut-and-tie models for the design

To achieve the design strut-and-tie model for the construction phase, a simplified load path was developed (see Fig. 9-7). The cross section is fully compressed at the connection left section even though a small tension occurs on the right side.

The refined strut and tie model shown at Fig. 9-8 is attained by dividing the resultant stresses at the D-region boundary into to several struts. The ties are dimensioned in Table 9-1. The compression fields are shown in Fig. 9-9, and these then join the continuity cables struts, keeping the connection between the two precast beams in compression. The vertical ties result from the anchorage deviation forces.

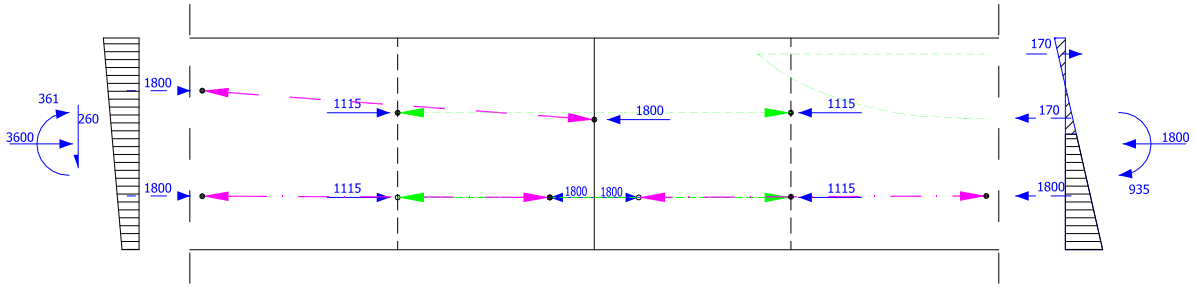


Fig. 9-7: Simplified load paths for construction phase

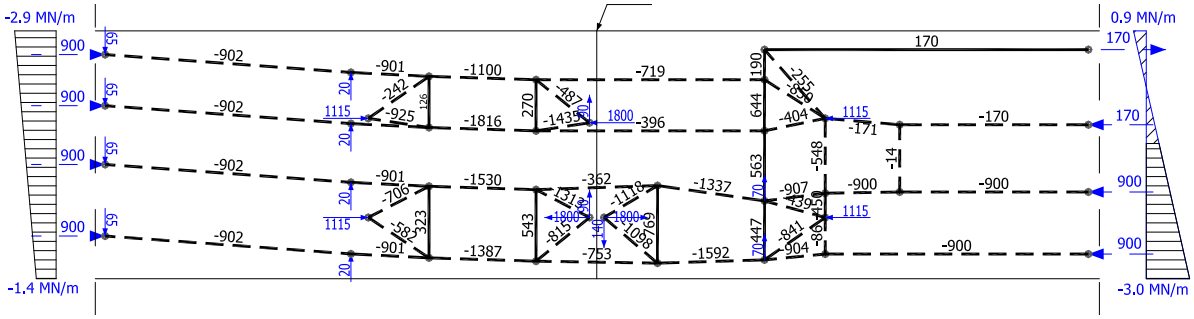


Fig. 9-8: Strut and tie model for construction phase
(decimal point instead of comma; see Editorial Comments on p. vi)

Table 9-1: Tie forces in the construction phase and required and adopted reinforcement

Force *T*	***A*****s**	***A*****s, adopted**	**Reinforcement**
170 kN	391 mm^2	1.407 mm^2	7ϕ16
644/0,4 = 1.610 kN/m	3.701 mm^2/m	4.520 mm^2/m	4×ϕ12//0,10
769/0,4 = 1.923 kN/m	4.419 mm^2/m	4.520 mm^2/m	4×ϕ12//0,10

This document is the intellectual property of the fib – International Federation for Structural Concrete. All rights reserved.
This PDF of fib Bulletin 61 is intended for use and/or distribution solely within fib National Member Groups.

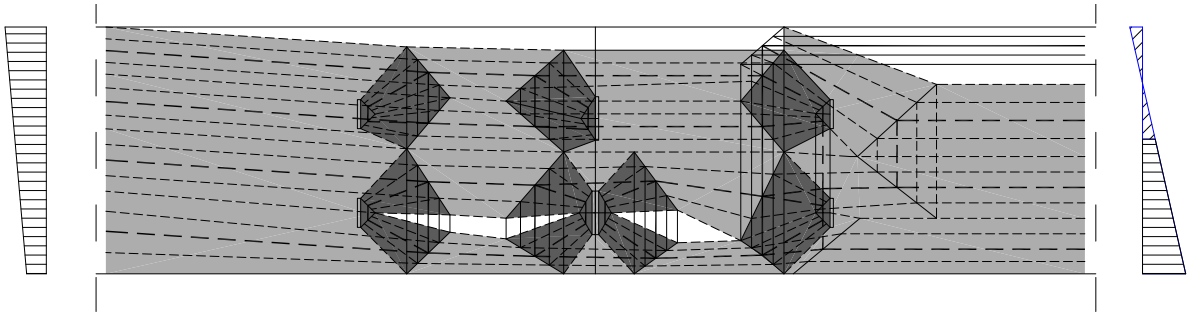


Fig. 9-9: Stress fields for construction phase

The eccentricity of the continuity cables and the connection plan deviation (see Fig. 9-5a) leads to the out of plane strut-and-tie model presented in Fig. 9-10. Note that this analysis is relevant essentially for continuity cables, since remain cables are along the beams plan neutral axis. The ties are dimensioned in Table 9-2. Even though, reinforcement near the joint must predict compression deviation for the remaining load cases.

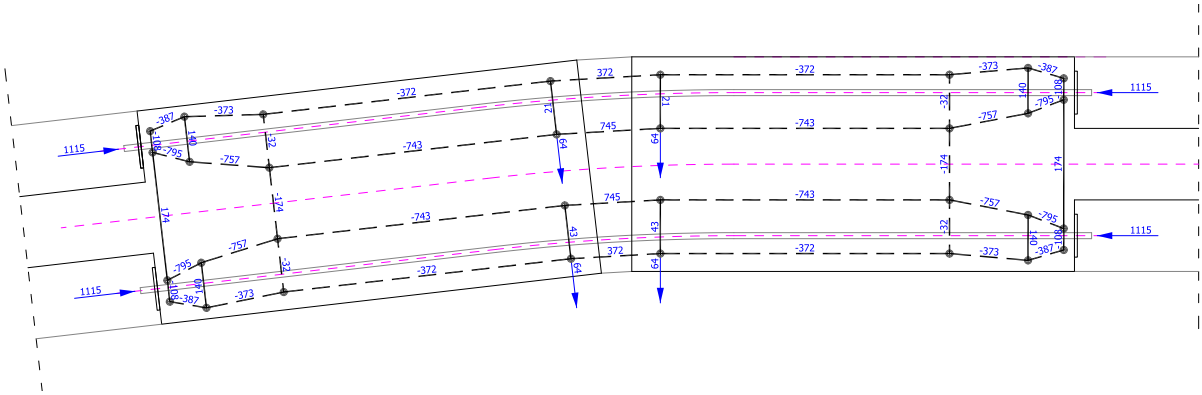


Fig. 9-10: Strut-and-tie model in third direction

Table 9-2: Construction phase tie forces, required and adopted reinforcement (plane model)

Force *T*	A_s	$A_{s,\ adopted}$	**Reinforcement**
174 kN	400 mm^2	804 mm^2	4ϕ16
140 kN	322 mm^2	3.390 mm^2	5×6ϕ12

For the ultimate limit state loads bending and shear modify the flow of forces. The strut-and-tie model should characterize the combinations of two different models, the model shown on Fig. 9-8 and a traditional shear transmission. This combination is presented in Fig. 9-11, and the relevant ties are dimensioned in Table 9-3.

This document is the intellectual property of the fib – International Federation for Structural Concrete. All rights reserved.
This PDF of fib Bulletin 61 is intended for use and/or distribution solely within fib National Member Groups.

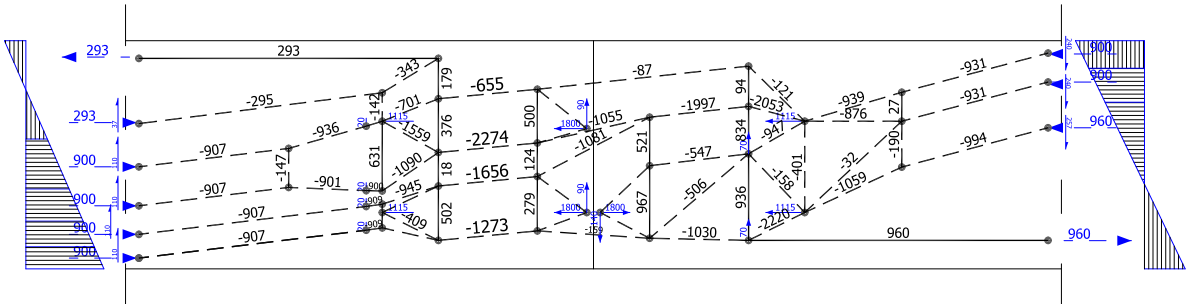


Fig. 9-11: Strut-and-tie model for ultimate limit state

Table 9-3: Tie forces for the ultimate limit state and required and adopted reinforcement

Force *T*	A_s	$A_{s,\,adopted}$	**Reinforcement**
293 kN	674 mm^2	1.407 mm^2	7ϕ16
960 kN	2.207 mm^2	1.796 mm^2+1.680 mm^2 (1)	5ϕ16+7ϕ12
967/0,5 = 1.934 kN/m	4.446 mm^2/m	4.520 mm^2/m	4×ϕ12//0,10

(1) Prestressing cables area ($\Delta\sigma_P$ = 452 *MPa*)

2.2 Check of nodes

In this particular case, the relevant nodes are the regions adjacent to the prestressing anchorage plates. According to sect. 5.6.2 of FIP Recommendations (1999) the concrete strength is given by $\sigma_{c,max} = 1,2\, f_{1cd}\sqrt{\frac{A_{c1}}{A_{c0}}} \le 3,88 \cdot f_{1cd}$. The relevant values are:

- for continuity cables (P_0=1.560 kN):

A_{c0}=0,15·0,30 = 0,045 m^2 and A_{c1}=0,25·0,40=0,10 m^2

$$\Rightarrow \sigma_{c,max} = 44,7 \text{ MPa} > 34,7 \text{ MPa}$$

- for beam prestressing cables (P_0=2.340 kN):

A_{c0}=0,31·0,31 = 0,096 m^2 and A_{c1}=0,75·0,75 = 0,56 m^2

$$\Rightarrow \sigma_{c,max} = 98,9 \text{ MPa} > 24,3 \text{ MPa}$$

3 Detailing

The reinforcement layout is shown in Fig. 9-12.

References

FIP Recommendations (1999): Practical Design of Structural Concrete.
FIP-Commission 3 "Practical Design", Sept. 1996. Publ.: SETO, London, Sept. 1999.
(Distributed by: *fib*, Lausanne. Web http://www.fib-international.org)

This document is the intellectual property of the fib – International Federation for Structural Concrete. All rights reserved.
This PDF of fib Bulletin 61 is intended for use and/or distribution solely within fib National Member Groups.

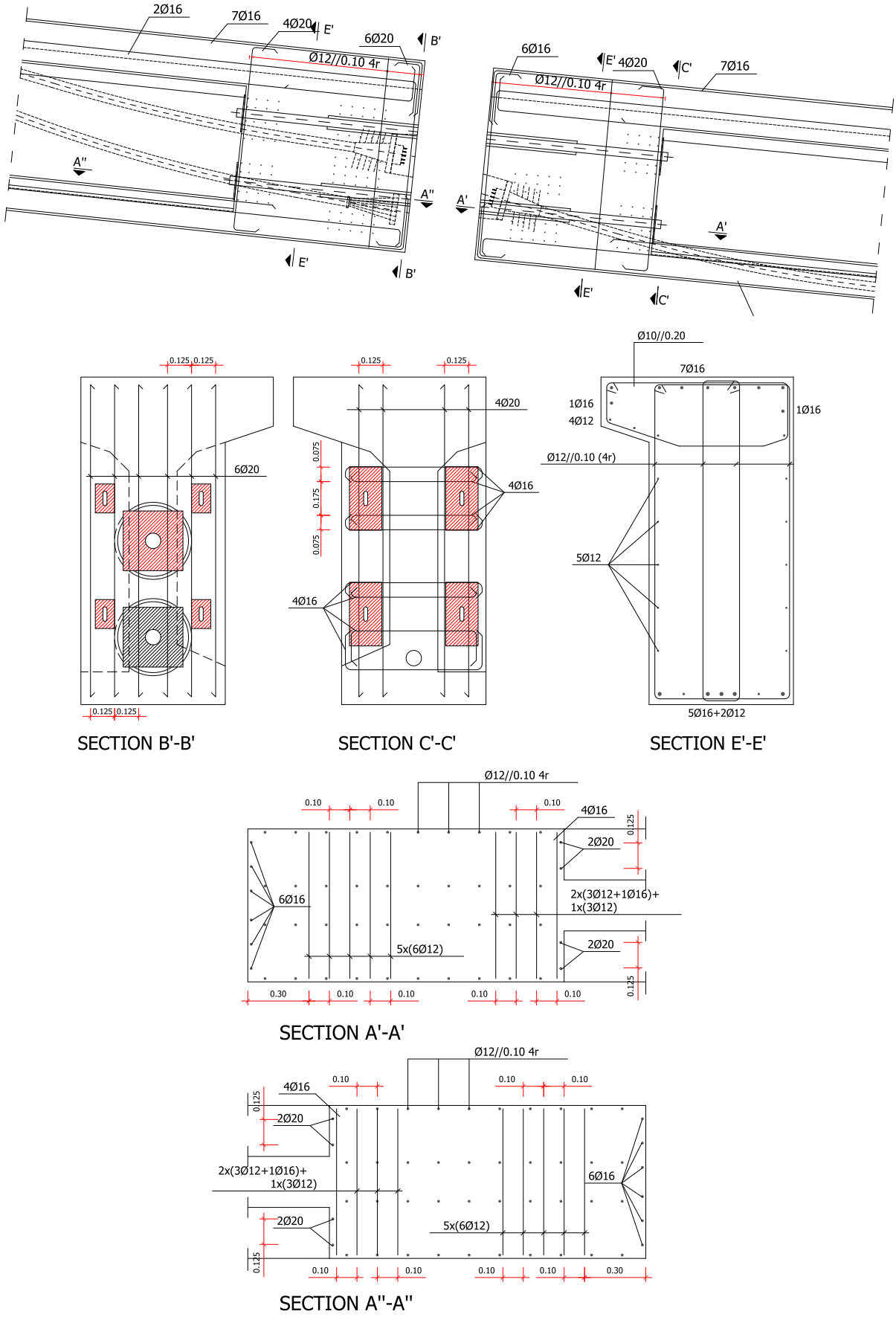


Fig. 9-12 – Connection detailing
(decimal point instead of comma; see Editorial Comments on p. vi)

This document is the intellectual property of the fib – International Federation for Structural Concrete. All rights reserved.
This PDF of fib Bulletin 61 is intended for use and/or distribution solely within fib National Member Groups.

This document is the intellectual property of the fib – International Federation for Structural Concrete. All rights reserved.
This PDF of fib Bulletin 61 is intended for use and/or distribution solely within fib National Member Groups.

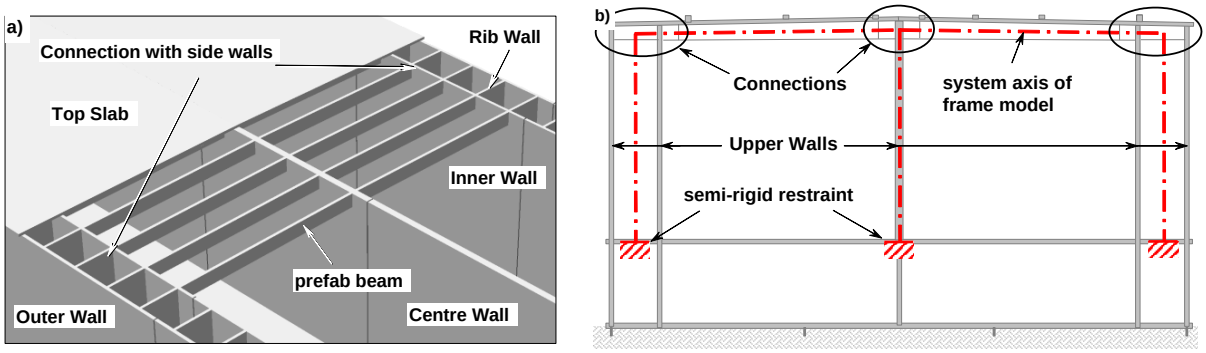
Example 10:
Clamped support of large prefabricated T-girder

Hannes Ludescher

1 Presentation of structure

The D-region presented in this example is part of a large offshore terminal built of reinforced, prestressed concrete. The terminal is a gravity-based structure (GBS) that serves as docking station for large tankers, storage facility and as basis for processing facilities. The two bearing chambers are covered by a roof composed of 35 m long T-girders and the Top Slab, see Fig. 10-1a. Including the 0,5 m thick Top Slab, the girders have a statical height of 3 m and a width of 0,8 m at midspan. In order to facilitate construction, web and lower flange of the T-girders are placed as prefabricated beams. The connections and the Top Slab are cast in place in various casting steps.

In the operational phase, the T-girders are clamped into the supports in order to provide higher stiffness for top side processing facilities. Thus, the girders are part of a frame constituted of the Upper Walls and the Top Slab which stiffens the terminal against transverse loading like waves or tanker impact, see Fig. 10-1b. For the analysis, the structure is sliced in individual frames with a width of 7,5 m corresponding to the beam spacing.



a) spatial view of structural members *b) section*

Fig. 10- 1: Overview over structure

2 Description of design task

D-region design concentrates on the connections at the girder ends. In this example, only the design for closing moments at connections with the side walls is documented. Closing moments result first of all from gravity loads on the Top Slab, but also from the static and dynamic (waves) water pressure on the Outer Walls. Accidental loading situations considered in design include tanker impact, earthquake and blast (explosion).

This document is the intellectual property of the fib – International Federation for Structural Concrete. All rights reserved.
This PDF of fib Bulletin 61 is intended for use and/or distribution solely within fib National Member Groups.

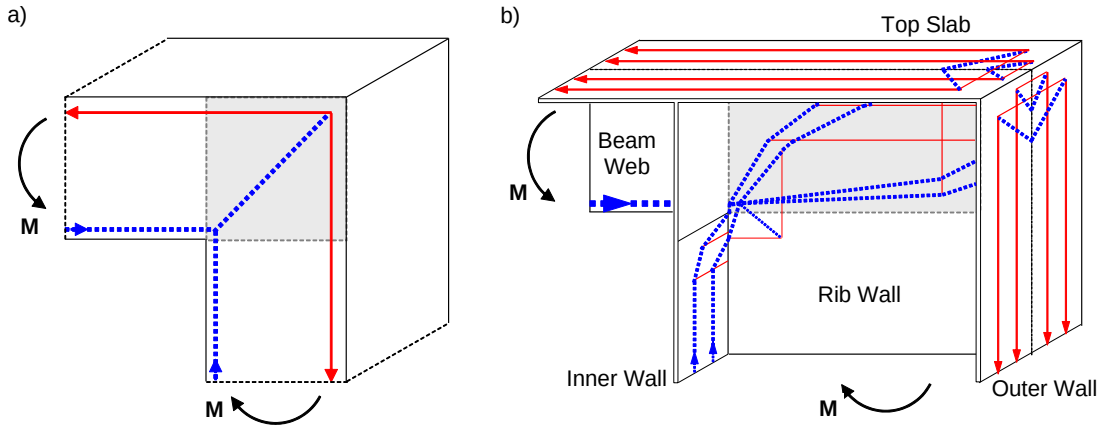
The entire structure is highly prestressed in order to minimise crack width and to increase stiffness. In the slabs and walls, centric prestressing ensures an average compression of 2 to 5 MPa. The T-girders have an average compression of about 6 MPa. For this reason, the structural elements behave in a relatively brittle manner and no redistribution of action effects is considered. Instead, section forces obtained from linear elastic analysis are used for design.

3 Qualitative modelling

The decomposition of the connection in various panels and the important contribution of prestressing make strut-and-tie modelling challenging. In order to have a sound basis, the design models are derived from simple, generic models for massive connections, see Fig. 10-2a. Fig. 10-2 b shows a connection with the actual geometry. The model illustrates that the various struts and ties are located in different planes. They have to be deviated to the main panel linking them before equilibrium can be established. The deviation of struts is based on an orthogonal reinforcement layout in all panels. Altogether, four shear panels can be distinguished:

- *Beam Web / Rib Wall*: This is the main panel linking all other panels. It includes the Beam Web and lower flange as well as the Rib Wall that quasi acts as a web for the Outer and Inner Walls. The entire transverse shear force of the frame system is transferred in this plane.
- *Top Slab*: The Top Slab acts as upper flange for the T-girder. Closing moments will primarily cause tension in this panel.
- *Outer Wall*: In the case of closing moments, the Outer Wall is the tension chord of the H-shaped cross section formed by the Outer Wall, Rib Wall and Inner Wall.
- *Inner Wall*: The Inner Wall is mainly subjected to compression for closing moments.

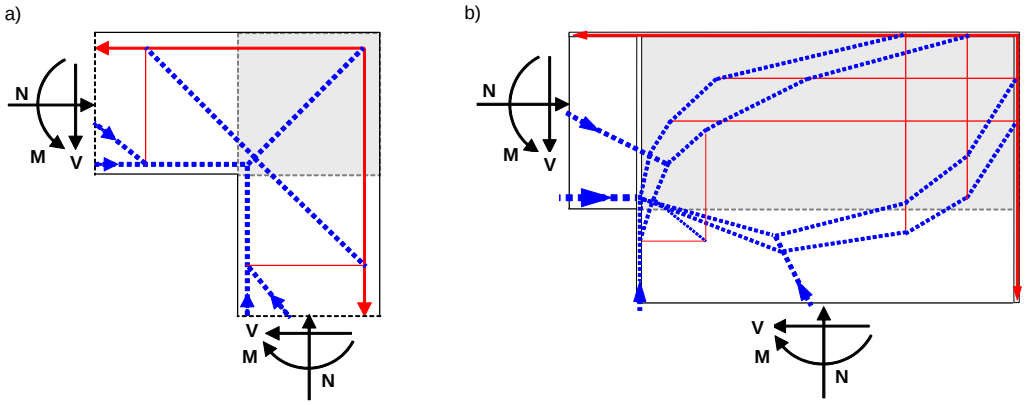
The models in Fig. 10-2 only include a closing moment, but not the corresponding transverse shear force. A better picture of the main shear panel including transverse shear in the frame system is shown in Fig. 10-3. Transverse shear does not affect the flanges and only results in minor changes to the model for bending only. Compressive stresses culminate in the inner corner of the connection, whereas the tensile stresses are spread over the outer corner.



a) massive cross-section *b) thin-walled cross-section*

Fig. 10-2: Closing moment for massive and thin-walled cross-sections

This document is the intellectual property of the fib – International Federation for Structural Concrete. All rights reserved.
This PDF of fib Bulletin 61 is intended for use and/or distribution solely within fib National Member Groups.

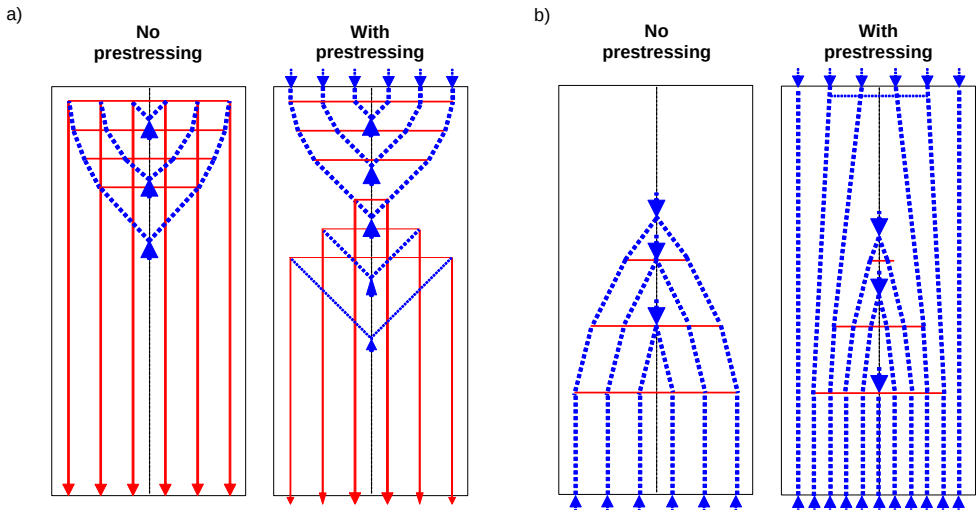


a) massive cross-section *b) web and rib wall of thin-walled cross-section*

Fig. 10-3: Extension of models in Fig. 10-2 for transverse shear

Prestressing has a major influence on the stress distribution in the connection. All panels are post-tensioned and post-tensioning anchorages are located in the connection. Top Slab, Outer and Inner Wall have an orthogonal, centric prestressing, whereas the Beam Web includes curved tendons in the direction of the beam. Prestressing transverse to the frame system is neglected in the framework of this example as well as membrane forces in the Top Slab due to the "global" behaviour of the terminal.

Fig. 10-4a illustrates the effect of post-tensioning on the stress distribution in Top Slab and Outer Wall. Longitudinal stresses are redirected to the centre by activating transverse reinforcement. The more the force transfer is pushed to the end of the panel, the higher the need of transverse reinforcement. Fig. 10-4b shows the effect of post-tensioning on the Inner Wall, which is dominated by compression.

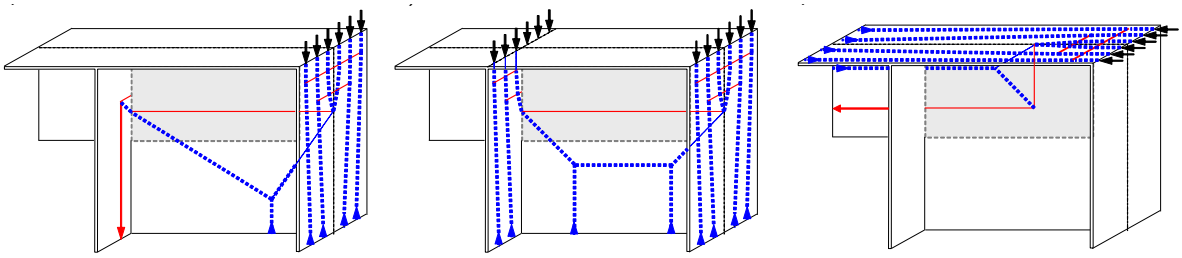


a) top slab and outer wall *b) inner wall*

Fig. 10-4: Effect of prestressing in Top Slab/ Outer Wall and Inner Wall.

This document is the intellectual property of the fib – International Federation for Structural Concrete. All rights reserved.
This PDF of fib Bulletin 61 is intended for use and/or distribution solely within fib National Member Groups.

The post-tensioning of the individual panels influences the entire connection because bending moments are introduced with respect to the neutral axis of the frame system and because compression spreads into the adjacent panels. This is illustrated in Fig.10-5. It shows in a qualitative manner how part of the post-tensioning spreads into the main panel, causing tensile stresses perpendicular to the compressive force flow.



a) Outer Wall *b) Outer and Inner Walls* *c) Top Slab*

Fig. 10- 5: Force flow for post-tensioning in the different structural members

In order to simplify the models, only the "direct" effect of post-tensioning is considered: Actually, post-tensioning of the Top Slab not only affects the T-girder, but also introduces a bending moment into the walls as the frame is a statically indeterminate system. Moments introduced into the connection will primarily go into the walls forming an H-shaped cross section that is much stiffer than the T-girder. The overall structural behaviour is fully considered in the "global" finite element analysis model for the entire structure that is used to define the section forces at the connection.

The qualitative models cannot be used directly for design, but they help to understand the structural behaviour and to develop design models. Especially as several shear planes are involved, it is important look at the connection as a whole in order to get close to an overall optimum.

4 Geometry and forces

As a first step to detailed modelling, a more precise description of the connection is necessary. Fig. 10-6 shows the dimensions and forces in vertical and horizontal cross sections (dimensions in metres, forces at service state in kN). The relevant tendons are shown explicitly in order to emphasise their significance for design. For the external equilibrium of the connection, the precise location and intensity of the various anchorages is important. The Rib Wall does not contain tendons apart from the continuous cables in the wall top.

In order to simplify installation of the approximately 2.200 kN heavy prefabricated beams, they are placed on temporary supports inside the Inner Wall. Consequently, the tendons in the prefabricated girder are anchored ahead of the final support. This requires particular attention to the transfer of transverse shear in that region.

The panels are about 0,5 to 0,6 m thick, which is sufficient for two orthogonal layers of non-prestressed reinforcement on each face and two layers of prestressed reinforcement in the centre. The Beam Web has a width of 0,8 m and widens to 1,5 m at the support. On the other side of the Inner Wall, the width decreases to 0,5 m, which is the general thickness of the Rib Wall. The total height of the T-girder is 3 m and the H-shaped composite wall section is 8 m high.

This document is the intellectual property of the fib – International Federation for Structural Concrete. All rights reserved.
This PDF of fib Bulletin 61 is intended for use and/or distribution solely within fib National Member Groups.

The geometry of the finite element model used for structural analysis does not correspond to the actual connection geometry used in design. Instead of a gradual thickness variation of the main panel, the computation model includes an abrupt change. "Global" structural analysis only uses 8-node solid finite elements with a relatively coarse mesh. No degeneration to 6-node prismatic elements is used in order to simplify post-processing of the section forces.

The variable width of the Beam Web / lower flange has an influence on the neutral axis of the T-girder and on the section forces, which reflect the eccentricity with a step in the bending moment.

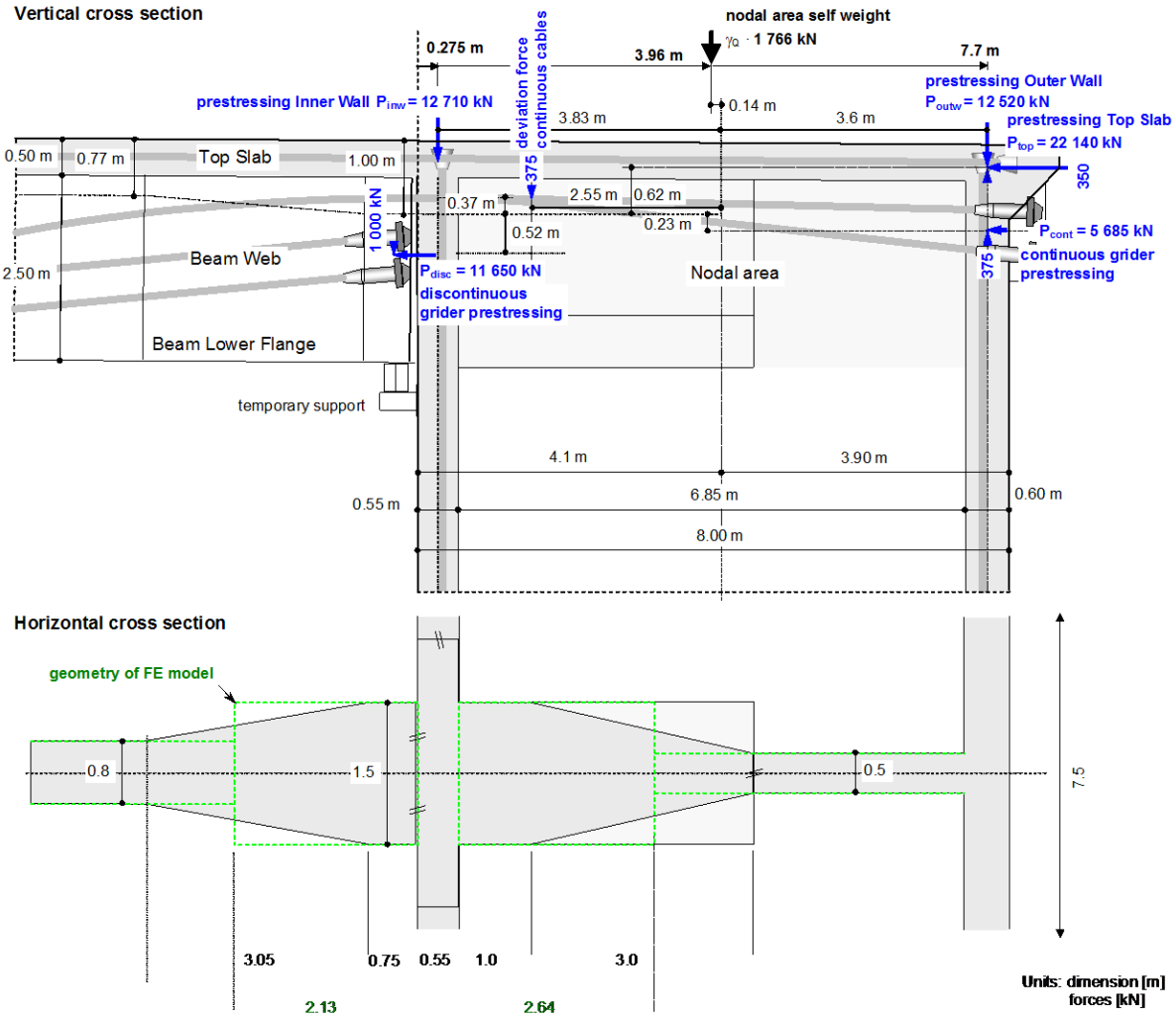


Fig. 10-6: Geometry and external forces for detailed analysis
(decimal point instead of comma; see Editorial Comments on p. vi)

5 Section forces

Post-processing provides a functionality to integrate section forces over defined cross sections. This way, the structure acting as a frame (see Fig. 10-1b) can effectively be designed as frame without neglecting the three-dimensional nature of the structure. For each defined frame section, the normal force *N*, shear forces *V* and bending moments *M* are determined. Fig. 10-7 gives a qualitative impression of bending moments M. At the connections, the results are not

This document is the intellectual property of the fib – International Federation for Structural Concrete. All rights reserved.
This PDF of fib Bulletin 61 is intended for use and/or distribution solely within fib National Member Groups.

always precise, and the input for connection design is obtained from extrapolation of section forces for adjacent sections. The extrapolation is complicated by the stepped variation of bending moments close to the connection caused by the thickness variation in the Beam Web / lower flange. Due to the larger web, the centre of gravity of the T-girder cross-section moves towards the bottom flange and an additional moment $M = N \cdot e$ is introduced.

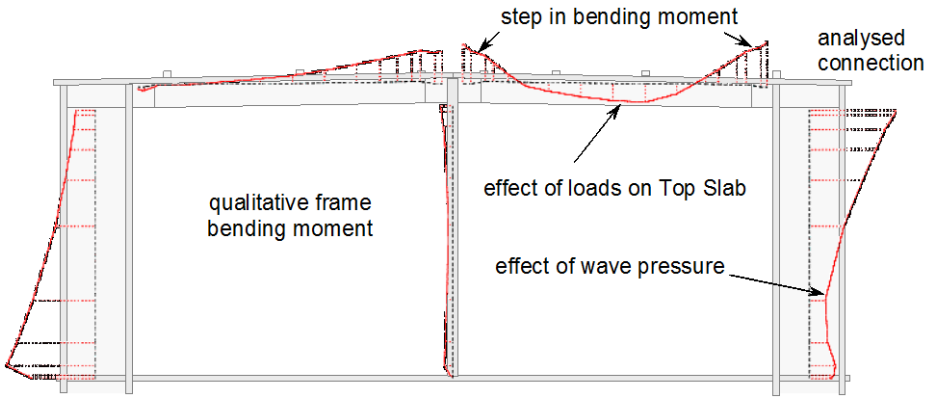


Fig. 10-7: Frame bending moment for design combination "Tow Wave"

For the nodal region, a free body diagram is set up in order to check equilibrium of forces, see Fig. 10-8. Some adjustments are required in order to satisfy the three conditions of equilibrium in the model plane. The large number of external forces acting on the connection, the difference of the FE model to the actually designed structure and the restraint of the connection out of plane make this task particularly complicated.

In Fig.10-8, the frame section forces are displayed as resultants in the cross section at the edge of the nodal region that are highlighted with dashed lines. The eccentricity of the resultant in the T-girder indicates tension in the upper flange (Top Slab), and the resultant for the walls indicates some tension in the Outer Wall despite the high vertical prestressing.

Weight and prestressing forces shown in Fig. 10-8 do not correspond to the values in Fig. 10-6 because different partial safety factors are applied. The forces in Fig. 10-7 apply to the design combination with maximum tension in the Top Slab, for which prestressing is assumed to 90% of the values for service state and self-weight is multiplied by the factor 1,3.

Structural design includes another combination with prestressing forces set to 110% of those for service state, which is used to verify concrete compression in critical regions. In the area of the connection, the T-girder cross-section previous to widening of the web / lower flange is most critical. At this cross section, particular attention is paid to compressive shear failure.

This document is the intellectual property of the fib – International Federation for Structural Concrete. All rights reserved.
This PDF of fib Bulletin 61 is intended for use and/or distribution solely within fib National Member Groups.

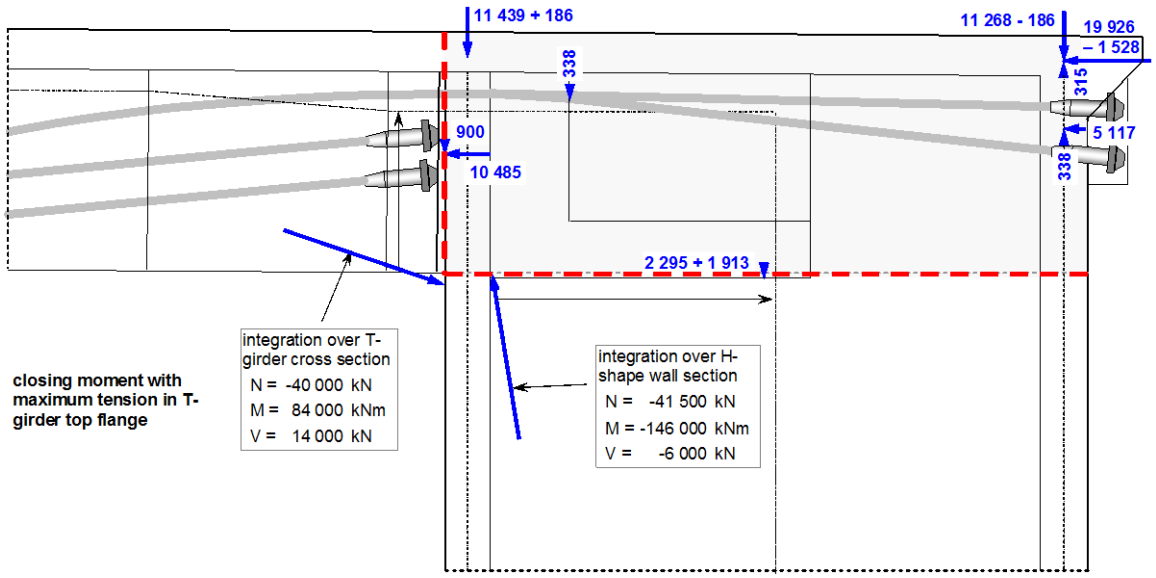


Fig. 10-8: Connection with resulting section forces for "Tow wave"

6 Model development

The development of the model starts with the T-girder cross-section at the edge of the nodal region. The inner forces *N*, *M* and *V* are modified in order to consider the anchorage of discontinuous post-tensioning cables. This is illustrated with resultant vectors in Fig. 10-9. The vector representing the total resultant of the inner forces in the girder is subdivided in two vectors, one that balances normal force and bending moment of the anchor force, and the residual that maintains the correct sum to the total resultant. In this vector analysis, the relation between shear force and normal force is assumed constant.

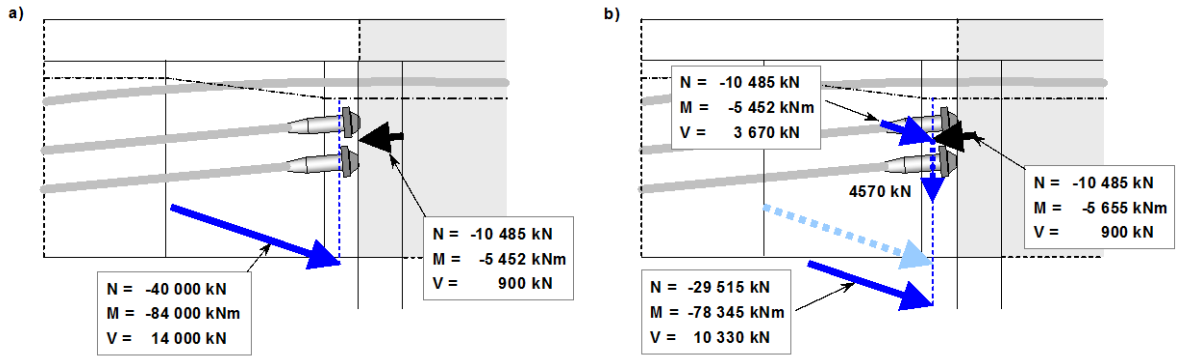


Fig. 10-9: Balancing of concentrated force at post-tensioning anchorage

This document is the intellectual property of the fib – International Federation for Structural Concrete. All rights reserved.
This PDF of fib Bulletin 61 is intended for use and/or distribution solely within fib National Member Groups.

Balancing normal force and bending moment at the anchorage of the post-tensioning cables results in a vertical force of 4.570 kN. For usual arrangements with post-tensioning anchors "behind" the support, this force goes directly into the support. In the present case, the force increases the shear in the construction joint between the precast beam and the nodal area of the connection. The transfer of this shear force is secured by the high axial compression in the construction connection that is provided by the continuous beam and slab post-tensioning.

The governing cross section with regard to connection design is situated "behind" the post-tensioning anchorages, where the favourable effect of the prestressing has decreased. For the residual forces, the tie in the Top Slab is determined by locating the tensile force in the centre of the Top Slab and by assuming an angle of the diagonal shear strut that is somewhat above the inclination of the resultant vector, see Fig. 10-12. The model for the beam is extended in order to include the beam cross section with reduced web thickness (b_w = 0,8 m instead of 1,5 m at connection). The model shows that the thickness of the Beam Web / lower flange (or the section modulus, respectively) reduces more quickly than the bending moment, because the height of the compression zone increases towards this section.

In analogy to the T-girder section forces, the section forces in the composite walls next to the connection are transformed in struts and ties. The angle chosen for the shear field results in a tensile force of 5.817 kN in the Outer Wall, see Fig. 10-12. Obviously, this tensile force has to be somehow linked to the tensile force in the Top Slab. Before the model for the Beam Web / Rib Wall can be developed further, models for the flanges have to be set up.

Fig. 10-10 shows the chosen *model for the Top Slab* together with the principal membrane forces according to finite element analysis. In a detailed manner, it shows the deviation of the Top Slab tensile and compressive forces towards the Rib Wall. The Strut-and-Tie model shows that this leads to considerable transverse splitting forces. They do not appear in the plot below because they are compensated by transverse prestressing in the Top Slab.

This document is the intellectual property of the fib – International Federation for Structural Concrete. All rights reserved.
This PDF of fib Bulletin 61 is intended for use and/or distribution solely within fib National Member Groups.

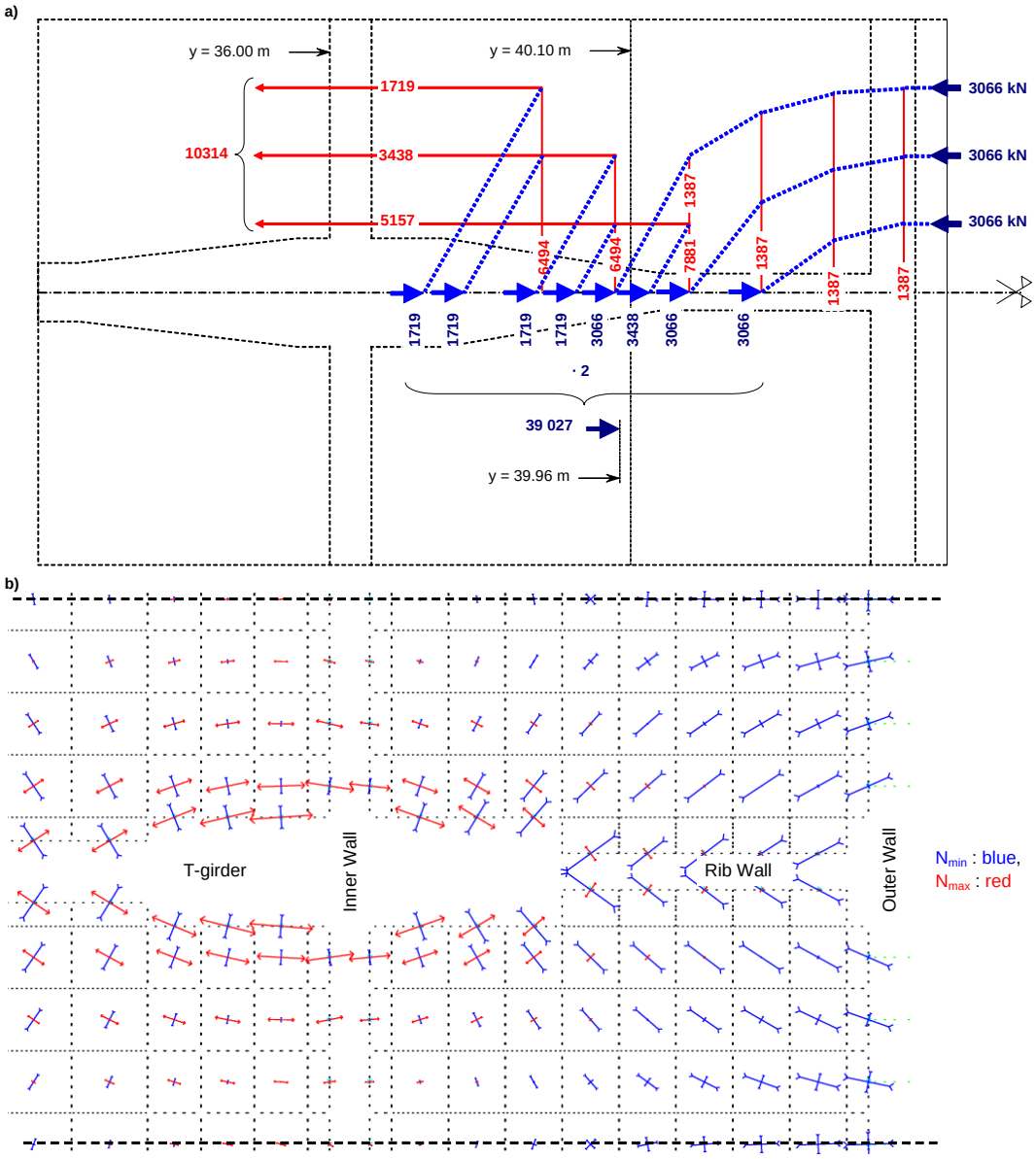


Fig. 10-10: Model for Top Slab vs. principal membrane forces (processed FE results) (decimal point instead of comma; see Editorial Comments on p. vi)

The model is set up in a way to direct the resultant of compressive forces to the centre of the Rib Wall. This resultant has to be deviated towards the T-girder bottom flange (see Fig. 10-12) which causes important vertical tension in the Rib Wall. Keeping the resultant near the centre allows distributing the reinforcement over a large area.

Just as for the Top Slab, a *model* is developed *for the Outer Wall*, see Fig. 10-11. The compression introduced on top of the wall by the four tendons is deviated towards the Rib Wall, just as the tension at the lower edge of the nodal region. The total compression introduced into the Rib Wall is divided into a fraction acting at the anchorage of the continuous beam cables and the rest, gathered in one resultant. The chosen model is again confronted with the result of the FE analysis. It shows that the splitting tension is mostly compensated by the horizontal prestressing in the Outer Wall, but for the rest it compares well.

This document is the intellectual property of the fib – International Federation for Structural Concrete. All rights reserved.
This PDF of fib Bulletin 61 is intended for use and/or distribution solely within fib National Member Groups.

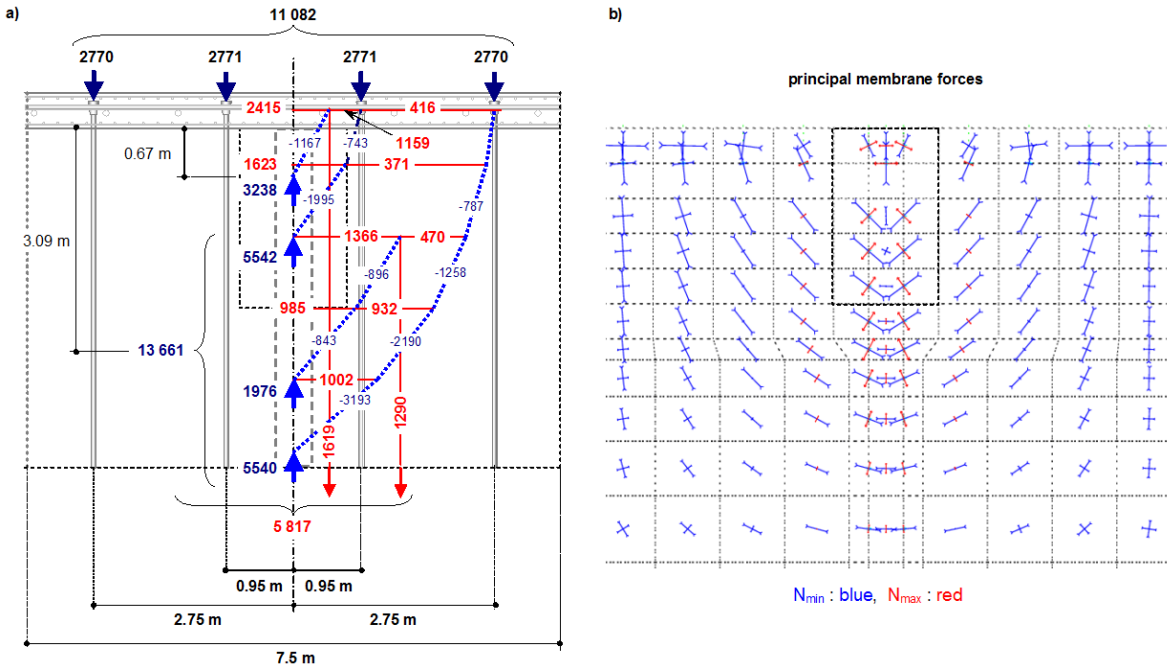


Fig. 10-11: Model for Outer Wall vs. principal membrane forces (processed FE results)
(decimal point instead of comma; see Editorial Comments on p. vi)

The models developed for the Top Slab and the Outer Wall serve as input the model for the Beam Web / Rib Wall, see Fig. 10-12. It connects the models for the other shear panels in Fig. 10-10 and Fig. 10-11. In order to simplify modelling, the compressive stresses in these panels are bundled in one or two resultants. The major results are the vertical tensile force of about 26,5 MN and the horizontal force of about 15 MN. The model also shows where these forces have to be anchored and, together with the models in Fig. 10-10 and Fig. 10-11, over which area the corresponding reinforcement can be distributed.

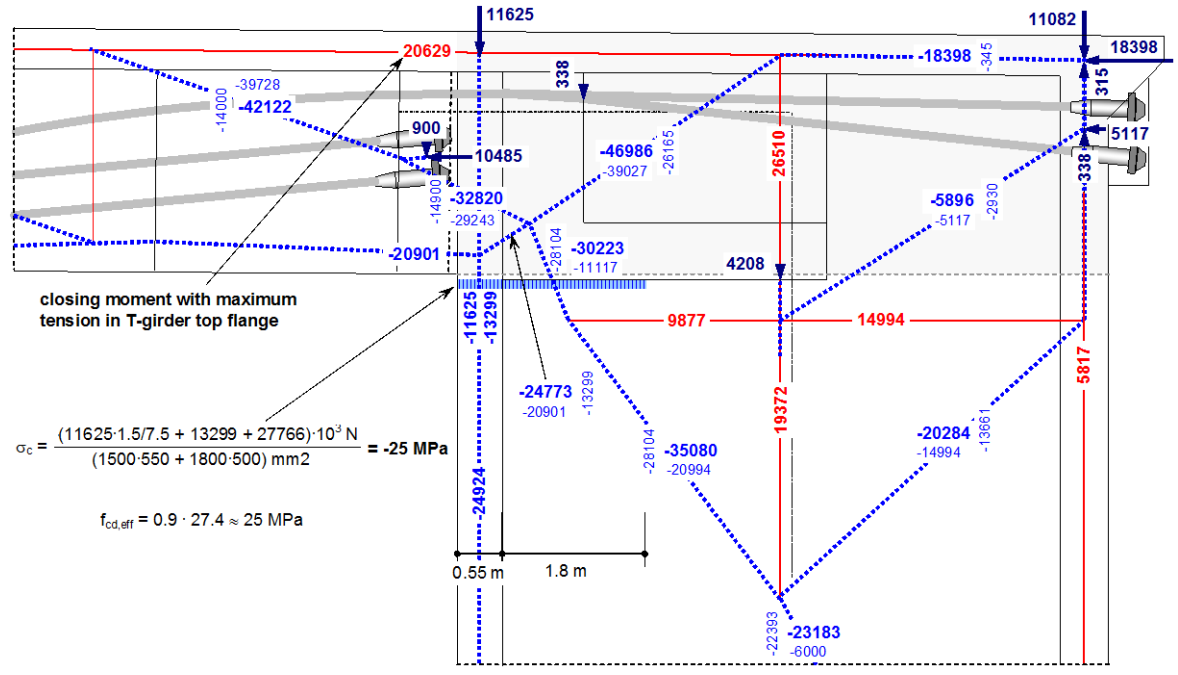


Fig. 10-12: Model for main shear panel
(decimal point instead of comma; see Editorial Comments on p. vi)

This document is the intellectual property of the fib – International Federation for Structural Concrete. All rights reserved.
This PDF of fib Bulletin 61 is intended for use and/or distribution solely within fib National Member Groups.

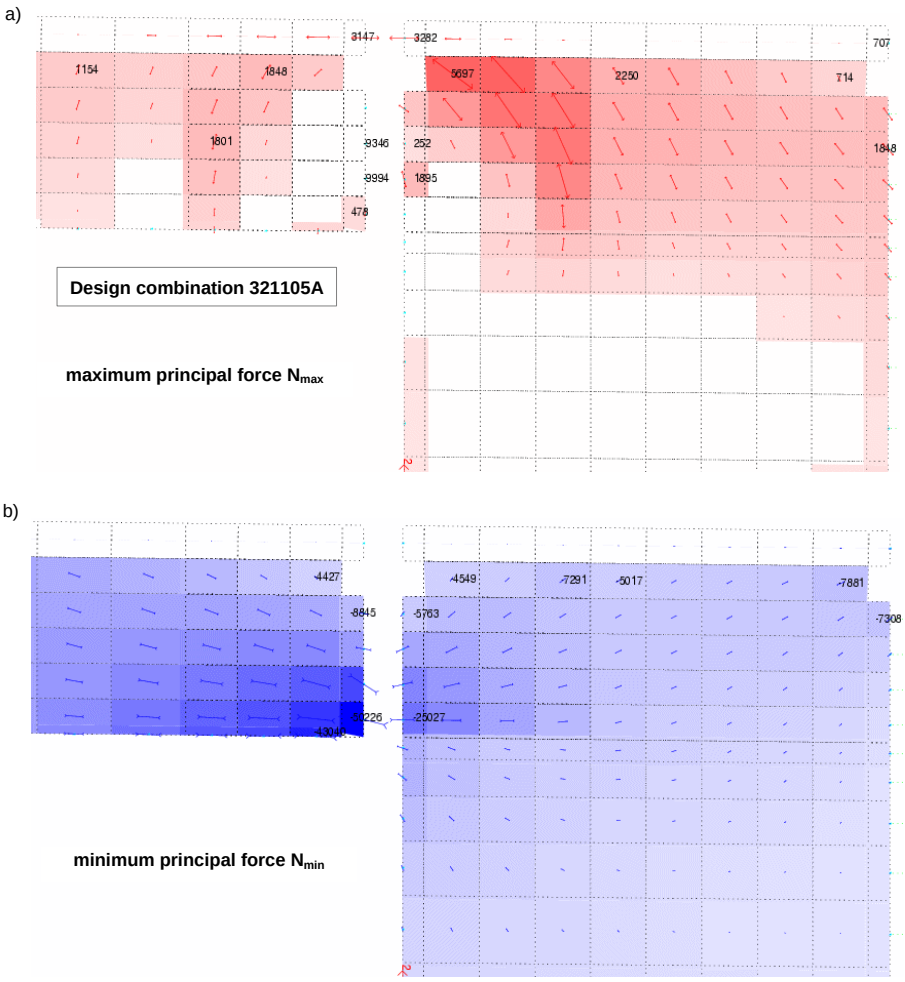


Fig. 10-13: Principal normal forces for "Tow wave", processed FE results

The model of Fig. 10-12 can be compared to the result of the FE analysis in Fig. 10-13. The FE model shows a high concentration of tensile stresses in the top left of the nodal region, whereas the tensile stresses do not extend very far below the level of the beam lower face. This stress distribution is a consequence of isotropic element models used in the linear elastic FE analysis. Contrary to isotropic finite elements, the orthotropic reinforcement used in design does not allow a direct transfer of skew principal tensile forces.

Using the strut-and-tie model, it is possible to distribute reinforcement more evenly and to estimate the impact on the adjacent structural elements. Concretely the model shows that the vertical tension can be assigned to vertical reinforcement of uniform intensity if this reinforcement is extended several Meters below the nodal region. The more the resultant of the vertical tension is moved away from the beam end, the smaller it gets. However, this will increase the splitting tension in the Top Slab.

This document is the intellectual property of the fib – International Federation for Structural Concrete. All rights reserved.
This PDF of fib Bulletin 61 is intended for use and/or distribution solely within fib National Member Groups.

7 Verifications

Based on the developed model, critical aspects can be evaluated in order to ensure safe and robust behaviour of the connection. Generally, concrete stresses have to be limited and sufficient reinforcement has to be provided and properly anchored. In the presented example, the focus is on the required reinforcement quantities. The selected design combination includes a load factor of 0,9 on prestressing effects. Maximum compression is found for the corresponding combination including a factor of 1,1.

- **Concrete stresses**: Fig. 10-12 and Fig. 10-13 show that maximum concrete compression occurs in the beam end. The governing cross section is located previous to the widening of the Beam Web. Verification of this section is covered by sectional design. The critical area for the Rib Wall is the vertical transition from the 1,5 m thick extension of the Beam Web to the ordinary Rib Wall with 500 mm thickness. For this section the extent of the compression zone in the Rib Wall is estimated to 1,8 m, see Fig. 10-12.

- **Reinforcement quantities**: The translation of tie forces into reinforcement quantities is described in the next section.

- **Reinforcement anchorage**: The model shows that standard solutions are sufficient for the anchorage of the main reinforcement. The tie forces are not influenced by the precise location of T-heads or other concentrated anchorages.

- **Required confinement**: In the area of maximum compression, the struts have to be confined by splitting reinforcement in the Beam Web and Rib Wall, see next section.

- **Stress transfer at casting joint**: According to Fig. 10-12, the shear force transferred at the casting joint is 14,9 MN. It acts in combination with a compression of -20,9 – 29,2 ≈ -50 MN. A friction coefficient of $\mu = 0{,}3$ is sufficient to ensure the force transfer. Due to more unfavourable conditions in other load phases, the casting joint includes shear keys and a rough surface resulting in a far higher friction coefficient.

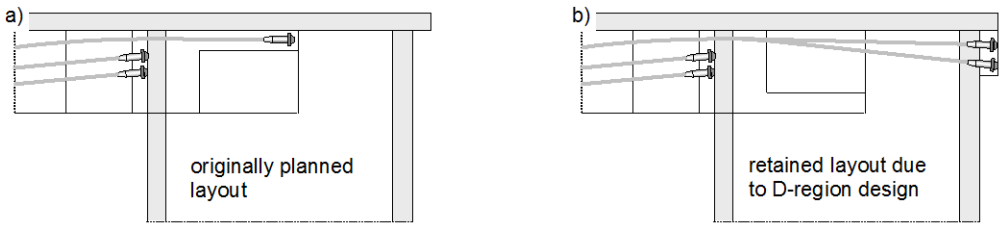
8 Application to reinforcement layout

Connection design is the result of a stepwise procedure with increasing level of detail. Previous to detailed design, dimensions and cable layout for the connection were determined with simplified “global” models without specific consideration of the force transfer in the connection. In addition, no opening moment had to be considered in the original design. Detailed design using Strut-and-Tie models lead to two major changes:

– The continuous beam cables originally planned to be anchored in the nodal region where extended to the Outer Wall, see Fig. 10-14. Ideally the anchorages had been placed even lower with the cables following the principal tensile forces (see Fig. 10-13 a) but this would have caused excessive friction losses due to the high curvature.

– The continuation of the beam lower flange into the nodal region was widened in order to accommodate important non-prestressed reinforcement. This reinforcement is activated by opening moments which are particularly delicate due to the premature anchorage of the discontinuous beam cables.

This document is the intellectual property of the fib – International Federation for Structural Concrete. All rights reserved.
This PDF of fib Bulletin 61 is intended for use and/or distribution solely within fib National Member Groups.



a) original layout *b) retained layout*

Fig. 10-14: Amendment of tendon layout

The specification of the required non-prestressed reinforcement is based on the overall system adopted for the structure. The main reinforcement consists of a grid of bars Ø25 mm or Ø32 mm with a spacing c = 200 mm which may be placed in bundles of two bars. The application of Strut-and-Tie modelling to reinforcement layout consequently necessitates assigning the ties an extent over which the reinforcement can be activated in agreement with the model.

For each of the shear panels, sketches are drawn that indicate intensity and length of the required reinforcement. Fig. 10-15 shows that the maximum intensity of non-prestressed reinforcement does not exceed 1,5Ø25 c 200 per layer in the Top Slab. This is due to the high intensity of prestressed reinforcement provided in the slab (cables of 19 strands of 0,6 inches spaced 1 m). The highest intensity of non-prestressed reinforcement is required in the Rib Wall which does not include post-tensioning cables (verticals of 2Ø32 c 200 in both faces, Fig. 10-16).

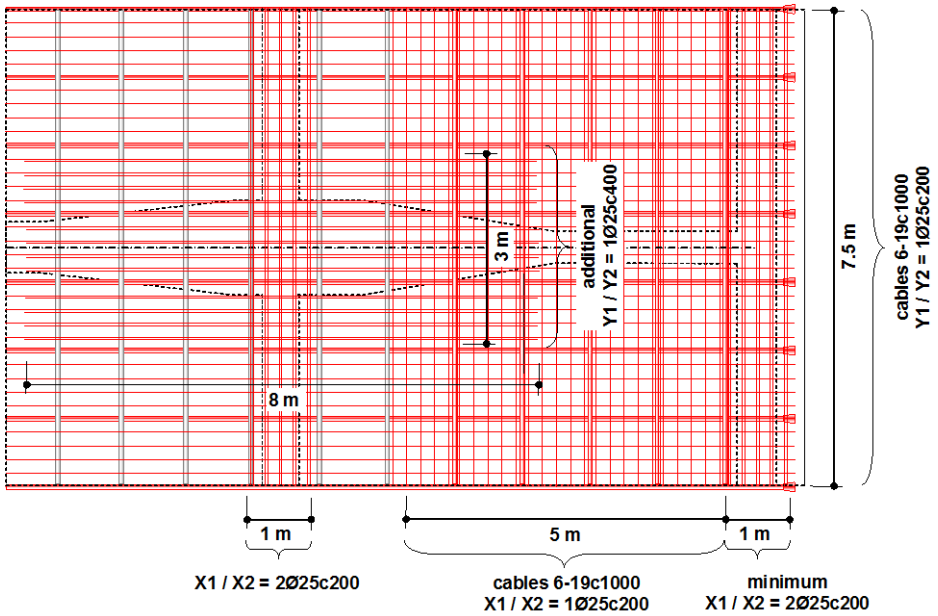


Fig. 10-15: Required reinforcement intensities in Top Slab above connection.

The actual reinforcement layout is strongly influenced by the construction method. As the connection is constituted of a precast beam, walls erected with slip-forming and a part of the nodal area cast in place, some splicing is required in the nodal region. The areas with splicing have stirrups providing lateral confinement. In addition lateral confinement is provided at geometrical discontinuities, see bottom of Fig. 10-16. The constructability of the layout is verified with a 3D-model, see Fig. 10-17.

This document is the intellectual property of the fib – International Federation for Structural Concrete. All rights reserved.
This PDF of fib Bulletin 61 is intended for use and/or distribution solely within fib National Member Groups.

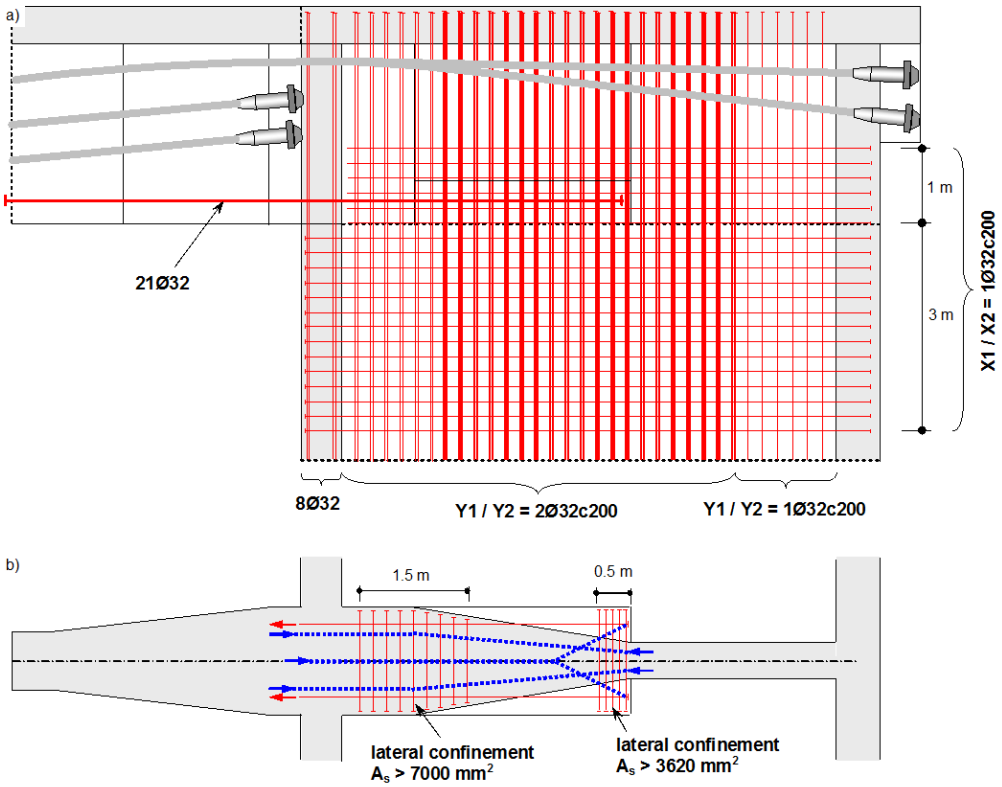


Fig. 10-16: Required reinforcement intensities in top of Rib Walls (decimal point instead of comma; see Editorial Comments on p. vi)

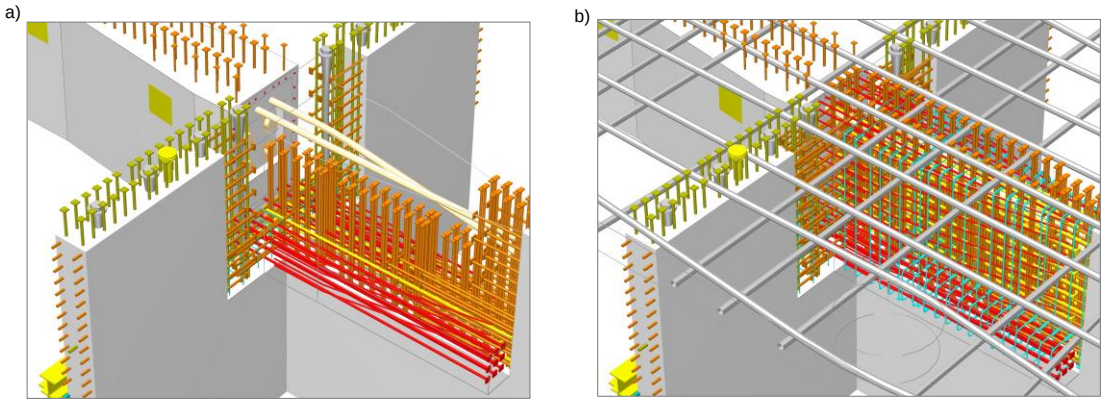


Fig. 10-17: Verification of constructability using 3D models

9 References

FIP Recommendations (1999): Practical Design of Structural Concrete. FIP-Commission 3 "Practical Design", Sept. 1996. Publ.: SETO, London, Sept. 1999. (distributed by: *fib*, Lausanne. Web http://www.fib-international.org)

fib Bulletin 16: Design Examples for the 1996 FIP Recommendations “Practical design of structural concrete”. *fib*, Lausanne, Jan. 2002

This document is the intellectual property of the fib – International Federation for Structural Concrete. All rights reserved.
This PDF of fib Bulletin 61 is intended for use and/or distribution solely within fib National Member Groups.

Example 11: Abutment Shear Wall of Viaduct 1 on Algarve Highway

Miguel S. Lourenço, João F. Almeida

1 Presentation of the structure

1.1 Description of the structure

The *Algarve SCUT Concession* is an expansion of the existing *Via do Infante* (*IC4*), connecting *Alcantarilha* to *Lagos* in the South of Portugal, which includes eleven current viaducts with a total extension of 4.376 m.

The viaducts superstructure consists of two parallel decks with 12,4 m width each. The decks has two longitudinal U-shape pre-fabricated, pre-tensioned beams, spaced 6,15 m between axles, directly supported on the piers and abutments with neoprene or pot type bearings (see Fig. 11-2). A 0,25 m thick reinforced concrete slab connects the longitudinal beams. The slab is cast *in-situ* through a non-effective prefabricated pre-slab.

The superstructure is fully continuous on its total length. Structural continuity is ensured by the reinforced concrete deck and by post-tensioned bars connecting the longitudinal beams over the supports.

In most of the viaducts, the soil conditions led to the adoption of a pile/pier solution which has low capacity to equilibrate horizontal forces. Accordingly, dampers devices were placed in the abutments in order to resist seismic actions.

The major viaduct, V1, has a total extension of 1.204 m, with spans of 32,0 m length. Only one expansion joint was applied, approximately in the middle of the total length of the viaduct, in which was placed a transition span of 25,0 m. Two continuous viaducts with 589,5 m length each are thus obtained. Fig. 11-1 shows the elevation and the plan view of the viaduct.

As mentioned before the seismic forces are equilibrated in the abutment, through the damping device system, and at the first three set of columns where was possible to apply a solution with direct foundations. The remaining columns a longitudinal sliding bearing at the top was provided.

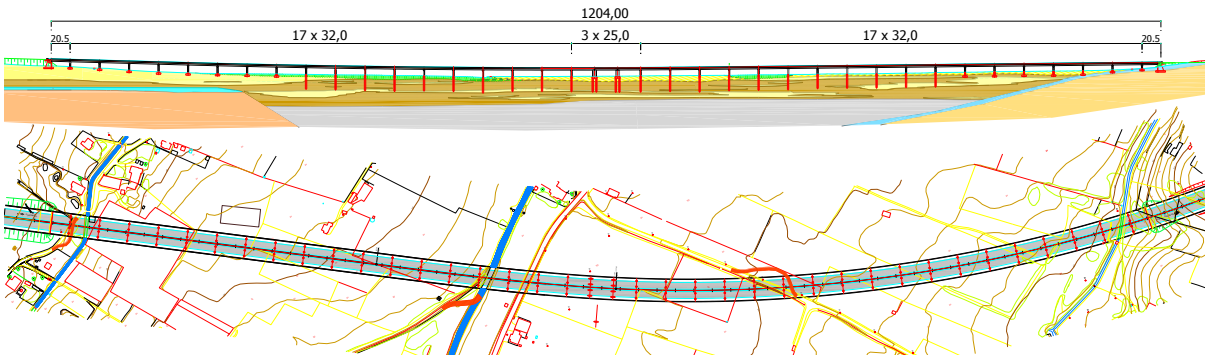


Fig. 11-1: Plan and elevation of viaduct 1

This document is the intellectual property of the fib – International Federation for Structural Concrete. All rights reserved.
This PDF of fib Bulletin 61 is intended for use and/or distribution solely within fib National Member Groups.

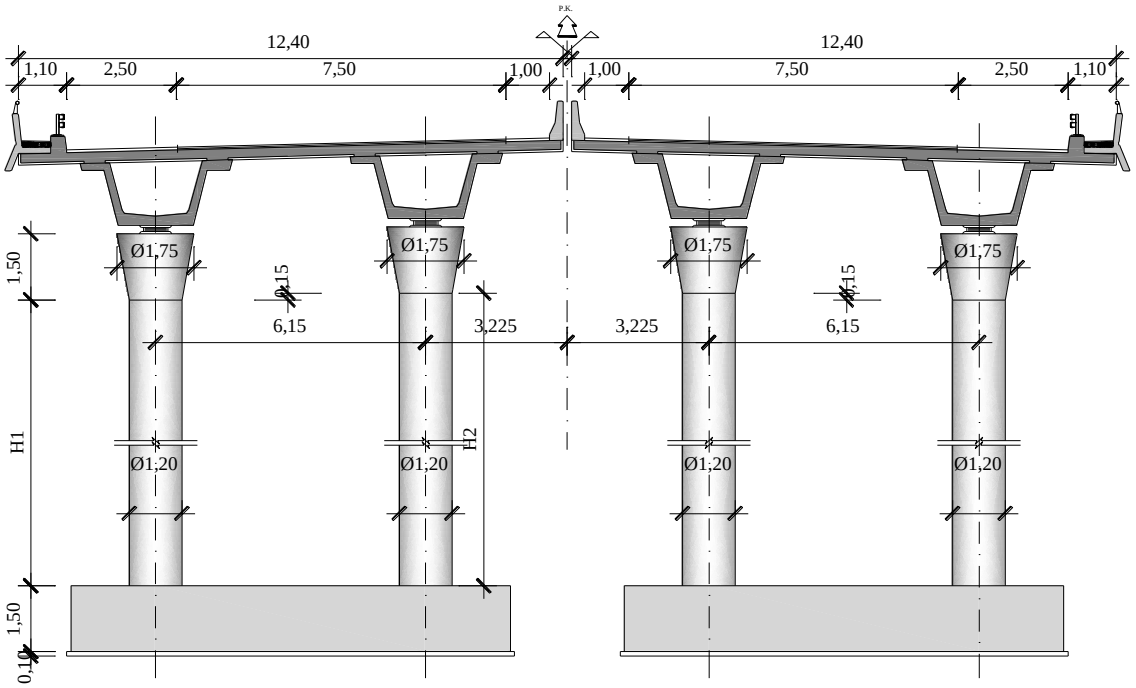


Fig. 11-2: Deck section

The fixed abutment has a total of four damping devices, one per beam, transmits the inertial forces of the deck, due to seismic action, to four vertical shear elements. The abutment geometry is shown in Figs. 11-3 to 11-6.

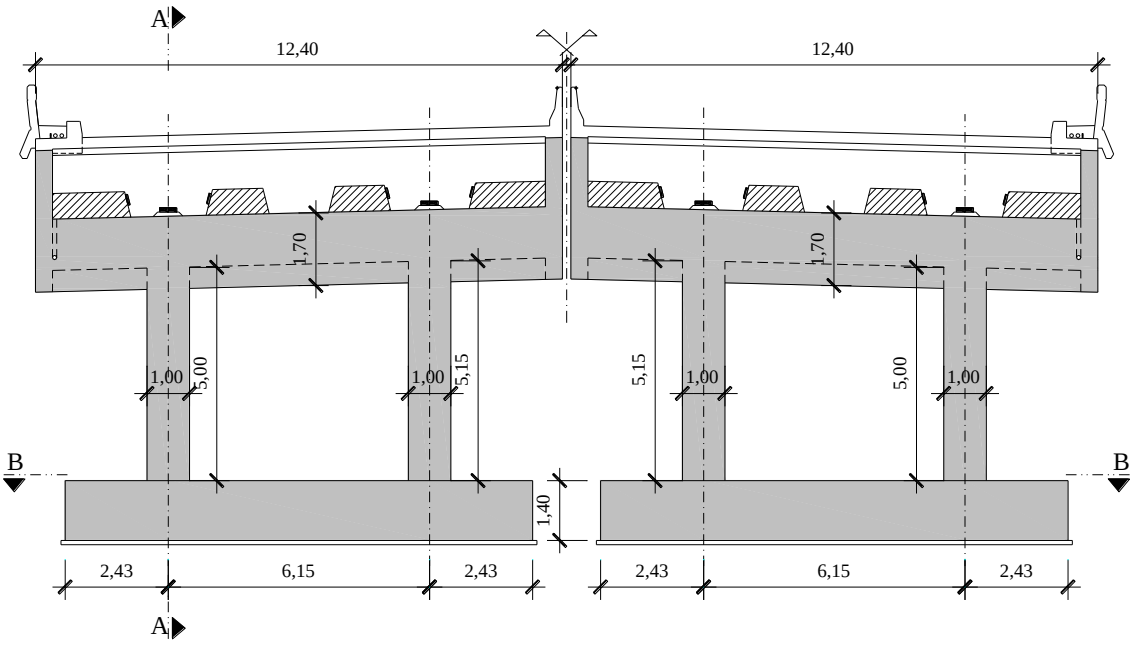


Fig. 11-3: Front view of the abutment

This document is the intellectual property of the fib – International Federation for Structural Concrete. All rights reserved.
This PDF of fib Bulletin 61 is intended for use and/or distribution solely within fib National Member Groups.

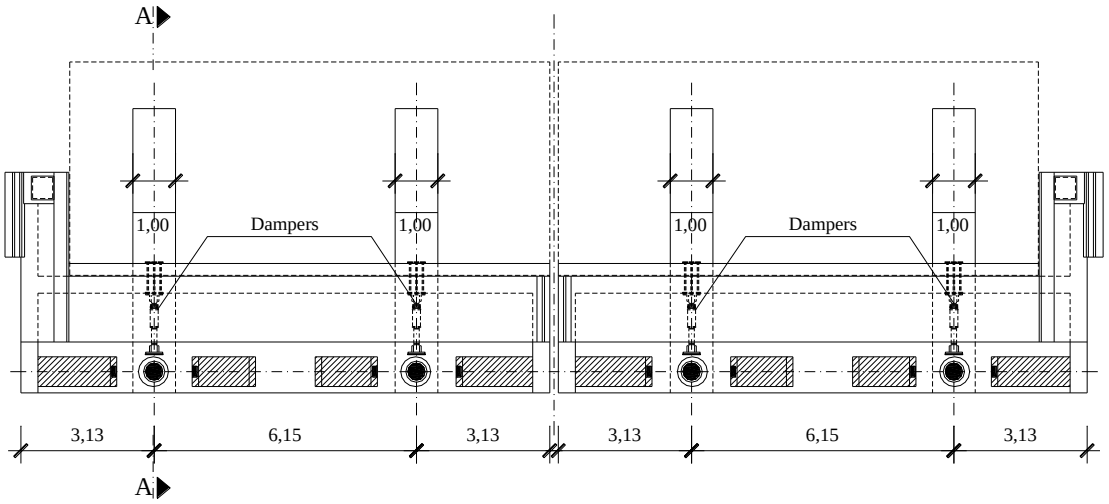


Fig. 11-4: Plan view

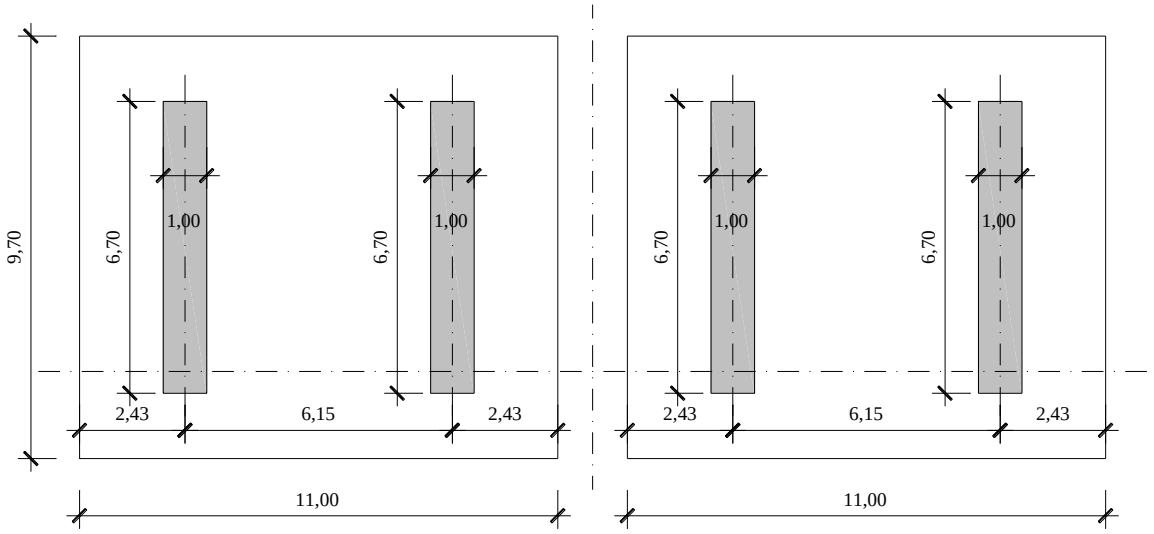


Fig. 11-5: Cross-section B-B

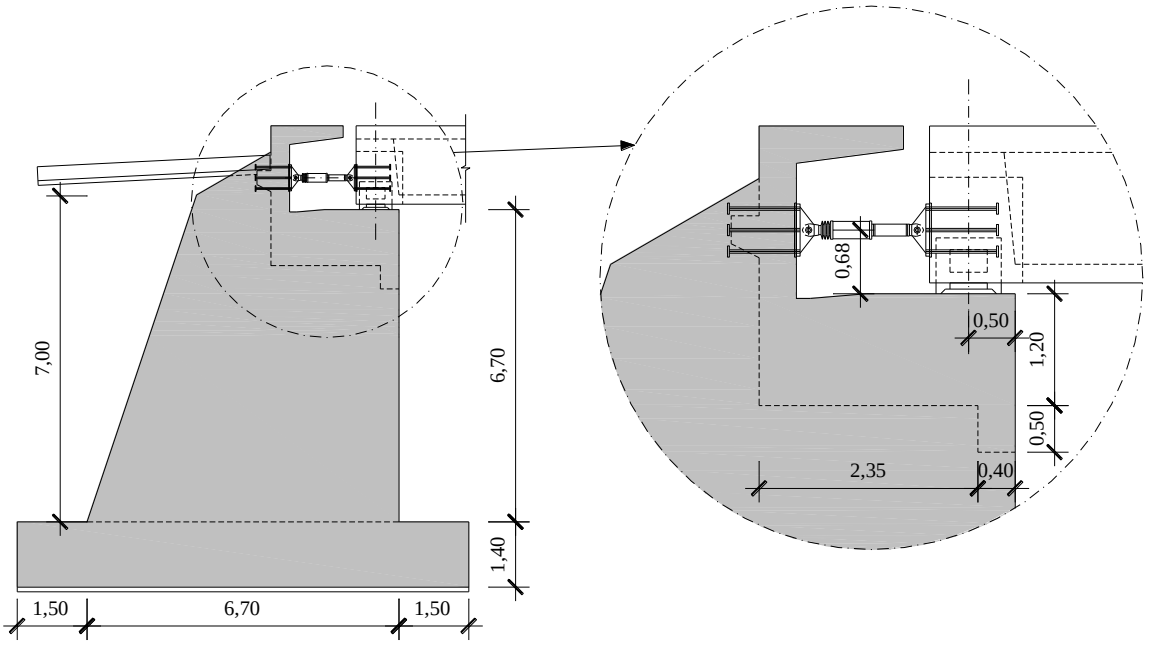


Fig. 11-6: Cross-section A-A

This document is the intellectual property of the fib – International Federation for Structural Concrete. All rights reserved.
This PDF of fib Bulletin 61 is intended for use and/or distribution solely within fib National Member Groups.

Time history analysis, along a 30 seconds earthquake, was developed resulting the seismic device forces and displacements shown on Fig. 11-7.

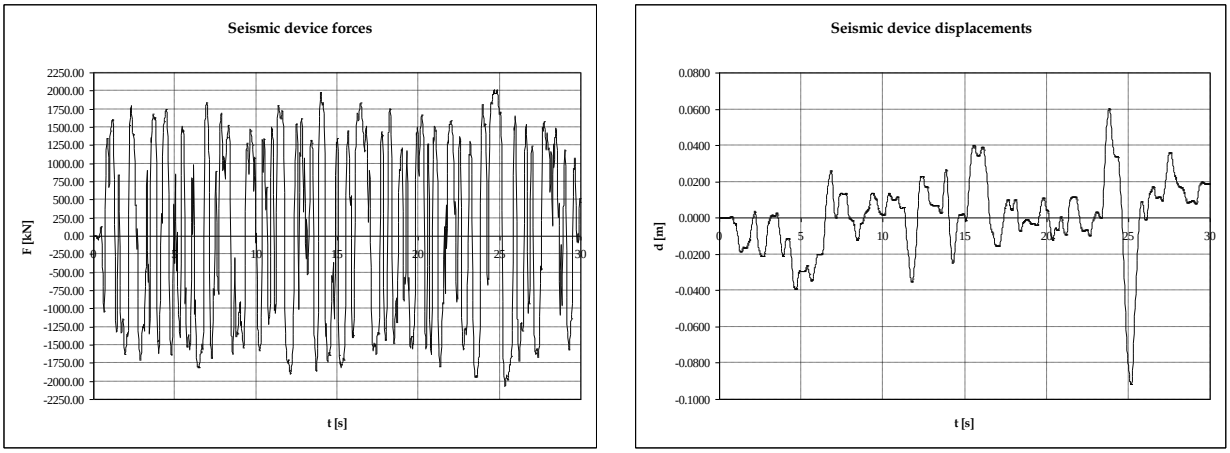
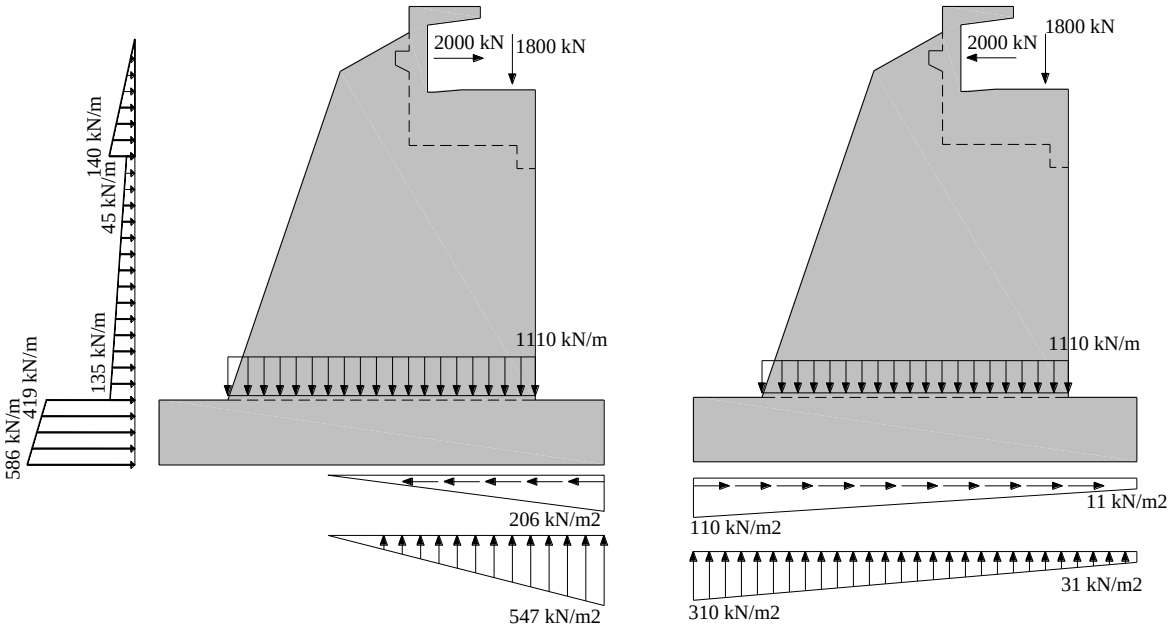


Fig. 11-7: Forces and displacements of damping device system

1.2 Description of the design task

1.2.1 Loads

For the seismic action load case, which is the most relevant for the design, the abutments are subject to several in-plane loads: the earth pressure, the dead weight of the deck, and the maximum forces transmitted by the damping devices. Since these loads can act in both directions two different load cases should be considered (see Figs. 11-8a and 11-8b).



a) seismic action pulling the abutment *b) seismic action pushing the abutment*

Fig. 11-8: Load cases for seismic action

This document is the intellectual property of the fib – International Federation for Structural Concrete. All rights reserved.
This PDF of fib Bulletin 61 is intended for use and/or distribution solely within fib National Member Groups.

The horizontal trapezoidal loads represent the soil pressure assuming $\phi=35^{\circ}$ and $\gamma_s=18$ kN/m^3. The active impulse (K_a) was assumed since it is concomitant with the seismic action. The horizontal and vertical concentrated loads at the top of the vertical shear wall represent the maximum seismic action transmitted by the damping device system and the vertical dead loads transmitted by the bearings, respectively. The uniform load at the top face of the foundation slab represents the soil self-weight of the backfill of the abutment. Finally, the resulting soil reactions at the foundation base are indicated for both load cases.

Concerning the mentioned loads, the following assumptions were considered:

- The horizontal soil pressure was conservatively disregarded when the seismic action is pushing the abutment.
- The self weight of the vertical shear wall was set to act at the top face of the foundation together with the soil self weight in the backfill, in order to simplify the strut-and-tie model. As shown later the self-weight of the shear wall has little influence in the design.

1.2.2 Design values for materials

Concrete: C25/30 $f_{ck} = 25$ MPa, $f_{1cd} = 0{,}85 \cdot 25 / 1{,}5 = 14{,}2$ MPa

Steel reinforcement: A500NR: $f_{yk} = 500$ MPa $f_{yd} = 500/1{,}15 = 435$ MPa

1.2.3 Statement of design problem

The strut-and-tie method is a preferential tool for the design and detailing of structural concrete discontinuity regions. This kind of regions should be analysed with the same level of accuracy as current regions, especially if subjected to relevant loads. This example shows a practical application of strut-and-tie models to the design of a viaduct shear wall fixed abutment under the dead and the seismic loads, following the FIP Recommendations (1999). The inertial forces of the deck, due to the seismic action, are transmitted to the abutment through damping devices, leading to considerable stresses in the abutment shear walls. The reversal loading leads to different strut-and-tie models for the analysis and detailing and node regions were checked assuming simplified considerations for concrete compression strength under cyclic loads. Local models are also developed for a proper detailing in critical regions.

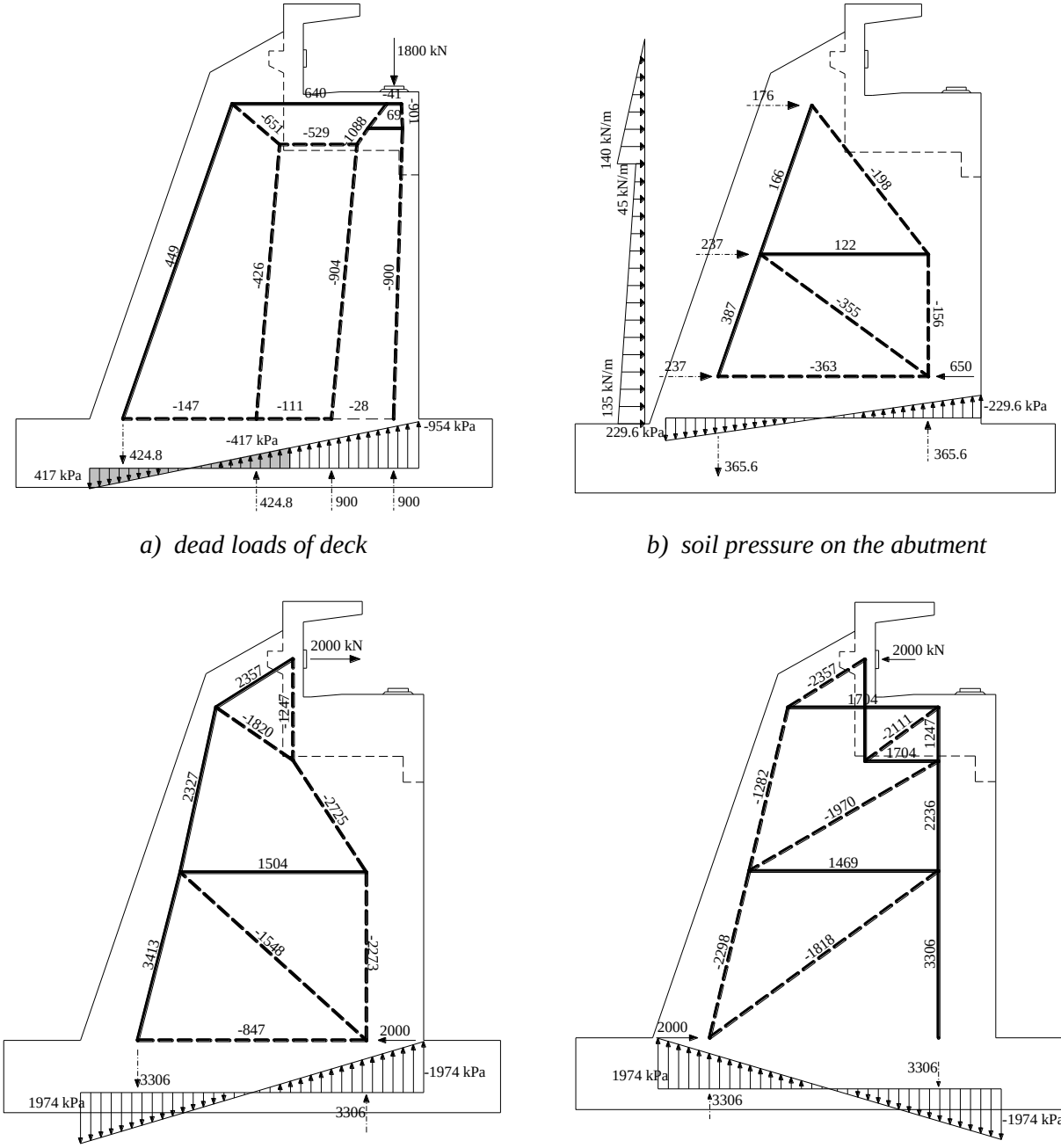
2 Design procedure

2.1 Strut-and-tie models for the design of the abutment

In order to easily understand the final design model, a strut-and-tie model for each load was developed, as shown in Fig. 11-9. A typical strut-and-tie model of an eccentric concentrated load, such as the case of an eccentric pre-stressed anchorage of a beam, was developed for the vertical force due to the deck's dead load (Fig. 11-9a). A common strut-and-tie model of a beam cantilever is produced by the soil pressure and the horizontal top force generated by the damping device (Fig. 11-9b and 11-9c). When the damping device is pushing the abutment, a strut-and-tie model similar to a dapped end beam is undertaken (Fig. 11-9d).

As shown in Fig. 11-10, the self-weight of the shear wall has no significant influence in global design model, since it generates low stresses in comparison with the other load effects.

This document is the intellectual property of the fib – International Federation for Structural Concrete. All rights reserved.
This PDF of fib Bulletin 61 is intended for use and/or distribution solely within fib National Member Groups.



a) dead loads of deck *b) soil pressure on the abutment*

c) seismic action pulling the abutment *d) seismic action pushing the abutment*

Fig. 11-9: Strut-and-tie models for each load case
(decimal point instead of comma; see Editorial Comments on p. vi)

This document is the intellectual property of the fib – International Federation for Structural Concrete. All rights reserved.
This PDF of fib Bulletin 61 is intended for use and/or distribution solely within fib National Member Groups.

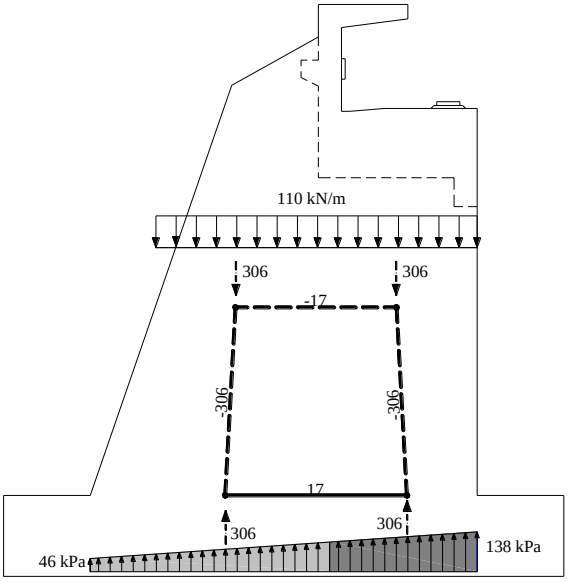
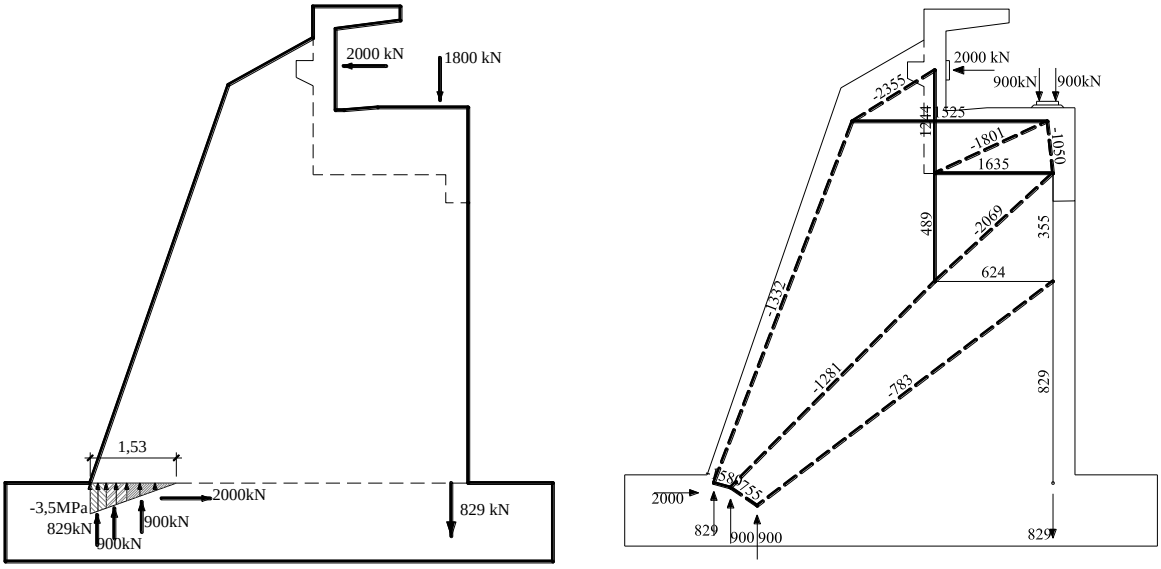


Fig. 11-10: Strut-and-tie model for the vertical shear wall self weight

The combination of each load distribution in the vertical shear wall leads to the resultants shown in Fig. 11-11 and Fig. 11-12 and the final models can be obtained by the superposition of the referred models. The above models are all based on the assumption of linear elastic response at the base of the wall, even though it should be remarked that their combination reflects the non-linear behaviour of a cracked section.

In Tables 11-1 and 11-2 are shown the forces of the ties obtained by the strut-and-tie models and the required and provided reinforcement.



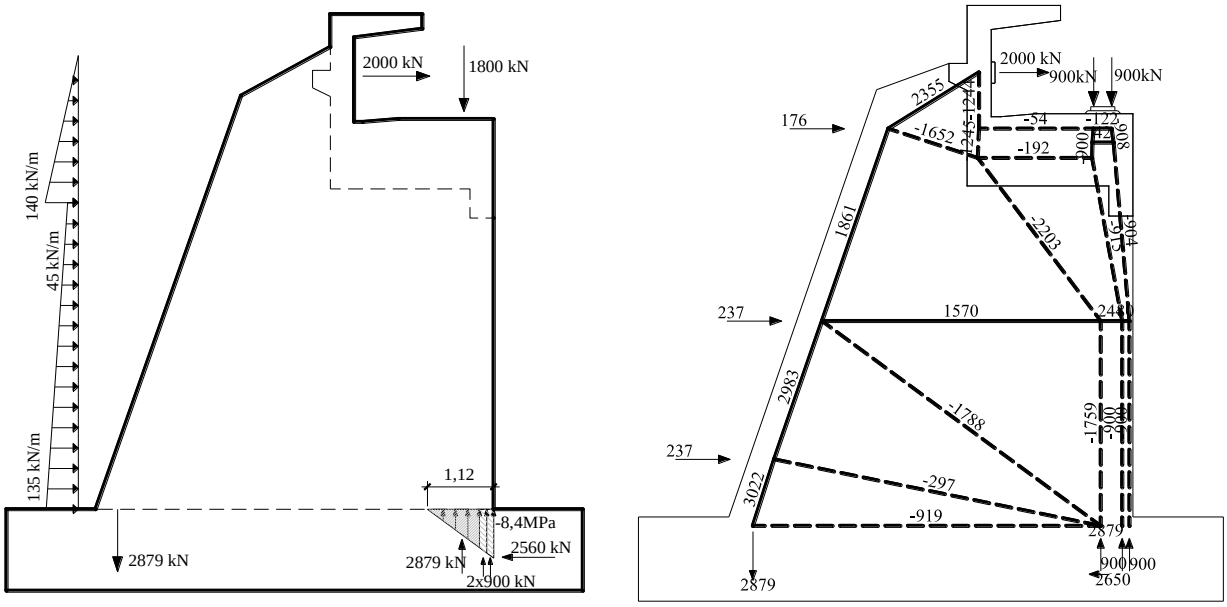
a) loads *b) strut-and-tie model*

Fig. 11-11: Loads and strut-and-tie model for the seismic action pushing the abutment

This document is the intellectual property of the fib – International Federation for Structural Concrete. All rights reserved.
This PDF of fib Bulletin 61 is intended for use and/or distribution solely within fib National Member Groups.

Table 11-1: Tie forces and required and provided reinforcement

Force T [kN]	**A_s [mm^2]**	**$A_{s,\,prov}$ [mm^2]**	**Reinforcement**
1.525	3.506	3.768	3×4ϕ20
1.244	2.860	3.768	2×5ϕ20+2ϕ20
829	1.906	2.946	6ϕ25
1.635/1,00=1.635 kN/m	3.759 mm^2/m	4.022 mm^2/m	4×ϕ16-0,20
624/1,77=353 kN/m	810 mm^2/m	2.260 mm^2/m	4×ϕ12-0,20



a) *b)) strut-and-tie model*

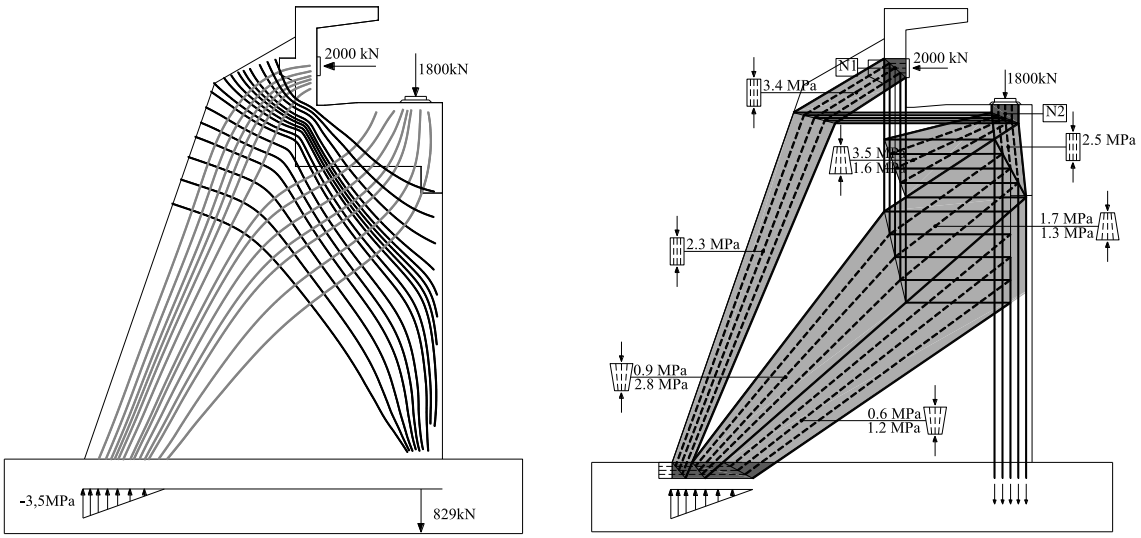
Fig. 11-12: Loads and strut-and-tie model for the seismic action pulling the abutment

Table 11-2: Tie forces, required and provided reinforcement

Force T [kN]	**A_s [mm^2]**	**$A_{s,\,prov}$ [mm^2]**	**Reinforcement**
3.022	6.950	11.256	6ϕ32 + 8ϕ32
1.570/3,1=506 kN/m	1.160 mm^2/m	2.260 mm^2/m	4×ϕ12-0,20

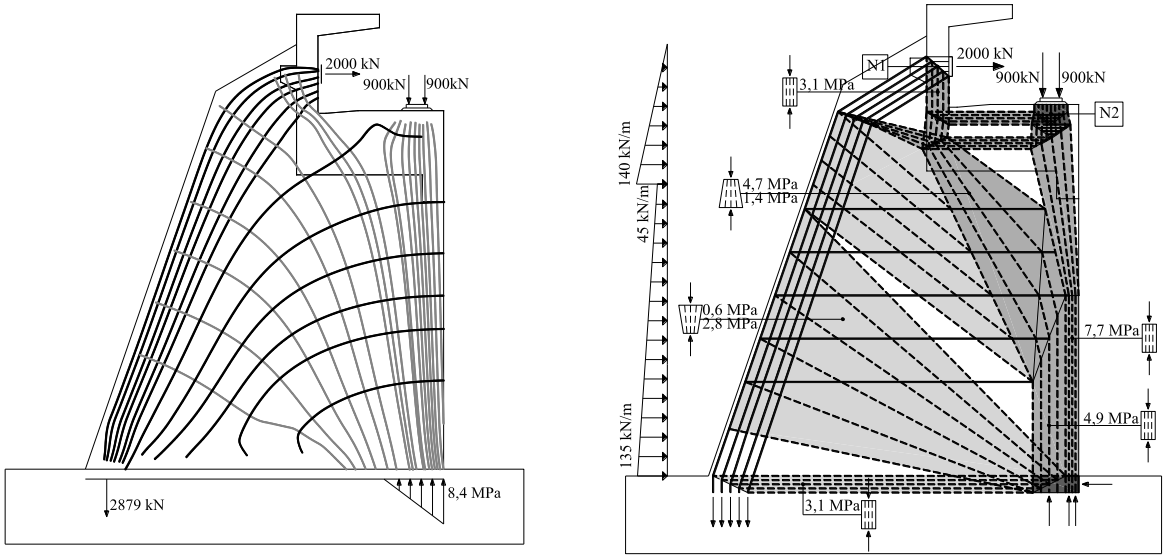
Fig. 11-14 illustrates the comparison between the finite element analysis elastic stress trajectories and the stress fields of the design models presented. In the first case, seismic action pulling the abutment - see Figs. 11-13a and b, the strut-and-tie model matches quite well the elastic stress trajectories obtained directly from the FEM analysis. The second model, seismic action pushing the abutment - see Figs. 11-14a and b, the stress fields are locally slightly deviated due to the adoption of an orthogonal reinforcement configuration.

This document is the intellectual property of the fib – International Federation for Structural Concrete. All rights reserved.
This PDF of fib Bulletin 61 is intended for use and/or distribution solely within fib National Member Groups.



a) elastic stress trajectories *b) stress fields*

Fig. 11-13: Elastic stress trajectories and stress fields for seismic action pushing the abutment



a) elastic stress trajectories *b) stress fields*

Fig. 11-14: Elastic stress trajectories and stress fields for seismic action pulling the abutment

2.2 Check of nodes

2.2.1 Seismic action pushing the abutment

The concrete regions adjacent to the pot-bearings and damping device, where important concentrated loads are applied, must be checked. Fig. 11-15 shows the nodes geometry and stresses for the seismic action pushing the abutment.

According to sect.5.3.2 of FIP Recommendations (1999) the effective concrete strength in CCT nodes must be multiplied by a reduction factor ν_2=0,85. The reversal loading due to the seismic action leads to cracking in the nodes region that can influence nodes strength. Therefore a smaller value of concrete effective compression strength was considered for checking the nodes N1 and N2 ($\nu_2 = 0{,}6$; $f_{cd,eff} = \nu_2 f_{1,cd} = 0{,}6 \cdot 14{,}17 = 8{,}5\ MPa$) related with the reduction factor for struts crossing normal crack widths.

This document is the intellectual property of the fib – International Federation for Structural Concrete. All rights reserved.
This PDF of fib Bulletin 61 is intended for use and/or distribution solely within fib National Member Groups.

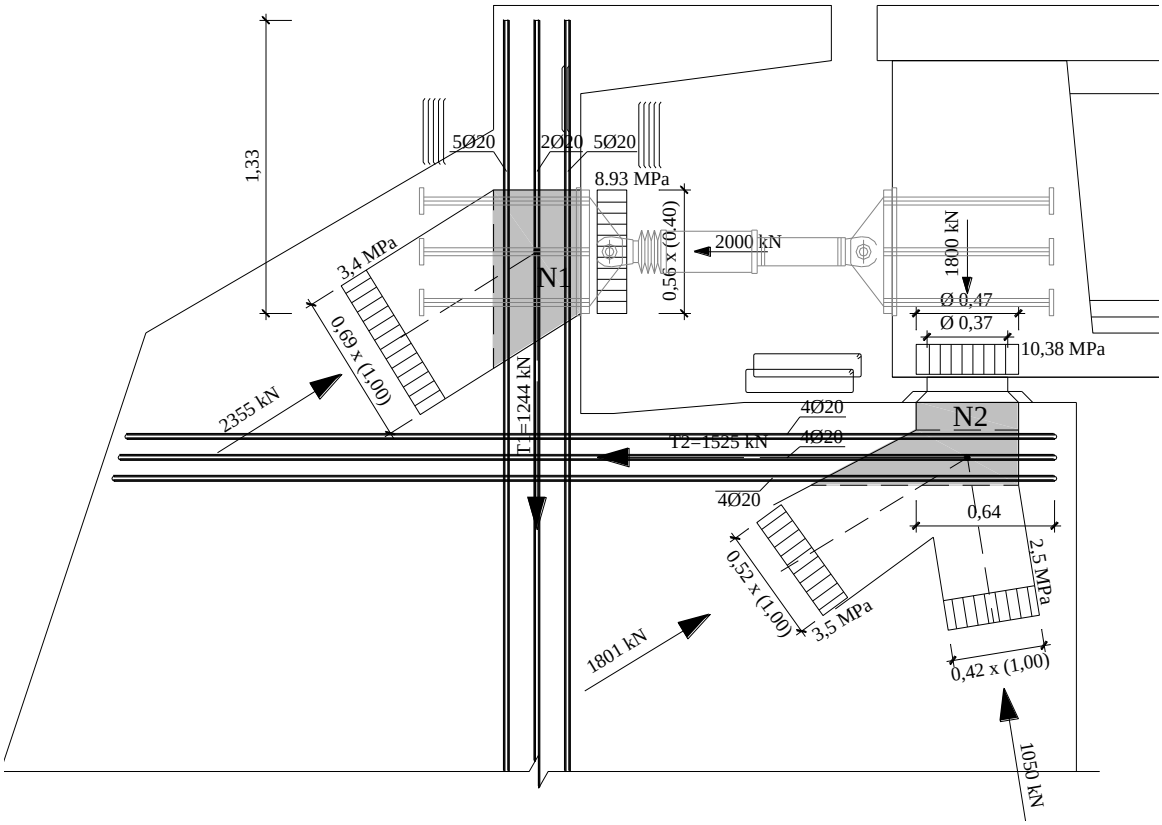


Fig. 11-15: Nodes N1 and N2 geometry for the seismic action pushing the abutment

Furthermore, under the support, the concrete compressive strength is $\sigma_{c,max} = 1{,}2\, f_{1,cd} \sqrt{\frac{A_{c1}}{A_{c0}}}$, according to sect.5.6.2 resulting in the following values:

- for node N1: $A_{c0}=0{,}56 \cdot 0{,}40=0{,}224\ m^2$ and $A_{c1}=1{,}16 \cdot 1{,}00=1{,}16\ m^2$

$$\Rightarrow \sigma_{c,max} = 38{,}69\ MPa > 8{,}93\ MPa$$

- for node N2: $A_{c0}=\pi \cdot 0{,}47^2 / 4=0{,}173\ m^2$ and $A_{c1}=\pi \cdot 1.0^2 / 4=0{,}785\ m^2$

$$\Rightarrow \sigma_{c,max} = 36{,}21\ MPa > 10{,}38\ MPa$$

The anchorage length of ties T1 and T2 are obtained from sect.5.6.4 of FIP Recommendations (1999).

$$l_{b,net} = \alpha_a l_b \frac{A_{s,req}}{A_{s,prov}} \quad \text{with} \quad l_b = \phi \cdot \frac{f_{yd}}{4 \cdot (1{,}05 \cdot f_{ctm})} = 0{,}02 \cdot \frac{435}{4 \cdot 1{,}05 \cdot 2{,}6} = 0{,}797\, m$$

where: α_a=1,0 and α_a =0,5 for nodes T1 and T2, respectively.

$$\left(\frac{A_{s,req}}{A_{s,prov}}\right)_{T1} = \frac{2.860}{3.868} = 0{,}739 \text{ and } \left(\frac{A_{s,req}}{A_{s,prov}}\right)_{T2} = \frac{3.506}{3.768} = 0{,}930$$

This results in the following anchorage lengths:

for T_1: $l_{b,net}$ = 0,59 m < 1,33 m and for T_2: $l_{b,net}$ = 0,37 m < 0,64 m

This document is the intellectual property of the fib – International Federation for Structural Concrete. All rights reserved.
This PDF of fib Bulletin 61 is intended for use and/or distribution solely within fib National Member Groups.

The node regions must also be checked in the transversal direction as shown in Fig. 11-16, since the compression field will spread over the depth of the wall (bottle effect), leading to a tension of approximately 25% of the applied load (FIP Recommendations 1999, sect.6.5.2.3).

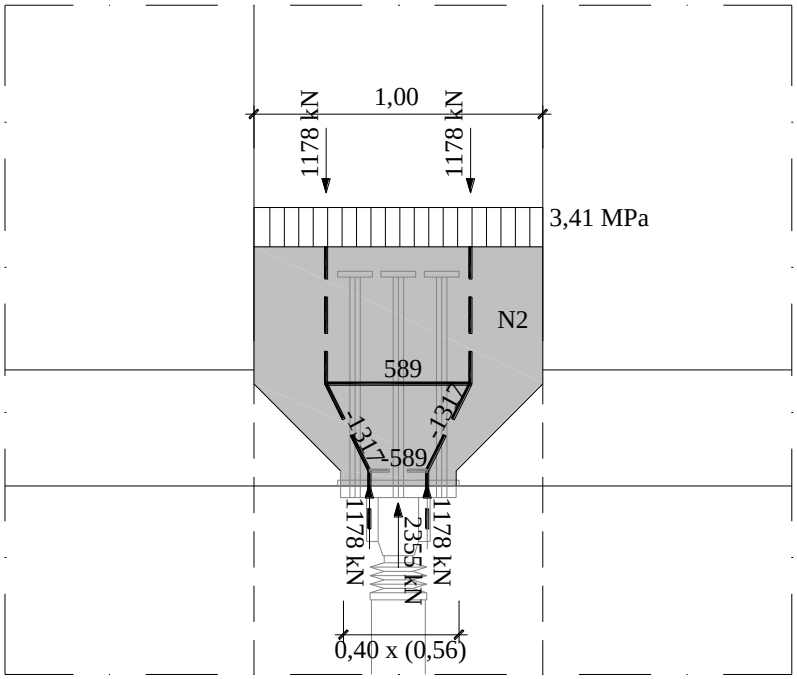


Fig. 11-16: Plan view of node N2

The maximum transverse tension is T=589 kN $\Rightarrow$ A_s=1.350 mm^2 < $A_{s,adopted}$ = 1.870 mm^2.

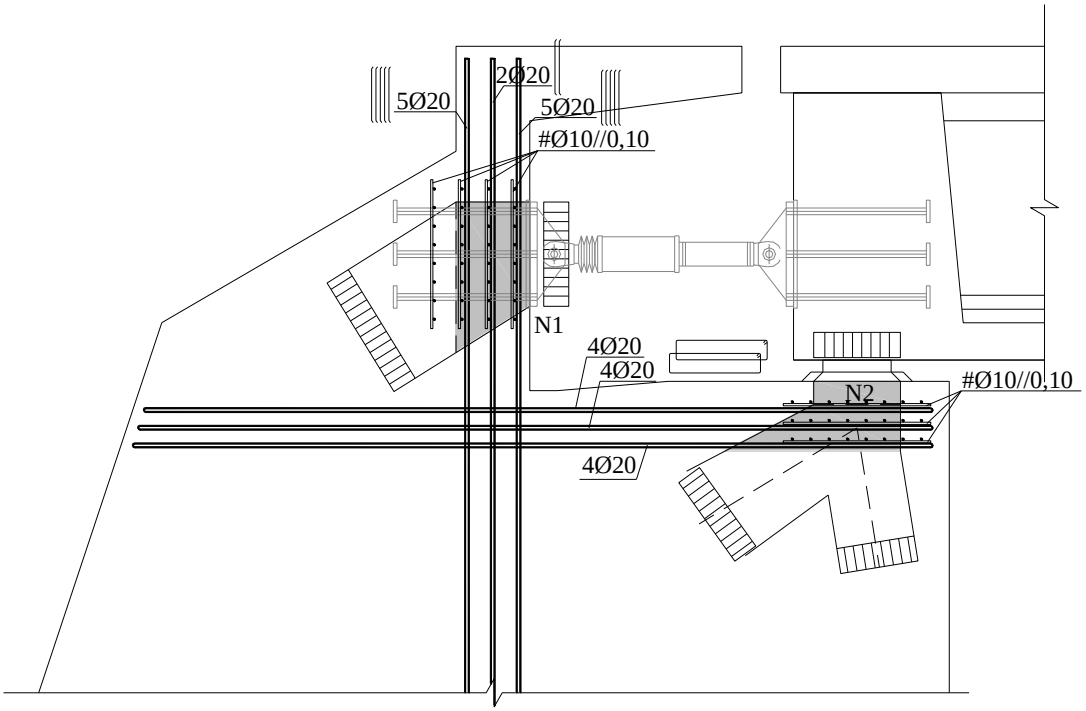


Fig. 11-17: Concentrated loads reinforcement layout

This document is the intellectual property of the fib – International Federation for Structural Concrete. All rights reserved.
This PDF of fib Bulletin 61 is intended for use and/or distribution solely within fib National Member Groups.

The interface between the vertical shear wall and the foundation slab must also be checked, since the inclined strut crosses the interface between concrete casted at different ages (see Fig. 11-18). According to FIP Recommendations 1999, sect. 6.4.7, the maximum shear forces across an interface, is given by:

$$\tau_{f,Rd}=\beta \cdot f_{ctd} + \mu\cdot\sigma_{cd} + \mu\cdot\rho\cdot f_{yd} = 0{,}4\cdot 1{,}2 + 0{,}9\cdot 2{,}6 = 2{,}82 \text{ MPa} > \tau_{f,Ed} = 1{,}96 \text{ MPa}$$

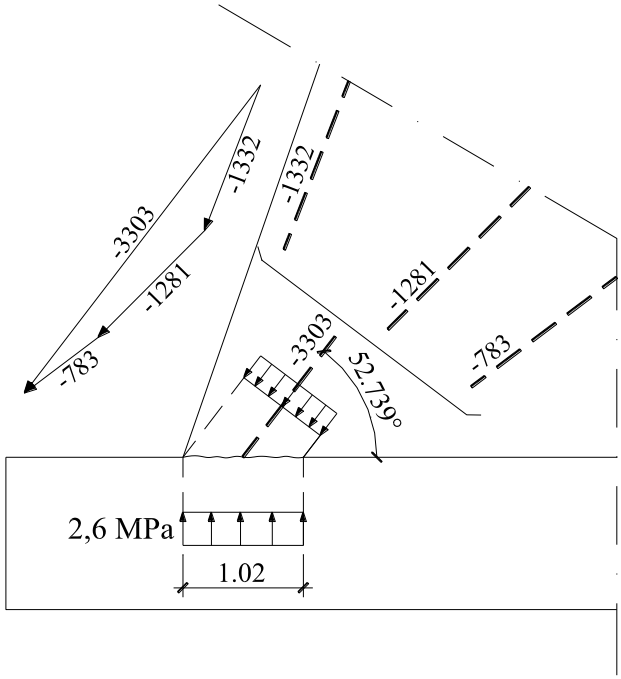


Fig. 11-18: Transfer of strut across joints

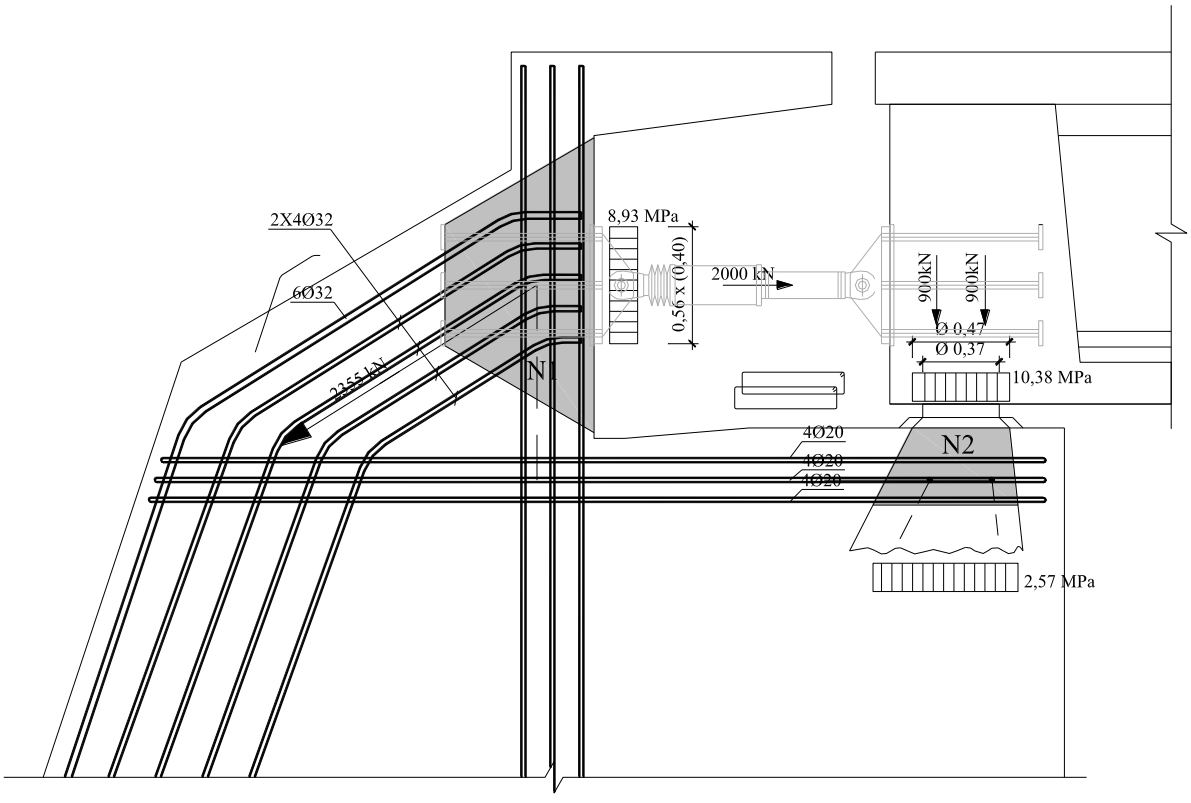


Fig. 11-19: Nodes N1 and N2 geometry for the seismic action pulling the abutment

This document is the intellectual property of the fib – International Federation for Structural Concrete. All rights reserved.
This PDF of fib Bulletin 61 is intended for use and/or distribution solely within fib National Member Groups.

2.2.2 Seismic action pulling the abutment

Concerning the loads when the seismic load is pulling the abutment the same nodes must be checked. The Fig. 11-16 shows the nodes geometry and stresses.

Local compression in node N2 was verified in the previous subchapter. Concerning the node N1, the maximum compression at each of the 8 anchor heads or studs of the damping device is given by (see also Fig. 11-20):

$$\sigma_{c,max} = 1{,}2 \cdot f_{1,cd} \sqrt{\frac{A_{c1}}{A_{c0}}}$$

A_{c0}=0,12 · 0,12 = 0,0144 m^2 and A_{c1}=0,15 · 0,15 = 0,0225 m^2 $\Rightarrow \sigma_{c,max}$ = 21,25 MPa

$$\sigma_{c,Ed} = \frac{2{,}0}{8 \cdot 0{,}12 \cdot 0{,}12} = 17{,}4 \text{ MPa} \quad < 21{,}25 \text{ MPa}$$

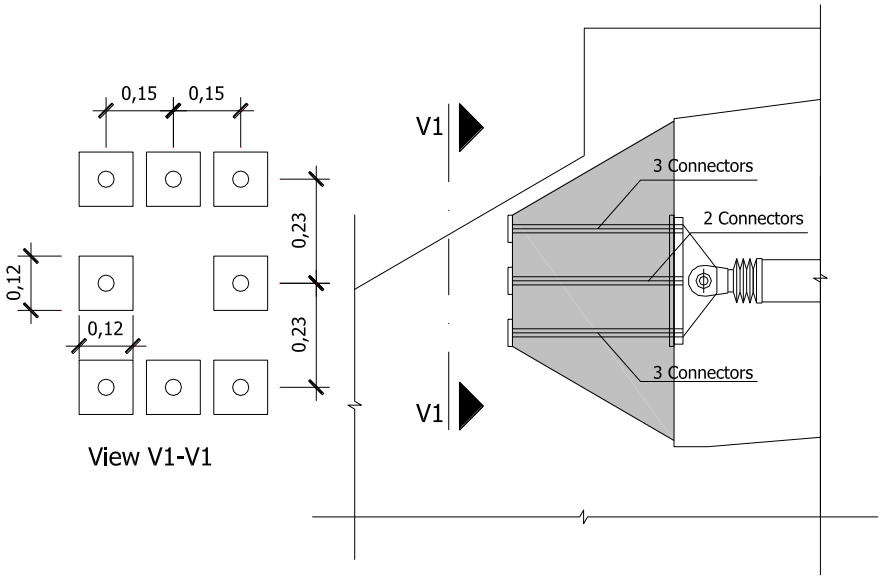


Fig. 11-20: Geometry of the connectors of the damping devices

The compression stresses must transfer the forces into the main tie of the shear wall which must be adequately anchored, thus a special analysis was developed. The provided anchorage length can be calculated according to the model showed in Fig. 11-21, which is similar to an interior anchorage zone, wherein all the force must be tied back.

This document is the intellectual property of the fib – International Federation for Structural Concrete. All rights reserved.
This PDF of fib Bulletin 61 is intended for use and/or distribution solely within fib National Member Groups.

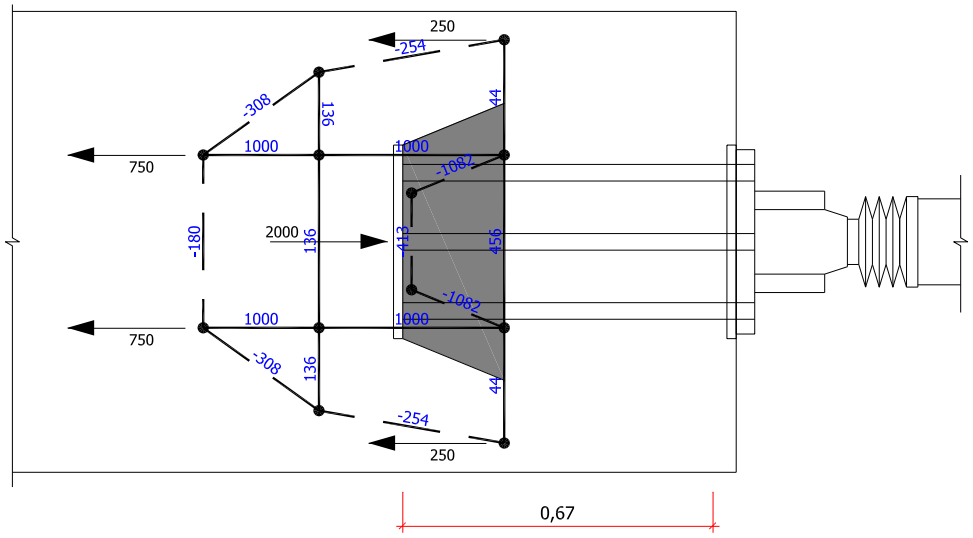


Fig. 11-21: Node N2 plan view for the seismic action pulling the abutment

The provided anchorage length is shown in Fig. 11-21 and the required anchorage length is given by:

$$l_{b,net} = \alpha_a l_b \frac{A_{s,req}}{A_{s,prov}}$$

with $$l_b = \varphi \cdot \frac{f_{yd}}{4 \cdot (1{,}05 \cdot f_{ctm})} = 0{,}032 \cdot \frac{435}{4 \cdot 1.05 \cdot 2.6} = 1{,}27 \text{ m}$$

α_a=1,0

$$\left(\frac{A_{s,req}}{A_{s,prov}} \right)_{T1} = \frac{2.355 / 435 \cdot 10^3}{14 \cdot 8{,}04 \cdot 10^{-4}} = 0{,}48$$

This results in the following anchorage length:

$l_{b,net}$ = 0,61 m < 0,67 m

Similar to the case of the seismic action pushing the abutment, the interface between the shear wall and the foundation slab must also be checked (see Fig. 11-22). According to the FIP Recommendations 1999, sect.6.4.7, the shear capacity, is given by:

$\tau_{f,Rd}=\beta \cdot f_{ctd} + \mu \cdot \sigma_{cd} + \mu \cdot \rho \cdot f_{yd}$ = 0,4·1,2 + 0,9·6,3 = 6,15 MPa > $\tau_{f,Ed}$ = 2,34 MPa

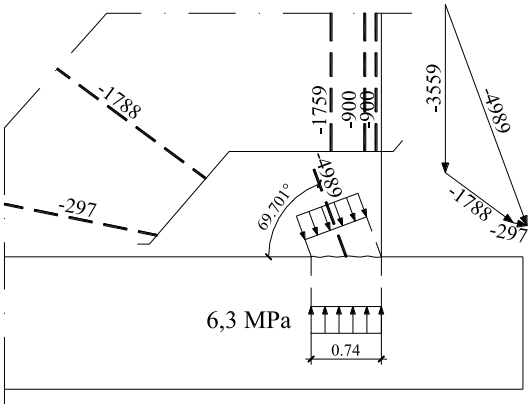


Fig. 11-22 - Transfer of strut across joints

This document is the intellectual property of the fib – International Federation for Structural Concrete. All rights reserved.
This PDF of fib Bulletin 61 is intended for use and/or distribution solely within fib National Member Groups.

3 Detailing

The detailing of the reinforcement is shown in Fig. 11-23 and it follows from the strut-and-tie design models presented before.

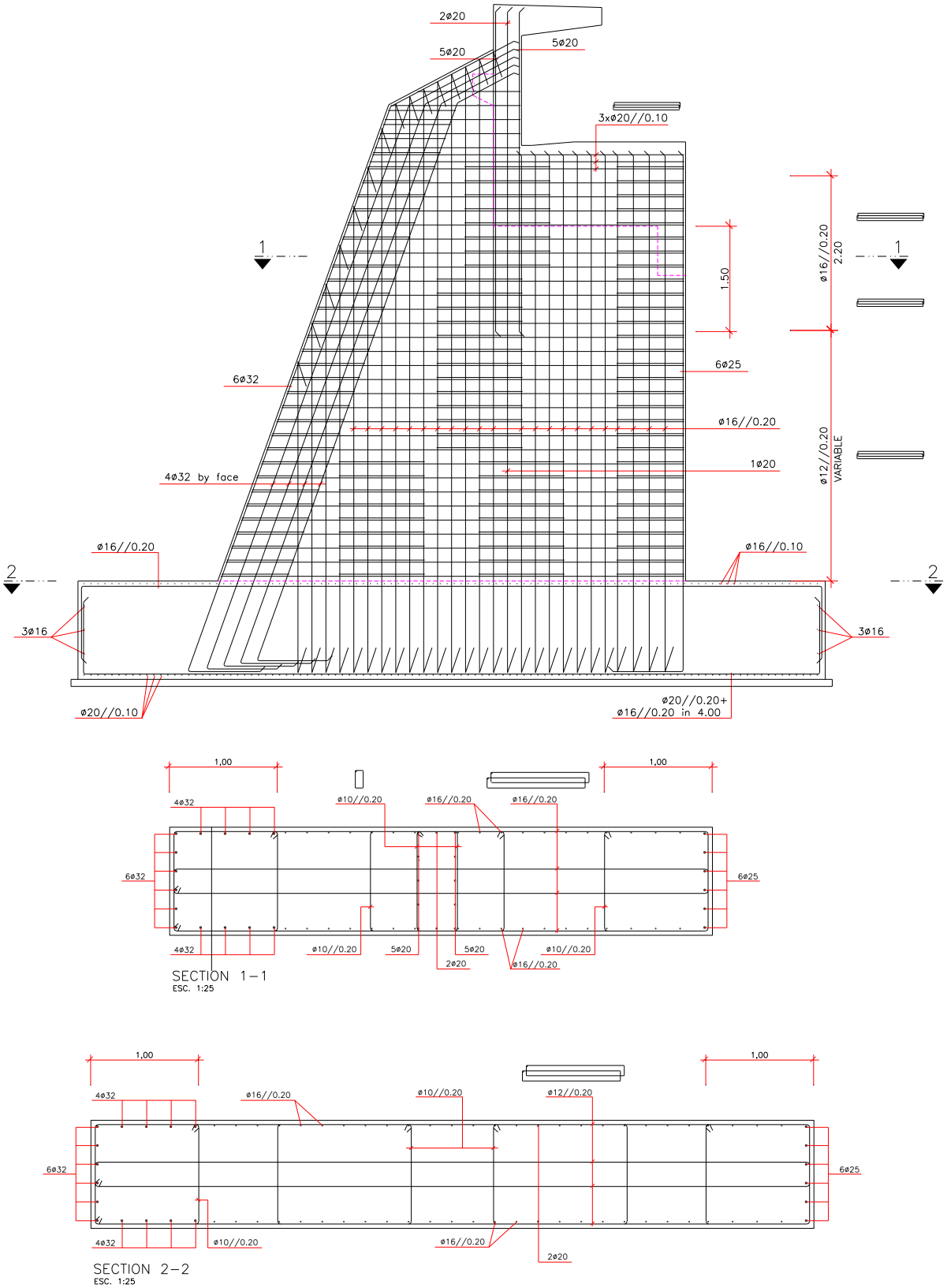


Fig. 11-23: Reinforcement for the abutment
(decimal is point instead of comma; see Editorial Comments on p. vi)

This document is the intellectual property of the fib – International Federation for Structural Concrete. All rights reserved.
This PDF of fib Bulletin 61 is intended for use and/or distribution solely within fib National Member Groups.

4 Summary and conclusions

The strut-and-tie method intends to reproduce the compression and tension fields due to the load path deviation within any structural concrete region. The application of the method to the design and detailing of a viaduct fixed abutment was shown to be particularly useful. The perception of the flow of forces provided by the method allowed a clear understanding of the region main behaviour and furthermore leaded to the proper analysis and detailing, under the applied loads. Different strut-and-tie models were developed due to the seismic action in both directions. Refined local models in critical regions allowed the definition of the appropriate reinforcement detail as well as the node checking.

References

FIP Recommendations (1999): Practical Design of Structural Concrete. FIP-Commission 3 "Practical Design", Sept. 1996. Publ.: SETO, London, Sept. 1999. (Distributed by: *fib*, Lausanne. Web http://www.fib-international.org)

This document is the intellectual property of the fib – International Federation for Structural Concrete. All rights reserved.
This PDF of fib Bulletin 61 is intended for use and/or distribution solely within fib National Member Groups.

Example 12:
Design of D-regions of the Enmedio stream bridge

Santiago Perez-Fadón Martínez, Carlos J. Bajo Pavía

1 The D-regions of the Enmedio stream bridge

The Enmedio stream bridge is located within the motorway of Málaga-Guadiaro, in the tract of Guadiaro-Estepona. It has a length of 158 m with two asymmetric spans of 106 and 52 m as shown Fig. 12-1, and is supported by a pier with a double wall. The deck is a mixture of a segmental cantilever deck and a composite box girder.

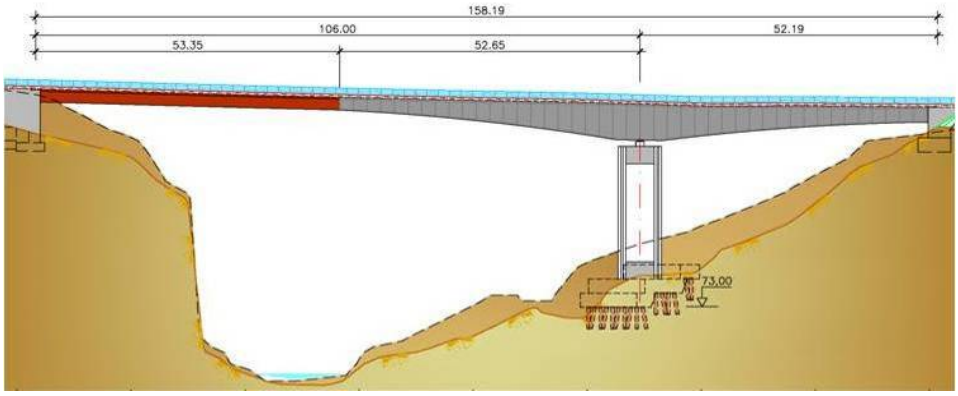


Fig. 12-1: View of the Enmedio stream bridge

Taking into account the basic characteristics of the bridge, the D regions have been identified (see Fig. 12-2), which were designed with strut-and-tie models. These regions are:

- 1: Support section of metallic deck - concrete segment
- 2: Deck support section on piers
- 3: Pier foundation by means of stepped pilecap
- 4 and 5: Anchorage at abutments with vertical prestressing and inverse bearing heel.

This document is the intellectual property of the fib – International Federation for Structural Concrete. All rights reserved.
This PDF of fib Bulletin 61 is intended for use and/or distribution solely within fib National Member Groups.

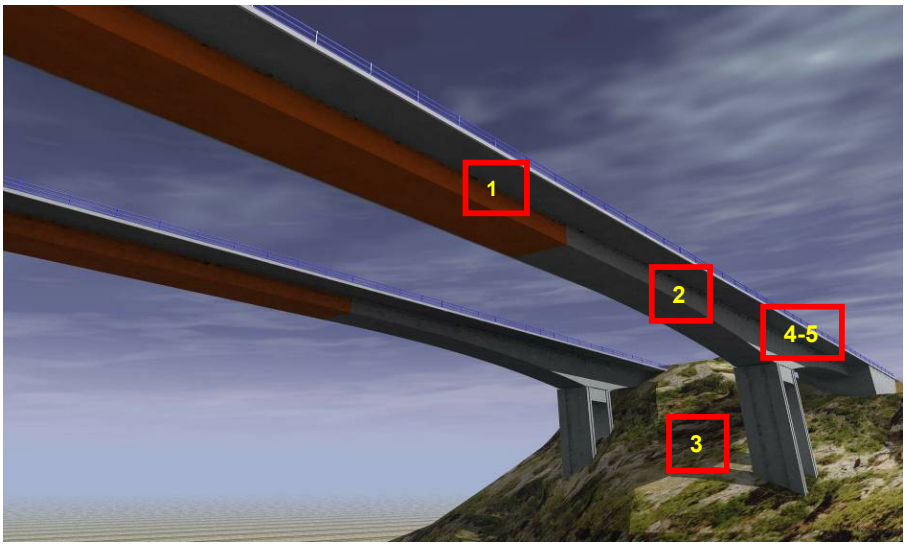


Fig. 12-2: D-regions of the Enmedio stream bridge

2 Support of steel deck on concrete segment

2.1 Design problem

Supports are singular points because of the high concentration of stresses due to local forces, and this excludes normally used analyses, but requires the evaluation with the strut-and-tie method. In the case of this bridge, the support consists of the steel deck resting on a concrete cantilever, with the addition of a prestressing force in both the top and the lower slab. The layout is shown in Fig. 12-3. The support introduces a vertical load on the concrete section in addition to the eccentric compressions generated by the prestressing force.

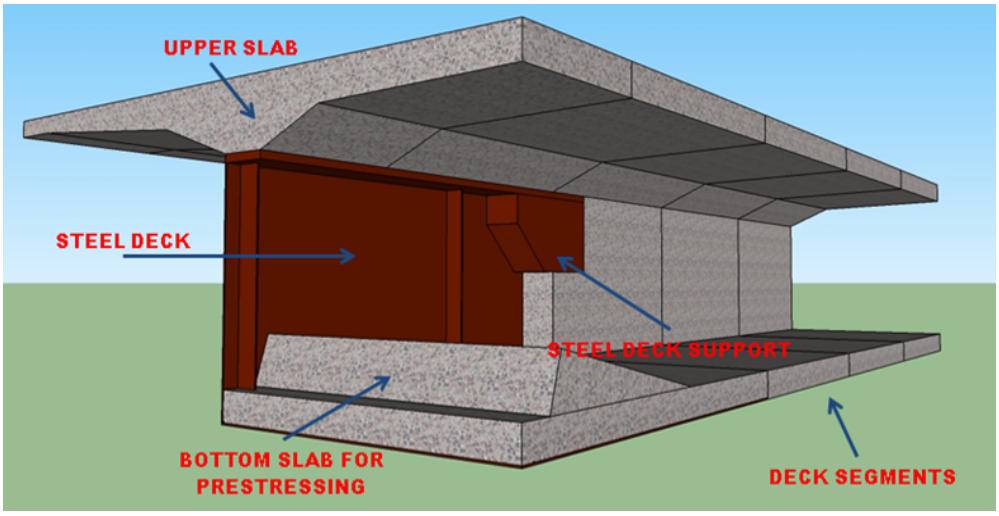


Fig. 12-3: Layout of steel girder supported by heel

2.2 Strut-and-tie model

The previously mentioned vertical force induces a shear force in addition to a bending moment which induces tension in the upper fibre of the deck and compression in the lower fibre. Therefore, the compression from the upper prestressing force reduces this tension stress and the resulting outline of forces is shown in Fig. 12-4, following FIP Recommendations

This document is the intellectual property of the fib – International Federation for Structural Concrete. All rights reserved.
This PDF of fib Bulletin 61 is intended for use and/or distribution solely within fib National Member Groups.

(1999). Compatibility should be considered by, at least, as close as possibly as the stress fields determined from a linear-elastic analysis, see Fig. 12-4. The support reactions appear at the right side of this Fig. 12-4.

Several models can be used to explain the behaviour of the stress fields. The one shown in Fig. 12-5 is the mixture between two different models. The first model is for the introduction of the vertical force in to the corbel and the second considers the spreading of this force in the web according to the common truss model in B-regions.

The analysis of the truss forces follows from the global balance of the structure. The external forces applied on the concrete segment are a vertical force of 2.000 kN due to the steel deck weight, a prestressing force of 3.500 kN applied at the top of the segment and a prestressing force of 500 kN applied at the bottom part. As a result, the three reactions shown in Fig. 12-5 are obtained:

$R_1 = -47$ kN; $R_2 = 2.845$ kN; $R_3 = 4.023$ kN

Each node is then solved, using the equilibrium equations to obtain the internal forces, and the balance is verified by checking the last two nodes.

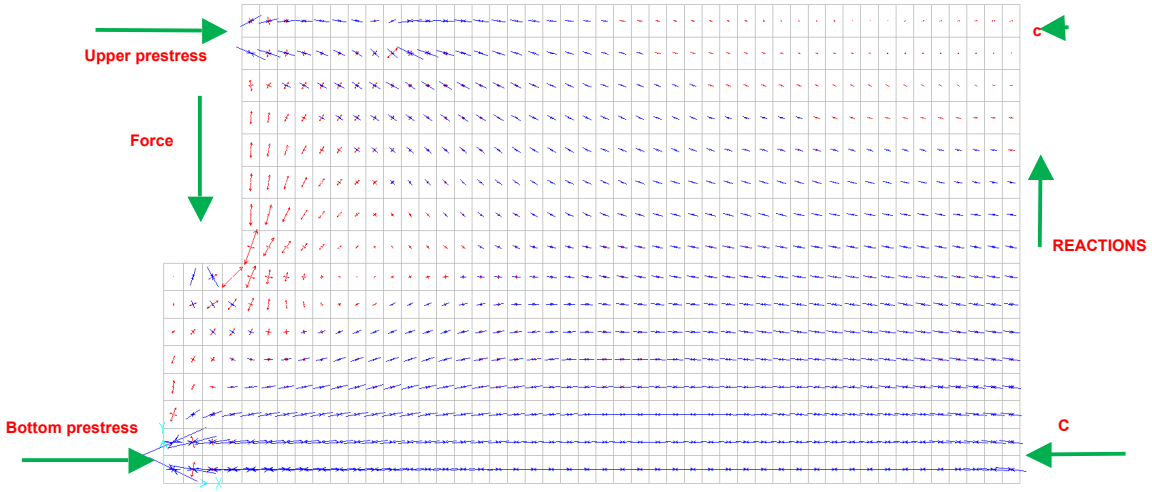


Fig. 12-4: Stress diagram for the support with forces and reactions

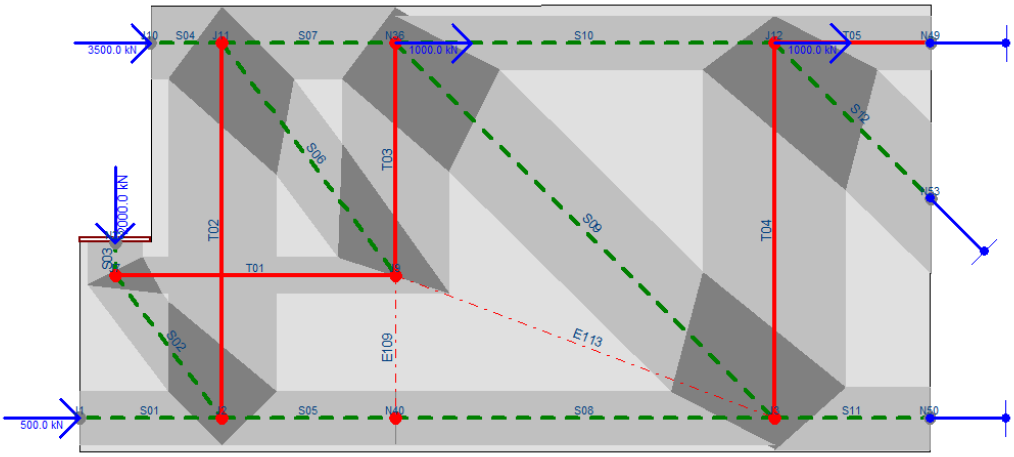


Fig. 12-5: Strut-tie-model for the corbel support

This document is the intellectual property of the fib – International Federation for Structural Concrete. All rights reserved.
This PDF of fib Bulletin 61 is intended for use and/or distribution solely within fib National Member Groups.

2.3 Check of struts

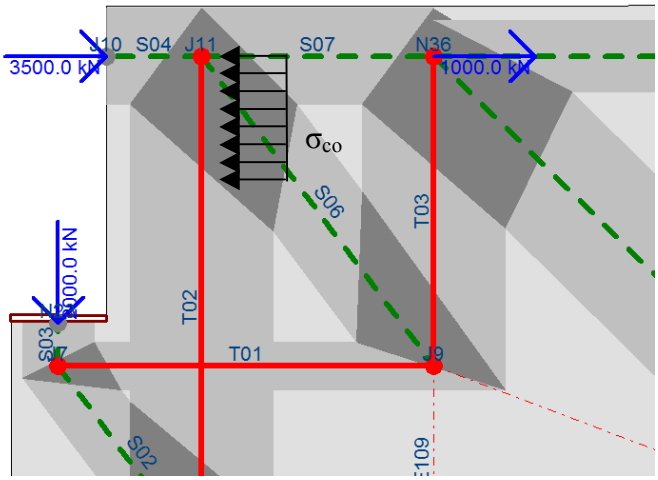
The materials used are concrete C-60 and reinforcement steel B 500-S. Following the Spanish code, EHE, the design values are:

$f_{cd} = 60/1{,}5 = 40$ MPa; $f_{yd} = 500/1{,}15 = 434{,}8$ MPa

The calculation of the stresses of each strut and each tie verifies that these design values are not exceeded.

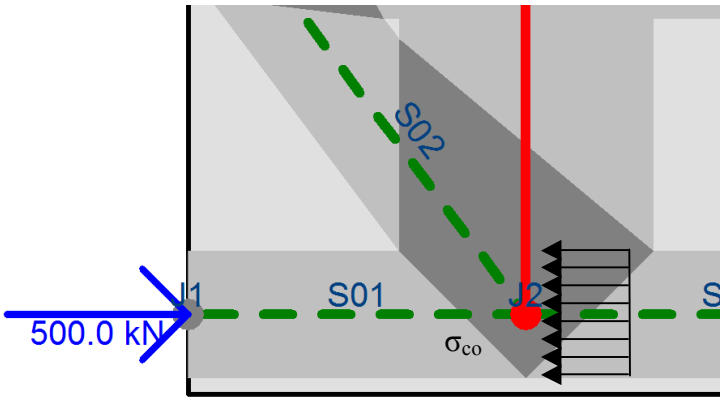
2.4 Check of nodes

The strut-and-tie model has two nodes that require an examination of stresses, and in each node a tie is anchored. The nodes and the calculated stresses are show in Fig. 12-6 and 12-7.



$$\sigma_{co} = 31\,\text{MPa} \le 0{,}80\,f_{cd} \text{ or } 0{,}85\,f_{cd}$$

Fig. 12-6: Node 1
(decimal is point instead of comma; see Editorial Comments on p. vi)



$$\sigma_{co} = 29\,\text{MPa} \le 1{,}20\,f_{cd}$$

Fig. 12-7: Node 2 (decimal is point instead of comma; see Editorial Comments on p. vi)

2.5 Design and layout of reinforcement

The necessary steel rebar area for each tie is shown in Table 12-1, and the selected reinforcement is sketched in Fig. 12-8.

This document is the intellectual property of the fib – International Federation for Structural Concrete. All rights reserved.
This PDF of fib Bulletin 61 is intended for use and/or distribution solely within fib National Member Groups.

Table 12-1: Design of reinforcement

Tie	*Force (kN)*	*Necessary Steel area (mm^2)*	*Reinforcement*
T01	+1.500	3.750	4ϕ25 in 2 layers at 200 mm
T02	+2.000	5.000	3 layers with 4ϕ25
T03	+2.000	5.000	3 layers with 4ϕ25
T04	+2.000	5.000	3 sϕ16 each 200 mm
T05	+ 47	120	not necessary

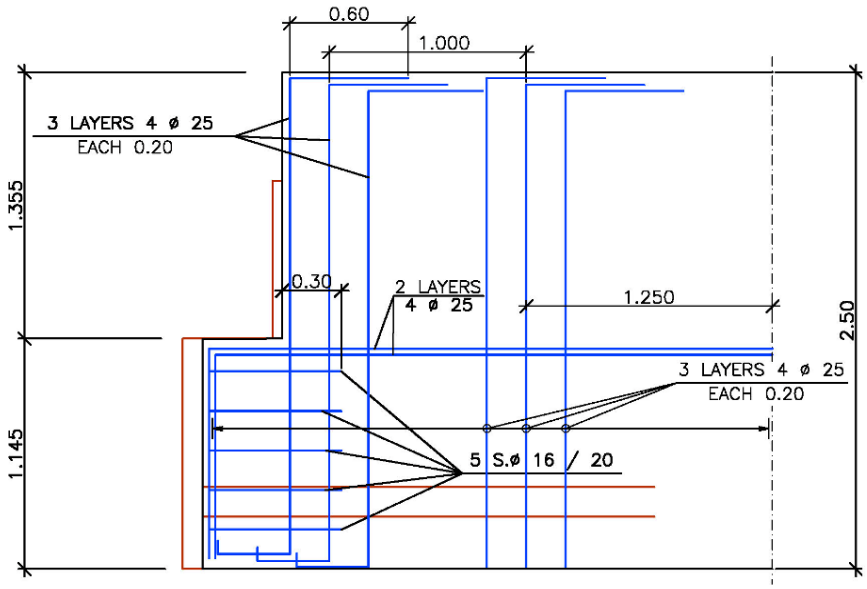


Fig. 12-8: Layout of the reinforcement support in the concrete segment (decimal is point instead of comma; see Editorial Comments on p. vi)

3 Diaphragm segment above pier

3.1 Introduction

Support deck zones on the piers are D-regions where high forces are introduced. In the case of the Enmedio stream bridge, the support also consists of the concrete segment that is supported by one pier. The diaphragm is made in a second stage and is connected with the webs along its surface. The problem analyzed here is how to handle the transfer of the shear force towards the pier supports because the webs of the segment do not coincide with the axis of the bearings.

This document is the intellectual property of the fib – International Federation for Structural Concrete. All rights reserved.
This PDF of fib Bulletin 61 is intended for use and/or distribution solely within fib National Member Groups.

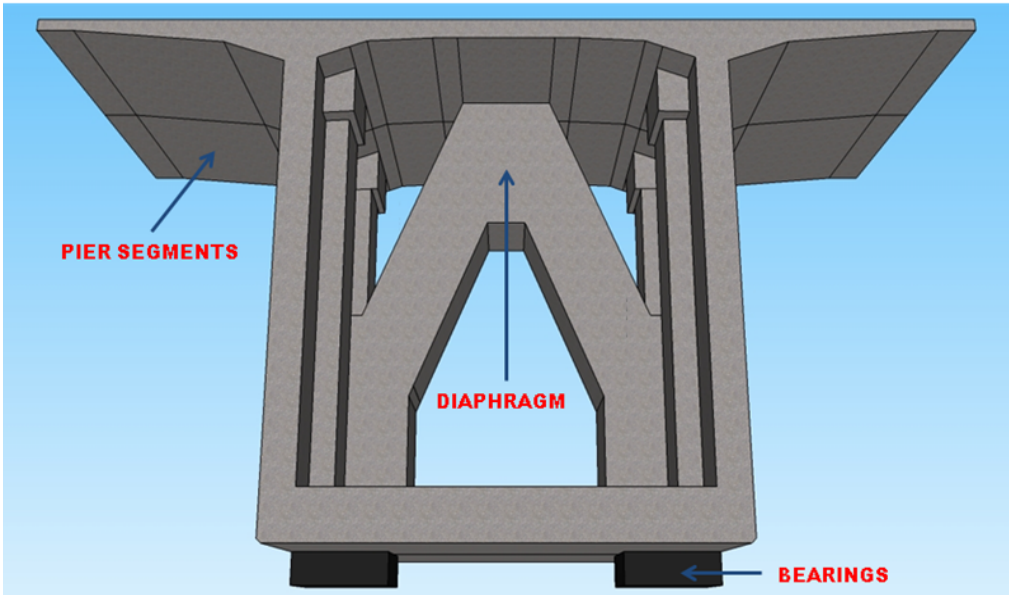
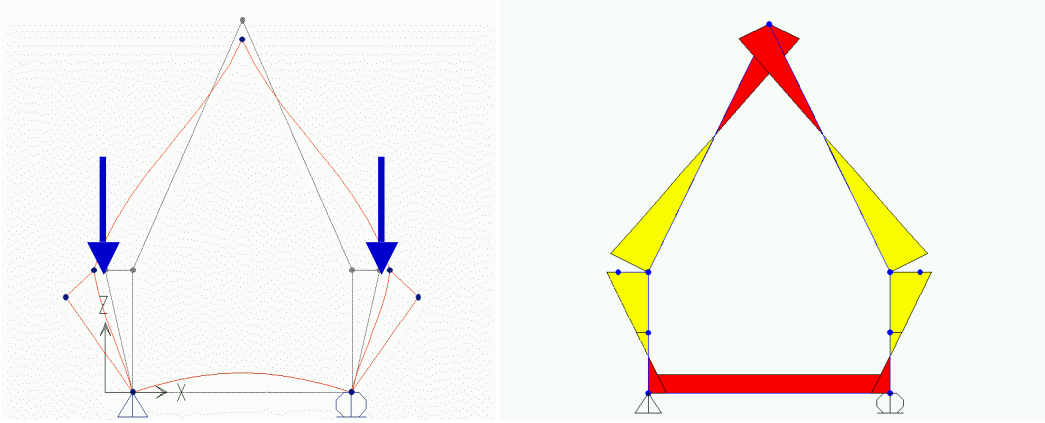


Fig. 12-9: Transverse section of the intermediate support

3.2 Analysis for flexure and torsion

Flexure occurs in the diaphragm due to the vertical forces of the webs of the segments. However, the axis of reaction on piers does not coincide with the axis of the webs due to the dimension of bearings, and this causes the flexure. The basic model for flexure is shown in Fig. 12-10.



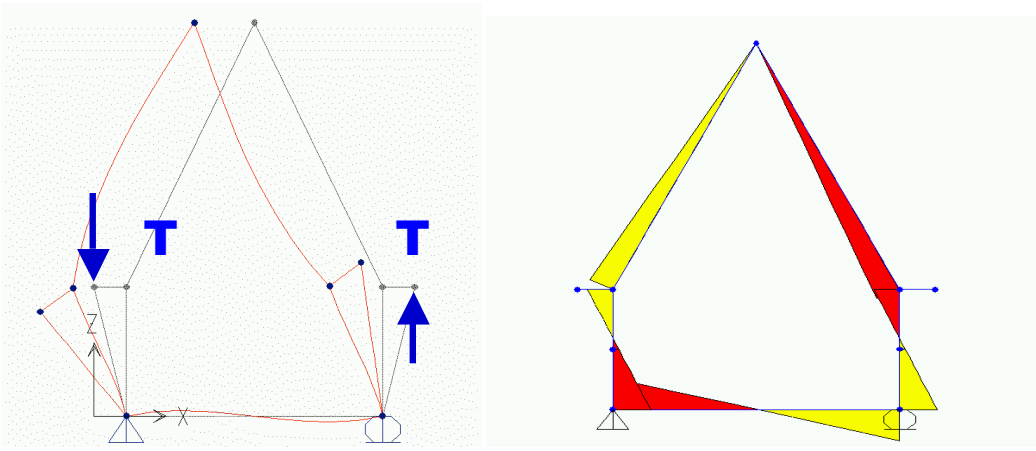
a) deformations *b) bending moments*

Fig. 12-10: Model for flexure of the diaphragm

The behaviour under torsion of the section, grossly calculated, is due to the action of a vertical force-couple, opposite to one another and acting in the webs of the section, see Fig. 12-11. The deformed shape due to the bridge torsion is directly related to the bending moment diagram.

Once the flexural and torsional effects have been analyzed in the diaphragm as an individual element, a strut-and-tie model can be developed including both D- and B-regions.

This document is the intellectual property of the fib – International Federation for Structural Concrete. All rights reserved.
This PDF of fib Bulletin 61 is intended for use and/or distribution solely within fib National Member Groups.



a) deformations *b) bending moments*

Fig. 12-11: Model for torsion of the diaphragm

3.2 Strut-and-tie model

The main function of such type of diaphragm is to avoid distortion inside the box section of the deck. Therefore, a field of tension and compression occurs when torsion occurs, and the inner forces are shown in Fig. 12-12. The torsion effect results in tension and compression fields in the triangular shape of the diaphragm. The forces due to flexure change when torsion forces appear, so that some strut may be changed into ties and also some ties into struts.

The new torsion forces are:

- two horizontal forces toward the left at the top nodes 46 and 49 of 850 KN.
- one force of 11.000 kN, vertical in the left web and one of 9.000 kN in the right web, both descending forces.
- A pair of forces of 850 kN horizontally towards the right in each one of the outer nodes of the inferior slab.
- The reactions in the supports from the forces R1 = 13.754 kN and R2 = 6.246 kN.

In Fig. 12-13, a detail of the model in the support areas is shown. It can be seen that inside two previous symmetric nodes some of the struts turn into ties due to the new forces applied.

This document is the intellectual property of the fib – International Federation for Structural Concrete. All rights reserved.
This PDF of fib Bulletin 61 is intended for use and/or distribution solely within fib National Member Groups.

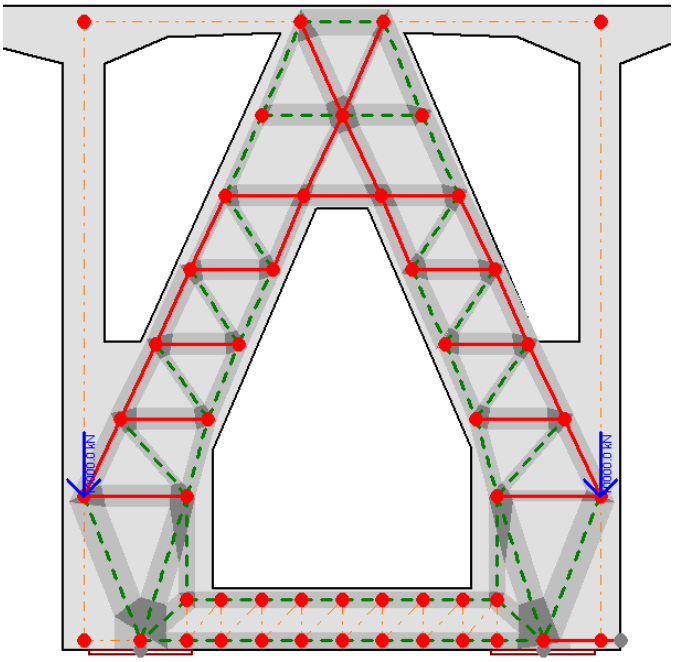


Fig. 12-12: Flexural model including applied forces

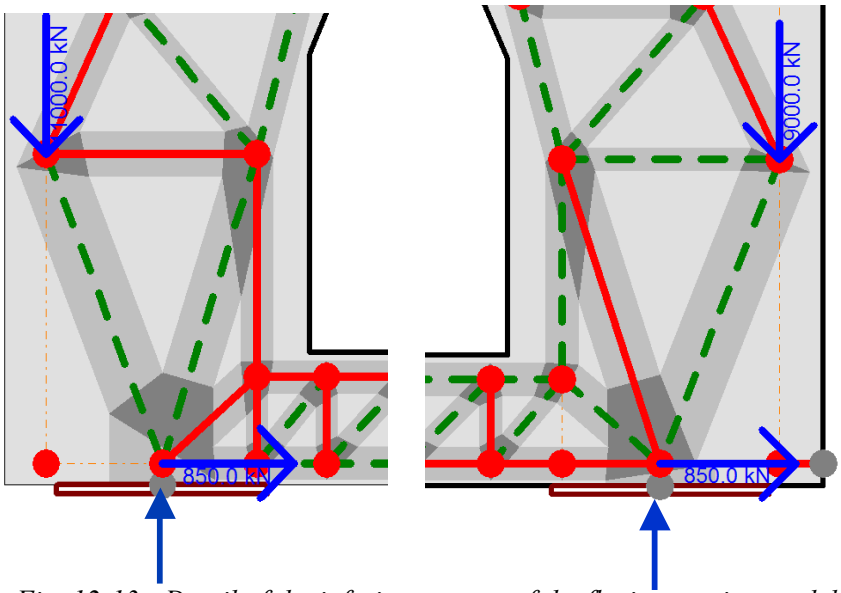


Fig. 12-13: Detail of the inferior corners of the flexion-torsion model

3.3 Solving the model

The inner forces of the model are shown in Fig. 12-14.

This document is the intellectual property of the fib – International Federation for Structural Concrete. All rights reserved.
This PDF of fib Bulletin 61 is intended for use and/or distribution solely within fib National Member Groups.

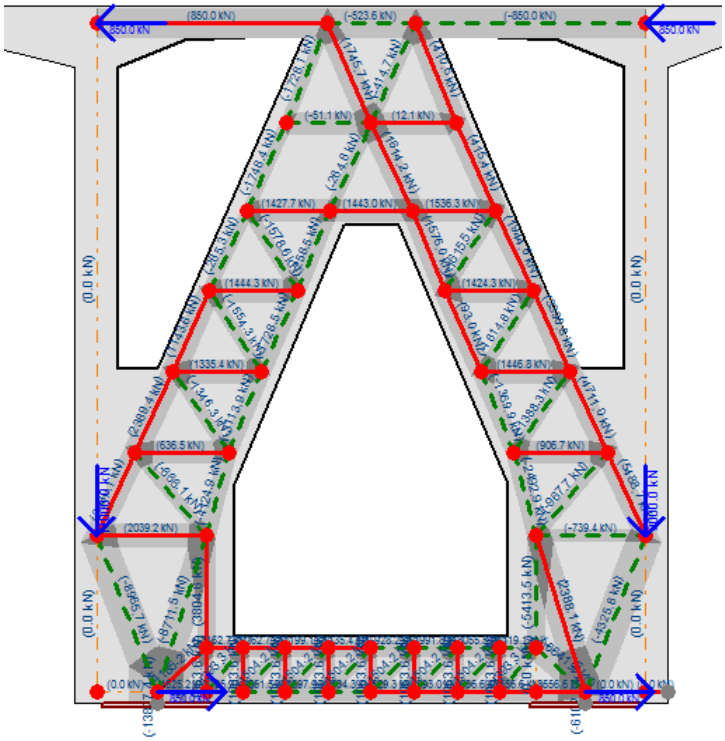


Fig. 12-14: Detail of the model and forces in elements

3.4 Check of struts

The strut calculations are performed based upon the mechanical characteristics of the model and the area of the transverse section of each element, producing the higher acceptable stress that is then compared with the calculated force.

The design material strengths for concrete grade C-60 and reinforcement B 500-S are determined for extended execution control with $\gamma_c = 1{,}50$ and $\gamma_s = 1{,}15$ to:

$f_{cd} = 60/1{,}5 = 40{,}00$ MPa

$f_{yd} = 500/1{,}15 = 434{,}8$ MPa

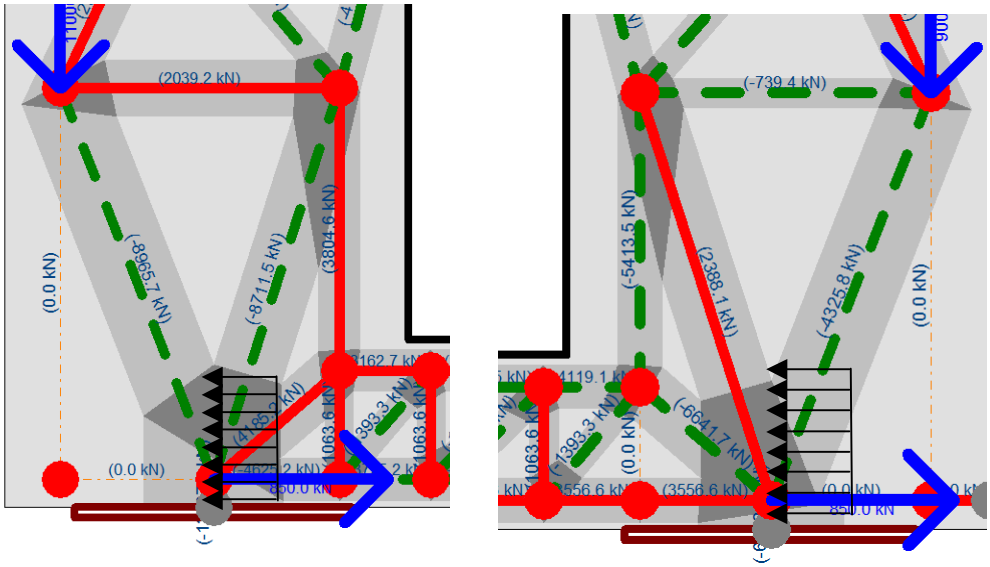
It has been verified that every strut is below the maximum compression admissible using the compression fields widths shown in the Fig. 12-14.

3.5 Check of nodes

It is necessary to check the stress of the multicompressed nodes located in the inferior corners of the model.

This document is the intellectual property of the fib – International Federation for Structural Concrete. All rights reserved.
This PDF of fib Bulletin 61 is intended for use and/or distribution solely within fib National Member Groups.

LEFT NODE: RIGHT NODE:



$\sigma_{CO} = 27,51$ MPa $\sigma_{CO} = 12,49$ MPa

Fig. 12-15: Check of nodes

3.6 Designing of ties and reinforcement.

The ties shown in Fig. 12-14 are dimensioned and the results are given in Table 12-2.

Table 12-2: Required reinforcement

Tension elements	Reinforcement
ST07, ST08, ST09, ST10, ST11, ST86, ST87, ST88, ST89	15 ∅32
ST16, ST35, ST40, ST45, ST48, ST53, ST56, ST59, ST61, ST67, ST69, ST75, ST76, ST80, ST82, E53	16 ∅32
ST17, ST19, ST21, ST23, ST25, ST27, ST29, ST31	8 stirrups ∅16
ST38, ST46, ST47, ST54, ST55, ST62, ST63, ST70, ST71, ST72, ST78, ST83	4 layers 6 ∅16 at 200 mm

The reinforcement of the diaphragm is shown in Fig. 12-16. The distribution of the reinforcing bars does not exactly fit to the model because the layout must cover the envelope of all possible models which could be applied.

Focusing on the point where the vertical force is applied on webs, it can be discussed which is the length in the webs over which the shear forces spread into the diaphragm. Therefore, avoiding any uncertainty, the reinforcement layout covers the complete web height along the connection surface between the diaphragm and the segment webs with couplers.

This document is the intellectual property of the fib – International Federation for Structural Concrete. All rights reserved.
This PDF of fib Bulletin 61 is intended for use and/or distribution solely within fib National Member Groups.

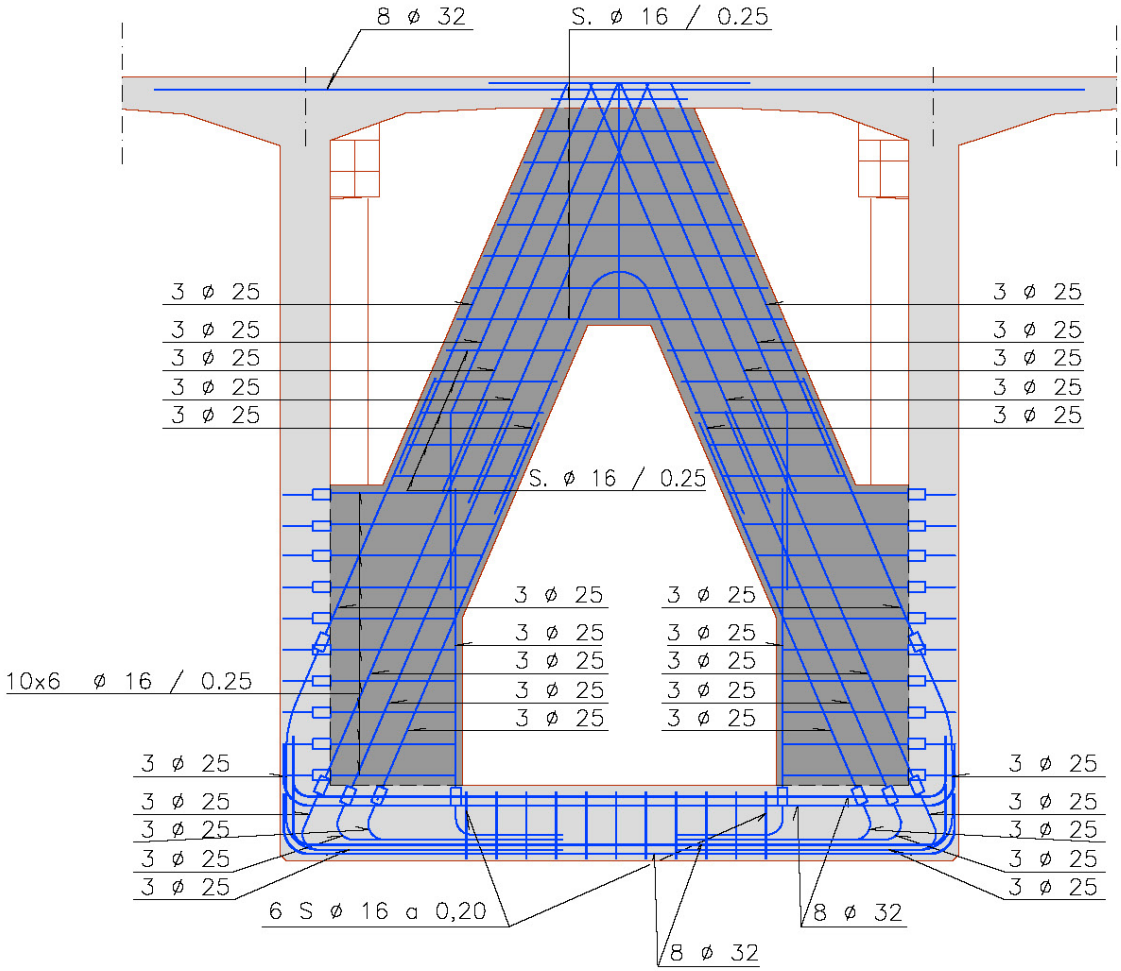


Fig. 12-16: Sketch of reinforcement of the pile diaphragm

4 Stepped pilecap

4.1 Design situation

The Enmedio stream bridge is located in an area of difficult topography that complicates the design of the foundation of the pier. The bridge pier is located on a leaning hillside on a stepped pile cap, as can be seen in Fig. 12-17. This design has been used to reduce the excavations in the hillside which would have affected the abutment foundation.

4.2 Selection the resistant model

Of all possible resistance models, the strut-and-tie model finally selected is the one shown in Fig. 12-18. It is the addition of the different pile cap steps considered each other as simple corbels. Once each different simple corbel is defined, the whole model is obtained by combining all simple models. Finally it comprises ties (in red) in the lower part of the pile cap and some stirrups which are located to resist shear forces, and struts (in green) under compression in the upper part. In the central area both elements are inserted to equilibrate the model.

This document is the intellectual property of the fib – International Federation for Structural Concrete. All rights reserved.
This PDF of fib Bulletin 61 is intended for use and/or distribution solely within fib National Member Groups.

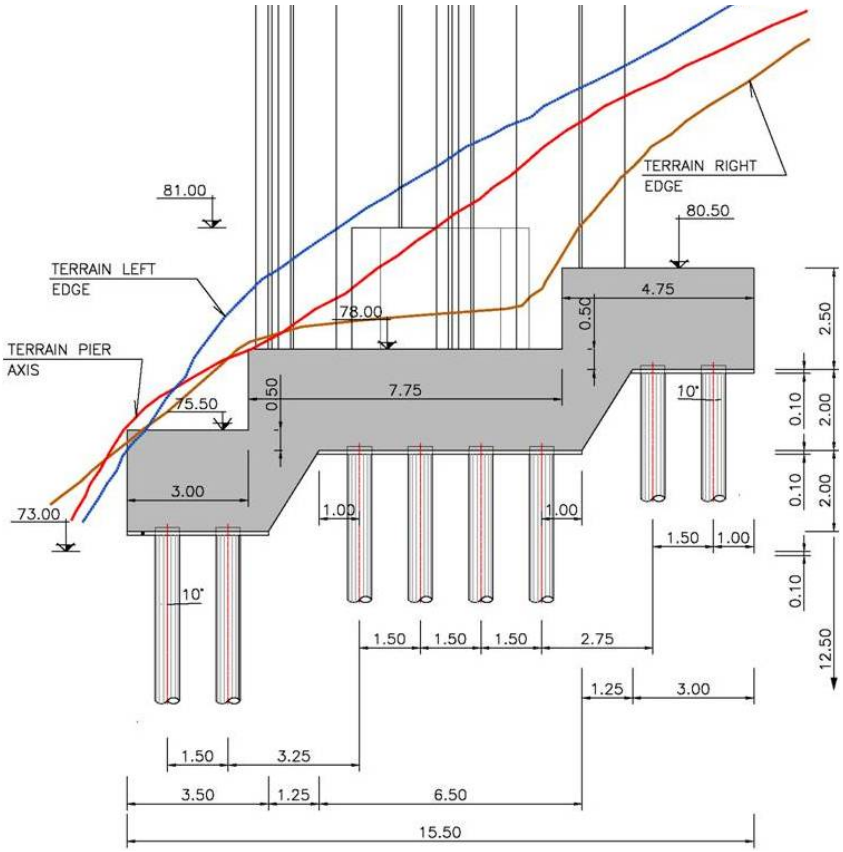


Fig. 12-17: Design of stepped pile cap (dimensions in m; decimal is point instead of comma – see Editorial Comments on p. vi)

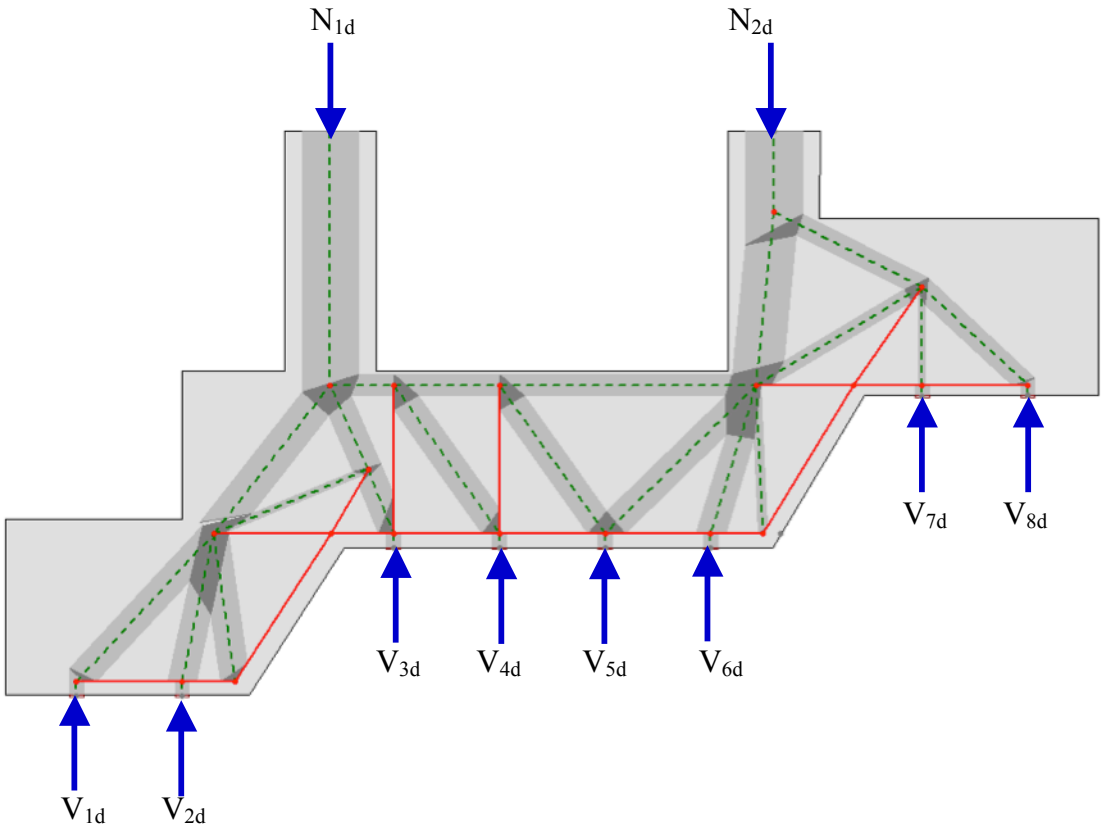


Fig. 12-18: Approach for selecting the model

This document is the intellectual property of the fib – International Federation for Structural Concrete. All rights reserved.
This PDF of fib Bulletin 61 is intended for use and/or distribution solely within fib National Member Groups.

The design loads (N_d) for the model are previously determined from the axial forces of each wall of the pier:

$N_{1d} = 1.799$ kN; $N_{2d} = 1.199$ kN

The reactions given in Table 12-3 are calculated at the edge of pile cap, considering it as a rigid solid and statically determinate. These forces are per row of micro-piles. The strut-and-tie model is shown in the previous Fig. 12-18 with the relative position of each load.

Table 12-3: Calculated pile reactions

Pile	Magnitude (kN)
V_{1d}	456
V_{2d}	438
V_{3d}	402
V_{4d}	384
V_{5d}	366
V_{6d}	348
V_{7d}	312
V_{8d}	294

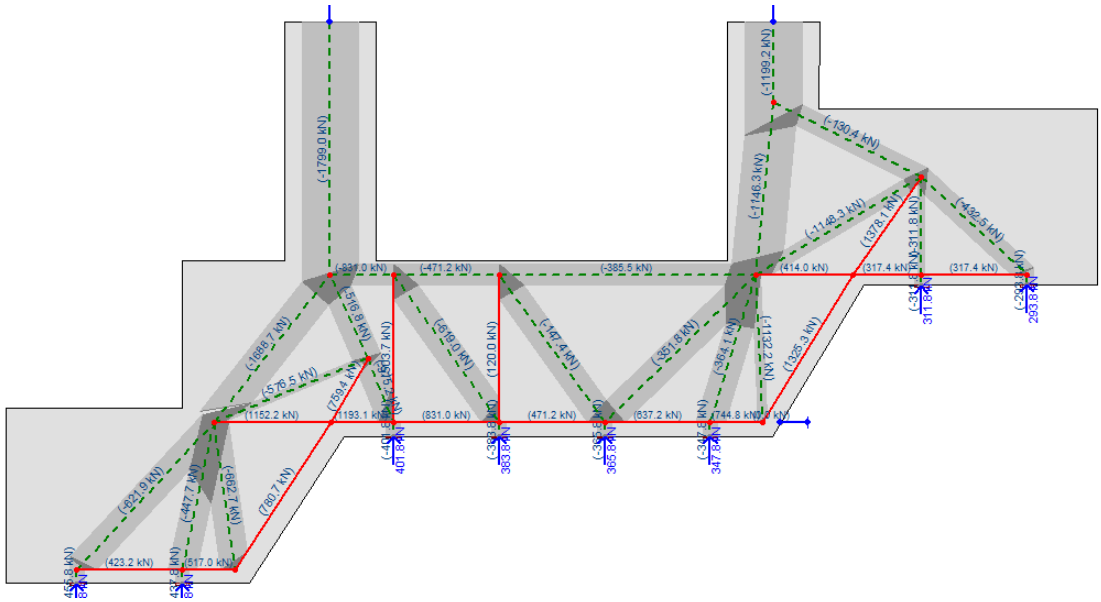


Fig. 12-19: Strut-and-tie model

4.3 Design and placement of reinforcement

The ties are sized in function of the area necessary to obtain an admissible stress with respect to the reinforcement, or limited, in this case to 400 MPa to avoid fissure problems and avoid experiencing defined conditions of compatibility. The required steel area is obtained as a result of dividing the force by the maximum stress. The results are given in Table 12-4.

This document is the intellectual property of the fib – International Federation for Structural Concrete. All rights reserved.
This PDF of fib Bulletin 61 is intended for use and/or distribution solely within fib National Member Groups.

Table 12-4: Required tie reinforcement

Tie	Force (kN)	Required steel area (mm^2)	Reinforcement
T01	423,2	1.058	4 ϕ 25
T02	517,0	1.293	4 ϕ 25
T03	780,7	1.952	4 ϕ 25
T18	759,4	1.899	4 ϕ 25
T04	1.152,2	2.881	4 ϕ 32
T05	1.193,1	2.983	4 ϕ 32
T06	831,0	2.078	4 ϕ 32
T07	471,2	1.043	4 ϕ 32
T08	637,2	1.593	4 ϕ 32
T09	744,8	1.862	4 ϕ 32
T10	1.325,3	3.314	6 ϕ 32
T11	1.378,3	3.446	6 ϕ 32
T16	414,0	1.035	4 ϕ 25
T17	317,4	794	4 ϕ 25
T12	317,4	794	4 ϕ 25
T13	503,7	1.260	25 ϕ 16
T14	120,0	300	25 ϕ 16

The proposed reinforcement layout is shown in Fig. 12-20.

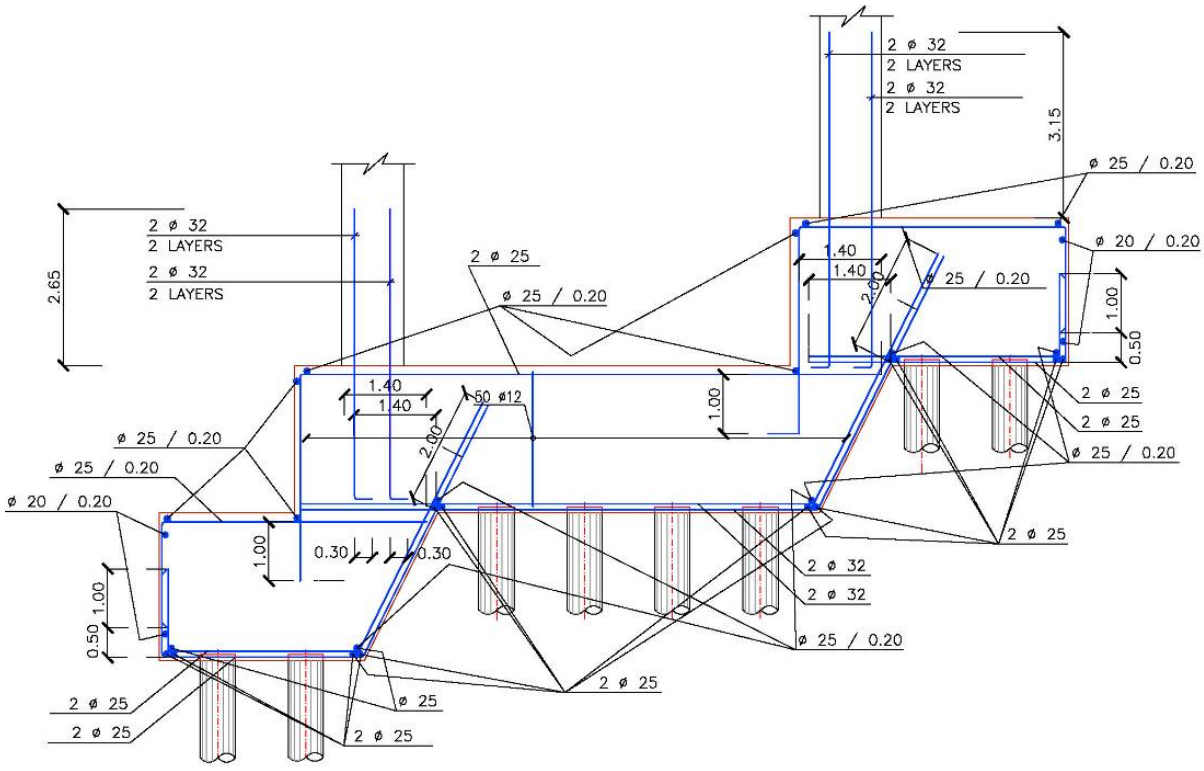


Fig. 12-20: Reinforcement layout for the stepped pile cap
(decimal is comma instead of point; see Editorial Comments on p. vi)

This document is the intellectual property of the fib – International Federation for Structural Concrete. All rights reserved.
This PDF of fib Bulletin 61 is intended for use and/or distribution solely within fib National Member Groups.

5 Anchored abutment

5.1 Strut-and-tie model for the diaphragm

For the Enmedio stream bridge the difficult topography also caused an asymmetrical solution for the bridge deck bridge, and this resulted in a weight unbalance between the main and the short span. As a result, there is an upward vertical load that must be supported. The uplift is corrected by means of a vertical prestressing tendons and a heel for temporary support of the deck during replacement of bearings or prestressing tendons, whose outline is shown in the following Fig. 12-21.

In addition to the heel and prestressing anchorages, internal concentrated forces and stresses are taken by a diaphragm located in a transversal section. The supporting force is the vertical action of the prestressing

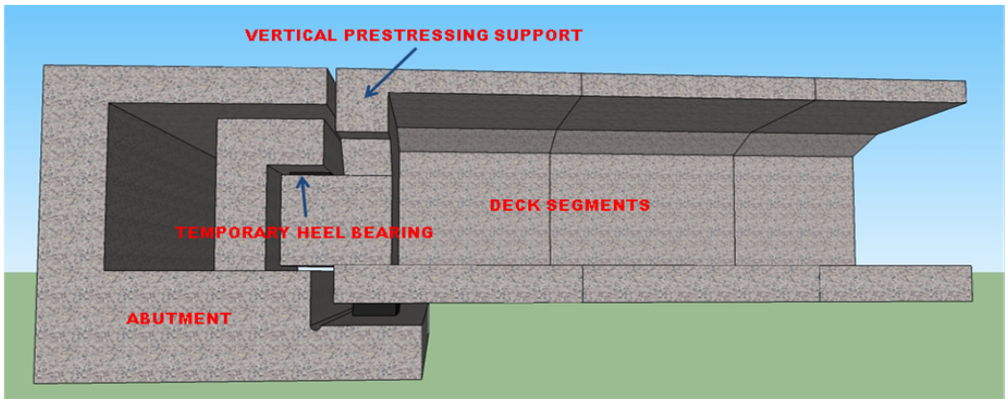


Fig. 12-21: Detail of the anchored abutment deck segment

The main stresses field in the diaphragm has been calculated with a finite element model in order to find the strut-and-tie model from the orientation of the linear-elastic principal stresses. The selected strut-and-tie model is shown in Fig. 12-22 in comparison to these principal stresses.

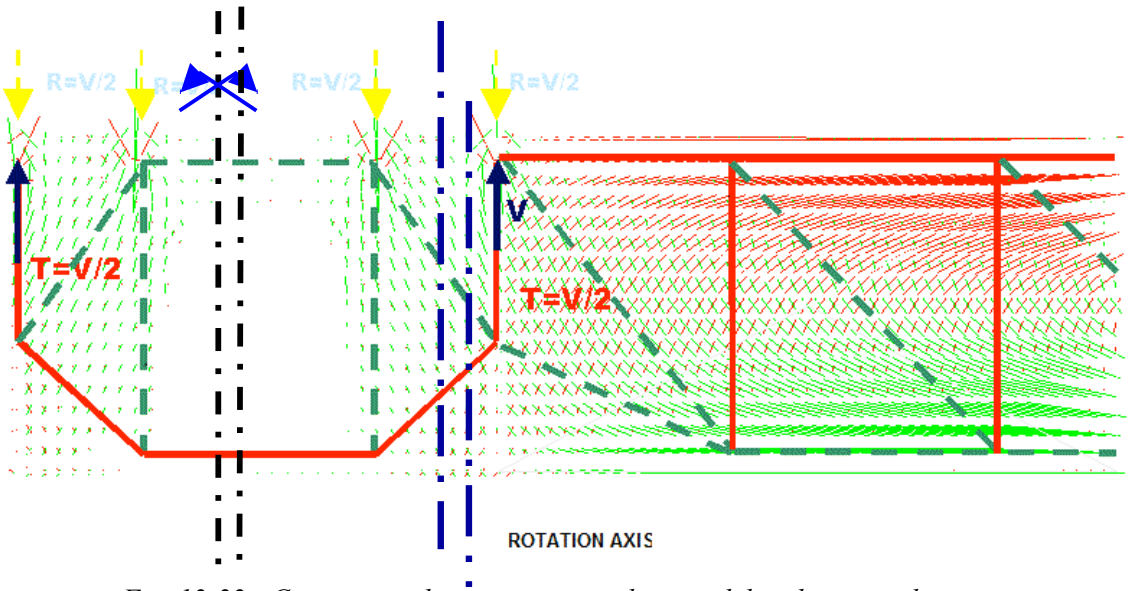


Fig. 12-22: Comparison between strut-and-tie model and principal stresses

This document is the intellectual property of the fib – International Federation for Structural Concrete. All rights reserved.
This PDF of fib Bulletin 61 is intended for use and/or distribution solely within fib National Member Groups.

In the left part of the previous Fig. 12-22, the principal stresses and the strut-and-tie model in the diaphragm are represented. The loads that are applied are the action introduced by the vertical prestressing and the shear force that comes from each web of the deck.

In the following Fig. 12-23, only the model of the diaphragm is shown. This model in Fig. 12-23 fulfils all requirements, but it is not optimal with respect to constructability since it includes oblique ties which require inclined reinforcement. Such reinforcements are unusual and would be difficult to install, and therefore the resistant model has been modified to that shown in Fig. 12-24.

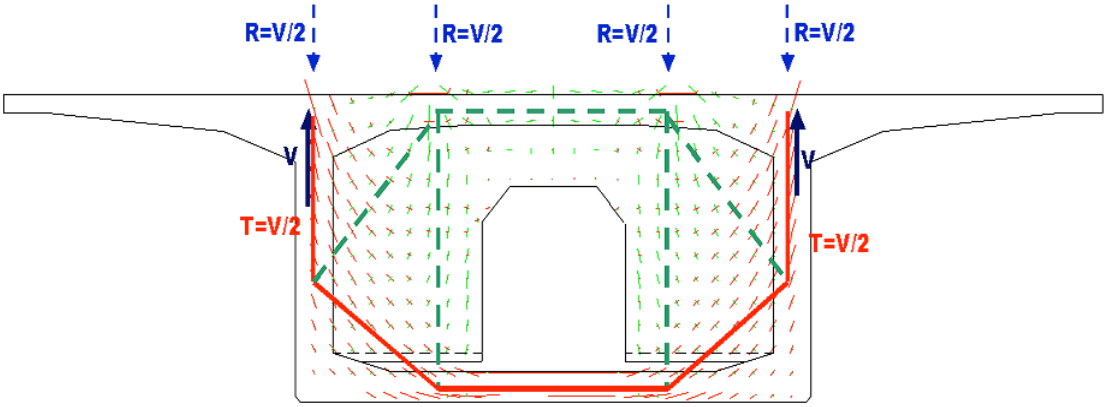


Fig. 12-23: Possible strut-and-tie model in the diaphragm

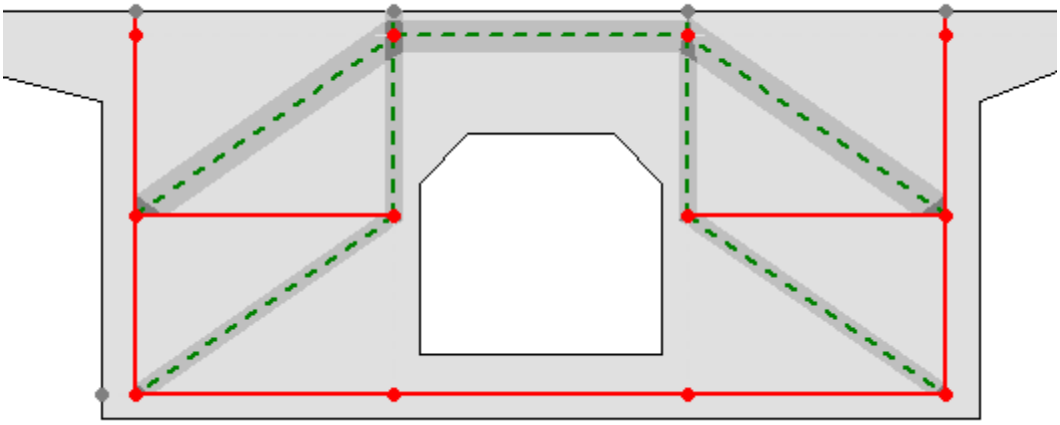


Fig. 12-24: Selected strut-and-tie model for the diaphragm

The design material strengths for concrete grade C-60 and reinforcement B 500-S are determined for extended execution control with $\gamma_c = 1{,}50$ and $\gamma_s = 1{,}15$ to:

$$f_{cd} = 60/1{,}5 = 40 \text{ MPa} \qquad f_{yd} = 500/1{,}15 = 435 \text{ MPa}$$

The ties are sized for a stress of only 400 MPa, and the results are shown in Table 12-5. The selected reinforcement is shown in Fig. 12-25.

This document is the intellectual property of the fib – International Federation for Structural Concrete. All rights reserved.
This PDF of fib Bulletin 61 is intended for use and/or distribution solely within fib National Member Groups.

Table 12-5: Area of necessary reinforcement

Tie	Force (kN)	Steel area (mm^2)	Reinforcement
E2, E7	+2.500	6.250	8 ϕ 32
E8, E9	+1.812	4.530	10 ϕ 25
E10, E15	+1.250	3.125	8 ϕ 25
E16, E17, E18	+1.812	4.530	10 ϕ 25

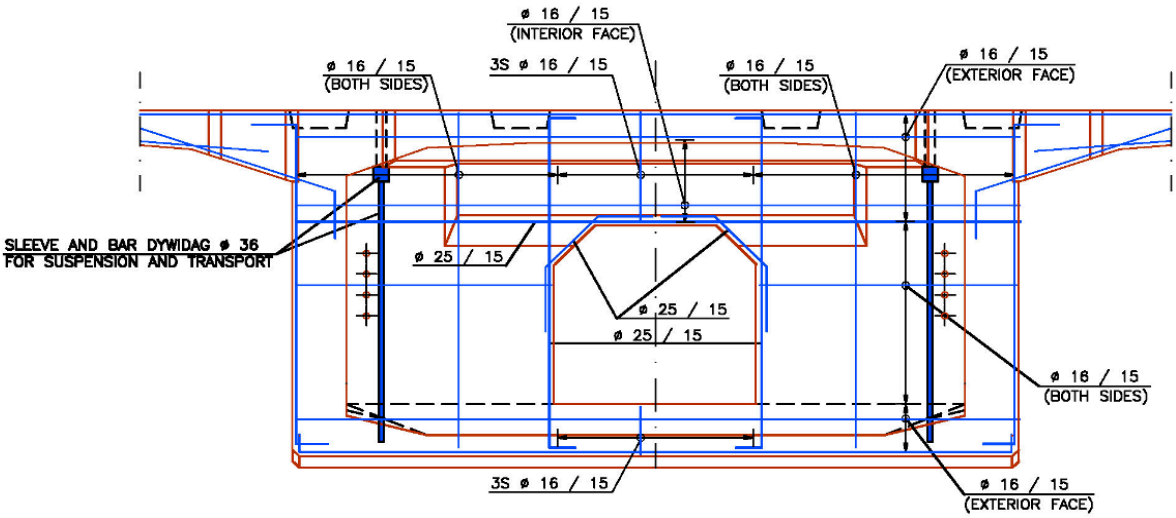


Fig. 12-25: Reinforcement of the diaphragm

5.2 Strut-and-tie model for the design of the heel

5.2.1 Design procedure

The design of the concrete heel to support the uplift is performed by means of the strut-and-tie method, and a three-dimensional strut and tie model has been developed (Fig. 12-26). Because of the difficulty in analyzing and visualizing a complex 3D-model, the model has been split into several 2D-models in order to evaluate the different paths of forces in different planes. Therefore, the following models have been adopted and are dealt with in the following section: one longitudinal model through the webs, a transversal model through a diaphragm, and a detailed model of the force transfer inside the heel.

This document is the intellectual property of the fib – International Federation for Structural Concrete. All rights reserved.
This PDF of fib Bulletin 61 is intended for use and/or distribution solely within fib National Member Groups.

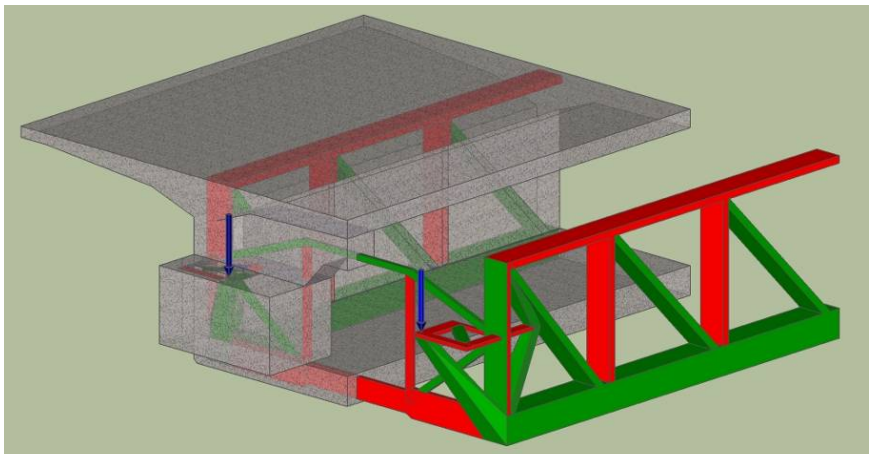


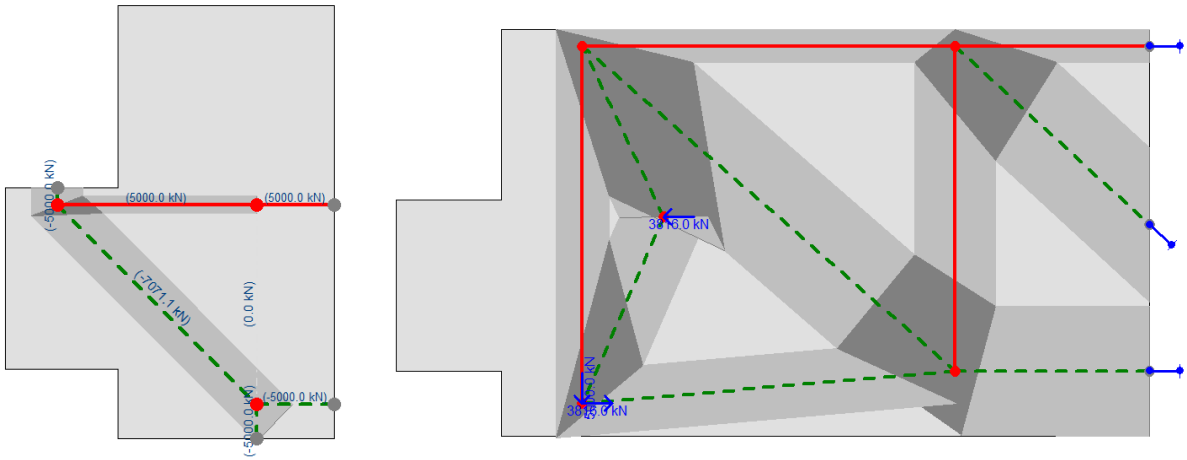
Fig. 12-26: Three-dimensional strut-and-tie model for the heel

5.2.2 Longitudinal strut-and-tie model

The determined design loads are applied to the model. In the example examined, the vertical force from the deck to be supported by the heel and stirrups is calculated as:

$N_{1d} = 5.000$ kN

The strut-and-tie model for this load is shown in Fig. 12-27, including the relative position of the applied loads.



a) model in corbel of heel *b) longitudinal view of*

Fig. 12-27: Strut-and-tie model for the heel

The design material strengths for concrete grade C-60 and reinforcement B 500-S are determined for extended execution control with $\gamma_c = 1{,}50$ and $\gamma_s = 1{,}15$ to:

$f_{cd} = 60/1{,}5 = 40{,}00$ MPa; $f_{yd} = 500/1{,}15 = 435$ MPa

The ties are dimensioned accordingly and the results are listed in Table 12-6.

This document is the intellectual property of the fib – International Federation for Structural Concrete. All rights reserved.
This PDF of fib Bulletin 61 is intended for use and/or distribution solely within fib National Member Groups.

Table 12-6: Necessary steel areas

Tie	Force (kN)	Necessary steel area (mm^2)	Reinforcement
T1	9.362	22.291	30 ϕ 32
T2	5.000	shear reinforcement	
T3	7.944	prestressing tendons	
T4	13.399	prestressing tendons	

5.2.3 Transverse strut-and-tie models

In this case, the whole reaction is divided into two parts in each of the two heels:

N_{1d} = 5.000 kN; N_{2d} = 5.000 kN

The reactions are calculated in each one of the considered supports of the model by applying the equilibrium equations to the entire structure of struts and ties.

The following model has been determined to represent the behaviour of the diaphragm, with the disposition of struts and ties as is indicated in the following Fig. 12-28.

The materials used are concrete C-60 and reinforcement steel B 500-S:

f_{cd} = 60/1,5 = 40 MPa; f_{yd} = 500/1,15 = 435 MPa

The ties are designed according to a lower limit of 400 MPa, and the required areas for the reinforcements are listed in Table 12-7.

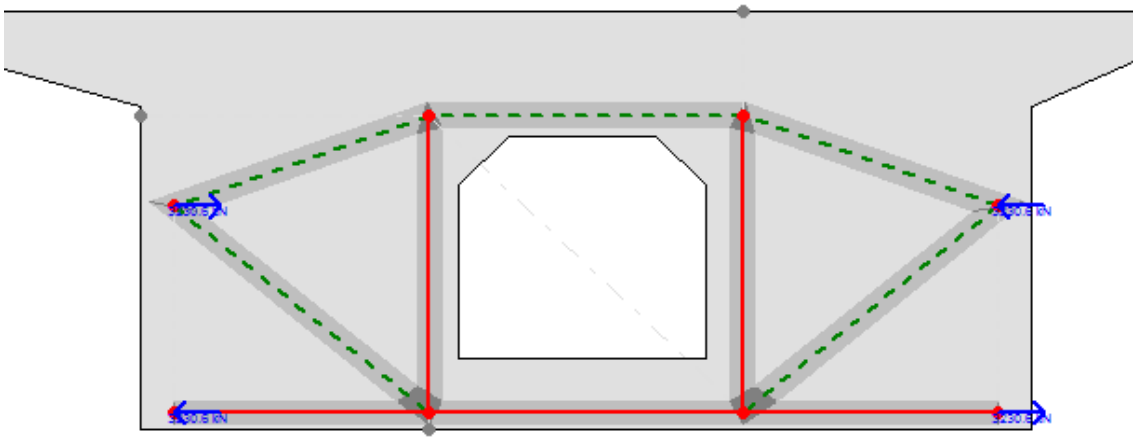


Fig. 12-28: Model utilized for the traverse diaphragm

Table 12-7: Required tie reinforcement

Tie	Force (kN)	required steel area (mm^2)	Reinforcement
T1	3.230,6	7.692	16 ϕ 25
T2	2.243,5	5.340	12 ϕ 25
T3	3.230,6	7.692	16 ϕ 25
T4	796,1	1.895	18 ϕ 16
T5	796,1	1.895	18 ϕ 16

This document is the intellectual property of the fib – International Federation for Structural Concrete. All rights reserved.
This PDF of fib Bulletin 61 is intended for use and/or distribution solely within fib National Member Groups.

5.2.4 Reinforcement of the heel

The reinforcement layout of the heel (as well as of the diaphragm) is shown in Fig. 12-29.

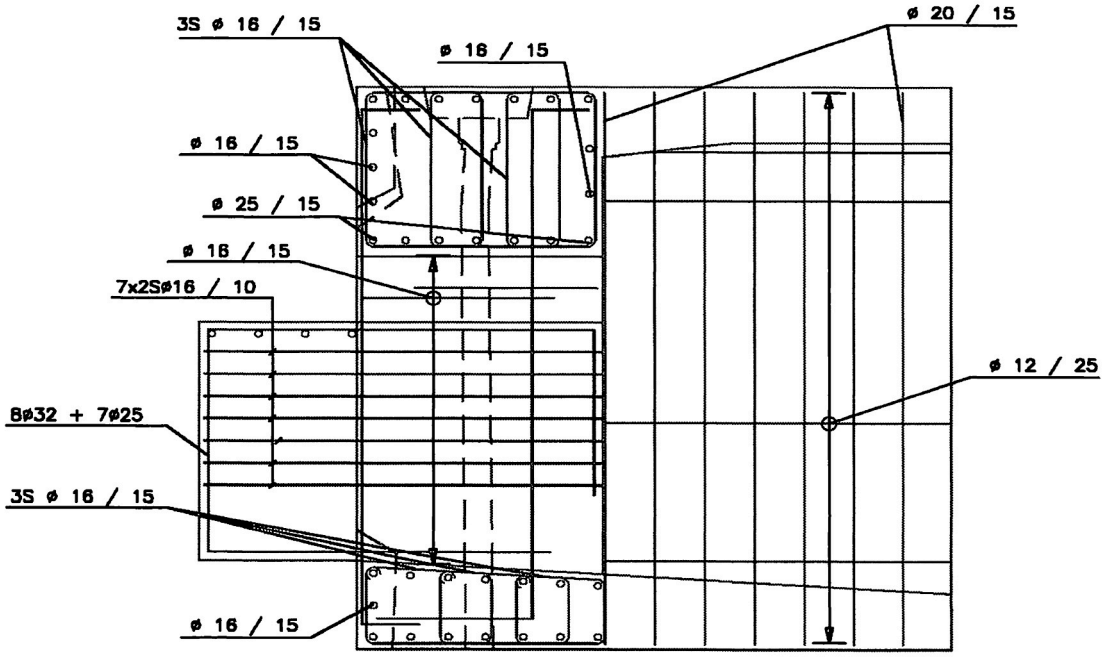


Fig. 12-29: Reinforcement of the heel (dimension of spacing in cm)

6 Conclusions

The strut and tie models for the five D-regions presented in this example are only some significant models that can be found within the complete design of a bridge. There are also many others strut and tie models related to discontinuity regions of the reinforced layout due to openings, reduction of concrete sections, etc.

The search of the different discontinuity regions in a bridge design process begins with the assumption that the whole bridge is a discontinuity region in which loads, supports and stresses paths must be found to assess the correct behaviour of the bridge. Then, secondary discontinuity regions have to be found where the loads are applied and where support have to be defined so that they can be designed with strut-and models.

Strut-and-tie models are not only a tool to dimension reinforcing bars in D-regions; these models force the designer in a global manner to think of the source of loads and how they are transferred through the concrete structure up to the different supports. Thereby a Finite Element Analysis model could be a great help to know the elastic path of the force distribution. Therefore, strut and tie models procedure is the educational way to acquire the knowledge of bridge behaviour or of any other structure.

This document is the intellectual property of the fib – International Federation for Structural Concrete. All rights reserved.
This PDF of fib Bulletin 61 is intended for use and/or distribution solely within fib National Member Groups.

References

ACI SP-208 (2002): see Reineck (2002)

fib Bulletin 16 (2002): Design Examples for the FIP Recommendations "Practical design of structural concrete". *fib*, Lausanne. January 2002

FIP Recommendations (1999): Practical Design of Structural Concrete. FIP-Commission 3 "Practical Design", Sept. 1996. Publ.: SETO, London, Sept. 1999 (Distributed by: *fib*, Lausanne. Web http://www.fib-international.org)

Reineck, K.-H. (2002): (Editor): Examples for the Design of Structural Concrete with Strut-and-Tie Models. ACI SP-208 (2002), ACI, Farmington Hills, MI

Schlaich, J.; Schäfer, K; Jennewein, M. (1987): Toward a Consistent Design for Structural Concrete. PCI-Journal Vol. 32 (1987), No.3, 75-150

CEB-FIP MC 90 (1993): Design of concrete structures. CEB-FIP-Model-Code 1990. Thomas Telford, 1993

EHE (1998) Instrucción de Hormigón Estructural, (distributed by: Ministerio de Fomento, SPAIN)

Monografía 6: Método de bielas y tirantes. ACHE, Spain.

This document is the intellectual property of the fib – International Federation for Structural Concrete. All rights reserved.
This PDF of fib Bulletin 61 is intended for use and/or distribution solely within fib National Member Groups.

This document is the intellectual property of the fib – International Federation for Structural Concrete. All rights reserved.
This PDF of fib Bulletin 61 is intended for use and/or distribution solely within fib National Member Groups.

Example 13: D-regions of the pylons of a cable-stayed bridge

Duc Thanh Nguyen

1 Description of design task

1.1 Geometry and loads

In frame of proof-check services for a new cable-stayed bridge four typical D-regions numbered from 1 to 4 of the pylon should be checked using strut-and-tie models (Fig. 13-1). The pylon has an H-form with two cross beams. The pylon legs and the cross beams have both rectangular sections with diaphragms at load transferring points. The main beam of the bridge is of composite box section which is supported at pylon vertically by the lower cross beam and horizontally by pylon legs at deck level. For accessible purpose a man hole is set at each diaphragm.

The forces to be transferred through the D-regions are gained from structural analysis and already factored according to relevant design regulations.

1.2 Design values for materials

Concrete: $f_{ck} = 35$ MPa $\Rightarrow f_{1cd} = \alpha f_{ck} / \gamma_c = 0{,}85 \times 35{,}0 / 1.5 = 19{,}83$ MPa

Reinforcement: $f_{yk} = 500$ MPa $\Rightarrow f_{yd} = f_{yk} / \gamma_s = 500 / 1{,}15 = 435$ MPa

1.3 Statement of design problem

This is an example for demonstrating the use of strut-and-tie models for the design of complicated D-regions of structural concrete. Not complete solution, but only chosen aspects are presented which are not sufficiently considered so far by conventional design methods (for instance, using finite element method). Assumptions shall be made based on experience and occasionally by using elastic finite element calculations. The design of the anchorage at nodes is critical.

In frame of this paper, only the check of two D-regions (D-region 1 and 2 in Fig. 13-1) is presented. As the results, the design of these regions could be confirmed. Suggestions for better reinforcement layout and also for a simpler geometry, however, were made as a help for future similar design problems. The check is carried out according to the FIP Recommendations (1999).

This document is the intellectual property of the fib – International Federation for Structural Concrete. All rights reserved.
This PDF of fib Bulletin 61 is intended for use and/or distribution solely within fib National Member Groups.

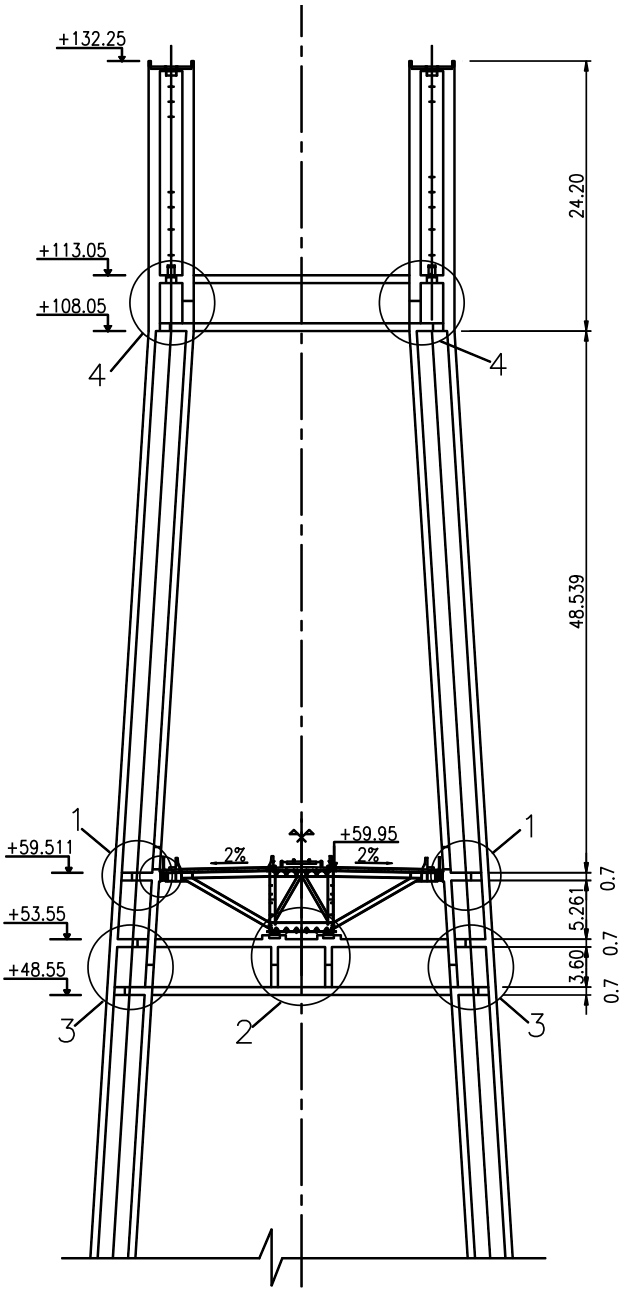


Fig. 13-1: Pylon and its typical D-regions (dimensions in m; decimal point instead of comma – see Editorial Comments on p. vi)

This document is the intellectual property of the fib – International Federation for Structural Concrete. All rights reserved.
This PDF of fib Bulletin 61 is intended for use and/or distribution solely within fib National Member Groups.

2 Design calculations

2.1 Design of D-region 1: Load transfer at the horizontal supports

For the horizontal supports the earthquake load case controls the design. A horizontal force of 10 MN will be placed at the centreline of the support (see Fig. 13-2). This force will first spread out through the diaphragm to the side walls of pylon and then along the side walls upwards and downwards.

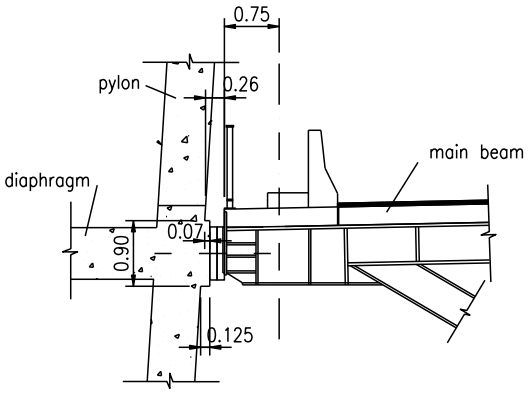


Fig. 13-2: Horizontal support at deck level
(decimal point instead of comma; see Editorial Comments on p. vi)

Strut-and-tie model in the diaphragm:

Due to the manhole two ties are assumed (see Fig. 13-3). A simple assumption for two mechanisms is made with 50% of the horizontal force for each mechanism. With geometry as in Fig. 13-3, the tie and strut forces can be calculated as follows:

$$T_1 = \frac{10\,\mathrm{MN}}{4} \times \cot 55^o = 1{,}75\,MN\,; \qquad T_2 = \frac{10\,\mathrm{MN}}{4} \times \cot 35^o = 3{,}57\,MN$$

$T_3 = 2{,}5$ MN; $T_4 = 5$ MN

$C_1 = (10\text{ MN} / 4) / \sin 55° = 3{,}05$ MN ; $C_2 = (10\text{ MN} / 4) / \sin 35° = 4{,}36$ MN

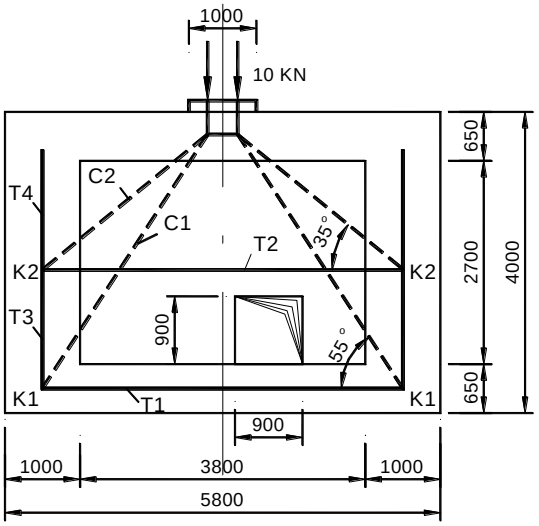


Fig. 13-3: Model in the diaphragm at the horizontal supports (dimensions in mm)

This document is the intellectual property of the fib – International Federation for Structural Concrete. All rights reserved.
This PDF of fib Bulletin 61 is intended for use and/or distribution solely within fib National Member Groups.

Check of the model in Fig. 13-3 with rebar layout in diaphragm shown in Fig. 13-4:

- Node at the support is a compression node. The effective concrete strength is:

$$f_{cd,eff} = \nu_2 \; f_{1cd} = 1{,}0 \; f_{1cd} = 1.0 \times 19{,}83 = 19{,}83 \text{ MPa}$$

Support area: $A_c = 1{,}0 \times 0{,}7 = 0{,}7 \; (m^2)$

Concrete stress: $\sigma_c = 10 \text{ MN} / 0{,}7 \text{ m}^2 = 14{,}3 \text{ MPa} \leq f_{cd,eff} = 19{,}83 \text{ MPa}$

- Tie T_1: Required reinforcement area is

$$A_{s,req} = T_1 / f_{yd} = (1{,}75 / 435) \times 10^6 = 4.023 \; (mm^2)$$

Available are 10∅1" (506 mm^2/bar), $A_{s,\,prov} = 5.060 \text{ mm}^2 > A_{s,req} = 4.023 \text{ mm}^2$

- Tie T_2:

$$A_{s,req} = T_2 / f_{yd} = (3{,}57 / 435) \times 10^6 = 8.207 \text{ mm}^2$$

Available are 18∅1", $A_{s,\,prov} = 9.108 \text{ mm}^2 > A_{s,req} = 8.207 \text{ mm}^2$

- Tie T_3 and T_4: use T_4 to find reinforcement for both.

$$A_{s,req} = T_4 / f_{yd} = (5 / 435) \times 10^6 = 11.494 \text{ mm}^2$$

Available are 25∅1" in 5 layers, each 5∅1", $A_{s,prov.} = 12.650 \text{ mm}^2 > A_{s,\,req} = 11.494 \text{ mm}^2$.

Nodes K_1 and K_2 are tension-compression nodes with two ties connected. The effective concrete strength is determined as follows:

$$f_{cd,eff} = \nu_2 \; f_{1cd} = 0{,}8 \times 0{,}8 \; f_{1cd} = 0{,}8 \times 0{,}8 \times 19{,}83 = 12{,}7 \text{ MPa}$$

The use of $\nu_2 = 0.8 \times 0.8$ is based on the fact that the concrete behavior with two ties is more unfavorable than that with only one tie. This is also adopted in AASHTO LRFD (1998).

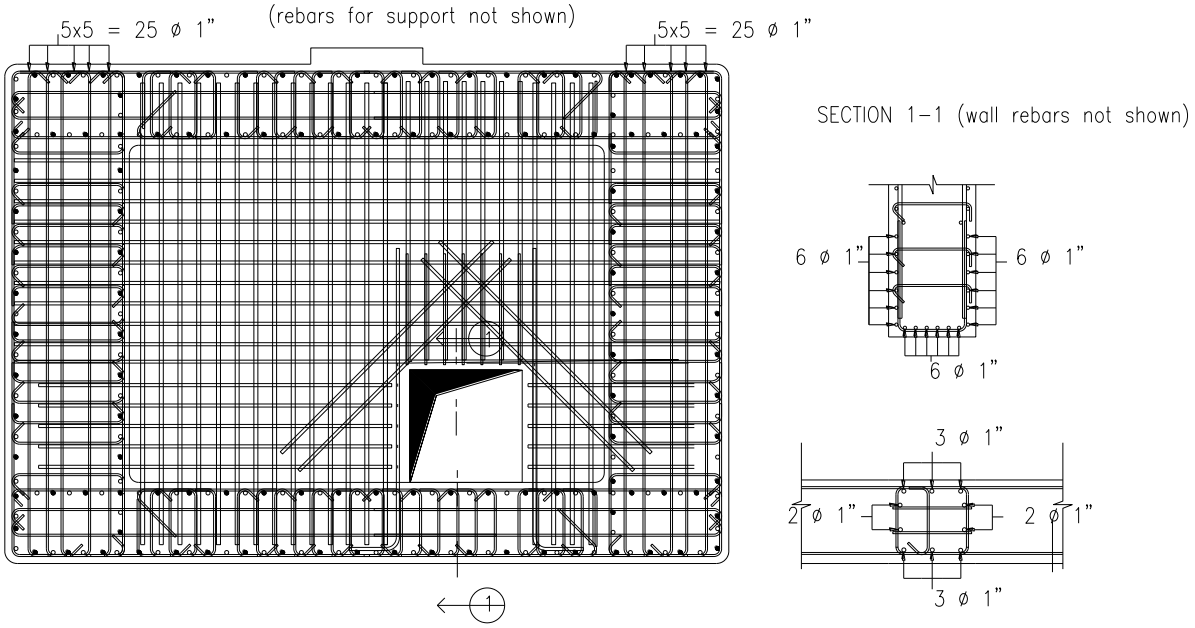


Fig. 13-4: Reinforcement layout in the diaphragm at the horizontal support

This document is the intellectual property of the fib – International Federation for Structural Concrete. All rights reserved.
This PDF of fib Bulletin 61 is intended for use and/or distribution solely within fib National Member Groups.

At node K_1, contact area of strut C_1 to the node is:

$$A_{c1} = (1{,}0 \times \sin 55^o + 0{,}65 \times \cos 55^o) \times 0{,}7 = 0{,}83 \ \ m^2$$

Concrete stress in this contact area:

$$\sigma_c = C_1 / A_{c1} = 3{,}05 / 0{,}83 = 3{,}65 \text{ MPa} << f_{cd,eff} = 15{,}86 \ \ \text{MPa}$$

Concrete stress at node K_2 is not to be checked because it is a smeared node.

Anchorage length of the hooked reinforcement bars of ties T_1, T_2, T_3 and T_4 is in this case bigger or equal to 800 mm ($> 0{,}7 \times 35 \varnothing = 0{,}7 \times 35 \times 25{,}4 = 711$ mm). So it is believed to be safe without a more detailed calculation.

Note that the model with tie T_2 and Strut C_2 can be refined by adding vertical ties between support and node N_2 (not shown in this example). The existing stirrups in the diaphragm (Fig. 13-4) are, according to a check using such a model, enough to cover the tie forces.

Model in the side walls

The transfer of the horizontal force further upwards and downwards in the side walls is a conventional shear force problem. So it is not considered in this paper. The model looks like in Fig. 13-5.

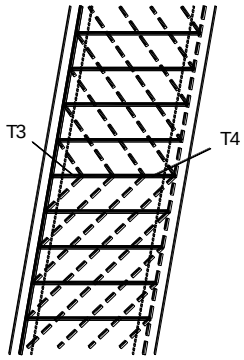


Fig. 13-5: Strut-and-tie model in the pylon side walls at the horizontal supports

2.2 D-region 2: Load transfer at vertical supports of lower cross beam

Configuration of the lower cross beam under the support is shown in Fig. 13-6. The vertical force to be transferred at each support is V = 42 MN. This force also spreads out through the diaphragm before coming to the side walls of the cross beam.

This document is the intellectual property of the fib – International Federation for Structural Concrete. All rights reserved.
This PDF of fib Bulletin 61 is intended for use and/or distribution solely within fib National Member Groups.

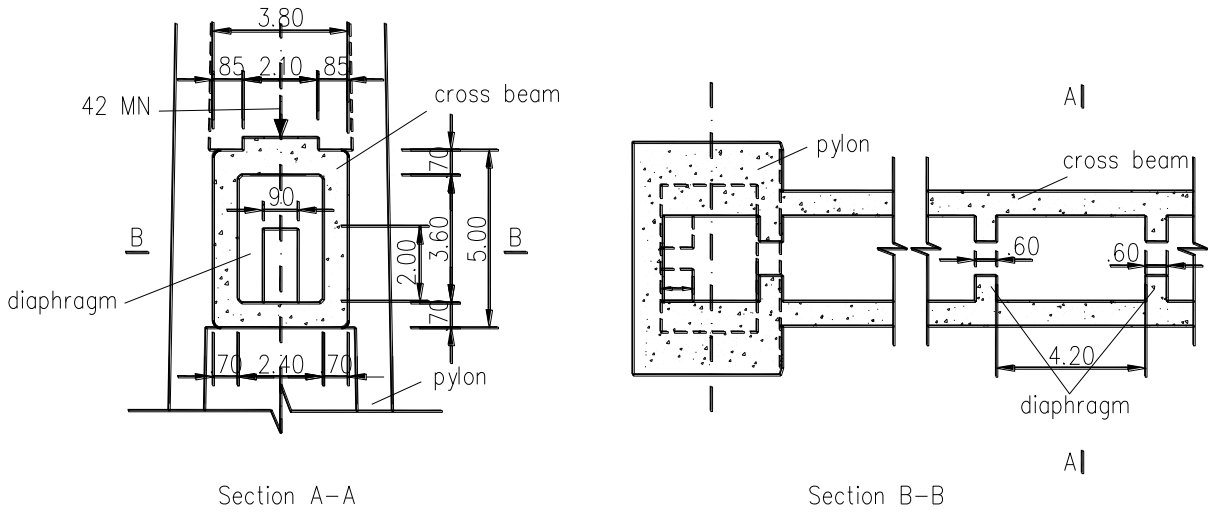
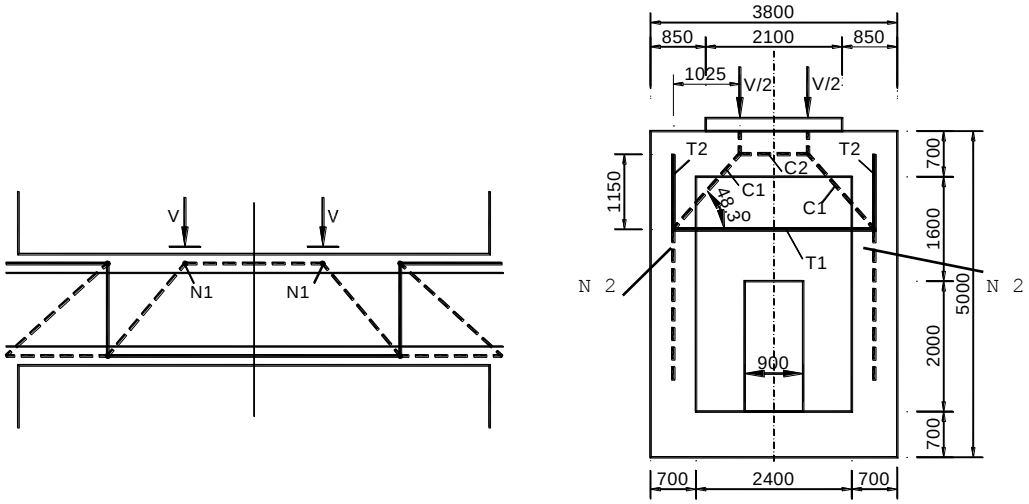


Fig. 13-6: Configuration of the lower cross beam and regions under the vertical supports (decimal point instead of comma; see Editorial Comments on p. vi)

Strut-and-tie models for the load transfer are shown in Fig. 13-7. In Fig. 13-7a the global model in the cross beam is presented while Fig. 13-7b shows the local model for the diaphragm only. For instance, the check of the model for the diaphragm (Fig. 13-7b) is done in the following.



a) global model for the cross beam *b) local model for diaphragm*

Fig. 13-7: Strut-and-tie model at the lower cross beam (dimensions in mm)

In the original design the reinforcement layout is as shown in Fig. 13-8.

According to Fig. 13-7b the strut-and-tie forces are as follows:

$T_1 = 21\ \text{MN} \times \cot 48{,}3^{o} = 18{,}71\ \text{MN}$; $T_2 = 21\ \text{MN}$

$C_1 = 21\ \text{MN} / \sin 48{,}3^{o} = 28{,}13\ \text{MN}$

This document is the intellectual property of the fib – International Federation for Structural Concrete. All rights reserved.
This PDF of fib Bulletin 61 is intended for use and/or distribution solely within fib National Member Groups.

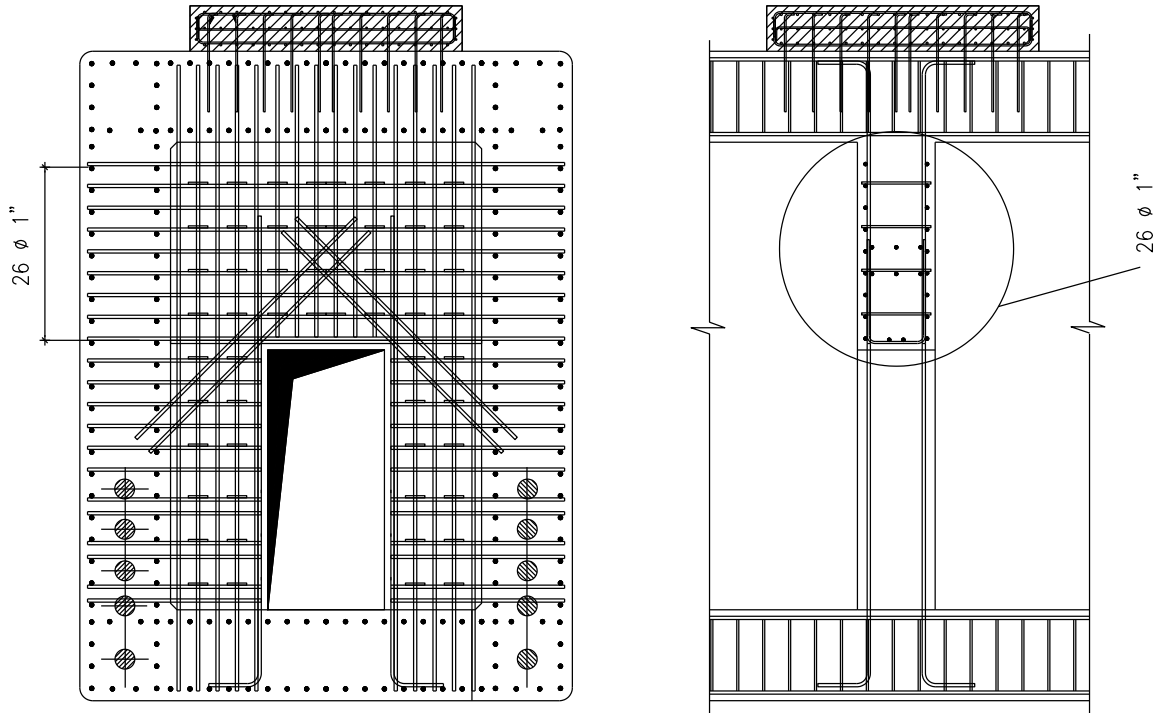


Fig. 13-8: Original reinforcement layout in diaphragm of the lower cross beam

Check of model:

- Node N_1 is a compression node, so $f_{cd,eff}$ = 19,83 MPa

  Support area: $A_c = 2{,}1 \times 0{,}6 = 1{,}26\ m^2$

  Actual concrete stress: $\sigma_c = V/A_c = 42\ MN/1{,}26\ m^2 = 33{,}3\ MPa > f_{cd,eff} = 9{,}8\ MPa$ (not OK)

- Tie T_1: $A_{s,req} = T_1 / f_{yd} = (18{,}7 / 435) \times 10^6 = 42.990\ (mm^2)$

  Available are 26 ∅1", $A_{s,\,prov} = 13.174\ mm^2 << A_{s,req} = 42.290\ cm^2$ (not OK!).

- Node N_2 is a tension-compression node with two ties. So the effective strength of concrete is $f_{cd,eff}$ = 12.7 MPa. Contact area between node N_2 and strut C_1 is

$$A_{c1} = (1{,}6 \times \cos 48{,}3^o + 0{,}7 \times \sin 48{,}3^o) \times 0{,}6 = 0{,}95\ m^2$$

Concrete stress in this contact area:

$$\sigma_c = C_1 / A_{c1} = 28{,}13 / 0{,}95 = 29{,}6\ MPa > f_{cd,eff} = 15{,}86\ MPa \text{ (not OK).}$$

The above check shows that the capacity of the model is not sufficient. The reason is that the thickness of the diaphragm is too small and too little reinforcement is available. Now the thickness of the diaphragm has been increased to 2,1 m and more reinforcing bars can be arranged in the diaphragm. With the new configuration in Fig. 13-9, the check is as follows.

- Node N_1: support area: $A_c = 2{,}1 \times 2{,}1 = 4{,}41\ m^2$

  Concrete stress: $\sigma_c = V/A_c = 42\ MN / 4{,}41\ m^2 = 9{,}52\ MPa < f_{cd,eff} = 19{,}8\ MPa$ (OK)

- Available bars for T_1: 40 ∅1.25" + 24 ∅1", $A_{s,\,prov} = 43.800\ mm^2 > A_{s,req} = 43.000\ mm^2$ (OK).

- Node N_2: Contact area between node N_2 and strut C_1 is

$$A_{c1} = (1{,}6 \times \cos 48{,}3 + 0{,}7 \times \sin 48{,}3) \times 2{,}1 = 3{,}25\ m^2$$

Concrete stress: $\sigma_c = C_1 / A_{c1} = 28{,}13 / 3{,}25 = 8{,}66\ MPa < f_{cd,eff} = 12{,}7\ MPa$ (OK).

This document is the intellectual property of the fib – International Federation for Structural Concrete. All rights reserved.
This PDF of fib Bulletin 61 is intended for use and/or distribution solely within fib National Member Groups.

Anchorage of the bars of tie T_1 at node N_2 must be secured by hooks as shown in Fig. 13-9. That means, with a thicker diaphragm for the cross beam the capacity of the model is now sufficient.

As shown in the check, the lower part of diaphragm beside the manhole in the original design has no influence to the capacity of the model and, therefore, can be omitted in the final design. The diaphragm in Fig. 13-9 has taken this into account.

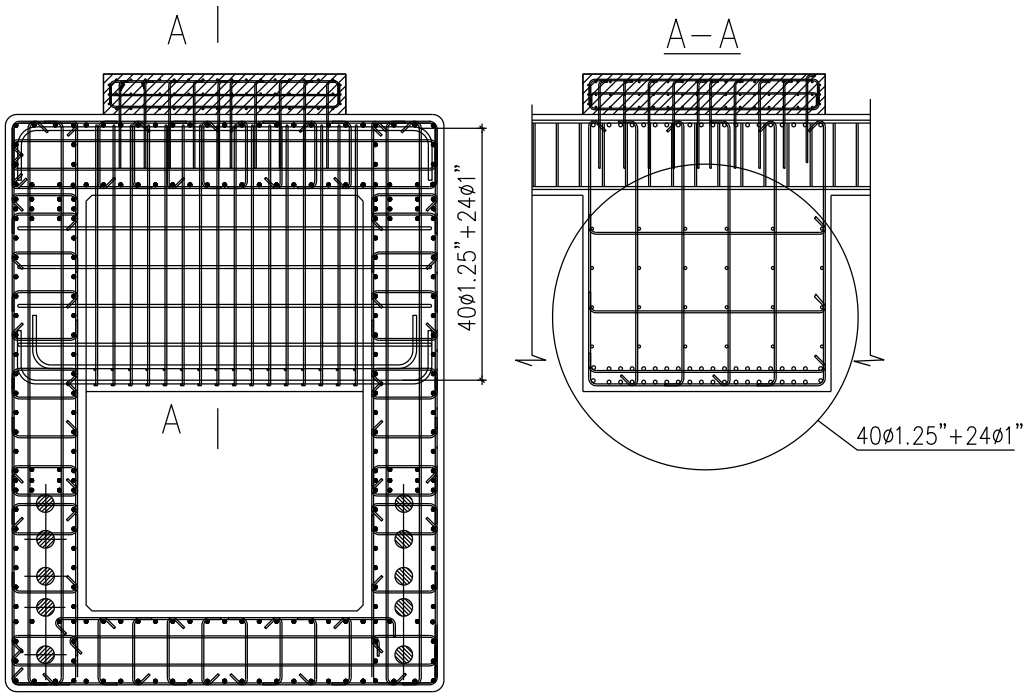


Fig. 13-9: Modified configuration of diaphragm at the lower cross beam and reinforcement layout (decimal point instead of comma; see Editorial Comments on p. vi)

4 Summary and conclusions

- Strut-and-tie models can follows very clearly flow of forces in D-regions of pylons of cable-stayed bridges
- In the practice, reinforcement must be arranged and anchored more carefully in these regions than it was done so far
- Geometry of the D-regions should be modified, may be more complicated or simpler

References

FIP Recommendations (1999): Practical Design of Structural Concrete.
FIP-Commission 3 "Practical Design", Sept. 1996. Publ.: SETO, London, Sept. 1999.
(Distributed by: *fib*, Lausanne. Web http://www.fib-international.org)

AASHTO LRFD (1998): AASHTO LRFD Bridge Design Specifications, American Association of State and Highway Transportation Officials 1998.

This document is the intellectual property of the fib – International Federation for Structural Concrete. All rights reserved.
This PDF of fib Bulletin 61 is intended for use and/or distribution solely within fib National Member Groups.

Example 14: Design of T-connections in an offshore terminal

Hannes Ludescher, Stein Atle Haugerud

1 Design process

The design of large offshore structures often requires dealing with a large number of D-regions. For this reason, a systematic approach has been developed that allows an efficient design of all relevant regions. The basis is an identification of regions and the classification with respect to their geometry and loading. It is important to identify all relevant regions in the first step, because errors are not caught by subsequent steps. The classification can subsequently be refined as the analysis is refined. The analysis is refined stepwise with an increasing degree of precision.

Fig. 14-1 gives an overview over the adopted methodology with the various steps passed in the framework of design. Some of the steps are closely linked, like classification and analysis of section forces. This way, the required depth of the analysis can be adapted in an iterative manner. In addition, the various steps are linked to B-region design which is also gradually refined. In an early project stage, the section forces may not be well known or still subject to modification due to enhancements in load modelling and optimisation of the overall project. Minor modifications in load modelling require verification of the chosen design, whereas major modifications may result in a re-design.

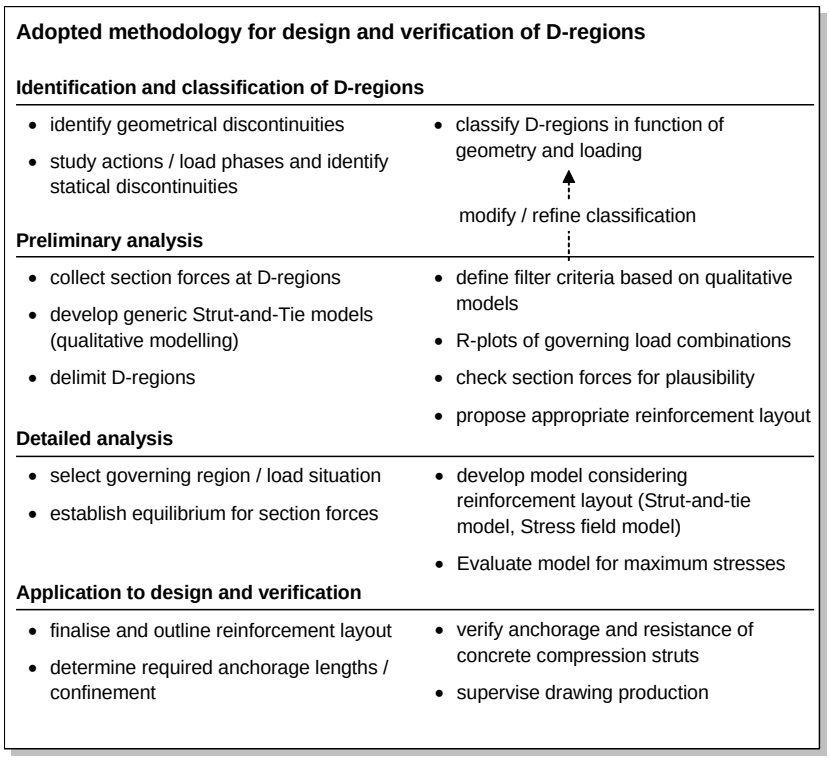
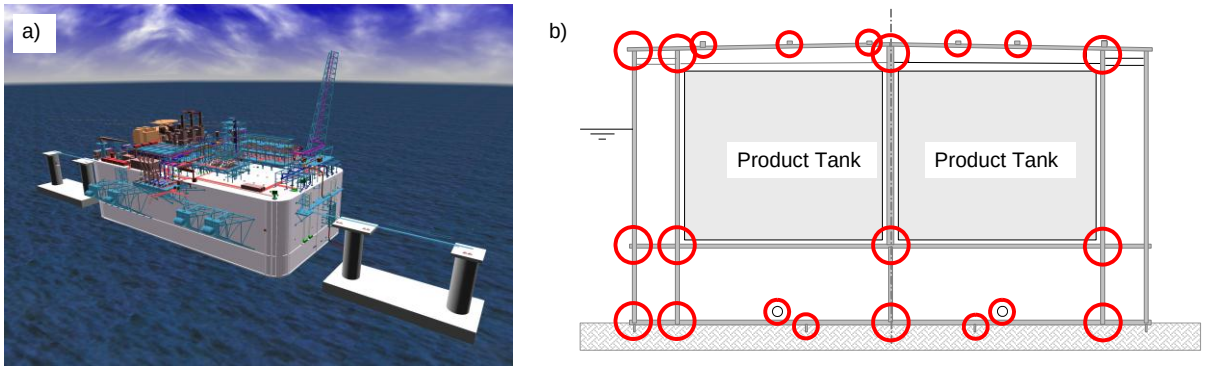


Fig. 14-1: Adopted methodology for the design of D-regions

This document is the intellectual property of the fib – International Federation for Structural Concrete. All rights reserved.
This PDF of fib Bulletin 61 is intended for use and/or distribution solely within fib National Member Groups.

2 Identification and classification of D-regions

Generally, D-regions can be found at geometric and / or static discontinuities. Examples for D-regions in offshore structures are connections, post-tensioning anchorages, holes, casting joints, anchorages of embedded items or pedestals. Fig. 14-2 gives an example of a gravity base structure and illustrates the number of D-regions that can be found in one cross section.



a) general view *b) vertical cross section with D-regions*

Fig. 14-2: Offshore terminal and its D-regions

In the following, the focus is set on connections linking the main structural elements, i.e. the plates and walls. These regions have a major influence on the main reinforcement and typically present the highest stresses. Holes and embedded items are often treated separately as "miscellaneous items", i.e. as various local exceptions to the pattern of the main reinforcement. For prestressing anchor heads and at casting joints, standard design solutions are usually sufficient.

The classification starts with subdividing the connections according to their geometry. This is illustrated by the junction of the base slab with the lower walls in Fig. 14-3. In these connections, the starter bars for the walls are anchored. In addition, some connections serve as anchorage for so called "skirts", which are short appendices sticking into the ground in order to increase shear resistance of the base slab. If the skirts are neglected because they introduce minor forces, the connections can be generally subdivided in L-shaped and T-shaped connections. The T-connections can be further subdivided into connections with 550 mm and connections with 450 mm thick walls, where the wall thickness reflects the intensity of loading assumed by the connection.

In addition to the geometry, loading on the structural elements is an important criterion for the grouping of connections. Offshore terminals can experience a large variety of sometimes complex loading situations like:

– application of post-tensioning to individual elements;
– filling of compartments for leakage testing;
– external water pressure during transport, including waves;
– non-uniform ground reaction / solid ballast filling during installation;
– filling of ballast compartments for stabilisation / increase of ground pressure;
– maximum sea water level plus waves during operation;
– earthquake, ship impact, explosion or other accidental situations.

This document is the intellectual property of the fib – International Federation for Structural Concrete. All rights reserved.
This PDF of fib Bulletin 61 is intended for use and/or distribution solely within fib National Member Groups.

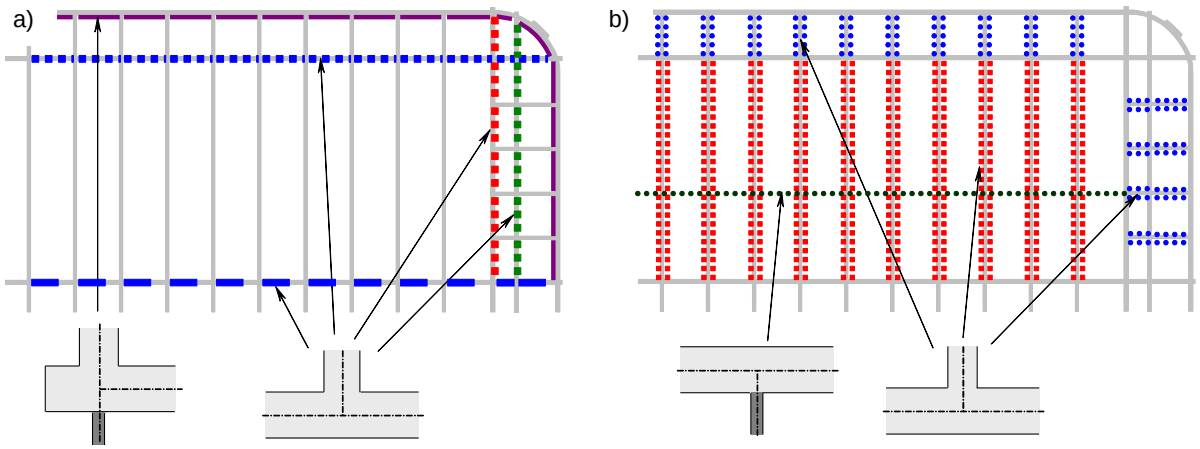
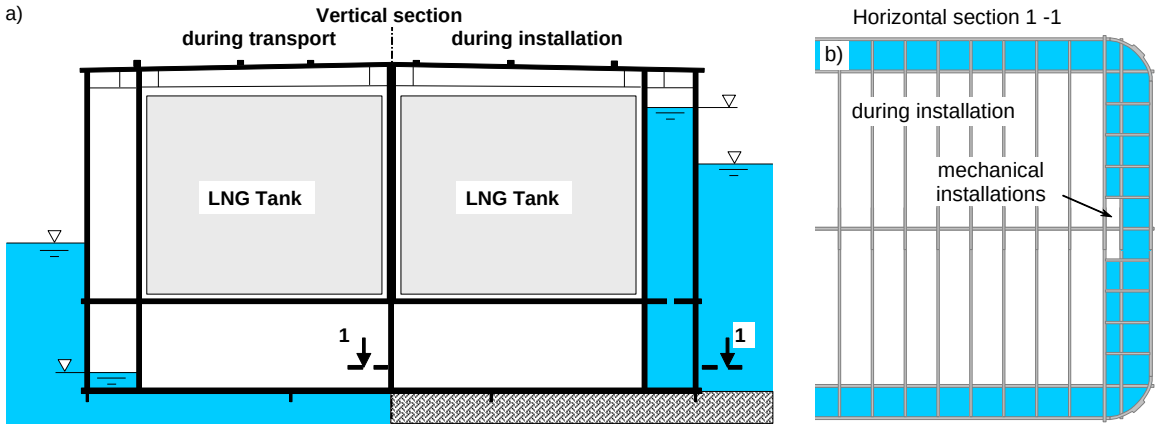


Fig. 14-3: Classification of connections in base slab.

Fig. 14-4 shows two load phases of the terminal shown in Fig. 14-2. For transport, the terminal floats like a boat and the "ground reaction" is hydrostatic water pressure. Ballast compartments are nearly empty, and the external water pressure including waves causes local bending of the outer walls whereas the terminal as a whole experience increased compression. During installation, on the other side, the ballast compartments are filled in order to press the terminal to the ground. Inner water level exceeds the outer water level and some walls are subjected to membrane tension.



a) vertical section during transport and installation *b) horizontal section*

Fig. 14-4: Water levels during transport and installation on site

The action effects at the connections result from local action (like water pressure on a wall) and from "global" action causing membrane forces in the plates and walls acting as shells. The dominant effect can vary from one load phase to another, and without structural analysis it is often difficult to tell which action is governing. For this reason, it can be necessary to refine connection classification based on the preliminary structural analysis.

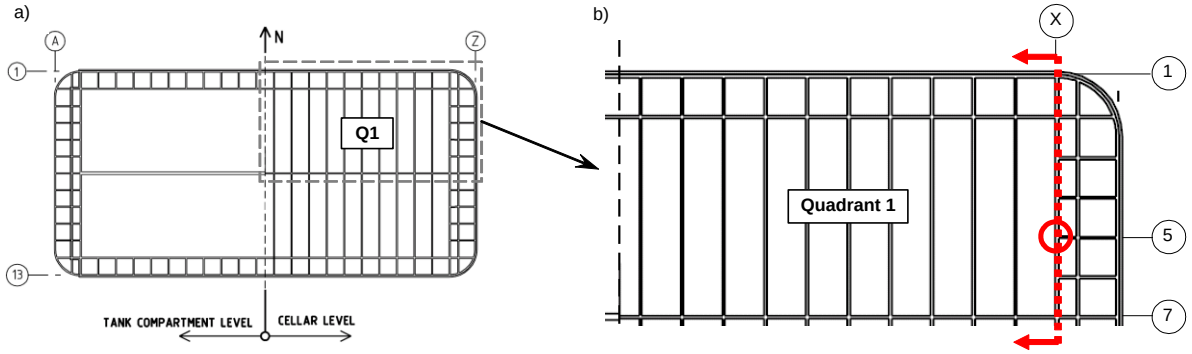
This document is the intellectual property of the fib – International Federation for Structural Concrete. All rights reserved.
This PDF of fib Bulletin 61 is intended for use and/or distribution solely within fib National Member Groups.

3 Preliminary analysis

3.1 Analysis of governing section forces

The analysis of section forces is of central importance for connection design. The character of the force flow determines which kind of model (2D or 3D) is appropriate for design, what the governing loading situations are and which regions experience maximum stresses. As named previously, also connection classification may require modification to consider particularities in the section forces of some regions.

First it is necessary to get an overview of character and intensity of the load situations that the connections are subjected to. This data is usually provided by structural analysis based on finite elements. In the case of offshore structures, the analysis is complicated by a high number of load cases that are combined to so-called “design combinations” in order to represent the various load phases. As an example, part of the sectional forces in an inner wall is shown subsequently. Fig. 14-5 indicates the analysed region of the terminal.



a) horizontal cross section at compartment and cellar level b) location of sections

Fig. 14-5: Horizontal cross section at compartment and cellar level and location of sections shown subsequently

Fig.14-6 shows the envelopes of maximum and minimum bending moments for a horizontal section through the wall in axis X, at approximately half of the wall height. The peak values can be found at the connections, where maximum bending moments are caused by water ballasting during installation and minimum bending moments are found for accidental flooding during operation.

The diagrams show high positive and negative moments at the connections, which is usually not the case for structures that are primarily subjected to gravity loads. This variety in loading situations makes connection design for offshore structures very challenging. Often there is not one governing situation, but several design combinations that have to be verified.

Fig. 14-6 also shows that the connections cannot be classified according to their geometry only. Whereas the T-connections ③X, ④X and ⑤X have similar moments, the T-connection ⑥X differs significantly. The reason is that only one compartment at the connection is filled with water during installation. The compartment containing mechanical installations remains empty, see Fig. 14-4b.

This document is the intellectual property of the fib – International Federation for Structural Concrete. All rights reserved.
This PDF of fib Bulletin 61 is intended for use and/or distribution solely within fib National Member Groups.

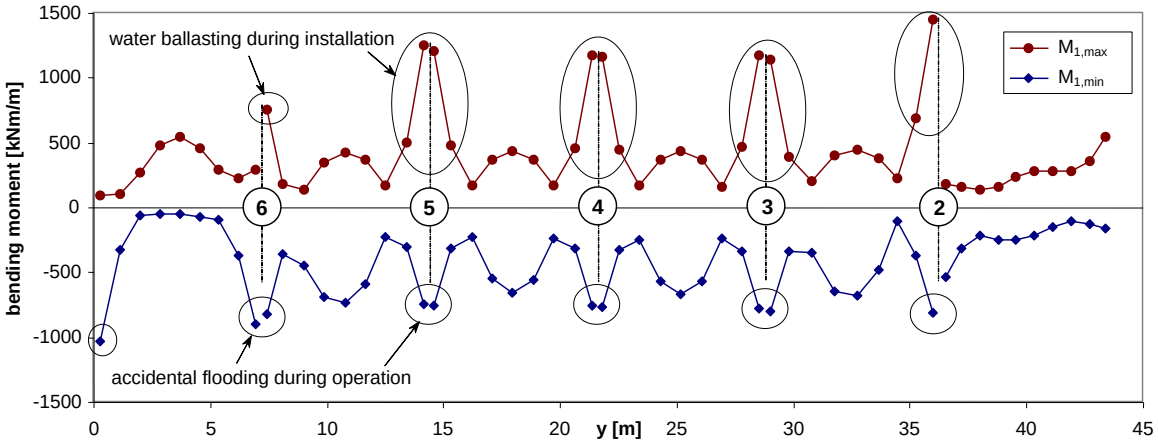


Fig. 14-6: Envelope curves for maximum / minimum bending moment in wall axis X

Fig. 14-6 only shows that the wall in axis X experiences important bending moments due to differential water pressure. More extensive information is obtained by plotting the section forces at a connection with a so called "rib wall" (axis ③ - ⑥) over the entire wall height, as done in Fig. 14-7. This figure contains envelope curves of the axial force ($N_{1,max}$, $N_{1,min}$), the in-plane shear ($N_{12,max}$, $N_{12,min}$) as well as of the bending moments and transverse shear forces next to the connection.

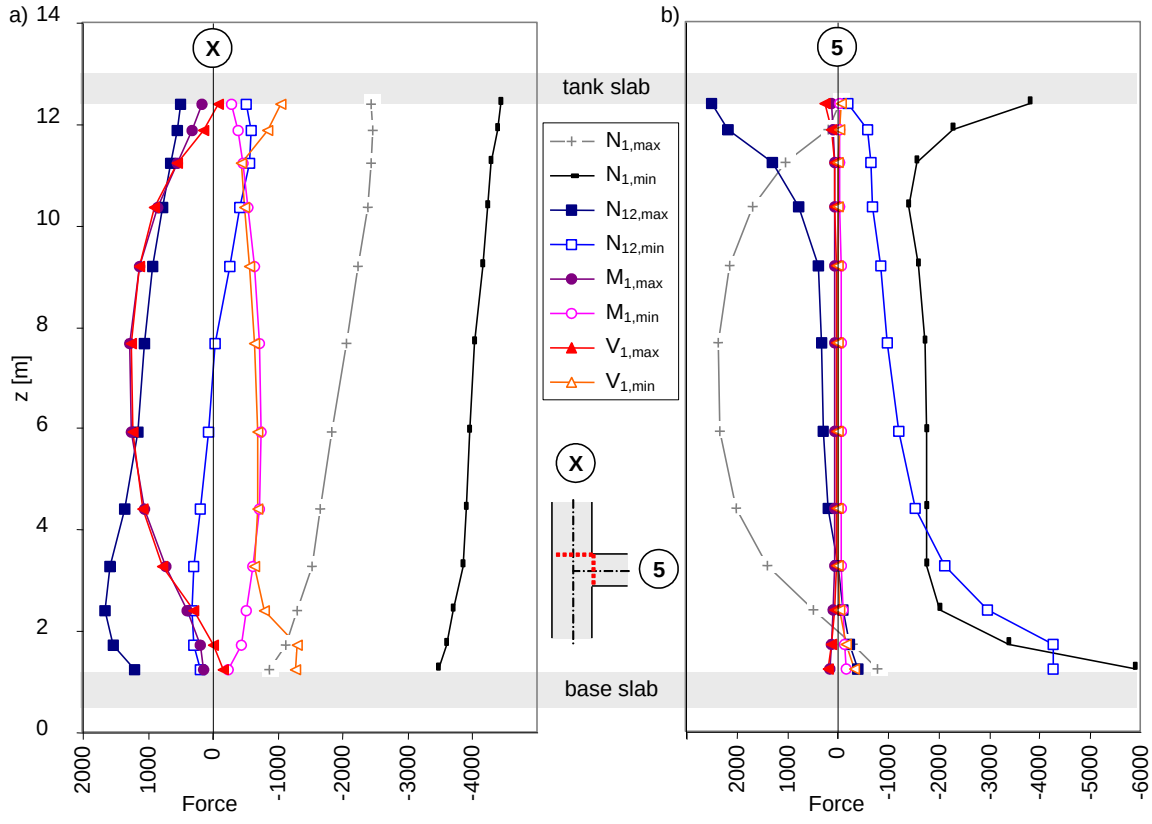
For the wall in axis X, the curves show variable axial compression which is mainly provided by post-tensioning. In-plane shear is relatively low. Bending moments attain their highest values at the middle of the wall height where the wall panel essentially acts as slab with one directional load bearing. Transverse shear forces generally have a similar course, with the exception of the minimum shear force showing a peak towards the base slab. The reason is a rotation of the base slab around the wall in axis X, which is restraint by the rib wall in axis ⑤.

The section forces of the rib wall in axis ⑤ are characterised by particular membrane forces (axial force and in-plane shear), whereas bending is practically negligible. High values for in-plane shear indicate that the wall primarily acts as shear panel stiffening the terminal in the longitudinal direction. Contrary to the wall in axis X, the rib wall experiences important axial tension during its loading history, mainly because it is not prestressed.

Envelope curves give a good overview over the various loading situations that can be found at connections. They also give good insight into the structural behaviour of the terminal. At the same time, they allow to verify if the section forces are plausible and comprehensible. This aspect is more difficult to judge if the study is reduced to isolated cross sections at the connections.

The disadvantage of envelope curves is that they do not show which section forces occur simultaneously. Usually, maximum bending moments / transverse shear forces do not coincide with maximum in plane shear N_{12}. However, the presence of in-plane shear in addition to bending often causes a shift in the most critical section. For this reason, the so-called "utilisation ratios" for reinforcement and concrete are plotted along the connection. Based on this overview, the detailed analysis can focus on the most utilised regions of a certain reinforcement layout.

This document is the intellectual property of the fib – International Federation for Structural Concrete. All rights reserved.
This PDF of fib Bulletin 61 is intended for use and/or distribution solely within fib National Member Groups.



a) innermost front wall *b) rib wall*

Fig.14-7: Envelope curves for section forces in innermost front wall and rib wall for vertical sections at connection ⑤/ X

In the specific case of connection ⑤X, D-region design has to cover the extreme bending moments and transverse shear forces in the continuous wall (axis X), and axial tension and extreme in-plane shear in the rib wall. A close analysis of the envelope curves reveals that the high bending moments in axis X and the tensile forces in ⑤ are linked, i.e. they result from the same loading situation. Using qualitative models, the number of loading situation to be verified can be further reduced.

3.2 Delimitation of D-regions

The delimitation of D-regions is the first step in the development of models for the structural analysis of D-regions. It is closely linked to the design procedures applied to the rest of the structure. The section forces at the connection indicate whether three-dimensional models should be used or whether two-dimensional models are sufficient. 3D models are far more difficult to visualise and analyse. For this reason, 2D models are used as much as possible.

Fig. 14-8a shows a connection in the base slab close to the intersection of two walls. For this connection, maximum stresses are found in between intersecting walls. Consequently, analysis can be based on 2D models in a plane transverse to the connection, see Fig. 14-8b. In other regions of the terminal, the model has to include intersecting walls.

This document is the intellectual property of the fib – International Federation for Structural Concrete. All rights reserved.
This PDF of fib Bulletin 61 is intended for use and/or distribution solely within fib National Member Groups.

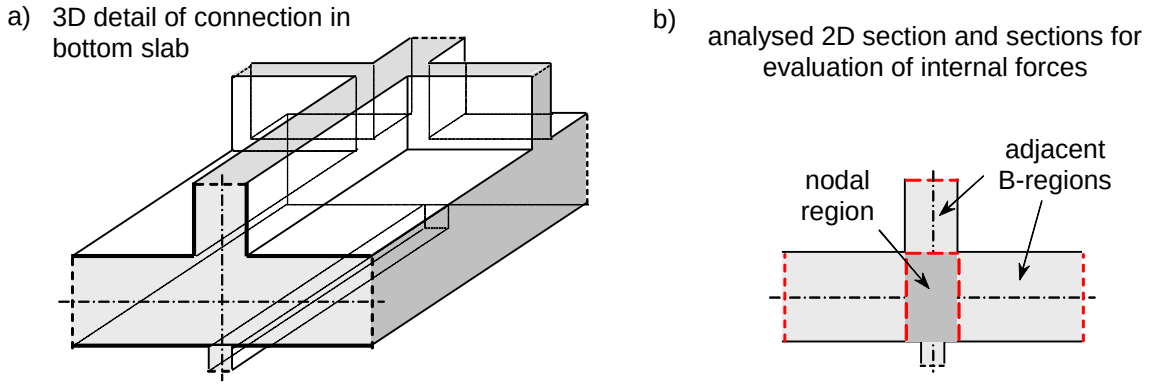


Fig. 14-8: Delimitation of connections

In the case of the analysed terminal, structural analysis provides section forces up to the edge of the nodal region. For this reason, B-region design is extended to these cross sections. In most cases, D-region design can thus be limited to the anchorage or deviation of forces in the nodal region and to the verification of concrete stresses.

D-region models have to extend beyond the actual nodal region, because the activated reinforcement is anchored in the adjacent B-region. By including two or more sections next to the nodal region, it is easier to understand the force flow and to guarantee compatibility of B- and D-region design.

3.3 Qualitative modelling

Qualitative strut-and-tie models help to understand the force flow in D-regions and enable to quickly develop appropriate reinforcement detailing. Based on qualitative models, the whole analysis can be effectively focussed on the most relevant topics. The models can show which connection type should be analysed in detail and which filter criteria can be used to identify the governing loading situations.

In the qualitative models continuous red lines show the reinforcement which is necessary for sustaining tensile forces. In the case of a continuous bar, this may only concern a part of it activated in a tensile zone. For clarity, the entire reinforcement is not shown although it might be required for proper anchorage.

In section 2, three types of connections have been identified (see Fig. 14-3): Cross (┼)-shaped connections, T-shaped connections and L-shaped connections. With the help of qualitative models it can be verified easily that cross-shaped connections do not require D-region design if the structural elements have constant thickness across the connection (no reinforcement terminated in the region). B-region design at the edge of the nodal region suffices to determine the required reinforcement intensity, and the concrete stresses do not increase inside the nodal region.

Qualitative modelling is illustrated in detail for T-shaped connections. This connection type is very frequent in the base slab and in the outer walls of the terminal shown in Fig. 14-5. It consists of a continuous element (slab or wall) which is usually prestressed and a discontinuous element. The analysis concentrates on the anchorage of the discontinuous element that requires appropriate detailing of the main reinforcement. Fig. 14-9 shows generic models for the various loading situations:

a) Dominant *compression*: Typical situation for a horizontal beam / plate supported by a column / wall; no particular difficulties in design.

This document is the intellectual property of the fib – International Federation for Structural Concrete. All rights reserved.
This PDF of fib Bulletin 61 is intended for use and/or distribution solely within fib National Member Groups.

b) Dominant *tension*: Corresponds to a horizontal beam / plate suspended by a tendon / wall; particular attention required to prevent tear-out of the tendon / wall.

c) and d) Dominant *bending moment*: Typical situation for external columns / walls of frame structures; solid anchorage of rib wall tension chord important.

e) Dominant *in-plane shear*: Typical situation for the web of beams with I – or T –shaped cross section.

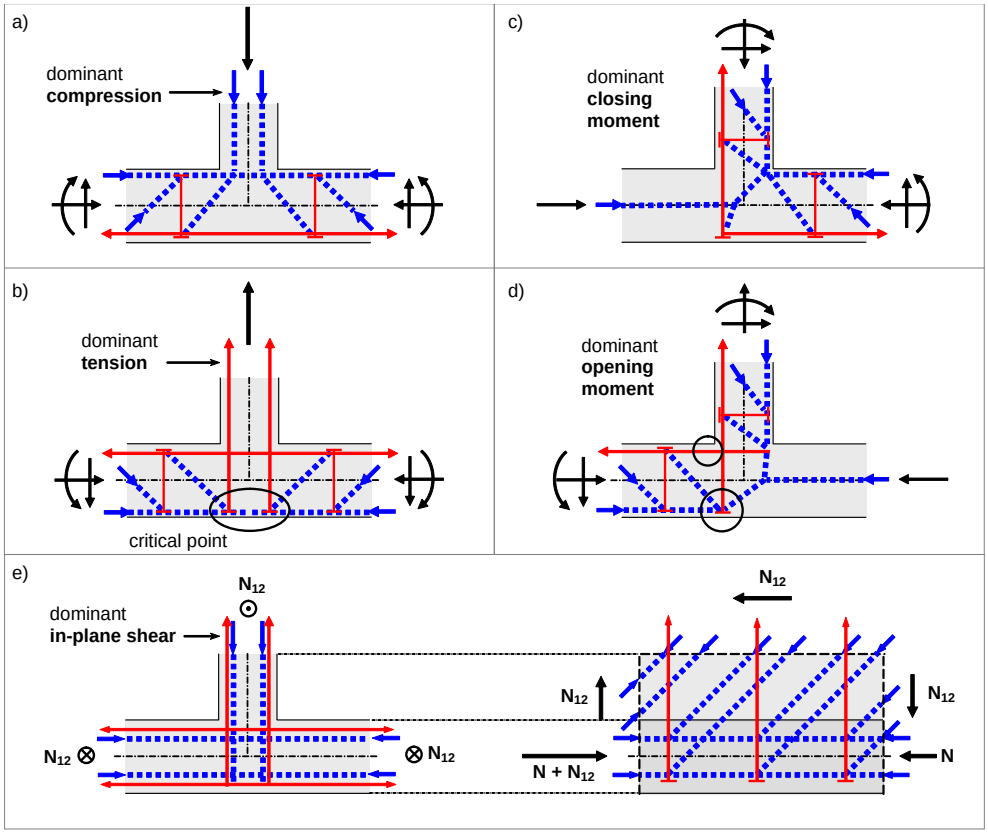


Fig.14-9: Generic strut-and-tie models for T-shaped connections

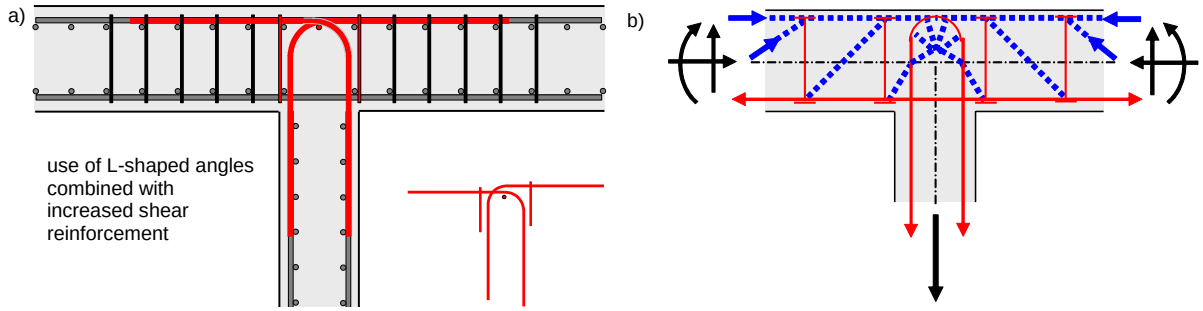
The most critical point is the anchorage of the main reinforcement of the discontinuous wall in the continuous wall, which is highlighted for cases b) and d). In order to provide a solid support for the last shear strut of the continuous wall, the precise design of this anchorage is decisive. If an opening moment is dominant, the location of this anchorage defines the statical height in the continuous element which again is determinant for the main reinforcement. Also in-plane shear in the discontinuous wall (case e) requires proper anchorage of the reinforcement. Contrary to cases b) and d), the precise location of the anchorage is less critical.

In the generic strut-and-tie models, reinforcement anchorage is symbolised by a T-head. T-heads are relatively expensive and complicate the use of bundles with two or more bars. On the other hand, T-headed bars do often simplify construction and decrease weight with respect to the anchorage with angles. For this reason, they are very popular in reinforced concrete offshore structures.

If the reinforcement is anchored with angles or loops, the generic models have to be refined in order to reflect the actual reinforcement layout. Fig.14-10, Fig. 14-11 and Fig. 14-12 show possible alternatives to the use of T-heads for the anchorage of the discontinuous main reinforcement. All possibilities have to be evaluated with respect to robustness, constructability and flexibility.

This document is the intellectual property of the fib – International Federation for Structural Concrete. All rights reserved.
This PDF of fib Bulletin 61 is intended for use and/or distribution solely within fib National Member Groups.

Fig. 14-10 shows a variant with L-shaped bars and a strut-and-tie model for the case of dominant tension in the discontinuous element. The model clearly shows that the L-bars do not provide the best support to the diagonal shear struts in the continuous element. The strut is anchored along the straight section of the bar because the angle itself is somewhat repellent. With respect to the solution with T-headed bars, shear reinforcement in the continuous element has to be increased adjacent to the connection. Inside the bends, one or two bars may be required to resist splitting tension. Concerning constructability, the solution is unfavourable because L-bars are difficult to place, particularly during slip-forming.

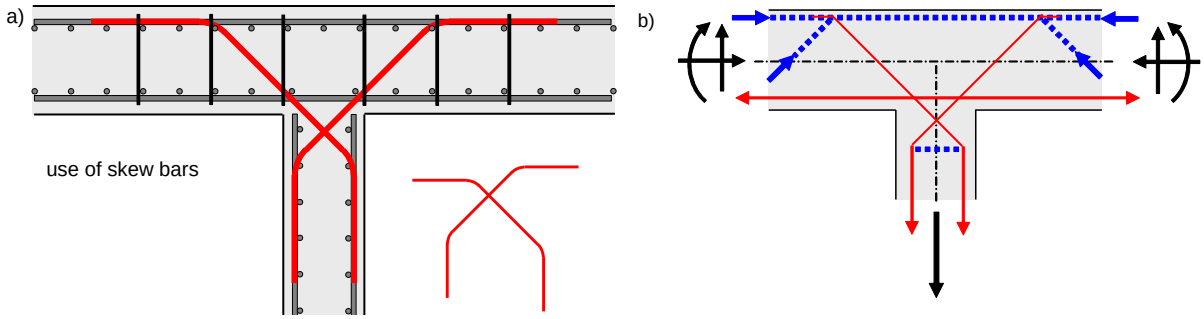


a) reinforcement layout using L-shaped bars *b) strut-and-tie model*

Fig. 14-10: Reinforcement layout and strut-and-tie model for T –shaped connection with dominant tension in discontinuous wall

Angles are cheaper than T-headed bars but they have important disadvantages with regard to construction. For bar diameters of 25 mm or more, they are very heavy which makes them difficult and dangerous to put in place. In the continuous element, the bars add to the continuous reinforcement that may already be constituted of two bars per bundle. If the continuous element is a slab, angle shaped bars are rarely an option.

Fig. 14-11 shows a possible layout with diagonal bars. For the case of dominant tension in the discontinuous element, this layout appears very efficient. Shear reinforcement can be decreased significantly and reinforcement congestion in the nodal region is avoided. On the other hand, the layout is absolutely inappropriate for bending moments or in-plane shear in the discontinuous element (Fig. 14-9c, d and e). In addition, diagonal bars are very difficult to put in place.

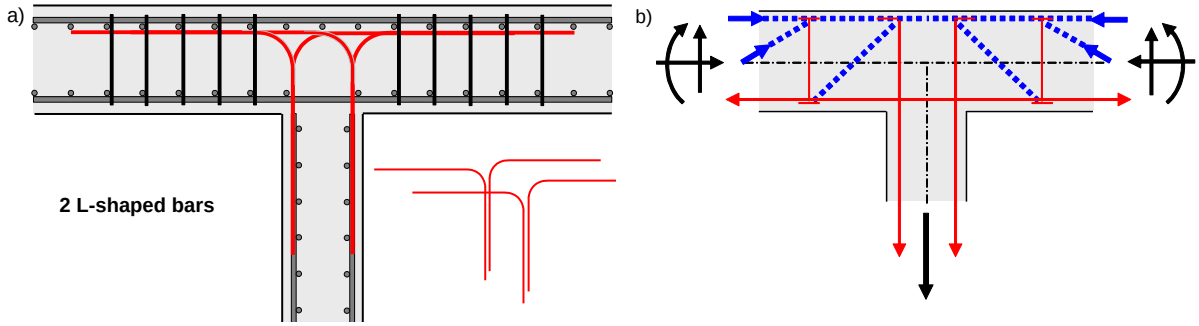


a) reinforcement layout *b) strut-and-tie model*

Fig. 14-11: Reinforcement layout using diagonal bars and corresponding strut-and-tie model for T–shaped connection with dominant tension in discontinuous wall.

This document is the intellectual property of the fib – International Federation for Structural Concrete. All rights reserved.
This PDF of fib Bulletin 61 is intended for use and/or distribution solely within fib National Member Groups.

In order to obtain a more polyvalent layout, different bars can be combined. A possible layout using a combination of L-shaped bars is shown in Fig. 14-12. The layout of Fig. 14-10 is amended by L-shaped bars with the angle directed outwards, thus providing good support to the diagonal shear strut. The drawbacks of this layout are its limitation to moderate forces and bad constructability. On top of the T, the first layer has to be reserved for the continuous reinforcement of the basic mesh which covers the support moment for the case of water pressure from the outside.



a) reinforcement layout with combination of L-shaped bars *b) strut-and-tie model*

Fig. 14-12: Reinforcement layout using a combination of L-shaped bars and corresponding strut-and-tie model for T –shaped connection with dominant tension in discontinuous wall

3.4 Definition of filter criteria

Filter criteria for the identification of governing loading situations are required if the structure is designed for a large number of design combinations. These filter criteria can be derived from collected section forces and qualitative Strut-and-tie models. Depending on the variety of loading situations and on the reinforcement layout, it may be necessary to define several criteria for the same connection.

Fig. 14-13 shows the example of a T-connection subjected to a dominant opening moment. In order to design the anchorage of the discontinuous reinforcement, the obvious filter criterion is maximum tension in the respective tie. In cases with important in-plane shear in the discontinuous element, this criterion will not yield the worst opening moment. Filtering for the maximum moment may lead to a design combination with high simultaneous compression. A better criterion is the maximum tension in the “inner” continuous reinforcement.

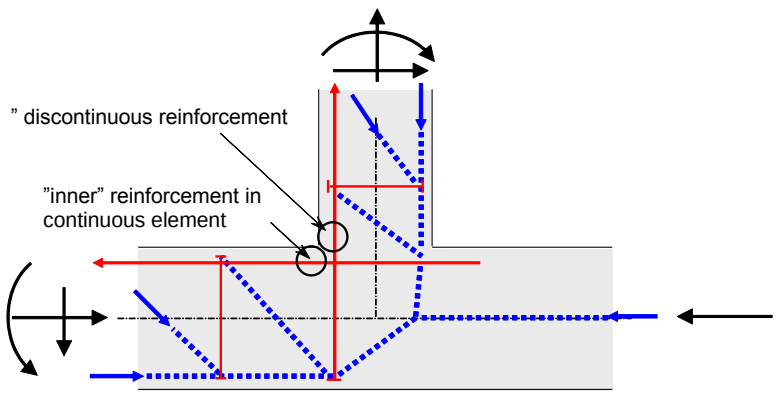


Fig. 14-13: Filtering for governing loading situation with opening moment.

This document is the intellectual property of the fib – International Federation for Structural Concrete. All rights reserved.
This PDF of fib Bulletin 61 is intended for use and/or distribution solely within fib National Member Groups.

Weight limits resulting from construction and transportation techniques for offshore structures often impose slender dimensions on the structural elements. For this reason, high compression is attained in certain regions. In these regions, filter criteria must be defined for the verification of maximum compression in D-regions.

3.5 Use of R-plots

R-plots are the best way to quickly determine the character of a loading situation and to compare the effect of different design combinations. Filter criteria do not guarantee that the most relevant loading situations have been determined. For this reason it is important to make a rough evaluation before detailed models are developed.

R-plots make it possible to visualise the section forces (normal force *N*, bending moment *M* and transverse shear force *V*) in a very concise manner, provided that the normal force differs significantly from zero. Hence, R-plots are best suited for prestressed structures and shell structures with significant membrane forces. The definition of a resultant vector in a cross section is illustrated in Fig. 14-14. Vector tips are marked with a punch that relates the resultant to the concrete compressive strength.

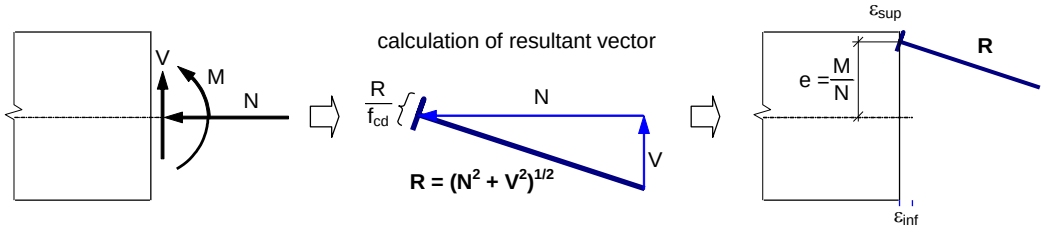


Fig. 14-14: Definition of resultant vectors

Although all the R-plots shown subsequently are two-dimensional, resultants actually are of three-dimensional nature in a spatial shell structure. A true representation of inner forces in the form of one resultant in space is not practicable because principal membrane forces and principal transverse shear forces are generally not aligned.

After delimitation of the D-region, the plane for its analysis is defined. R-plots will display a projection of *N*, *M* and *V* into this plane and neglect out of plane components like in-plane shear or the torsional moments. In regions with important out of plane components, it is useful to indicate this in the R-plot.

Fig. 14-15 shows an example of an R-plot for a T-connection. Resultants are drawn for the cross sections immediately adjacent to the connection as well as for the next section used in B-region design. These cross sections are indicated with dashed lines. The resultant for a cross section can be found by production of this line on either side of the section. For small values of *N* or large eccentricities *M*/*N*, respectively, the resultant may lie far beyond the cross section. The resultants are defined as force vectors acting on the connection, i.e. a vector pointing to the nodal region signifies axial compression. Resultants with positive normal force are drawn in red in order to reflect the importance of axial tension for design. In addition to the resultants, the plane of axial strains (assuming linear elastic behaviour) is indicated for every section.

This document is the intellectual property of the fib – International Federation for Structural Concrete. All rights reserved.
This PDF of fib Bulletin 61 is intended for use and/or distribution solely within fib National Member Groups.

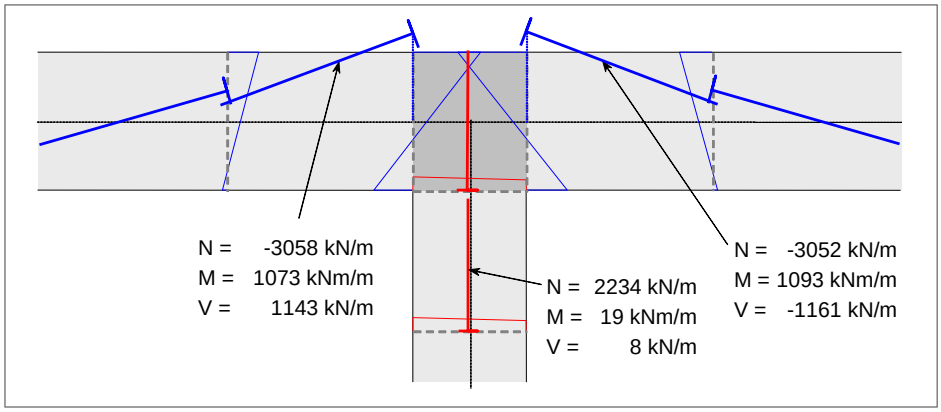


Fig. 14-15: R-plot for T –connection subjected to dominant tension in discontinuous wall

The plotting of resultants can be computerised, although there are few programs that provide this functionality. Depending on the analysis package and on the loading situation, the forces acting at the edge of the nodal region are not in equilibrium. In Fig. 14-15 for example, the normal force in the discontinuous element N = 2.234 kN/m is not equilibrium with transverse shear in the continuous element 1.143 + 1.161 = 2.304 kN/m. It may be necessary to append external forces at the "free" face of the nodal region or to consider transfer of forces out of plane. In offshore structures, the difference may result from modifications in certain force components in order to include the effect of water pressure in cracks.

Another example of an R-plot is shown in Fig. 14-16. As a next step to detailed modelling, the section forces at the edge of the nodal region are modified in order to establish equilibrium with respect to the centre of the nodal region. For transparency, the original forces obtained from the B-region design (post-) processing application are shown in parenthesis. The remaining unbalance F_{vert} = 50 kN/m is in equilibrium with water pressure on the "free" face of the nodal region.

Fig. 14-16 does not only show N, M and V at the nodal region, but also in-plane shear in the various cross sections. Whereas it is negligible to the right of the nodal region, in-plane shear is important in the other sections. In addition to section forces, Fig. 14-16 includes a precise localization of the connection cross-section as well as the identification of the design combination.

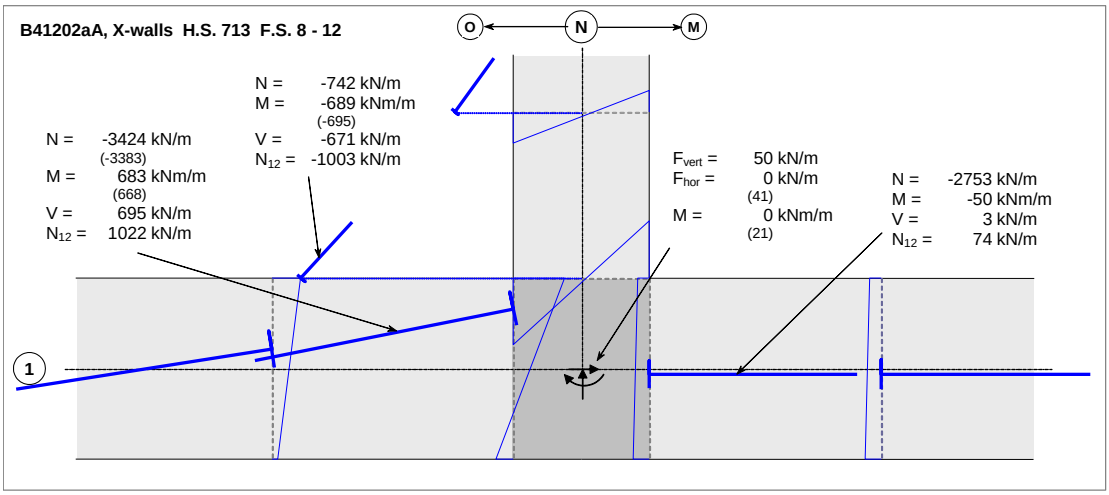


Fig. 14-16: R-plot for T –connection subjected to dominant closing moment.

This document is the intellectual property of the fib – International Federation for Structural Concrete. All rights reserved.
This PDF of fib Bulletin 61 is intended for use and/or distribution solely within fib National Member Groups.

4 Detailed analysis

4.1 Development of stress field models

In the case of simple D-regions like T-connections, design can often be based on preliminary analysis. Sectional design is mostly sufficient to determine the main reinforcement quantities, and D-region design helps to select reinforcement detailing in the region. Detailed analysis is then used to verify the regions with maximum utilisation according to standard provisions. In more complex D-regions where sectional design is not applicable, detailed analysis is required to determine not only reinforcement detailing but also the reinforcement quantities.

Small and simple D-regions make it possible to develop quite sophisticated models like stress-field models relatively straightforward. *Stress-field models* give a detailed picture of concrete stresses and are primarily useful for checking the concrete stresses at ultimate limit state. With respect to finite element models, these models have limited precision because simple stress distributions are assumed for the various stress fields and reinforcement is not activated in compression. On the other hand, these models are suitable for ultimate limit state with highly cracked cross sections. They provide a clear graphical illustration of the areas where the admissible concrete compressive strength $f_{cd,eff}$ is fully utilised.

Fig. 14-17 shows schematically how stress fields and the according struts and ties are developed on the basis of section forces at the edge of a connection. The development starts with setting up the input parameters

- Section forces N, M and V.
- Cross-section dimensions (section height, neutral axis, statical height of tensile reinforcement).
- Effective concrete compressive strength $f_{cd,eff}$ defined in function of the reinforcement layout, according to applicable standard.
- Inclination of diagonal stresses θ / θ_1 defined in function of the section forces, within the limits set by the applicable standard.

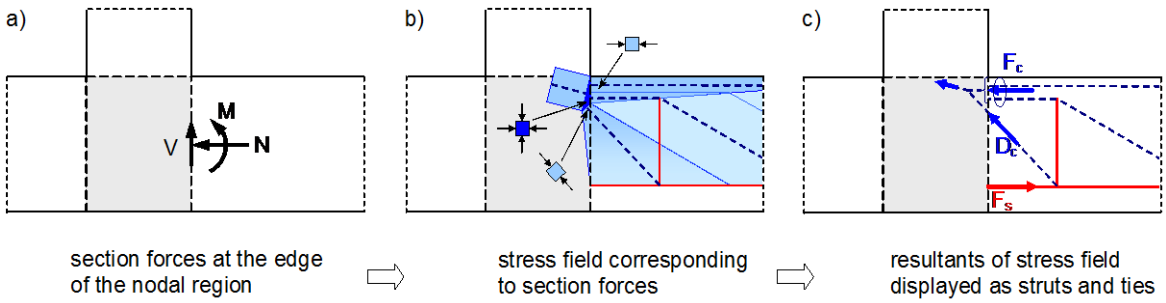
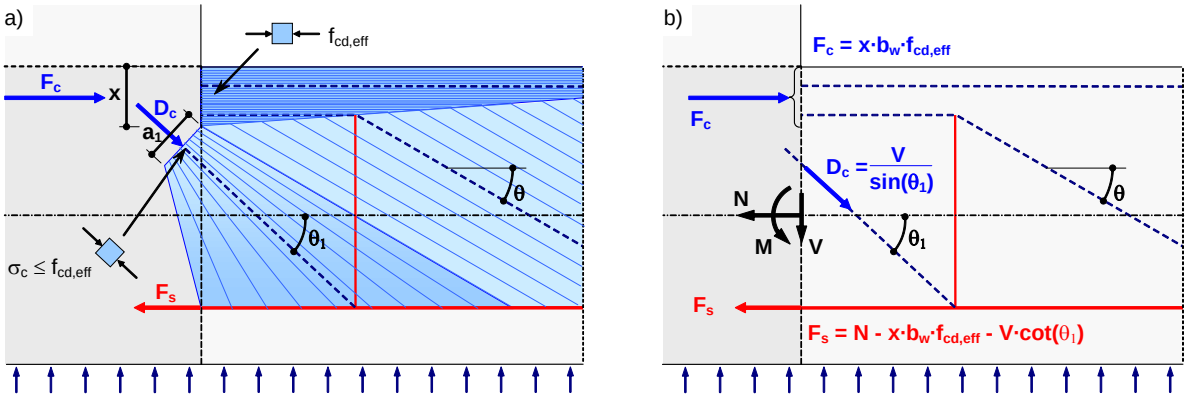


Fig. 14-17: Typical stress field at connection and deduction of strut-and-tie model

Fig. 14-18 shows the definition of the stress field model more in detail. In general, five stress fields are defined next to the nodal area. (1) The strut where the effective concrete strength $f_{cd,eff}$ is fully utilized in the axial direction. (2) The diagonal strut with regular inclination θ which touches the nodal zone at the tip. (3) The accompanying field of stirrups balancing the vertical component of the diagonal strut at both ends. (4) The fan shaped field of diagonal compression next to the nodal area. (5) The accompanying field of stirrups balancing the vertical component of the fan.

This document is the intellectual property of the fib – International Federation for Structural Concrete. All rights reserved.
This PDF of fib Bulletin 61 is intended for use and/or distribution solely within fib National Member Groups.

The height x of the compression zone depends on the internal lever arms of the struts and ties which again depend on x. The solution can be obtained by iteration or by solving a quadratic equation. The solution shows that x is a function of θ but not of θ_1. Principally the angle of the fan shaped compression field θ_1 can be varied between θ and $\theta_{1,max}$. The maximum angle $\theta_{1,max}$ is defined by the concrete stresses at the tip of the fan which may not exceed the effective compressive strength $f_{cd,eff}$. The angle θ_1 defines the stress level in the main tensile reinforcement. The force F_s decreases for increasing angles θ_1 due to the increased lever arm of internal forces. Often θ_1 is set to $\theta_{1,max}$ in order to minimise F_s and in order to obtain stress compatibility at the node where the struts F_c and D_c meet. The connection of struts with equal stresses in a CCC node creates a zone with hydrostatic compression in compliance with stress field theory. In certain cases, however, it is useful to treat θ_1 as free parameter for better agreement with other components of the model.



a) stress fields *b) strut-and-tie model*

Fig. 14-18: Definition of typical stress field at connection

The admissible concrete compressive strength $f_{cd,eff}$ is chosen according to the standard applied for the project, in Norway usually NS 3473:2003. Like other standards (e.g. EN 1992-1-1:2004, sect. 6.5.4), it defines $f_{cd,eff}$ in function of the state of stress in the considered zone. One-directional tension or ties anchored in one direction is considered by a minor reduction of the design compressive strength f_{cd} and two-dimensional tension or ties anchored in two directions in a major reduction.

4.2 Examples

Depending on the requirements defined by the client, D-regions and concrete stresses will be documented more or less extensively. It can be acceptable to analyse just one or two loading situations for each reinforcement layout. A more extensive way is to document each loading situation that is governing with respect to the selected filter criteria, for each of the D-region groups identified in the classification. Fig. 14-19 gives an overview over the number of cases analysed in the lower level walls of the cited offshore terminal.

The first example in Fig. 14-20 shows a T-connection (wall–wall junction) that is subjected to "internal" water pressure on the continuous wall which causes high tension in the discontinuous wall (N = 2.049 kN/m) and high bending moments and transverse shear forces in the continuous wall. The section forces for this loading situation are similar to the situation presented by the R-plot in Fig. 14-15. The forces at the edge of the nodal region are listed next to the corresponding element in the figure. The main task in designing the region is to assure the proper anchorage of the discontinued reinforcement in the region, see Fig. 14-9b.

This document is the intellectual property of the fib – International Federation for Structural Concrete. All rights reserved.
This PDF of fib Bulletin 61 is intended for use and/or distribution solely within fib National Member Groups.

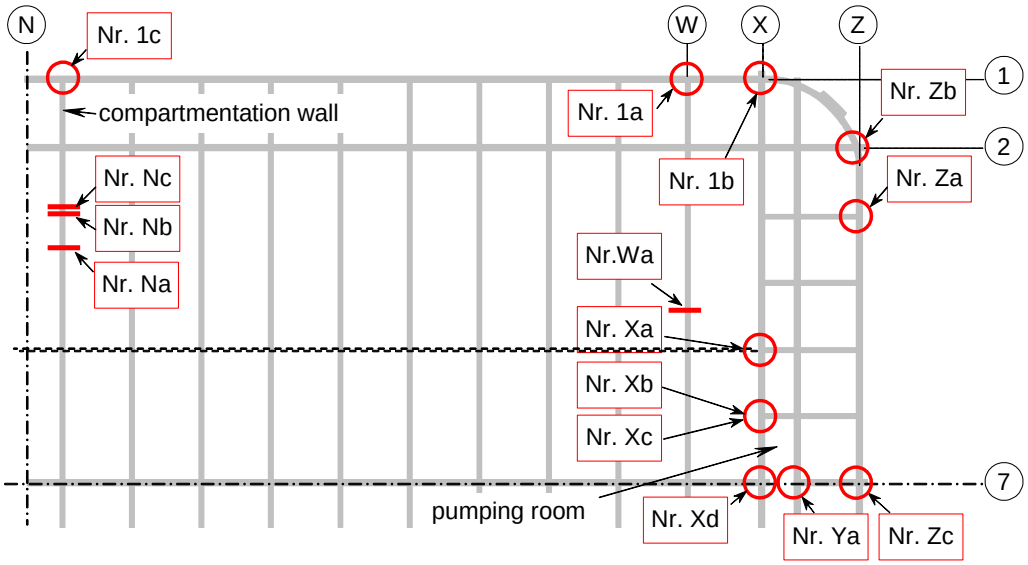


Fig. 14-19: Location of analysed connections in lower level walls

In addition to axial tension, the discontinuous wall is subjected to in-plane shear (N_{12} = -1.626 kN/m). However, the model in Fig. 14-20 represents only stresses due to bending / normal forces. In-plane shear is considered by providing sufficient capacity in the main reinforcement to take the tensile component, assuming a 45° inclination of the membrane forces. This means, the main reinforcement of 2Ø32 c200 has to cover the tensile force of 1.313 kN/m shown in Fig. 14-20 plus the contribution of in-plane shear N_{12} / 2 = 813 kN/m.

The development of the model starts with defining the stress fields at the edge of the nodal region. First, the concrete stress in the compression chord of the continuous wall is set to $f_{cd,eff} = 0{,}9 \cdot f_{cd}$. The reduction is due to the anchorage of the T-headed bars in this zone. In addition, the compression chord is not well confined: out-of-plane compression of about $\sigma_{c,perp}$ = -2,5 MPa does not compensate for the danger of concrete spalling towards the free surface. The main reinforcement located in the strut is not considered which simplifies design and makes it more robust.

Next, the angles for the shear fields θ and θ_1 are defined. High angles θ_1 result in a concentration of concrete stresses towards the compression chord, whereas low angles increase the force in the tension chord. Generally, rather low angles θ_1 are chosen. This choice results in higher requirements to the tension chord but it ensures good anchorage of the discontinuous bars. The utilisation ratio of the main tensile reinforcement is not increased beyond 90 to 95% because in-plane shear is not modelled very accurately.

In the presented example, the angles θ and θ_1 are restricted to combinations resulting in a continuous force in the tension chord across the nodal region. Thus, the stress distribution in the nodal region is obtained straight forward by connecting the struts and ties in the adjacent elements. The correctness of the model is confirmed if the equilibrium is fulfilled in every node and if the inclination of struts corresponds with their horizontal and vertical force components.

This document is the intellectual property of the fib – International Federation for Structural Concrete. All rights reserved.
This PDF of fib Bulletin 61 is intended for use and/or distribution solely within fib National Member Groups.

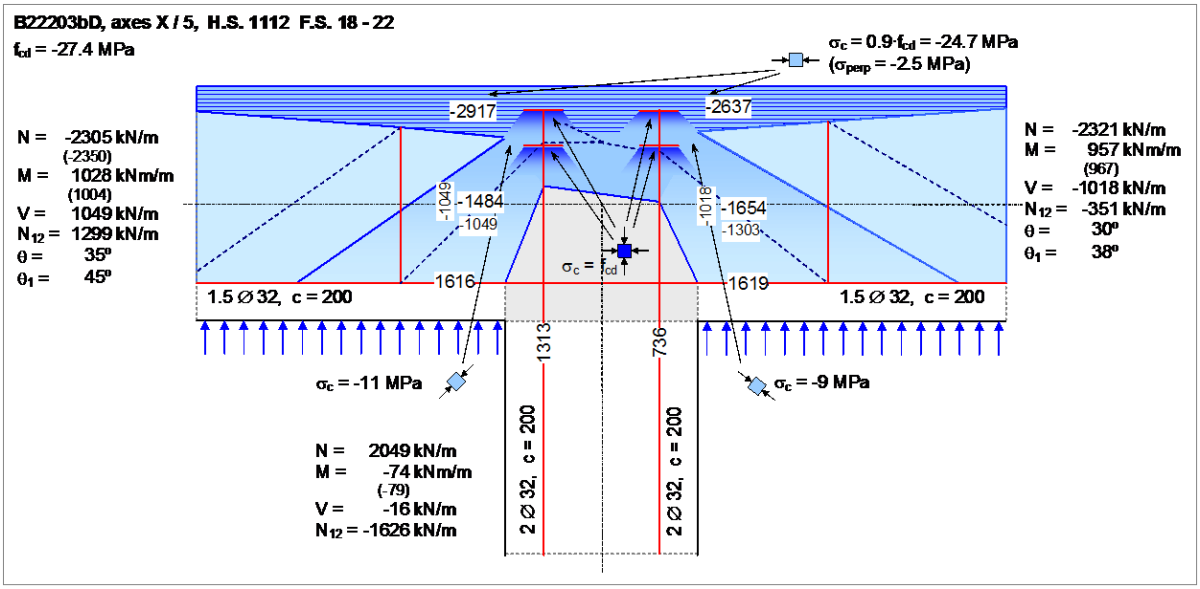


Fig. 14-20: Detailed model for example 1 – T-joint with dominant tension in discontinuous wall

The objective is not to model the stress distribution very accurately and theoretically exact. In view of the high number of connections and load combinations work has to concentrate on the critical points:

- By limiting the concrete strength used in the stress field model, concrete stresses are automatically verified.
- By connecting struts and ties at the anchorage of reinforcement, the proper stress transfer can be evaluated graphically.

The reinforcement to be anchored in the connection consists of 2Ø32 mm, centre to centre distance 200 mm, in both faces. This reinforcement should be anchored as far as possible towards the compression face of the continuous wall. The best solution from the structural viewpoint is probably a combination of T-headed and L-shaped bars. Since L-shaped bars Ø32 mm are very heavy and difficult to place, have a large bending radius and require a lot of space for anchoring the legs in the continuous wall, all bars are anchored with T-heads.

Given the spacing of 200 mm, it is not possible to anchor both T-headed bars in a bundle outside of the main reinforcement in the continuous wall. The stress field model shows that one bar is enough to suspend the shear force in the continuous wall, whereas the other bar can serve for in-plane shear. According to Fig. 14-9e, the precise location of the anchorage is less critical for in-plane shear.

The close placement of T-heads causes locally high concrete stresses that can exceed f_{cd}. This is admissible due to three-dimensional compression in these areas. It is preferable to hook the outer T-heads into the continuous reinforcement in order to obtain a better distribution of compressive stresses. In addition, this detailing allows the connection to perform better for closing moments.

The next example shows a similar situation (water pressure on the continuous wall suspended by the discontinuous wall), with the difference that section forces are at a distinctly lower level, see Fig. 14-21 compared to Fig. 14-15. The discontinued reinforcement consists of 1Ø25 mm, c = 200 mm instead of 2Ø32 mm, c = 200 mm. As this situation is governing over a large extent of T-connections, different detailing is chosen.

Fig. 14-21 highlights a particularity of the section forces: axial tension in the discontinuous wall includes the effect of water pressure in cracks. For pure tension at the shown level, the

This document is the intellectual property of the fib – International Federation for Structural Concrete. All rights reserved.
This PDF of fib Bulletin 61 is intended for use and/or distribution solely within fib National Member Groups.

cross section is theoretically cracked. Infiltrating water will build up water pressure on the crack faces and thus increase the tensile forces in the reinforcement. In order to establish equilibrium, the additional tension is conservatively balanced by an increase of transverse shear forces in the continuous wall. Actually, the crack pressure has no effect on shear forces in the continuous wall.

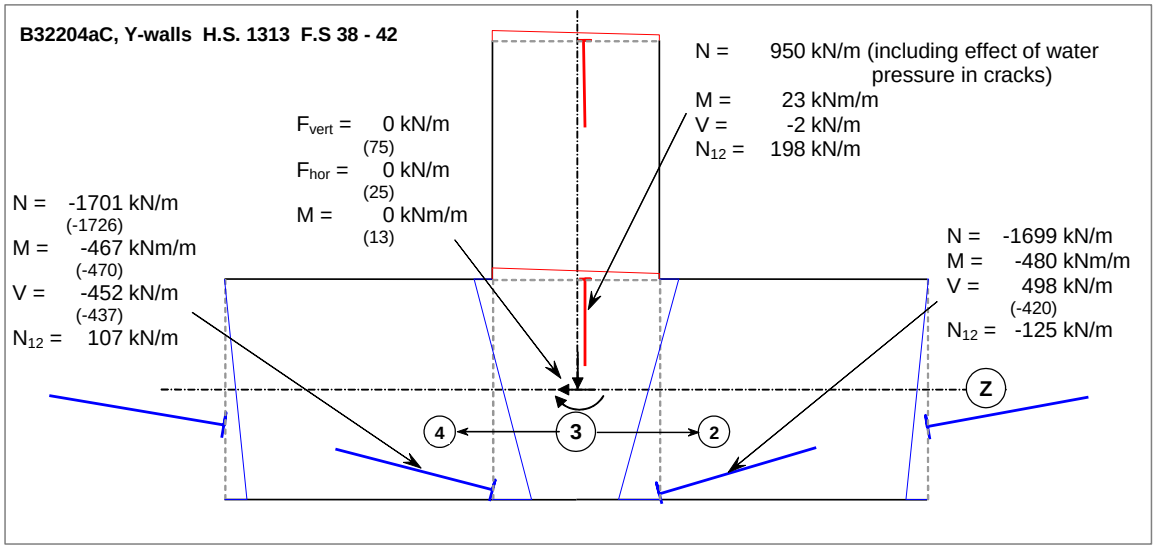


Fig. 14-21: R-plot for example 2 – T-connection with moderate tension in discontinuous wall

In order to anchor the discontinuous reinforcement in the continuous wall, L-shaped bars are chosen. They perform just as good for in-plane shear and for closing moments as T-headed bars and are cheaper. For opening moments or suspended loads, as in the example, L-shaped bars provide a lower resistance than T-headed bars. The transverse shear force in the continuous wall has to be anchored mostly along the straight section of the L-bar in the nodal area, which is only possible for relatively small angles θ_1. The performance is enhanced by placing extra shear reinforcement next to the nodal region as shown in Fig. 14-10a.

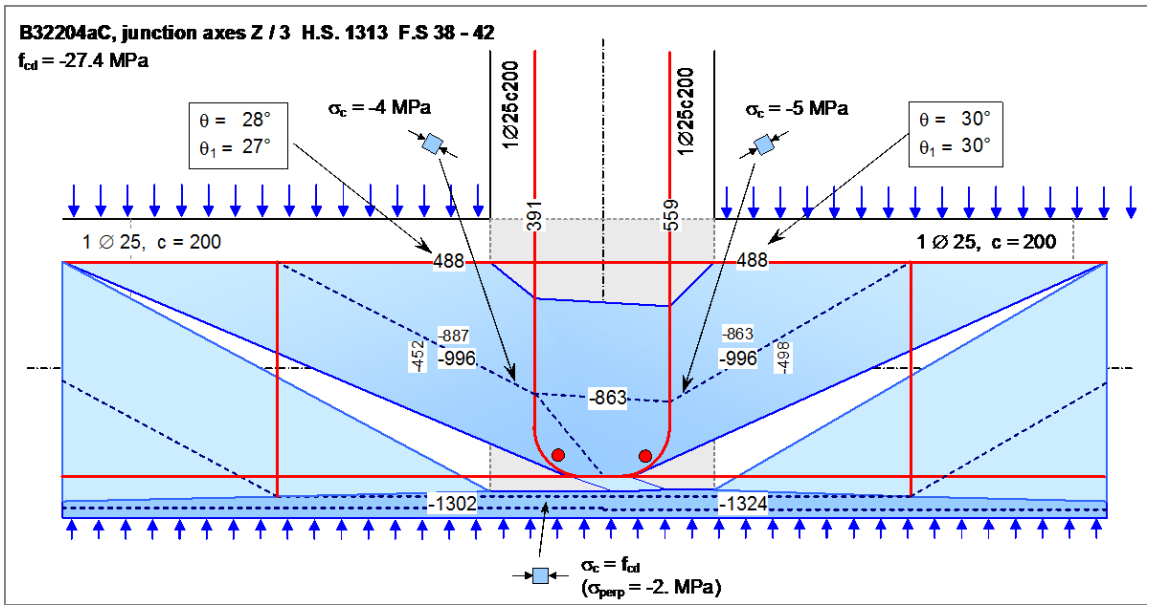


Fig. 14-22: Stress field model for example 2 – T-connection with moderate tension in discontinuous wall

This document is the intellectual property of the fib – International Federation for Structural Concrete. All rights reserved.
This PDF of fib Bulletin 61 is intended for use and/or distribution solely within fib National Member Groups.

Just as for the previous example, the weak point of the model is the missing confinement of the compression chord at the free face of the nodal region. According to the model in Fig. 14-22, minor shear forces might require to activate concrete tensile strength in this zone. The criticality of this problem can be evaluated by assuming concrete spalling of the compression chord exterior of the zone confined by shear reinforcement. If the reduced cross sections are still able to sustain service loads without excessive deformations (progressive collapse excluded), design is considered safe.

The third example shows a T-connection subjected to a dominant closing moment, see Fig. 14-23. The section forces are illustrated with the R-plot in Fig. 14-16. Contrary to the previous examples, all structural members are now subjected to axial compression. In addition to the closing moment (M = -689 kN/m), the discontinuous wall transfers notable in-plane shear (N_{12} = -1.003 kN/m). The continuous wall is dominated by axial compression.

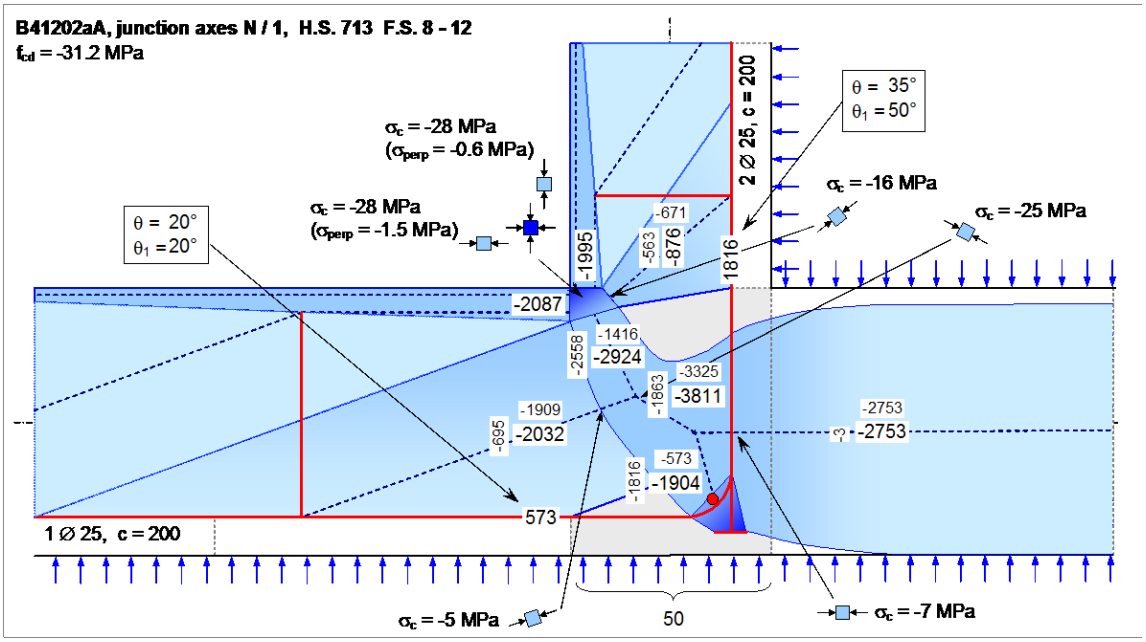


Fig. 14-23: Stress field model for example 3 – T-connection with dominant closing moment

Connection design is made for accidental limit state ALS, for which higher utilisation of material strength is admitted. The major design task again is to anchor the discontinuous reinforcement consisting of 2Ø25 mm, c = 200 mm. In this case, a combination of L-shaped angles and T-headed bars is applied, with a bar placed in the bend of the angle for a better support of the strut in the nodal region.

The last example deals with a T-connection that is subjected to an opening moment combined with axial tension and in-plane shear in the discontinuous wall (Fig. 14-24 and 14-25). The difference to the closing moment of the previous example is well illustrated by the R-plot in Fig. 14-25. A comparison of the various R-plots shows how useful this tool is for the preliminary evaluation of loading situations.

Heavy reinforcement is required for the force transfer between the continuous and the discontinuous wall (2Ø32 mm, c = 200 mm), which is anchored in the same manner as in the first example. One T-head is placed outside of the main reinforcement in the continuous wall, and the other at the inside. The external T-head effectively deflects the compression chord of the continuous wall, which fully utilises its capacity. The inner T-head suspends the shear force in the continuous wall and takes up in-plane shear.

This document is the intellectual property of the fib – International Federation for Structural Concrete. All rights reserved.
This PDF of fib Bulletin 61 is intended for use and/or distribution solely within fib National Member Groups.

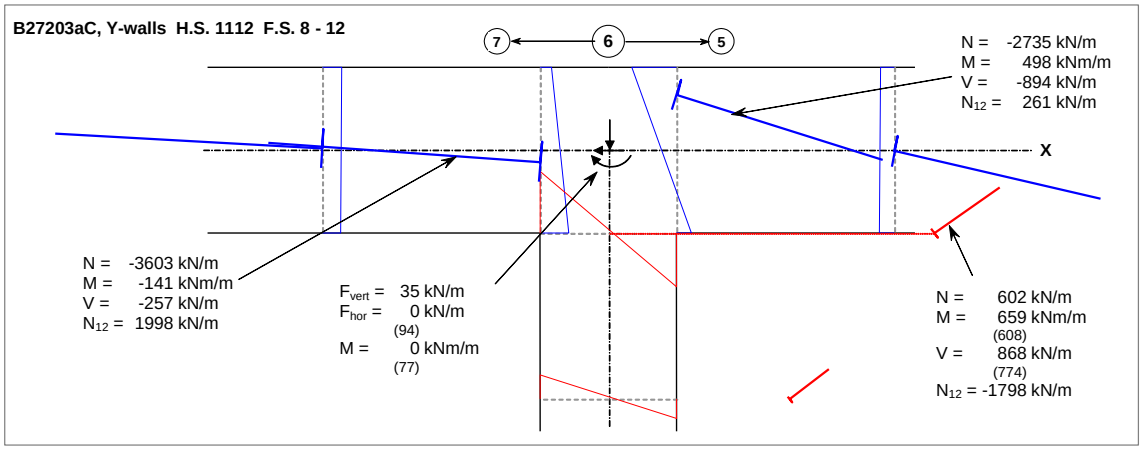


Fig. 14-24: R-plot for example 4 – T-connection with dominant opening moment

The precise location of the external T-head is particularly important because it determines the statical height in the continuous wall. The reduction in the effective cross section height due to the opening moment is not covered by B-region design. For this reason it is necessary to verify reinforcement intensities determined by sectional design for this loading situation. Also the shear reinforcement in the continuous wall contributes in confining the cross section and has to be verified for the minor decrease in effective height for shear transfer.

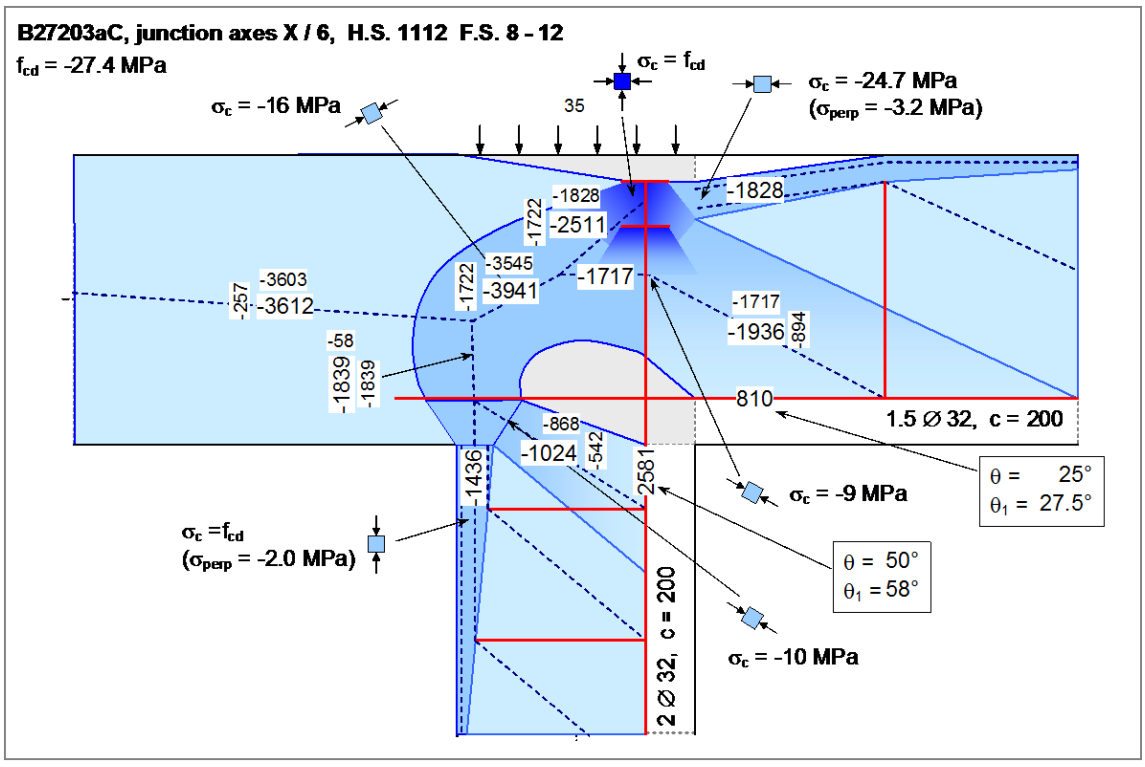
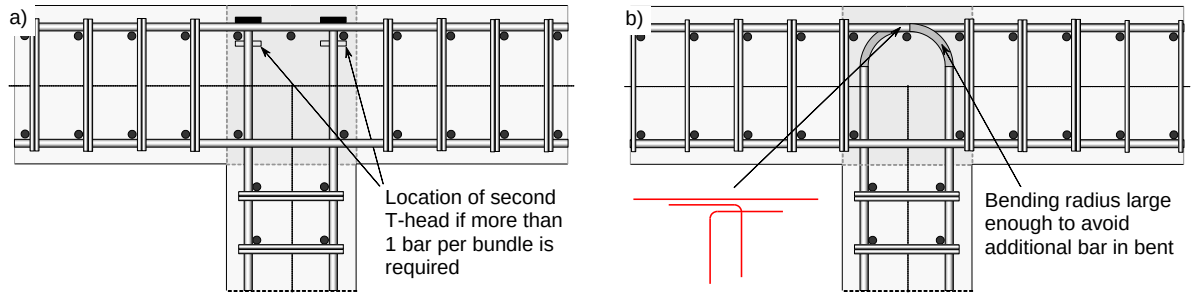


Fig. 14-25: Stress field model for example 3 – T-connection with dominant opening moment (decimal point instead of comma; see Editorial Comments on p. vi)

This document is the intellectual property of the fib – International Federation for Structural Concrete. All rights reserved.
This PDF of fib Bulletin 61 is intended for use and/or distribution solely within fib National Member Groups.

5 Application to design

Detailed analysis models cannot be handed on directly to draftsmen. They are used to outline reinforcement in collaboration with specialists for construction. Detailing decides whether the structure behaves as assumed in the model. Sometimes it is necessary to follow up particular solutions in order to make sure they are understood and effectively put in place on the construction site.



a) layout with T-heads *b) layout with L-bars*

Fig. 14-26: Typical reinforcement layouts adopted for T-connections

First, stress fields or struts and ties, respectively, have to be associated with the structure. A tie can represent several bars, and it takes engineering judgement to determine how far bars can be spread in agreement with the model. The extent of struts is partly defined in stress field models, partly it has to be estimated. The corresponding stress level gives an indication of an average utilisation in the concerned region and serves as a guideline in comparing various solutions. The absolute value must always be seen in context of the form of the strut and of the lateral confinement. Solutions adopted for connections between slabs and walls may not be appropriate for connections between beams and columns, due to their missing compression out of plane.

Not all the required reinforcement is necessarily represented by a tie in the model. It is more efficient to use models for the main intensities and use guidelines and engineering judgement for detailing. In many cases, standards include guidelines for good detailing, like placing bars in bends of an angle-shaped bar for a better distribution of concrete stresses. In other cases, additional stirrups or other means of confinement generally increase robustness.

Non-structural criteria sometimes force to use sub-standard solutions, including splicing or anchoring in unfavourable locations. Especially in these cases it is necessary to insist on confinement, even though the utilisation of this reinforcement might be difficult to quantify and it might complicate drawing production and construction. The solutions shown in Fig. 14-26 are not optimal from a structural viewpoint, like the anchorage of the second T-head or the missing bar in the bend but they present an acceptable compromise between robustness and constructability.

The selected reinforcement is outlined and described together with specification for its anchorage or splicing. A proper documentation is very important because it might include aspects considered in modelling that are easily forgotten in the subsequent process. Often questions arise during construction when it is very important to respond quickly without having the time to reconsider all aspects integrated in a model.

This document is the intellectual property of the fib – International Federation for Structural Concrete. All rights reserved.
This PDF of fib Bulletin 61 is intended for use and/or distribution solely within fib National Member Groups.

In the case of the presented T-connections, drawing production is governed by B-region design. D-region design might require minor but important specifications like the precise location of T-heads or local increases of shear reinforcement, which are cumbersome to specify in drawings. In order to ensure that these details are understood and correctly implemented, follow-up of drawing production and construction is important.

References

FIP Recommendations (1999): Practical Design of Structural Concrete.
FIP-Commission 3 "Practical Design", Sept. 1996. Publ.: SETO, London, Sept. 1999.
(Distributed by: *fib*, Lausanne. Web http://www.fib-international.org)

fib Bulletin 16 (2002): Design Examples for the FIP Recommendations "Practical design of structural concrete". *fib*, Lausanne. January 2002

NS 3473:2003: Design of concrete structures – Design and detailing rules.
Norges Standardiseringsforbund, 6th edition Sep. 2003.

This document is the intellectual property of the fib – International Federation for Structural Concrete. All rights reserved.
This PDF of fib Bulletin 61 is intended for use and/or distribution solely within fib National Member Groups.

This document is the intellectual property of the fib – International Federation for Structural Concrete. All rights reserved.
This PDF of fib Bulletin 61 is intended for use and/or distribution solely within fib National Member Groups.

Paper 15:
Strut-and-tie models utilizing concrete tension fields

Karl – Heinz Reineck

1 Introduction

In codes the utilization of the concrete tensile strength has often been denied and explicitly been ruled out. Yet, there are many concrete members where concrete tensile stresses are not resisted by reinforcement and so the concrete tensile strength is utilized to some extent, and many examples for that are given by Reinke (1986).

Firstly to be mentioned is the fundamental basis for structural concrete of bond and anchorage of reinforcement in concrete members, which cannot be explained without utilizing concrete in tension. This is clearly demonstrated by the strut-and-tie model shown in Fig. 15-1, which was proposed by Tepfers (1973), Schober (1984) and others. However, this dependency on the concrete tensile capacity is covered in the design by using shear stresses for the bond strength.

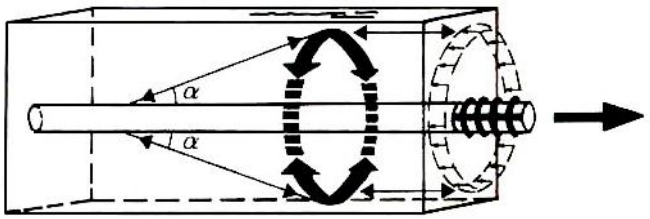


Fig. 15-1: Model for bond between reinforcing bars and concrete [Tepfers (1973)]

Secondly, there are plain concrete members, like footings, which do not contain any reinforcement and obviously rely on tensile stresses in the concrete. As shown in Fig. 15-2 the linear elastic analysis yields the stresses and trajectories from which the cracking load may be determined. However, in design no explicit limits or design values are given for the concrete tensile strength but detailing rules for the geometry of such footings, as shown in Fig. 15-3.

Thirdly, the ultimate capacity of members without shear reinforcement has been defined by nominal shear stresses or shear forces, for which empirically derived design values are given (Fig. 15-3). In Fig. 15-4 the basis for such formulae for the shear capacity is briefly summarized and an example given with the formula of JSCE (1986) proposed by Okamura and Niwa (1987). The main parameters are also listed in Fig. 15-4. However, such empirically derived design equations do not give any insight into the structural behaviour and the flow of the forces within the member, in contrast to the truss model for members with shear reinforcement, as indicated in Fig.2. Therefore, the state of stress in the web and the role of the concrete tensile strength is not clear. In the following the shear transfer in members without shear reinforcement is explained and a simple truss model with inclined concrete ties in the web is derived.

This document is the intellectual property of the fib – International Federation for Structural Concrete. All rights reserved.
This PDF of fib Bulletin 61 is intended for use and/or distribution solely within fib National Member Groups.

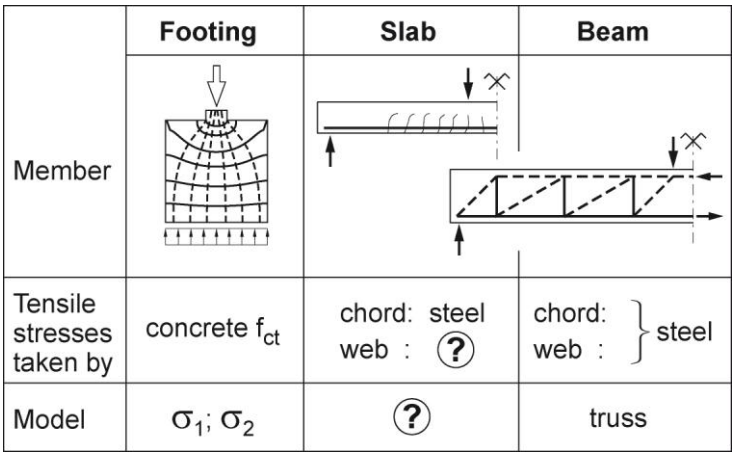


Fig. 15-2: Comparison of models for structural concrete members

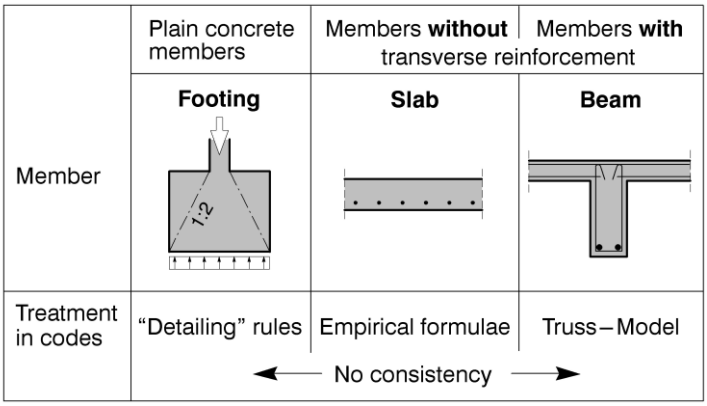


Fig. 15-3: Different treatment in codes of structural concrete members

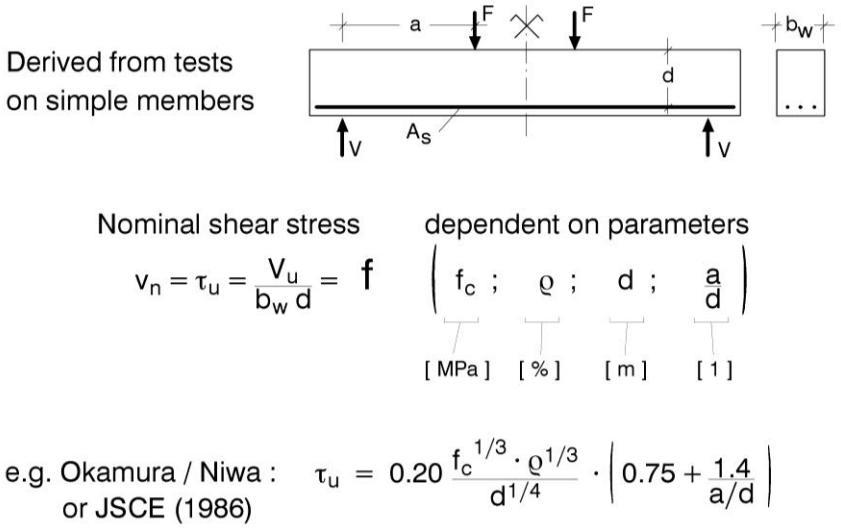


Fig. 15-4: Empirically derived formulae for members without shear reinforcement (decimal point instead of comma; see Editorial Comments on p. vi)

This document is the intellectual property of the fib – International Federation for Structural Concrete. All rights reserved.
This PDF of fib Bulletin 61 is intended for use and/or distribution solely within fib National Member Groups.

2 Models for members without shear reinforcement

For structural concrete members without shear reinforcement different theories have been developed in the last decades, and surveys are given in the reports CEB Bull. 237 (1997) and chapter 4 of ASCE-ACI 445 (1998).

Frequently, the shear transfer in a member without shear reinforcement is explained by an arch for a member with distributed loads or by an inclined strut between a point load and the support of a member. These models comply with the static theorem of the theory of plasticity and should yield a lower bound for the capacity. However, the model does not comply with the development of the crack pattern as shown in Fig. 15-5, because the inclined strut of the model crosses the failure crack which opens widely prior to the failure. The reason for this discrepancy between test and the theory is that the basic assumption of the theory of plasticity is not fulfilled, which is that the materials are ductile. This is not the case for the sudden and brittle failure in the webs of members without shear reinforcement.

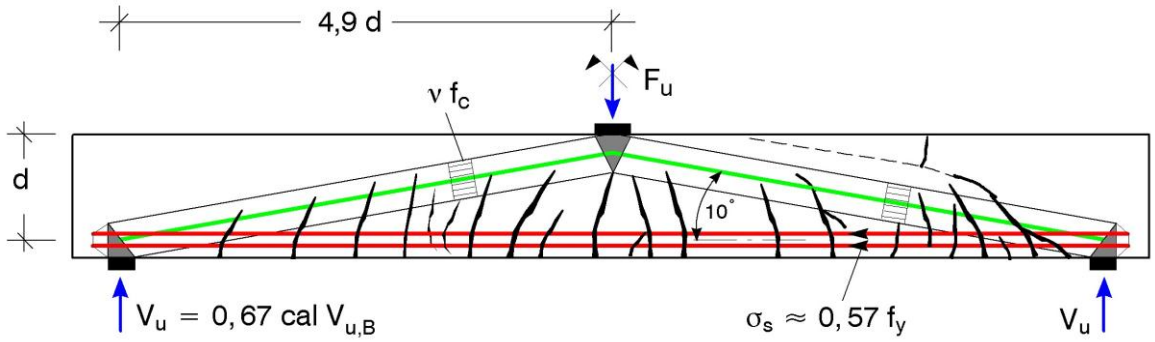


Fig. 15-5: Discrepancy between the crack pattern near failure and strut-and-tie model with an inclined strut for a member without shear reinforcement subjected to a point load

Any theory must therefore start with the crack pattern before the failure crack appears and suddenly leads to failure, and this is done with the so-called tooth-model shown in Fig. 15-6. The different shear transfer actions are shown in Fig. 15-6, and these are the forces due to friction or aggregate interlock along the inclined cracks, the dowel action of the longitudinal reinforcement and the transfer of shear stresses in the compression zone. In addition there may be the transfer of residual concrete tensile stresses across cracks. All these shear transfer actions are related to concrete tensile stresses. Further explanations are given in the above mentioned survey reports.

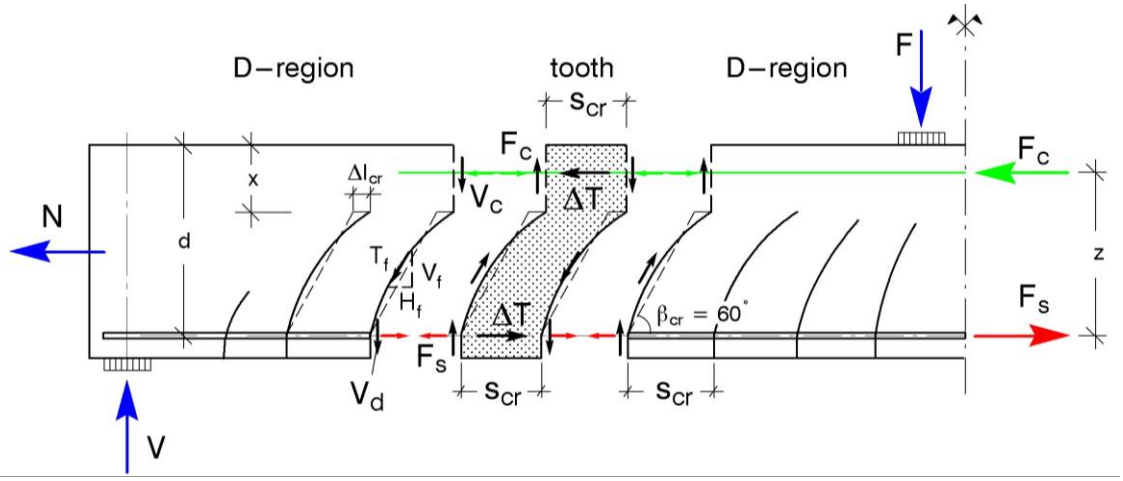


Fig. 15-6: Crack pattern prior to failure and tooth model with shear transfer actions

This document is the intellectual property of the fib – International Federation for Structural Concrete. All rights reserved.
This PDF of fib Bulletin 61 is intended for use and/or distribution solely within fib National Member Groups.

In the past one or the other shear transfer action has been used either alone or in combination with one other action for modelling the failure and predicting the ultimate shear capacity, and mostly no considerations of compatibility were performed. However, Reineck (1990, 1991) presented a theory considering all transfer actions and determining their contribution by analysing the deformations and introducing a compatibility condition. In the following a brief survey is given with special emphasis on the state of stress in the web.

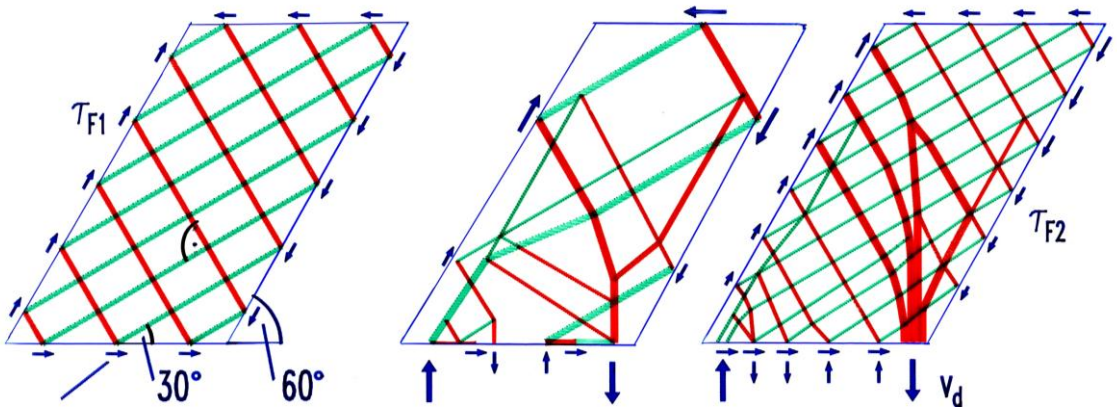
3 Tooth model and related truss model

The tooth model shown in Fig. 15-6 consists of the concrete between the cracks, which is stressed by the different shear transfer actions. Since the tooth is uncracked a linear elastic analysis may be carried out. The crack spacing at midheight of the cracks is decisive for the geometry of the tooth, and a value of $s_{cr} = 0{,}7 \cdot h_{cr}$ was assumed, with h_{cr} being the crack height. The crack spacing near the longitudinal reinforcement is smaller and it depends on the reinforcement ratio, but it is only relevant in a small area around the reinforcement. The crack angle is about 60° and for simplicity a straight crack is assumed.

Fig. 15-7 shows the stresses in the tooth induced by the forces due to friction (Fig. 15-7a) and the dowel action (Fig. 15-7b). In each case the combination of the forces is such that the tooth is in equilibrium. The constant friction forces at the crack in Fig. 15-7a are the simplest distribution and induce an inclined biaxial tension-compression field, with the angle of $30° = \beta_{cr}/2$ for the principal compression field. The force due to the dowel action shown in Fig. 15-7b has to be transferred by confined tensile stresses into the tooth. However the dowel action also induces friction stresses due to the relative displacements of the teeth, and these increase from bottom to the top and this again results in a biaxial tension-compression field in the upper part of the tooth.

In both cases the biaxial tension-compression field in the tooth is governing and this justifies to simplify the state of the stress by the truss model shown in Fig. 15-8, see also Fig. 6.40 in the FIP Recommendations (1999). The dowel action thereby is not explicitly modelled. The inclined concrete ties at an angle of 60° do not cross the crack, but at the crack only tangential forces exist due to the combined action of tension and compression, and theses tangential forces have to be taken by friction of the crack faces. This truss model shows that the longitudinal reinforcement may be staggered, and the force F_s in the tension chord can be determined from the truss analogy (with $\theta = 30°$ and $\alpha = 60°$) as follows:

$$F_s = M/z + 0{,}5 \cdot V \cdot (\cot\theta - \cot\alpha) = M/z + 0{,}58 \cdot V \qquad (1)$$



a) friction stresses *b) simple and refined model for dowel action and related friction*

Fig. 15-7: Stress fields between the inclined shear cracks due to friction along the cracks and due to the dowel action of the longitudinal reinforcement

This document is the intellectual property of the fib – International Federation for Structural Concrete. All rights reserved.
This PDF of fib Bulletin 61 is intended for use and/or distribution solely within fib National Member Groups.

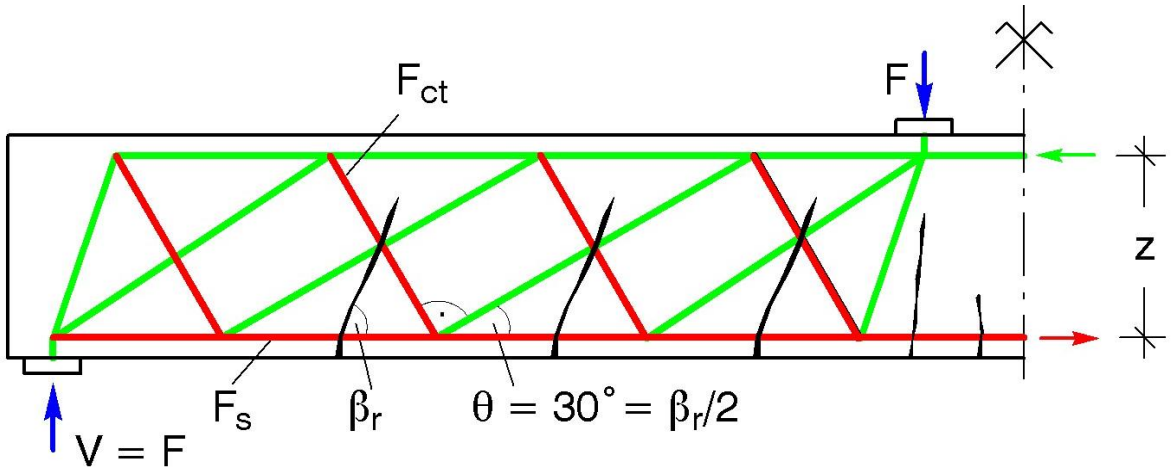


Fig. 15-8: Simple truss model for the state of stress in the web according to Fig. 15-7

The model proposed by Reineck (1990, 1991) does apart from a small region near the crack tip not consider the transfer of residual tensile stresses across the crack, which occur in the fracture process zone up to very small crack widths of about 0,16 mm, as shown in Fig. 15-9. This effect can only play a role for very shallow members, where at failure only small crack widths appear. This is demonstrated in Fig. 15-10, where the residual tensile stresses are plotted along the crack for members with depths of d = 0,125 m up to 0,72 m: the higher the depth the larger the crack widths at midheight of the crack at failure. Consequently, the shorter is the extension of the fracture process zone, and since a portion of theses tensile stresses is already utilized in the zone very near to the crack tip in the theory by Reineck (1990, 1991), the remaining vertical component of the resultant tensile force T_{ct} is therefore very small for the higher members.

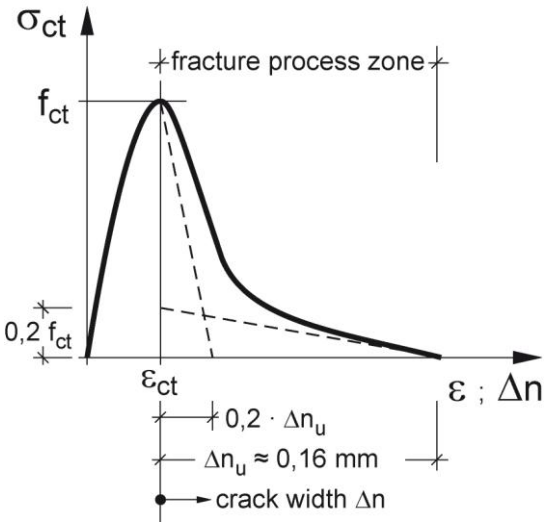


Fig. 15-9: Concrete tensile stresses versus strain respectively crack width [Reinhardt (1986)]

This document is the intellectual property of the fib – International Federation for Structural Concrete. All rights reserved.
This PDF of fib Bulletin 61 is intended for use and/or distribution solely within fib National Member Groups.

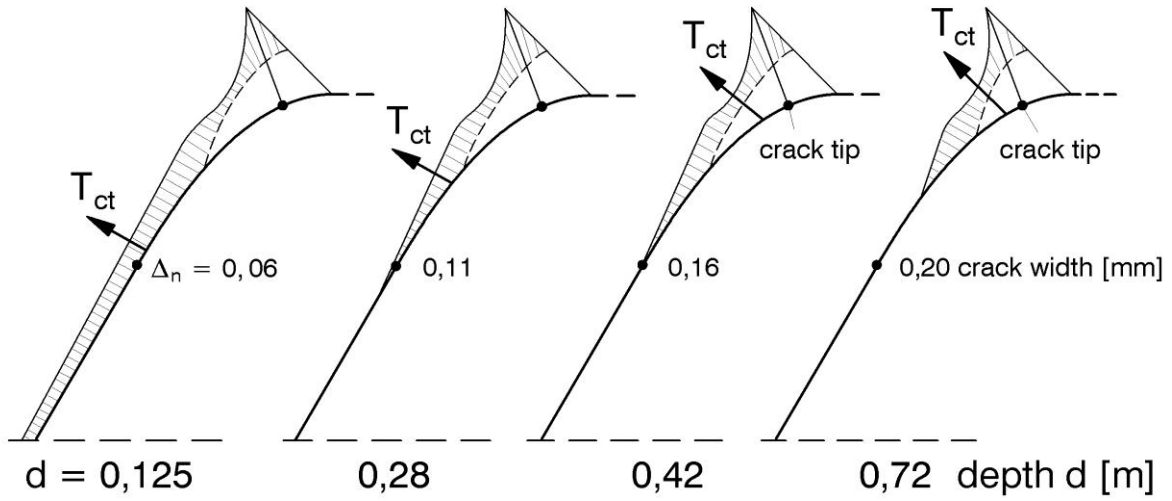


Fig. 15-10: Distribution of residual tensile stresses in the fracture process zone acc. to Fig. 15-9 for members with different depths from d = 0,125 m up to d = 0,72 m with crack widths at failure as calculated by Reineck (1990, 1991)

4 Ultimate shear for members without shear reinforcement

The truss model of Fig. 15-8 very well demonstrates the load transfer in the B-region with shear force by means of concrete ties perpendicular to the inclined struts, and thus it is clear that the concrete tensile strength is utilized. However, the ultimate capacity is not attained by the concrete ties reaching the concrete tensile strength but by the limited capacity of the friction along the cracks and the dowel action. The main contribution is that of the crack friction or aggregate interlock and Fig. 15-11 shows the constitutive law as assumed by Reineck (1990, 1991) based on Walraven (1980). The relationship between the friction stress τ_r and the slip Δs depends on the crack width Δn, and the simple equation given in Fig. 15-11 decreases linearly for increasing crack width. Thereby the normal stress σ_n is not utilized for members without shear reinforcement.

This dependency on the crack width now requires to calculate the crack widths as well as the slip in the slab without shear reinforcement, and Fig. 15-12 demonstrates this for a straight crack with a horizontal branch as simple model for a curved crack shape. For a certain rotation φ a constant slip Δs and a linearly increasing crack width Δn occur over the crack height. If now the depth d of the member (Fig. 15-12a) is doubled to $2 \cdot d$ also all other geometric values are doubled and thus also the crack width. The consequence of the increased crack width is that the friction stress is reduced and thus the vertical component of its resultant, i.e. the shear force. This explains the so-called size effect on the shear capacity of members without shear reinforcement.

This tooth model requires refined analyses of the kinematics and assumptions for the constitutive laws, and this was done by Reineck (1990, 1991) for members without shear reinforcement. He derived an explicit relationship for the ultimate shear force, and for RC members without axial forces with a/d = 5 this relationship is given by:

$$V_u = \frac{0{,}4\, f_{ct}\, b_w\, d + V_d}{1 + 0{,}64\, \dfrac{f_{ct}}{f_{1c}}\, \lambda} \qquad (2)$$

This document is the intellectual property of the fib – International Federation for Structural Concrete. All rights reserved.
This PDF of fib Bulletin 61 is intended for use and/or distribution solely within fib National Member Groups.

with : f_{ct} = axial concrete tensile strength
V_d = shear force due to dowel action
f_{1c} = uniaxial concrete compressive strength = $0{,}95 \cdot f_{c,cyl}$
b_w = width of member
d = depth of member

The parameter λ in Eq.(2) is a dimension-free value for the crack width defined as follows:

$$\lambda = \frac{\varepsilon_{sy}}{\omega} \frac{d}{\Delta n_u} = \frac{f_{1c}}{E_s \, \rho} \frac{d}{\Delta n_u} \tag{3a}$$

With: Δn_u = 0,9 mm = critical crack width
ε_{sy} = f_{sy} / E_s = yield strain of longitudinal steel
ρ = $A_s /(b_w \, d)$ = reinforcement ratio
ω = $\rho \, f_{sy} / f_{1c}$ = mechanical reinforcement ratio

Since the uniaxial concrete strength f_{1c} is given and the parameters E_s and Δn_u are constants, the Eq.(3a) may be simplified to:

$$\lambda = \alpha \cdot d / \rho \tag{3b}$$

where: $\alpha = f_{1c} /(E_s \cdot \Delta n_u)$ = factor (3c)

Therefore, the parameter λ for the crack width likewise covers the influence of the depth d as well as of the reinforcement ratio ρ. The larger the crack width the less is the capacity of the friction forces along the crack, which are the main component for the transfer of the shear force. Thereby, the role of the reinforcement ratio cannot be ignored, because the crack width increases with decreasing reinforcement ratio. Likewise, if the depth increases the value λ for the crack width increases and thus the shear capacity decreases. These facts can be seen from Fig. 15-13, where Eq.(2) is plotted versus the parameter λ for two concrete strengths.

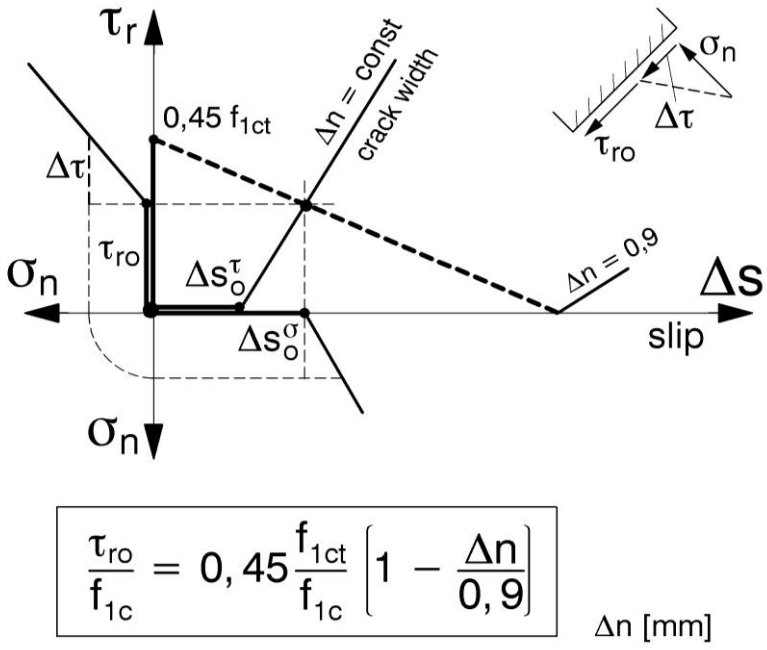
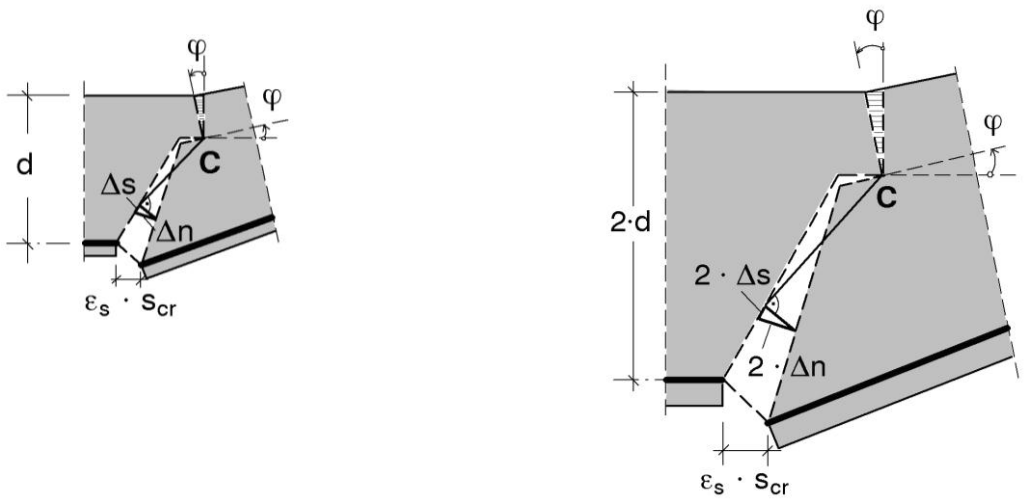


Fig. 15-11: Simple constitutive law for the crack friction or aggregate interlock

This document is the intellectual property of the fib – International Federation for Structural Concrete. All rights reserved.
This PDF of fib Bulletin 61 is intended for use and/or distribution solely within fib National Member Groups.



a) rotation for the depth d *b) rotation for the depth 2·d*

Fig. 15-12: Crack width and slip for a simple crack shape due to a rotation φ

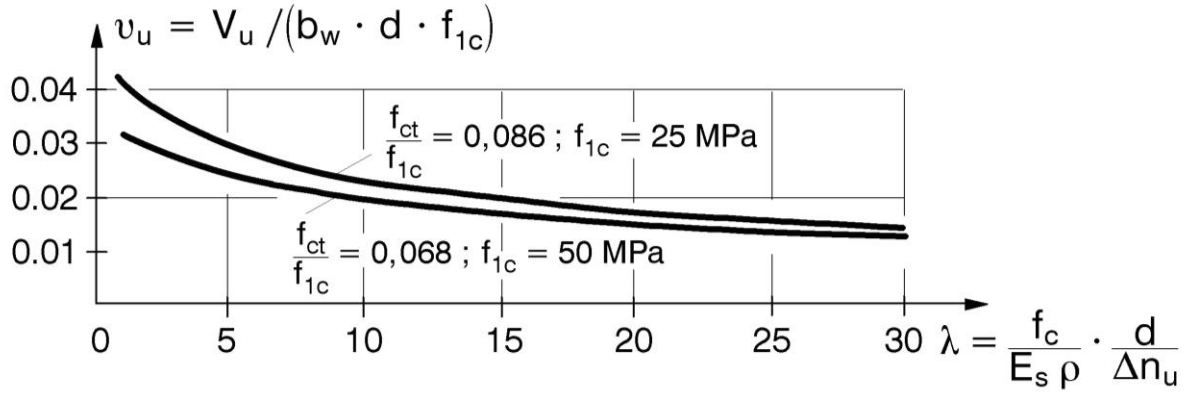


Fig. 15-13: Non-dimensional shear force υ_u plotted versus the parameter λ for the crack width in a dimensioning diagram for members without shear reinforcement according to Reineck (1990, 1991)

5 Transition from B- to D-region

The truss model of Fig. 15-8 also explains the transition from B- to D-regions in members without shear reinforcement and enables the design of the D-regions. For this an example is given in the following.

First a refined strut-and-tie model with stress fields is presented in Fig. 15-14 for the end support of the truss model in Fig. 15-8. The inclined concrete tension field of the B-region needs to be split into two resultants, because the lower part of the tension field cannot extend up to the top chord. The result is that the D-region consists of bi-axial tension-compression fields as well as fan-shaped compression fields in between. The resultant strut in the D-region has two slightly different inclinations, but the force of the tension chord to be anchored at the end support is determined at the end of the B-region, i.e. where the last strut crosses the axis of the reinforcement, and for common dimensions for the loading plate and the distance of the reinforcement from the bottom face it is:

$$F_{sA} = 0{,}86 \cdot V \qquad (4)$$

This document is the intellectual property of the fib – International Federation for Structural Concrete. All rights reserved.
This PDF of fib Bulletin 61 is intended for use and/or distribution solely within fib National Member Groups.

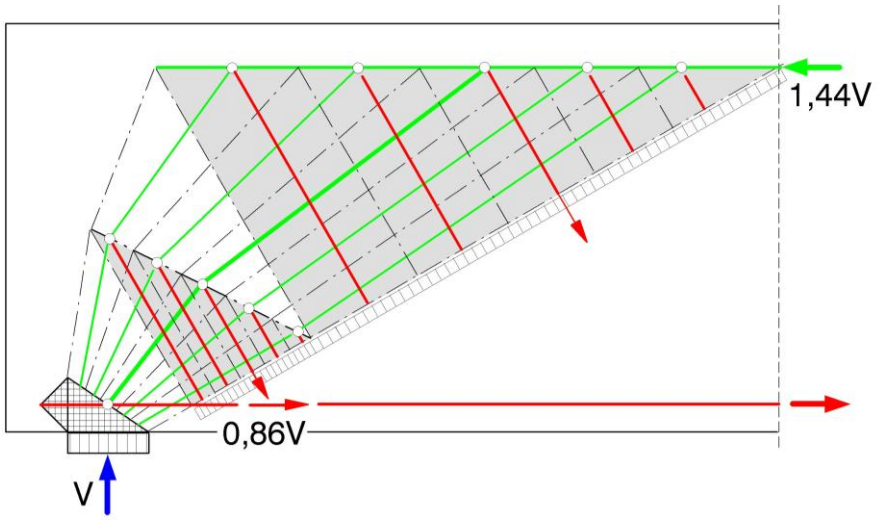


Fig. 15-14: Refined strut-and-tie model and stress fields for the end region of the model in Fig. 15-8

The truss model of Fig. 15-8 for members without transverse reinforcement is the basic model for investigating the flow of the forces and the shear transfer in slabs. For these members the modelling with concrete tension fields is indispensable. This is especially important for the transition of the B-regions to the D-regions of these members, like e.g. for a slab with dapped beam ends shown in Fig. 15-15. Often only stirrups are provided at the end of the beam as hanging-up reinforcement. The strut-and-tie model in Fig. 15-15 shows the transition to the strut-and-tie model in the B-region of Fig. 15-8. At node (N4) an inclined concrete tie T_{ct} is required, which however transfers in this case 2/3 of the shear force, and this will exceed the capacity of concrete in tension. In addition, this tie is the resultant of a stress field in pure tension, and there is no compression field perpendicular to it, so that at an inclined crack the resultant force could be a tangential force to be taken by friction. Therefore, stirrups have to be provided in this region further away from the end of the slab, as shown in Fig. 15-16.

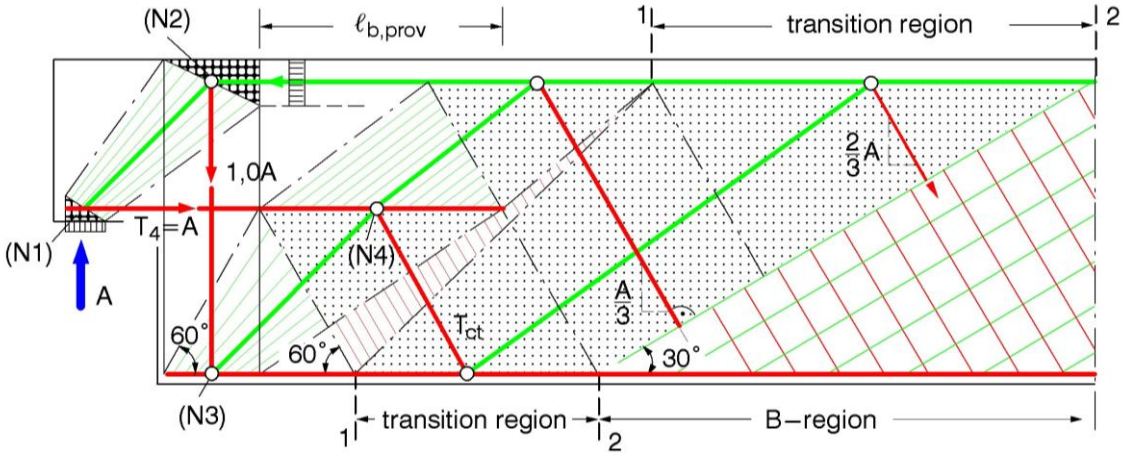


Fig. 15-15: Strut-and-tie model for dapped beam end with stirrups only at the end of the beam

This document is the intellectual property of the fib – International Federation for Structural Concrete. All rights reserved.
This PDF of fib Bulletin 61 is intended for use and/or distribution solely within fib National Member Groups.

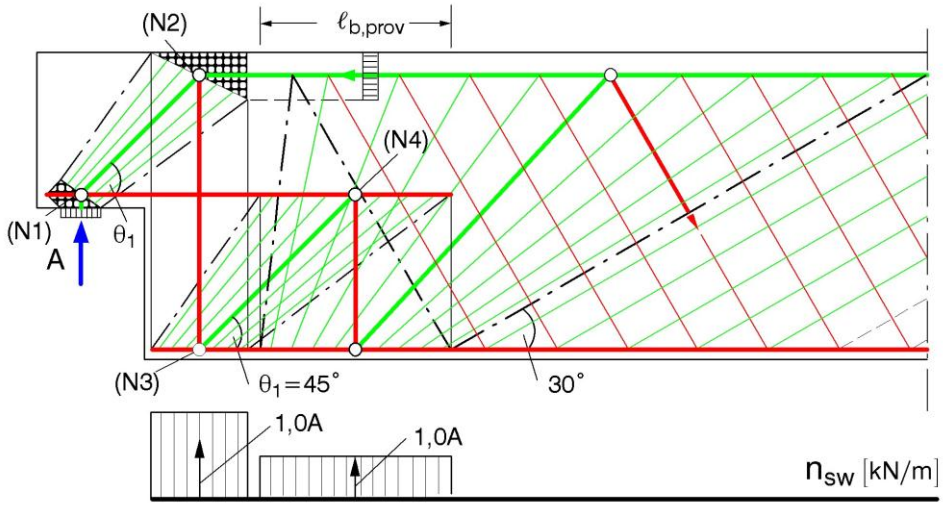


Fig. 15-16: Strut-and-tie model for dapped beam end with required stirrups in the slab further away from the end of the beam

This example for a D-region of a slab demonstrates the need for the strut-and-tie model with inclined concrete ties shown in Fig. 15-8, which clearly describes the transfer of the loads for a slab without shear reinforcement. Thus a gap is closed in the design concept with strut-and-tie models, so that they can be applied for all types of structures with and without shear reinforcement. The designer can understand the load transfer, as requested by Schlaich et al. (1987, 1991), and he is able to detect problems and to solve them, especially in D-regions like that of a dapped-end of a slab in Fig. 15-15.

6 Closing remarks

The utilization of the concrete tensile strength in the design and structural behaviour of structural concrete members is nowadays generally acknowledged. However, the design procedures rarely give explicit relationships to design values for the concrete tensile strength, but rather use shear stresses like the bond strength. Therefore, the modelling with concrete tension fields at the ultimate limit state is mostly critically looked at, and this especially refers to members without shear reinforcement, like slabs and shells. For most it is rather acceptable to check the capacity by means of an empirically derived formula, which does not provide any insight into the structural behaviour and the load transfer. Likewise do many researchers derive such empirical formulae or propose theories by only looking at a critical section without describing how the load or shear force is transferred from that section to the support.

However, the concept of strut-and-tie models can only be applied to members without shear reinforcement if concrete ties and concrete tension fields are defined, and this is achieved by the truss model with inclined concrete ties. Only such a model allows to look at the load transfer and to follow these up into the D-regions and supports, and this was demonstrated by the dapped end of a slab. The model made clear that a critical region exists where the load transfer only relies on pure tension and therefore stirrups additional stirrups have to be provided.

However, modelling with concrete in tension does not mean that also the capacity may be checked by assuming that the concrete tensile strength is attained in the ties. This could lead to dangerous designs. The concrete tension fields in members without shear reinforcement only exist in combination with compression fields perpendicular to it, so that in any inclined crack the state of stress results in tangential forces at the crack faces which can be taken by

This document is the intellectual property of the fib – International Federation for Structural Concrete. All rights reserved.
This PDF of fib Bulletin 61 is intended for use and/or distribution solely within fib National Member Groups.

friction. Therefore, any assessment of the capacity requires to determine the crack width which defines the capacity of the friction. In practice this will be difficult to do in a rigorous way but only as a rough check, in order to decide whether it is not better to provide reinforcement, as in case of the above given example.

References

ASCE-ACI 445 (1998): Recent approaches to shear design of structural concrete. State-of-the-Art-Report by ASCE-ACI Committee 445 on Shear and Torsion. ASCE-Journ. of Struct. Eng. 124 (1998), No.12, 1375-1417

CEB Bull. 237 (1997): Concrete Tension and Size Effects. Contributions from CEB Task Group 2.7. Comité Euro-International du Beton, Lausanne 1997

FIP Recommendations (1999): Practical Design of Structural Concrete.
FIP-Commission 3 "Practical Design", Sept. 1996. Publ.: SETO, London, Sept. 1999
(Distributed by: *fib*, Lausanne. Web http://www.fib-international.org)

JSCE (1986): Standard Specification for design and construction of concrete structures - 1986, Part 1 (Design). Japan Society of Civil Engineers. Tokyo 1986

Okamura, H.; Niwa, J. (1987): The essence of the revision of JSCE "Standard specification for design of concrete structures". Civil Engineering Dep., Univ. of Tokyo, Japan, May 1987

Reineck, K.-H. (1990): Ein mechanisches Modell für den Querkraftbereich von Stahlbetonbauteilen (Mechanical model for the behaviour of reinforced concrete members in shear). Dissertation, Institut für Tragwerksentwurf und Konstruktion, Universität Stuttgart, Febr. 1990, 1-273

Reineck, K.-H. (1991): Ultimate shear force of structural concrete members without transverse reinforcement derived from a mechanical model.
ACI-Struct. Journ. V.88 (1991), No.5, Sept./Oct., 592-602

Reinhardt, H.W. (1986): The role of fracture mechanics in rational rules for concrete design. IABSE Survey S-34/86 in IABSE Per. 1/1986

Reinke, H.G. (1986): Zum Ansatz der Betonzugfestigkeit bei der Stahlbetonbemessung mit Stabwerkmodellen. Diss., Univ. Stuttgart, 1986

Schlaich, J. (1991): The need for consistent and translucent models. IABSE Report V.62 (1991), 169-184

Schlaich, J.; Schäfer, K; Jennewein, M. (1987): Toward a consistent design for structural concrete. PCI-Journ. V.32 (1987), No.3, 75-150

Schober, H. (1984): Ein Modell zur Berechnung des Verbundes und der Risse im Stahl- und Spannbeton. Diss., Institut für Massivbau, Univ. Stuttgart, 1984

Tepfers, R. (1973): A theory of bond applied to overlapped tensile reinforcement splices of deformed bars. Publ. 73:2. Div. of Concrete Structures, Chalmers University of Technology, Göteborg. 1973 (Second printing 1976).

Walraven, J.C. (1980): Aggregate interlock: a theoretical and experimental analysis. Dr.-thesis, Delft Univ. Press, 1980, 1-197

This document is the intellectual property of the fib – International Federation for Structural Concrete. All rights reserved.
This PDF of fib Bulletin 61 is intended for use and/or distribution solely within fib National Member Groups.

This document is the intellectual property of the fib – International Federation for Structural Concrete. All rights reserved.
This PDF of fib Bulletin 61 is intended for use and/or distribution solely within fib National Member Groups.

Paper 16: Gaining experience with strut-and-tie models for the design of concrete structures

Karl-Heinz Reineck, Miguel S. Lourenço, João F. Almeida, Stein Atle Haugerud

1 Summary and conclusions of examples

The primary aim of this Bulletin was to present examples where the application of the design with strut-and-tie models is demonstrated as presented in the chapter 6.5 of the FIP Recommendations 1999 "Practical Design of Structural Concrete". This Bulletin is a follow-up of the fib Bulletin 16 (2002). The examples in this Bulletin deal with structures taken from the practice of the Working Group members, and they cover critical details in buildings, several bridges, and even of a special structure like a concrete offshore terminal.

In concluding, the examples fully demonstrated that the modern concepts of the FIP Recommendations (1999) "Practical Design of Structural Concrete" enabled practising engineers to solve even quite complicated problems by using strut-and-tie models.

However, there are some topics still to be investigated and some of them were discussed in the Working Group and are briefly addressed in the following. One topic is dealt with separately in Paper 15, since it turned up in several examples and posed problems in the application. It deals with the modelling of structural concrete members without shear reinforcement, and it presents a truss model with concrete ties respectively concrete tension fields.

2 Gaining experience in designing structural concrete with strut-and-tie models

2.1 Brief review on the development of strut-and-tie models

Strut-and-tie models have been used for a long time to design special regions like corbels, deep beams or dapped-end beams of structural concrete members. Schlaich (1984) started a new development and proposed to consistently cover the design of structural concrete members using strut-and-tie models. He discerned B-regions (B for bending or Bernoulli) and discontinuity regions (D-regions), whereby the latter may be due to concentrated loads (e.g. supports or anchorage zones of prestressing tendons), due to geometrical discontinuities (e.g. frame corners or openings in members) or due to the combination of both (e.g. corbel with point load at a column). For all these D-regions strut-and-tie model is often the most practical design tool.

Since then the method has been further developed, and the work by Schlaich and Schäfer (1984, 2001) and Schlaich, Schäfer and Jennewein (1987) was instrumental in this respect. Reineck (1996) supplemented this work with special emphasis on the shear design and the design of D-regions of beams, and later in 2005 with the design of D-regions of prefabricated members with many numerical examples like corbels, dapped-end beams and beam webs with openings. A fundamental work is also that by Muttoni, Schwartz and Thürlimann (1996) who put an emphasis on stress field design.

This document is the intellectual property of the fib – International Federation for Structural Concrete. All rights reserved.
This PDF of fib Bulletin 61 is intended for use and/or distribution solely within fib National Member Groups.

For the CEB-FIP MC 90 (1993) the design with strut-and-tie models was summarized in the extensive review by Schäfer (1999). For the ACI community Marti (1985) gave a survey, and Cook and Mitchell (1988) presented tests on some D-regions to verify the method. ASCE-ACI Committee 445 (1998) presented this topic within the state-of-the-art report on shear design, and later in 1997 this Committee published an extensive bibliography. In ACI SP-208 (2002) MacGregor (2002) presented and justified App. A of ACI 318-08 (2002) for the design with strut-and-tie models, followed by Mitchell et al. (2002) giving comparisons with tests, and then in ACI SP 208 a set of examples followed. Recently ACI SP 273 was published with further examples for the design with strut-and-tie models based on App.A of ACI 318-2008.

Especially worth mentioning are the FIP Recommendations (1999) "Practical Design of Structural Concrete". The structure of this code-like document is fully based on the design using strut-and-tie models and thus this design concept is consistently integrated in the code. The logic is that the elements for the design, which are the struts, ties and nodes (including anchorages and splices), are defined prior to the applications for the design of B-regions (with flexural and shear design) and D-regions. The section on D-regions contains an extensive collection of basic examples from buildings and bridges. The application of this code was demonstrated in *fib* Bulletin 16 (2002) by several examples from practice.

Because the provisions for design using the strut-and-tie model (STM) were incorporated in codes like CSA (1984), NS 3473 (1989), CEB-FIP MC 90 (1993), AASHTO (1994), FIP Recommendations (1999), DIN 1045-1 (2001, 2008), ACI 318-08 (2002) or EC 2 (2005), practicing engineering have increasingly been using strut-and-tie models for the design of concrete structures. As a help in their work the following documents can be regarded as basic ones, where the method is described and many applications are presented: Schlaich and Schäfer (1984, 2001), Schlaich, Schäfer and Jennewein (1987) and Schäfer (1999) and Muttoni, Schwartz and Thürlimann (1996).

The method provides a simple, yet reliable tool to evaluate consistently structural concrete members. It revives the idea of understanding the flow of forces within the members, and it provides an unprecedented awareness of structural behaviour. Some of the recognized advantages of this technique are:

- Visualization of the load path throughout any region due the inherent graphical interaction, providing an insight into the behaviour of the structure under the applied loads, prior to any detailed analysis.
- Complying with the lower bound of the theory of plasticity; this is particularly useful for design purposes since the ultimate load obtained is a lower bound of the actual failure load.
- Improved consistency in design concepts by allowing the treatment of discontinuity regions (D-regions) and B-regions with comparable accuracy.
- Account for the concrete behaviour after cracking.
- Adequate treatment of the reinforcement layout emphasizing the essential role of detailing in the design process. The method allows the definition of the necessary amount and correct distribution of reinforcement, as well as defining the geometry of nodes and the anchorage lengths for the local design of the support widths.

This document is the intellectual property of the fib – International Federation for Structural Concrete. All rights reserved.
This PDF of fib Bulletin 61 is intended for use and/or distribution solely within fib National Member Groups.

2.2 Validity of different models

The design method using strut-and-tie models (STM) is based on some general principles and rules for the modelling, but still different assumptions can be made with respect to e.g. the location of nodes and of struts and ties. Therefore, different engineers may propose different strut-and-tie models for the same D-region or the same design problem. In some design cases the differences in the results may be significant and may lead to quite different amounts of required reinforcement. The reason lies in the basis of the method using strut-and-tie models (STM), and this is briefly addressed here with reference to Reineck (2002).

When using STM the following two conditions must be fulfilled: equilibrium and strength limits for the elements of strut-and-tie models. These two conditions comply with the lower bound theorem or static solution of the theory of plasticity, i.e. equilibrium and yield conditions are fulfilled. This means that compatibility is not fulfilled, and this is the reason why different solutions are possible leading to different ultimate loads. However, any consideration of compatibility requires a non-linear analysis and assumptions for the constitutive laws for the elements of STM. In order to overcome the difficulty, Schlaich et al. (1987) and Schäfer (1999) recommended, for simplicity, to orientate the model following the stress fields of a linear elastic analysis. This has the following advantages:

- the changes in the inner flow of forces are small from the elastic state of stresses to the cracked state of the member until the ultimate load is reached for the assumed model, and thus not much ductility is required.
- the model can also be used for checking the serviceability limit state (SLS).

This recommendation can easily be followed due to the fact that linear elastic analyses are readily available and are normally performed anyway, especially for cases of unknown D-regions. In such cases no experimental evidence is available, which could justify a strut-and-tie model deviating much from the elastic stress fields, and so it is a conservative measure to follow this recommendation.

With respect to the ductility, which is assumed to be given in the theory of plasticity, it should be noted that normally a design with strut-and-tie models leads to a failure governed by yielding of the reinforcement and not by crushing of the struts. This is also due to the fact that the widths of the struts are often determined by given dimensions of loading plates or statical conditions, so that mostly the stress limits for struts are not attained. This is contrary to the theory of plasticity where always minimum widths of struts are assumed so that stress limits are attained in all struts.

The fact that in a design with strut-and-tie models different models can be found for a given problem and that not a single unique solution can be expected has puzzled many engineers when STM were presented to them as a design tool and has lead sometimes to a certain mistrust against the use of STM. Obviously in structural engineering the engineers are trained to always find the exact solution, but this is only true under given conditions and restrictions, e.g. when analyzing a structure for given geometry and loading according to the linear elastic theory. However, contrary to the analysis in a conceptual design of a structure an engineer accepts and investigates a variety of solutions for the same given task, and he has many options to satisfy the given conditions and requirements for safety, economy and quality. This is demonstrated by Fig. 3 in Part 5 of ACI SP 208 showing the variety of bridges which a designer may consider for his design in the first design phases or in the conceptual design. In view of this it should be accepted that also in structural concrete design different solutions are possible, and thus different strut-and-tie models may be favoured by different engineers. Such different models may all show the required capacity of the member in a test, as was shown for dapped beam ends (see section 2.3).

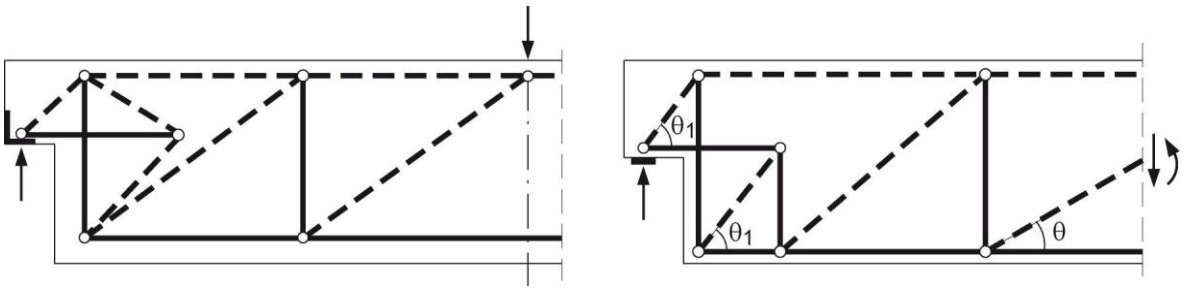
This document is the intellectual property of the fib – International Federation for Structural Concrete. All rights reserved.
This PDF of fib Bulletin 61 is intended for use and/or distribution solely within fib National Member Groups.

2.3 Dapped beam end

Dapped beam end is a frequently occurring D-region especially for precast beams, and it is also treated in Example 12 of this Bulletin. This D-region is a good example to illustrate how different models may be equally valid. Fig. 16-1 shows two different models in question. The model 1 in Fig. 16-1a requires a concentration of stirrups at the face of the beam end, whereas the model 2 in Fig. 16-1b leads to a second tie T_2 for anchoring the tie T_4 and thus allows to distribute the stirrups over some length. Every model has some advantages but also some disadvantages were seen by different researchers, as discussed in Part 5 of ACI SP 208 as well as by Reineck (2005).

The validity for the model 1 in Fig. 16-1a was demonstrated by tests of Cook and Mitchell (1988), as explained in Part 3 of SP 208. The model 2 in Fig. 16-1b is based on tests by Steinle and Rostásy (1974) and Steinle und Hahn (1988, 1995), who found that the high amount of reinforcement according to model 1 was not fully utilized and that the total force did not exceed the support force. This behaviour is explained by model 2 in Fig. 16-1b.

Therefore it must be concluded that both models may exhibit the full desired capacity and must be regarded as equally valid. The prerequisite for this is that the dapped beam end is properly designed and detailed for each case, i.e. that especially the nodes and anchorages do not lead to a premature failure.



a) model 1 by Cook and Mitchell (1988), see Fig. 9c in Part 3 of ACI SP 208

b) model 2 of FIP Recommendations (1999)

Fig. 16-1: Different models for dapped beam ends

2.4 Point load near a support

The strut-and-tie model for the D-region with a point load near a support is a frequently occurring case, and in the FIP Recommendations (1999) the model shown in Fig. 16-2 is proposed. This model is internally statically indeterminate, and therefore an empirically derived rule is given in the FIP Recommendations (1999) for which portion F_2 of the applied load is directly transferred to the support. The remaining part F_1 is transferred by the truss action requiring a vertical tie in the middle of the D-region, and it depends on the distance of the load from the support axis according to the following relationship:

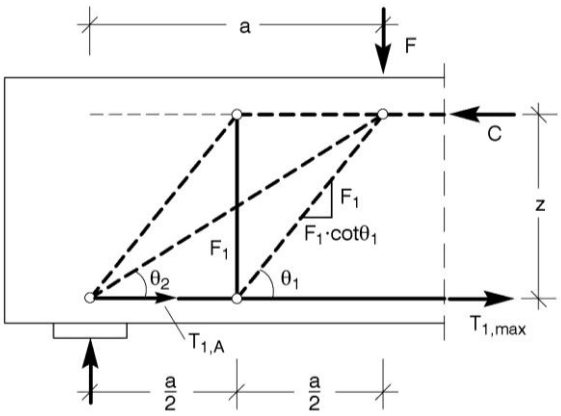
$$F_1 / F = (2\,a/z - 1)/3 \qquad (1)$$

where: a = distance of load from support axis

z = inner lever arm

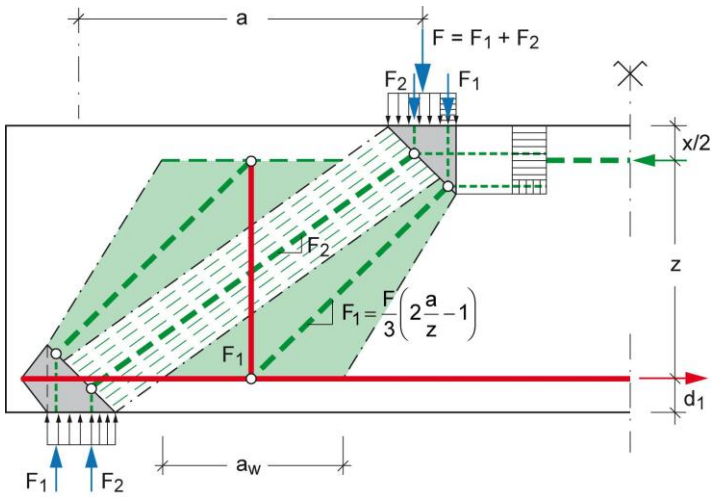
This relationship shows the increasing necessity for transverse reinforcement in the range between $a = 0{,}5 \cdot z$ and $a = 2 \cdot z$, and so a consistent transition is guaranteed from a deep beam with loads near the support to a slender beam. In the latter case the total applied load has to be transferred my means of a truss and no direct load transfer to the support by an inclined strut is possible. Therefore, the model of Fig. 16-2 is a proper and practical solution.

This document is the intellectual property of the fib – International Federation for Structural Concrete. All rights reserved.
This PDF of fib Bulletin 61 is intended for use and/or distribution solely within fib National Member Groups.



$$T_{1,A} = T_{1,max} - F_1 \cdot \cot\theta_1 = F \cdot \frac{a}{z} - F_1 \frac{a}{2z} = \frac{a}{z}\left(F - \frac{F_1}{2}\right)$$

a) simple combined model according to Schlaich and Schäfer (2001)



b) refined model with stress fields according to FIP Recommendations (1999)

Fig. 16-2: Model for point loads near the support with two load paths

In the FIP Recommendations (1999) only the refined model of Fig. 16-2b is presented, which however is kinematic and actually requires iterations to find the exact solution, as described by Reineck (2005). The simple model of Fig. 16-2a is very practical, since the force $T_{1,A}$ to be anchored at the support can be easily be determined to:

$$T_{1,A} = (F - F_1/2) \cdot a/z \qquad (2)$$

Altogether the model in Fig. 16-2 provides a clear transition from loads very near to the support up to slender cases with a > d. However, it has been discussed controversially in the last years in ACI Subcommittee 445-A "Strut-and-tie models" while working on the two Special Publications ACI SP208 (2002) and ACI SP 273 (2010). In most design examples of both SP´s the simple model with the direct load transfer of the load to the support by an inclined strut was selected, i.e. $F_1 = 0$. Mostly additional reinforcement was provided in accordance with A.3.3 of Appendix A. In this case the force in the tension chord is constant from support to support, and the anchorage at the support has to be designed for a tie force of 100% of the maximum tension chord force. In fewer examples the model with only the truss action was selected, i.e. $F_2 = 0$ and $F_1 = F$, so that many stirrups have to be provided in this D-region. This model is obviously conservative, especially if the load is very near to the support. The controversial discussion referred to the first case when the direct strut action was used for slender cases, but this needs further clarification and comparisons with tests.

This document is the intellectual property of the fib – International Federation for Structural Concrete. All rights reserved.
This PDF of fib Bulletin 61 is intended for use and/or distribution solely within fib National Member Groups.

2.5 Design with strut-and-tie models and stress fields

Sometimes a conflict is seen between the design with strut-and-tie models and the design with stress fields, whereby the latter is regarded by some as superior. For practical design proposals this separation or any classification can be regarded as unnecessary and not justified in view of the correct definitions of the elements of strut-and-tie models. These definitions are given in sect. 5.1 of the FIP Recommendations (1999) and are as follows:

- a strut represents the resultant of either a parallel of a fan-shaped compression stress field;
- a tie is the resultant of a layer of reinforcing bars or prestressing reinforcement, like in tension chords, or a resultant of distributed reinforcement like stirrups in webs;
- a node is a confined volume of concrete where struts either intersect or are deviated by ties anchored in the node.

These elements are visualized in Fig. 16-3 with the strut-and-tie model and the stress fields for the end support region of a beam.

These definitions clearly demonstrate that all these elements represent stress fields and not discrete elements. The stress fields for the strut and ties are uniaxially stressed and the nodes are either bi -or triaxially stressed, which may be only in compression or in tension and compression. Therefore, there is basically no difference between strut-and-tie model design and stress field design.

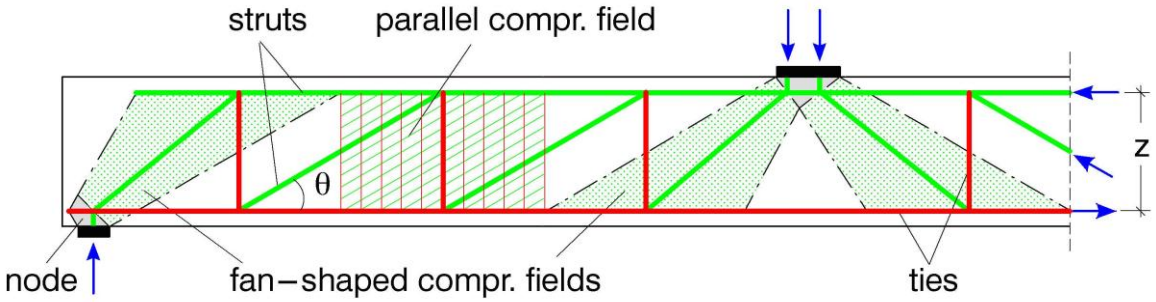


Fig. 16-3: Strut-and-tie model for the end support region of a beam

With these elements also continuous beams can be completely modelled, as demonstrated in Fig. 16-4 for a beam with a cantilever. In this model now no effort is made to establish or draw a complete truss, but the truss in the B-region is only indicated by the resultant ties representing the stirrup forces that cross the borderline of each D-region. This means that for a given strut angle θ it is not possible to construct a complete truss between the fixed D-regions. If in the left end-region of the beam in Fig. 16-4 the truss is continued in the B-region for the given angle θ, then it will not meet the truss constructed to the left from the D-region at the point load. However, this is not necessary, as it is a misconception that a complete truss must exist. For example, if a steeper strut angle is assumed in order to achieve a complete truss, then higher amounts of stirrups are calculated than required for the angle θ corresponding to the shear design. Unfortunately, many examples with this procedure were published. If on the other hand a flatter angle θ is used to achieve a complete truss, then it would lead to less amounts of stirrups than required for θ based on a shear design, which would be unsafe.

This document is the intellectual property of the fib – International Federation for Structural Concrete. All rights reserved.
This PDF of fib Bulletin 61 is intended for use and/or distribution solely within fib National Member Groups.

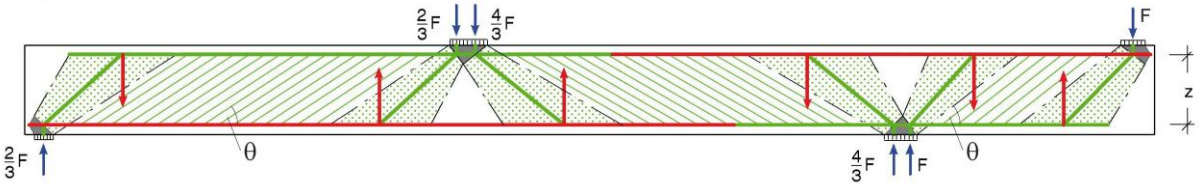


Fig. 16-4: Truss model and stress fields for a beam with a cantilever

This example demonstrates that strut-and-tie models should not be understood as a system made up of discrete elements ties and struts. Therefore also, the end region of the beam shown in Fig. 16-3 is actually a special case where the distance of the load from the support was such selected, that the truss model with the given angle θ fitted exactly between the D-regions. The stress fields in B-regions are defined by the angle θ derived from the shear design as stated in sect. 6.4.3.3 of the FIP Recommendations (1999), and the B-regions can be of any length between the fan-shaped stress fields of the D-regions, and they are always in equilibrium.

This already demonstrates that it is important to also consider the stress fields since they determine the distribution of the reinforcement, like e.g. for the stirrups in B-regions or for the stirrups over the length a_w in Fig. 16-2. Actually, the design could directly be performed with stress fields rather than starting with a discrete strut-and-tie model.

However, the above example of a beam was relatively simple because the D-regions were separated by B-regions, so that the stress conditions at the borders of the D-regions were clearly defined by that of the B-regions. The situation is different if a structure only consists of D-regions, which intersect and where no B-region can be discerned in between. In such cases the design should really start with finding a strut-and-tie model which is in equilibrium with the applied loads, whereby often simple models should be selected in the beginning of the design process before developing more refined ones. It should be reminded that the main design task for structural concrete members is to identify regions in tension and to determine the required amount of reinforcement, and for this only the forces of the ties are needed.

A direct start with a stress field design is difficult and carries the danger of losing the overall view on the flow of forces or state of stress. Therefore, the first step is normally always to find a strut-and-tie model, to determine the major reinforcement and to identify possible problems with nodes, e.g. with anchorages of reinforcing bars. The construction of the stress fields follows in a second or even third step after having finalized a satisfactory strut-and-tie model in order to determine the lengths over which reinforcements have to be distributed and to check critical struts or nodes.

It should be reminded that simplicity was an important aim apart from consistency in the design when developing strut-and-tie models, as explained by Breen (1991) and Schlaich (1991) and in the Summarizing Statement of the IABSE-Colloquium Stuttgart 1991 “Structural Concrete”.

2.6 SLS-checks with strut-and-tie models

The design method strut-and-tie models complies with the lower bound theorem or static solution of the theory of plasticity in the sense stated above in sect. 2.2. Therefore many have concluded that this method cannot be used for the Serviceability Limit State (SLS) in order to check for example crack widths in a D-region. However, this is a misunderstanding, since the design method strut-and-tie models is not based on the theory of plasticity in a strict sense, and this is the reason that in the above statement “complies” with the lower bound theorem was used instead of “based on”. The reason for this distinction is especially that only in very

This document is the intellectual property of the fib – International Federation for Structural Concrete. All rights reserved.
This PDF of fib Bulletin 61 is intended for use and/or distribution solely within fib National Member Groups.

rare cases the strength limits are utilized in struts and compression stress fields, as can be seen in the above examples. This is simply demonstrated by a strut representing a fan-shaped stress fields, since only at the narrowest width at the border of the node the highest stress occurs. This stress is mostly lower than the strength limit, because other conditions define the geometries of the stress fields, such as selected widths of support or loading plates or given widths of supports (like e.g. columns).

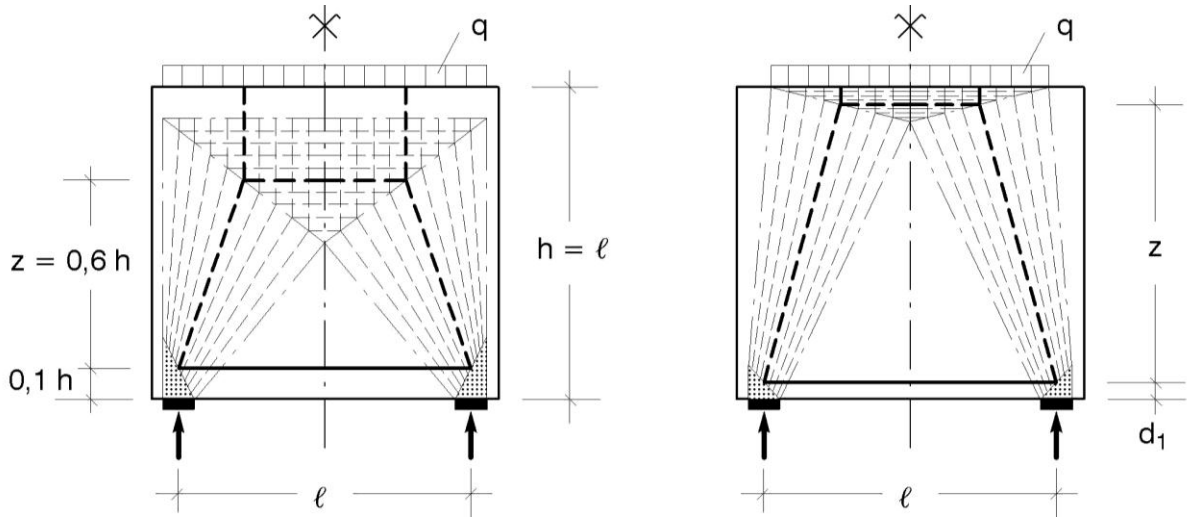
For checking the crack widths in a D-region the ties must be looked at, and this means that only the cracking behaviour in axial tension of a reinforced concrete member needs to be known. However, this is the case because this forms the basis for all relationships for crack widths, like e.g. in sect. 7.4.3.1 of the CEB-FIP MC 90 or section 7.5.3.2 of the FIP Recommendations (1999). Based on the latter a check of the crack width was performed for a D-region of the Example 1 in *fib* Bulletin 16 (2002).

The only problem for such a check at SLS is the uncertainty whether the model correctly reflects the state of stress of a cracked member under service load (SLS), since the model was selected for ultimate load level (ULS). This uncertainty is due to the fact that compatibility is not considered, see sect. 2.2. However, here it is of advantage if the recommendation by Schlaich et al. (1987) and Schäfer (1999) is followed to orientate the model at the stress fields of a linear elastic analysis.

This recommendation could mean that a conservative amount of reinforcement is selected, as e.g. for the deep beam shown in Fig. 16-5a showing the model orientated at the stress fields of a linear elastic analysis. However, the inner lever arm could be far higher and even the maximum value could be assumed shown in Fig. 16-5b, when the compression zone is fully utilized. This certainly leads to a more economical design of the reinforcement, but it may lead to excessive cracking at SLS so that a check is recommended for this, which then would be performed on basis of the model in Fig. 16-5a.

For models based on the theory of plasticity there is also the uncertainty, whether the structure exhibits the ductility required for the redistribution from model A to model B in Fig. 16-5. For deep beams enough experimental evidence is available, especially due to the tests performed by Leonhardt and Walther (1966), which lead to the classical design rules for deep beams still valid today. As an example the test on the deep beam WT2 is shown in Fig. 16-6, which is often used by researchers for comparing results of their analyses with tests. The failure photo in Fig. 16-6b proves that the deep beam actually attained the state assumed for the model B of Fig. 16-5b. The failure occurred at a support pressure of $p_A = 1{,}275 \cdot f_{1c}$. However, for calculating the failure load the strut-and-tie model had to be refined and to include the forces in the reinforcing bars distributed over the full height of the deep beam, as shown in Fig. 16-6c. Fig. 16-6d shows that quite high strains were attained in the reinforcing bars, with e.g. $\varepsilon_s = 6{,}34$ ‰ in the bottom bars and even $\varepsilon_s = 4{,}12$ ‰ in the bar at about mid-height. This means that in order to attain this stage the crack widths were quite high and this is confirmed by the photo in Fig. 16-6b.

This document is the intellectual property of the fib – International Federation for Structural Concrete. All rights reserved.
This PDF of fib Bulletin 61 is intended for use and/or distribution solely within fib National Member Groups.



a) model A orientated at linear elastic analysis *b) model B based on theory of plasticity*

Fig. 16-5: Strut-and-tie models for a deep beam subjected to distributed loads

This deep beam exhibited the required ductility to utilize the maximum inner lever arm and thus the highest possible load, and the reason for this is that the critical node at the support was well designed. The reinforcing bars had small diameters and were distributed over a certain height over the support. This was not the case for the deep beam WT1b, which had the same reinforcement at midspan but failed prematurely at a far lower load due to an anchorage failure at the support, as can be seen in Fig. 16-7a. The reason was that some of the main bars were bent up over the support thus weakening the tie anchored at the support. The failure occurred at a support pressure of only $p_A = 1{,}055 \cdot f_{1c}$.

The deep beam WT3 shown in Fig. 16-7b had double the amount of main reinforcement than WT2, but attained only a slightly higher load, since the failure occurred at a support pressure of $p_A = 1{,}335 \cdot f_{1c}$. The crack in the middle came only up to half the height, so that the model explaining the ultimate load is nearer to the model of Fig. 16-5a. Obviously the pressure at the node over the support cannot be increased much more beyond the biaxial compressive strength, which is $f_{2c} = 1{,}2 \cdot f_{1c}$ according to Eq.(5.19a) of the FIP Recommendations (1999). With support pressures of $p_A = 1{,}275 \cdot f_{1c}$ for WT2 and $p_A = 1{,}335 \cdot f_{1c}$ for WT3 this biaxial strength f_{2c} was exceeded by 6% respectively by 11%.

The common practical rule of orientating the model at the elastic stress fields is appropriate, and therefore in EC 2, Part 1-1 (2005) it is stated as follows:

"...if the struts and ties follow the main compression and tension elastic stress trajectories, the ultimate limit state model can be used to check service behaviour...".

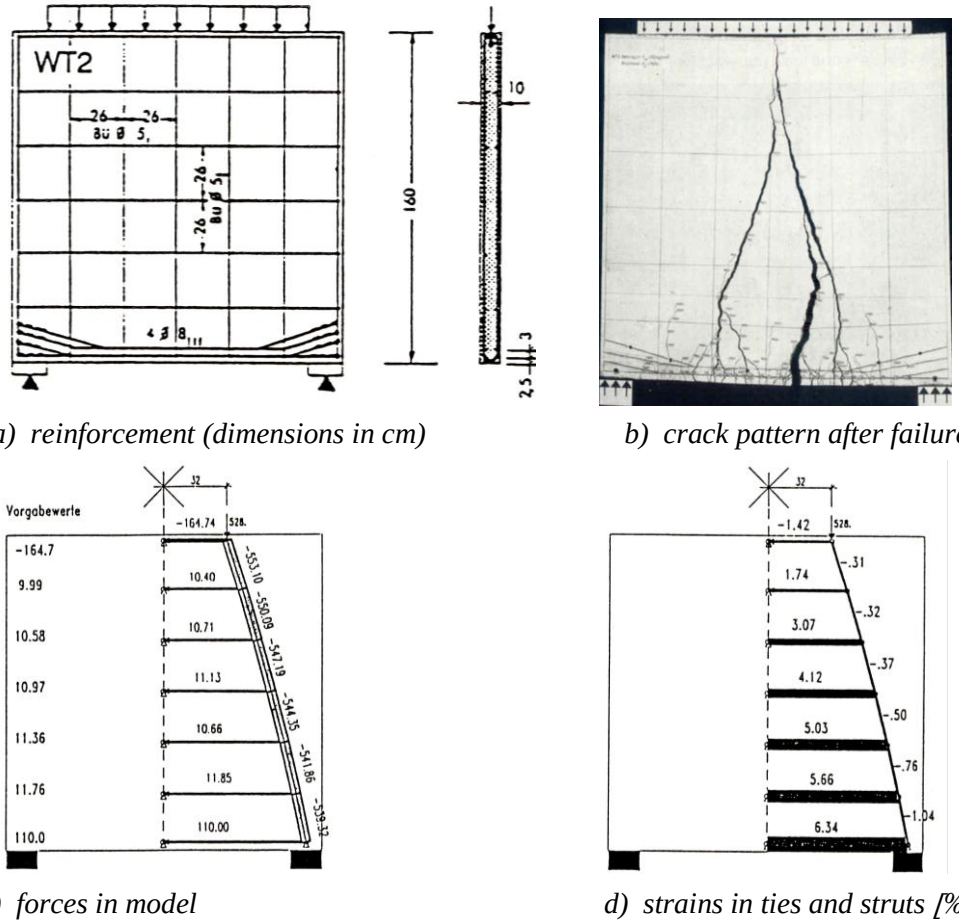
However, this should not be interpreted as a perfect mapping of the elastic trajectories. An important issue to develop a suitable strut-and-tie model is to follow the practical reinforcement layout, so that mainly the struts are close to principal compressive stress trajectories. An illustration of the application of elastic stress trajectories for the development of the design strut-and-tie model is presented in Example 13 of the current Bulletin.

Note that the engineer does not need to develop an elastic analysis in every practical situation. The models presented by e.g. Schlaich et. al. (1987), Schlaich and Schäfer (1991), *fib* Bulletin 3 (1999) and FIP Recommendations (1999) cover most current cases. For internally hyperstatic models the reference solution is known for almost every practical situation, so that the designer have no difficulties in finding a suitable strut-and-tie model for the design.

This document is the intellectual property of the fib – International Federation for Structural Concrete. All rights reserved.
This PDF of fib Bulletin 61 is intended for use and/or distribution solely within fib National Member Groups.

To illustrate that a suitable strut-and-tie model can be found without previously having performed an elastic analysis, Fig. 16-8 shows a strut-and-tie model for the vertical loads of a pier of a viaduct. Two models M1 and M2 may be discerned in Fig. 16-8a. It is easily recognized that the model M1 bears similarities with a common model for deep beam, and so a suitable inner level arm of $z = 0{,}7 \cdot l$ can be assumed. The remaining struts and ties of model M2 can be compared with a model corresponding to a deep beam with suspended loads, and again though the same ratio for the inner level arm $z_1 = 0{,}7 \cdot l_1$ was assumed. In this way it is possible ensure good service behaviour and moreover, to calculate crack widths at SLS with the same model as was used for ULS.

In concluding it can be stated, that the recommendation by Schlaich et al. (1987) and Schäfer (1999) to orientate a strut-and-tie model at the stress fields of a linear elastic analysis is a practical and conservative recommendation. However, the fact remains that the selected model does not reflect cracking and thus not the redistribution of forces up to the service load level (SLS). This fact has led to further developments in the last years to use non-linear analyses and to combine it with the strut-and-tie model concept, and this topic is further dealt with in the following chapter 3.

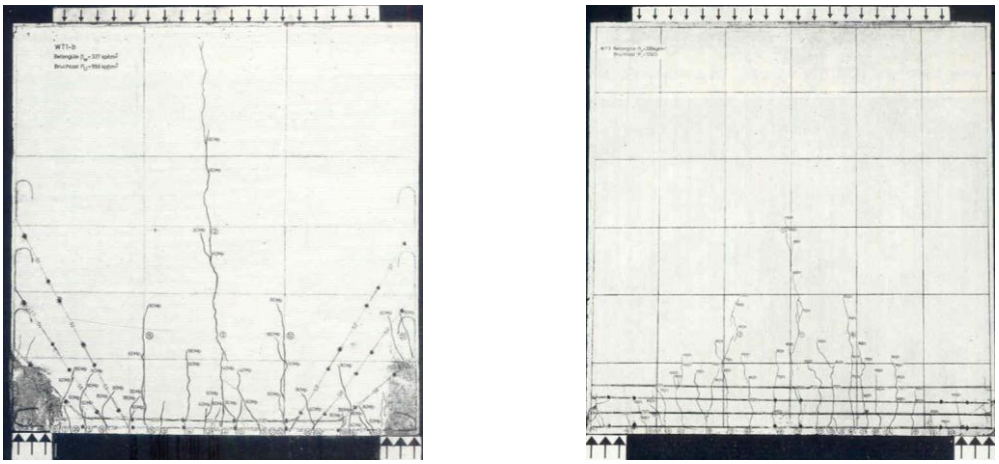


a) reinforcement (dimensions in cm) *b) crack pattern after failure*

c) forces in model *d) strains in ties and struts [‰]*

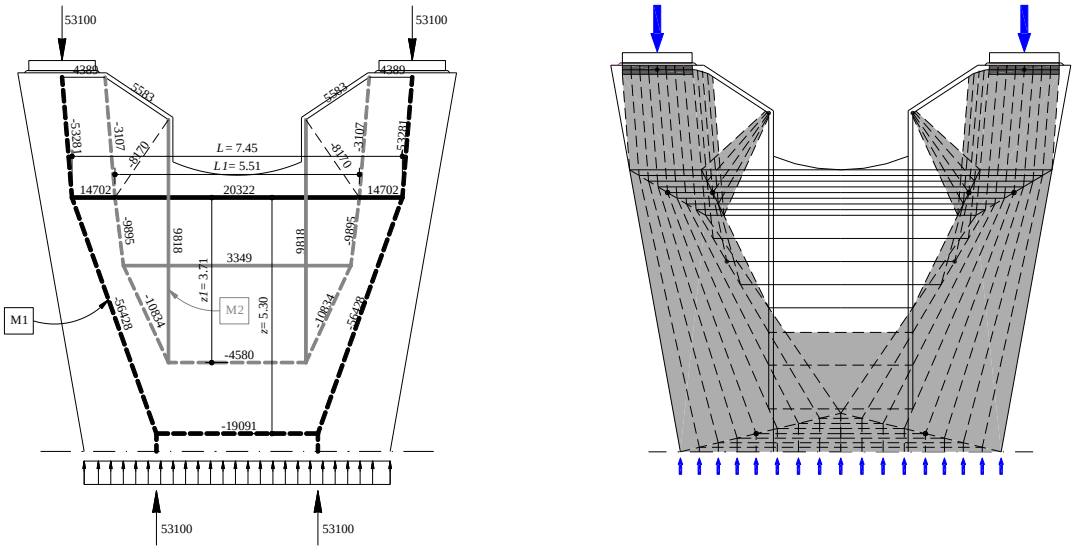
Fig. 16-6: Test on the deep beam WT2 by Leonhardt and Walther (1966) and model for explaining the failure load according to Rückert (1994)
(decimal point instead of comma; see Editorial Comments on p. vi)

This document is the intellectual property of the fib – International Federation for Structural Concrete. All rights reserved.
This PDF of fib Bulletin 61 is intended for use and/or distribution solely within fib National Member Groups.



a) deep beam WT1b b) deep beam WT3

Fig. 16-7: Failure photo of the tests on two deep beams by Leonhardt and Walther (1966)



a) strut-and-tie models M1 and M2 b) stress fields

Fig. 16-8: Models for a bridge pier
(decimal point instead of comma; see Editorial Comments on p. vi)

3 Recent developments

3.1 Introduction

The increase of computational capabilities in the last decade has allowed numerical models to be widely used in the analysis, leading to a further level of complexity in structural engineering. In fact, one could be tempted to think that structural analysis is only a matter of computational capacity, and the only significant aspects necessary to model structural concrete would be the size of the region mesh and the definition of the material nonlinear behaviour with almost unlimited accuracy. However, structural engineers should not merely engage in countless calculations and checks, losing sight of the overall behaviour of the structure. The prediction of the structural behaviour together with a critical analysis of the outputs is highly important for a good design and detailing. The structural design based on strut-and-tie models can effectively address this problem of structural judgement.

This document is the intellectual property of the fib – International Federation for Structural Concrete. All rights reserved.
This PDF of fib Bulletin 61 is intended for use and/or distribution solely within fib National Member Groups.

However, despite of all its unquestionable advantages, the strut-and-tie method is not widely disseminated because of several constraints to its practical application. One of the aspects frequently pointed out is the uncertainty in selecting a suitable model leading to the discussion on the validity and uniqueness of models, see section 2.2. Moreover, some engineering judgment is required to come up with the design model and to find an equilibrated strut-and-tie model can be time consuming if the designer is not familiarized with the technique. Serviceability and ductility topics are usually indirectly checked through semi-empirical rules. In a simplified way, service behaviour is ensured by following the model main compression and tension stresses through elastic stress trajectories although, in many cases, they are unsuited for detailing purposes. On the other hand, after developing a specific model for a structural concrete region, the doubt whether the structure has enough ductility to adapt itself to the chosen model could remain.

The need for systematic procedures for establishing and calculating models were evident in the early 1990's. One of the first researchers working on the automatic tools for the development of the strut-and-tie models was Schlaich, M. (1989). Based on a discrete truss mesh of a structural concrete region, the computer program developed returns to the elastic solution, the plastic approach and the solution with minimum reinforcement. Almost at the same time Hajdin (1990), in Zurich, used uniform stressed triangular meshes for the development of stress field models in reinforced concrete walls.

The simplified energetic criteria mentioned by Schlaich et al. (1987) to choose a model out of several possible ones, is the base for the work of some other researchers:

- "in selecting the model, it is helpful to realize that loads try to use the path with the
- least forces and deformations. Since reinforced ties are much more deformable than
- concrete struts, the model with the least and shortest ties is the best".

The application of an energetic criterion to perform nonlinear analysis of stress field models was initially proposed by Rückert (1991, 1993, 1994), Sundermann and Mutscher (1991) and later Sundermann (1994). The procedure consists in adapting model geometry according to the principle of minimum strain energy taking into account nonlinear behaviour for concrete and steel reinforcement. Numerical results based on nonlinear stress field models shown a reasonable agreement for deep beams when compared with the tests by Leonhardt and Walther (1966).

Kuchma and Tjhin (2000) presented a discussion of strut-and-tie method and provided an introduction to the strut-and-tie method (STM). In addition an overview was given on the Computer-Aided Strut-and-Tie (CAST) design tool, which is a user friendly freeware program to design structural concrete regions with strut-and-tie models.

Elia et al. (2002) delineated an interactive procedure to design strut-and-tie models using an evolutionary structural optimisation method. In this methodology the difference is measured between the strain energy of the design strut-and-tie model and the optimal solution, and it allows an evaluation of the ductility capacity of the structure.

Salem (2004) developed a micro truss model with small isotropic truss members are used and the macro strut-and-tie model is automatically obtained. The proposed model can be used for checking nonlinear behaviour of reinforced concrete structures and was validated with experimental results.

Vitone et al. (2006) applied the load path method to assess strut-and-tie models at different stages: uncracked, cracked phase and ultimate load. The application to frame corners with opening moments and with specific reinforcement detailing was analysed.

This document is the intellectual property of the fib – International Federation for Structural Concrete. All rights reserved.
This PDF of fib Bulletin 61 is intended for use and/or distribution solely within fib National Member Groups.

Kostic (2006) presented a procedure initially proposed by Bendsoe et al. (1994) and Biondini et al. (1996) where an initial mesh is generated with a series of joints connected by bars. This renders the continuum system into a n-times statically indeterminate truss model. Some elements are not as efficient in transmitting the forces as others and can thus be removed until an optimized strut-and-tie model is obtained.

Ruiz et al. (2007a) presented an approach for the automatic development of stress fields using the finite element method. A computer aided program considering nonlinear finite element triangles implemented the main hypotheses of the stress field method to develop suitable stress fields. Ruiz and Muttoni (2007b) developed comparisons with tests were performed for the validation of this approach. The methodology was also used on a well-known deep beam with opening, first presented by Schlaich et al. (1987).

Lourenço (2010) presented a considerable improvement of the work developed by Rückert (1991) and Sundermann (1994). The proposed technique "Adaptive Stress Field Models" employs the convenient simplifications inherent to the stress field models to develop a tool for the nonlinear analysis of discontinuity regions, allowing to study service behaviour, ductility, and, more generally to assess models. The interpretation of the flow of forces provided by the method offer a unique awareness of the structural behaviour during the loading process, essential for an adequate judgement of the outputs. The internal stress redistributions due to the nonlinear behaviour of the materials are accomplished by the introducing the adaptive structures concept to stress field systems, in particular model follows energy. The model configuration at each load step is thus obtained following the least complementary energy. It intends to follow consistently the stress field model concept, by setting an initial stress field distribution and the appropriate variables that will be adjusted are chosen: geometry and/or forces of the model. The mechanical properties of the compression and tension elements are obtained directly from the geometry of the stress fields, accounting for the nonlinear constitutive relationships of the materials. Special attention is given to the behaviour of reinforced concrete ties, since the global energy is greatly influenced by the tension stress fields. Therefore, the reinforced concrete tie elements behaviour was obtained following the tension chord model concept by Marti et al. (1998). The proposed technique was validated by comparing the numerical results with several outcomes from tests and other numerical methods.

3.2 Use of programs for assessing models at the Serviceability Limit State

The following analyses for assessing models for the Serviceability and Ultimate Limit State were developed with the adaptive stress field concept.

In discontinuity regions, considerable redistributions usually occur after cracking and frequently leading to proper service behaviour. This particular subject is observed in e.g. deep beam regions, in which the cracking of the bottom tie induces significant internal stresses redistributions and a rapid increase of the inner level arm, reducing significantly the bottom tie stresses at service and ultimate loads, especially in case of low reinforcement ratios.

This redistribution of stresses was confirmed by the well-known tests on deep beams by Leonhardt and Walther (1966). As mentioned before, two geometrically identical deep beams WT2 and WT3 were tested with rather different reinforcement layouts, see Fig. 16-9. The main reinforcement of the deep beam WT3, obtained by a strut-and-tie model based on the elastic theory (i.e. assuming an inner level arm of $z \approx 0{,}7 \cdot h$), is compared with WT2 in which half of the reinforcement ratio was adopted. It could be expected that the ultimate load is much lower for WT2 than for WT3, but the experimental ultimate loads reached quite similar values for both deep beams. In both cases, the failures were governed by the compression stresses over the supports. In the deep beam WT2 the bottom reinforcement yielded and in WT3 steel stresses of 370 MPa were obtained.

This document is the intellectual property of the fib – International Federation for Structural Concrete. All rights reserved.
This PDF of fib Bulletin 61 is intended for use and/or distribution solely within fib National Member Groups.

The considerable redistribution of internal stresses immediately after cracking is clearly illustrated by the stress field configurations presented in Figs. 16-10a and 16-10b. In WT2 with the lower reinforcement ratio almost the whole depth of the deep beam was utilized, leading to moderate steel strains at the ultimate load. A final remark concerning generally simply supported beams is that despite of such remarkable internal redistributions the steel stresses and crack width at SLS remained at quite appropriate levels. For a service load of P_{serv} = 600 kN the crack widths w_k= 0,04 mm (WT3) and w_k = 0,06 mm (WT2) were observed and also achieved numerically (Fig. 16-11).

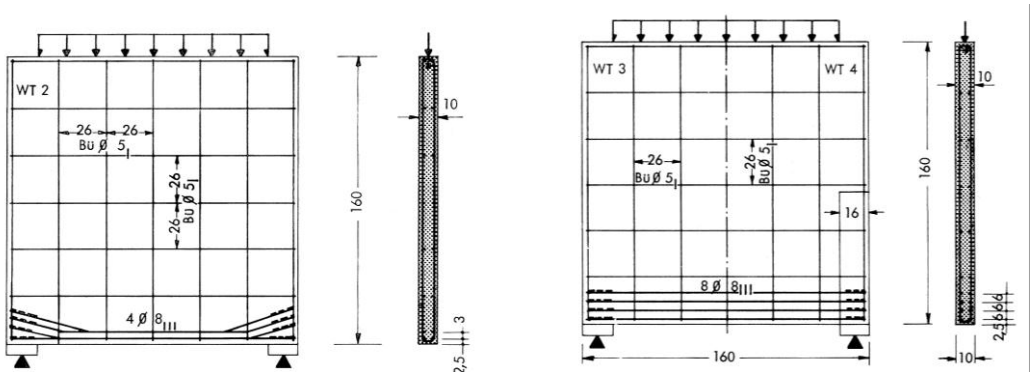
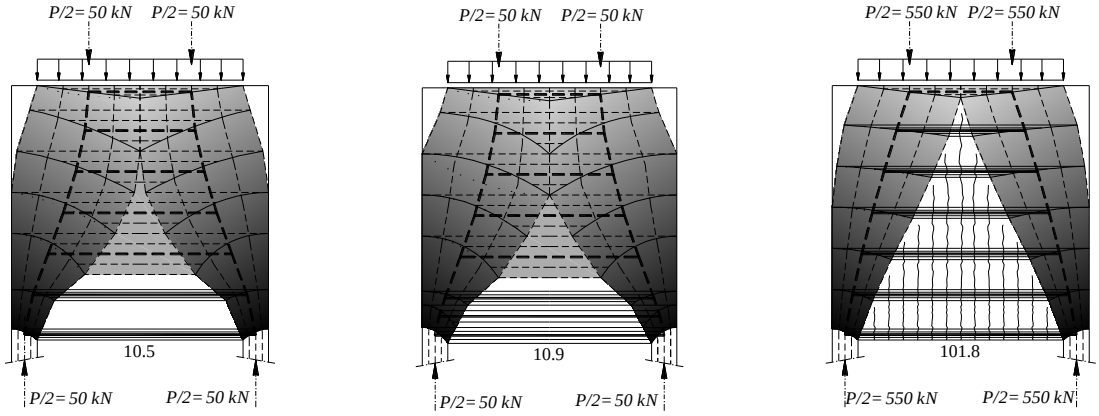
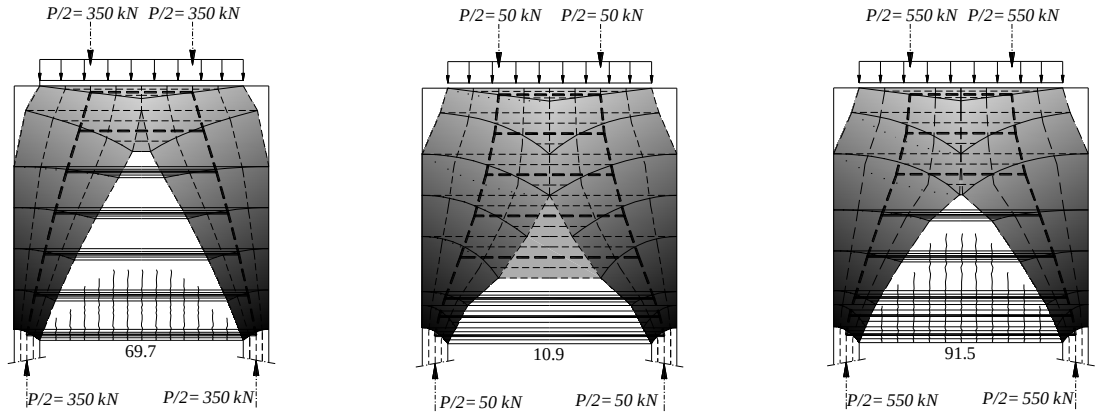


Fig. 16-9: Deep beams WT2 and WT3 tested by Leonhardt and Walther (1966) (dimensions in cm)



a1) uncracked stage *a2) service load* *a3) ultimate load*

a) development of stress fields for deep beam WT2

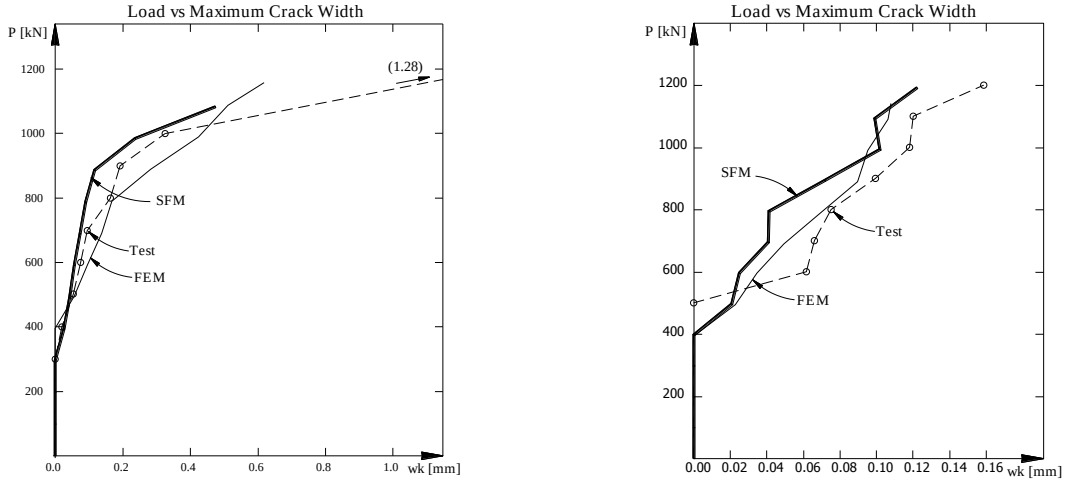


b1) uncracked stage *b2) service load* *b3) ultimate load*

b) development of stress fields for deep beam WT3

Fig. 16-10: Development of stress fields with increasing loads acc. to Lourenço (2010) (decimal point instead of comma; see Editorial Comments on p. vi)

This document is the intellectual property of the fib – International Federation for Structural Concrete. All rights reserved.
This PDF of fib Bulletin 61 is intended for use and/or distribution solely within fib National Member Groups.



a) crack widths for WT2 *b) crack widths for WT3*

Fig. 16-11: Measured crack widths in deep beam tests and comparison with numerical results acc. to the adaptive stress field analysis (SFM) and a nonlinear finite element analysis (FEM) acc. to Lourenço (2010) (decimal point instead of comma; see Editorial Comments on p. vi)

3.3 Use of programs for assessing models at the Ultimate Limit State

An unpredicted concrete failure is mainly conditioned by the reduction of the compressive concrete strength due to the presence of high transverse strains. Usually this phenomenon becomes perceptible only for large crack widths, associated with yielding of the reinforcement. However, in most practical cases this effect is not relevant, because compressive stresses within the regions are usually lower than the effective strength due to other conditions for selecting the dimensions for nodal regions. However, this aspect can occur in some discontinuity regions, such as the corbel with suspended loads shown in Fig. 16-12. In this particular model the load transfer is assumed by vertical and inclined reinforcement, leading to the superposition of two different models. The compressive stresses σ_c must cross the diagonal tie with significant transverse strains induced which may reduce the strength of the strut. Anyway, the concrete stresses in the CTT node at the top face of the corbel must be limited to its effective strength, see FIP Recommendations (1999).

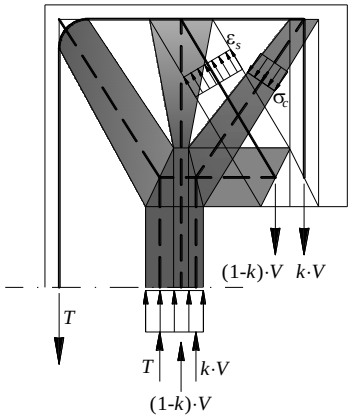
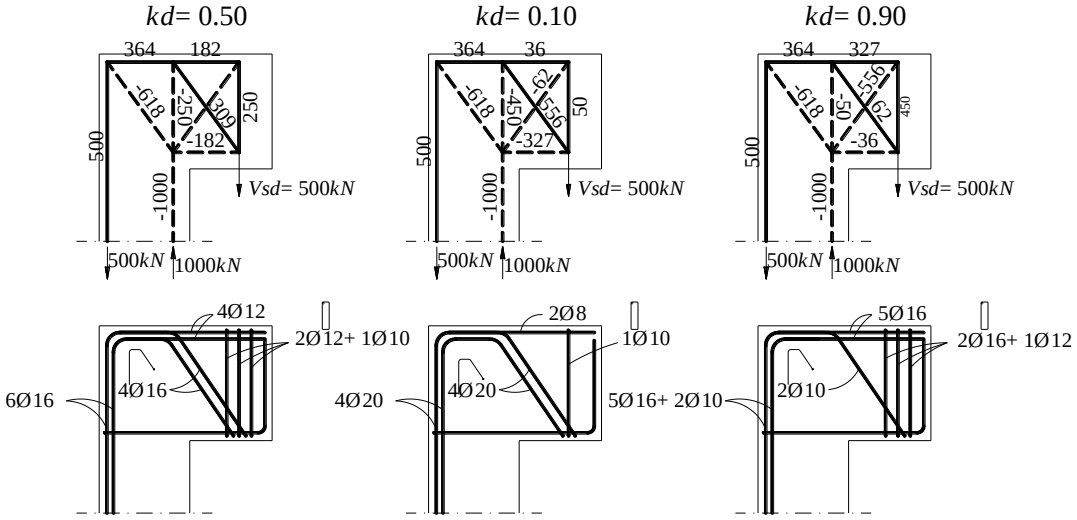


Fig. 16-12: Superposition of two strut-and-tie models for a corbel with a suspended load

This document is the intellectual property of the fib – International Federation for Structural Concrete. All rights reserved.
This PDF of fib Bulletin 61 is intended for use and/or distribution solely within fib National Member Groups.

For this corbel with a suspended load an adaptive stress field analysis was developed for each reinforcement layout, and Fig. 16-13 shows three possible strut-and-tie models for different amounts of inclined and vertical reinforcement. The adaptive variable k_d represents the fraction of the load that is suspended by stirrups. To properly simulate the global behaviour, the analysis considers the reduction of the compressive strength of concrete for the diagonal strut crossing the diagonal tie. In this way it is possible to evaluate the influence of the diagonal cracking in the compression field and predict an eventual premature failure. The design load was achieved in all cases and low to moderate compressive stresses were obtained. Fig. 16-14 shows the development of the diagonal compressive stresses with increasing loading for each reinforcement layout. As expected, the diagonal compression stresses are higher for the reinforcement layout with higher amounts of stirrups, although still below the effective concrete strength.



a) model 1 (kd = 0.5) *b) model 2 (kd = 0.1)* *c) model 3 (kd = 0.9)*

Fig. 16-13: Three possible strut-and-tie models for three corbels with different amounts of diagonal and vertical reinforcements (decimal point instead of comma; see Editorial Comments on p. vi)

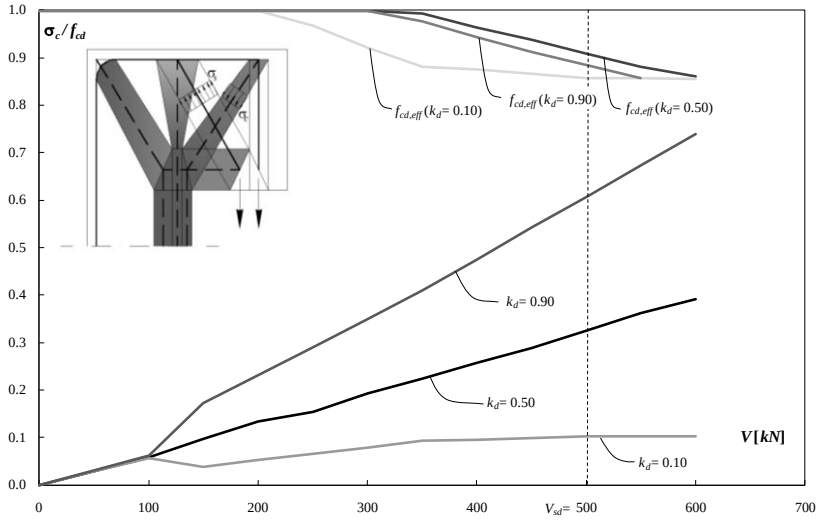


Fig. 16-14: Diagonal compressive stresses related to the effective concrete strength in the corbels of Fig. 16-13

This document is the intellectual property of the fib – International Federation for Structural Concrete. All rights reserved.
This PDF of fib Bulletin 61 is intended for use and/or distribution solely within fib National Member Groups.

3.4 Concluding remarks

The assumption that the structure is able to adapt itself to the selected design model was confirmed in several studies for different discontinuity regions. The deformation capacity of the materials after yielding allows considerable stress redistributions and successive formation of new statical systems. In practical applications, strut-and-tie models should, in general, be used together with a well distributed minimum reinforcement, which should prevent premature failures at the cracking load.

In general the engineer has plenty of freedom for choosing the model for the design of discontinuity regions, and his judgement based on previous experience should not be underestimated. The discussed common rules for the development of a suitable strut-and-tie model should be respected, preventing extreme redistributions that can cause a premature failure.

4 Conclusions and proposals for future work

Owing to its simplicity and rational analytical approach, the strut-and-tie method (STM) has gained widespread use and recognition in recent years. As outlined in Sec. 2.1 the general concept of strut-and-tie modelling is well developed and experimentally validated. The STM has also emerged as a code-worthy methodology and provisions for STM have now found place in most major design codes. The applicability of the STM concept to 'real-life' design problems has been widely demonstrated through a variety of design examples presented in this and the previous Bulletin 16 (2002) as well as in ACI SP 208 and SP 273. Several issues pertaining to model formulation have been addressed through these examples. Stemming from the discussions within the Working Party, there are still some aspects of modelling and practical application of STM that deserve further investigation.

Although the strut-and-tie method is conceptually simple, finding a suitable model is the most challenging task since the choice of model is mainly based on intuition and experience. As indicated in Sec. 3.2 the assessment of models at service load level has shown that relative high stress redistributions can be tolerated without much affecting the service behaviour. A systematic assessment of design models for frequent appearing discontinuity regions would provide valuable insight in how much freedom exists in developing appropriate models.

While STM design provisions mostly agree on the general principles of strut-and-tie modelling, some discrepancies occur in the values for the effective compressive strengths. Only few codes specify strength modifications for high strength and lightweight concrete, since research so far mainly considered concrete of normal strength and density. Thereby the relevance of the post-peak behaviour in uniaxial compression, whether brittle or less brittle, needs further assessment. However, it should be noted that this topic should not be overemphasized, since for well-designed structures or D-regions the failure is governed by yielding of the reinforcement rather than by compression failures.

Another relevant topic is the use of STM for seismic design. There is limited evidence on the behaviour of STM designed members subjected to reversed cyclic loading. Consequently, to what extent current STM provisions, derived for monolithic loading, are applicable for reversed cyclic loading is subject to debate and a topic for further research. Application of STM to assess the strength and behaviour of D-regions subjected to seismic loading should therefore be studied more closely to provide some general guidance, first of all directed towards strength-based design. The limitations for performance-based design are more obvious, as a conventional strut-and-tie analysis does not provide information about deformation capacities.

This document is the intellectual property of the fib – International Federation for Structural Concrete. All rights reserved.
This PDF of fib Bulletin 61 is intended for use and/or distribution solely within fib National Member Groups.

Lastly, there are aspects concerning realization of 3D models, for which little or no guidance is found in the STM provisions. Often the decomposition of a 3D region into planar models is sought to avoid the complexity of 3D models. Such a 2D analogy is often possible, but where this is not the case, e.g. in large pile foundations, the formulation of a spatial model can be quite intricate as well as finding consistent geometries for the 3D nodal zones. For complex nodal geometry strength factors developed for biaxial stress state may be inappropriate. Further research should be performed on efficient concepts for developing 3D nodal zones as well as suitable failure criteria be defined the effective strengths of 3D nodes.

It is proposed that the outlined topics and issues are addressed and presented for the benefit of practicing engineers in a separate technical publication devoted to special aspects of modelling and applying STM. If relevant, supplements and modifications to the FIP Recommendations (1999) should also be proposed herein.

References

Abbreviations: AASHTO = American Association of State Highway and Transportation Officials
ACI = American Concrete Institute
ASCE = American Society of Civil Engineering
BuStb = Beton- und Stahlbetonbau
CEB = Comité Eurointernational du Beton (until 1998
fib = Fédération Internationale du Béton (since 1998; merged from CEB and FIP)
FIP = Fédération Internationale de la Précontrainte (until 1998)
IABSE = International Association for Bridges and Structural Engineering
= IVBH = Internationale Vereinigung für Brücken und Hochbau

AASHTO (1994): AASHTO LRFD Bridge design specifications, section 5 Concrete Structures. American Ass. of State Highway and Transportation Officials, Washington, D.C., 1994

ACI SP-208 (2002): see Reineck (2002)

ACI SP-273 (2010): see Reineck and Novak (2010)

ACI 318 (2008): Building Code Requirements for Structural Concrete (ACI 318-08) and Commentary. American Concrete Institute, Farmington Hills, MI. 2008

ACI 445 (1997): Strut-and-Tie Bibliography. (Edts: Anderson, N. S.; Sanders, D.). Reported by ACI/ASCE Committee 445-Shear and Torsion. ACI, Farmington Hills, MI. 1997

ASCE-ACI 445 (1998): Recent approaches to shear design of structural concrete. State-of-the-Art-Report by ASCE-ACI Committee 445 on Shear and Torsion. ASCE-Journ. of Struct. Eng. 124 (1998), No.12, 1375-1417

Bendsoe, M.P., Ben-Tal, A., Zowe, J. (1994): Optimization methods for truss geometry and topology design. Structural optimization Vol.7 (1994), 141-159

Biondini F., Bontempi F., Malerba P.G. (1996): Ricerca di Modelli Strut-and-tie mediante programmazione Lineare. Studi e Ricerche No. 17, 121-156.

Breen, J.E. (1991): Why Structural Concrete? p. 15-26 in: IABSE Colloquium Structural Concrete, Stuttgart April 1991. IABSE Rep. V.62, 1991

CAST: Computer Aided Strut-and-Tie (CAST Software). University of Illinois Strut-and-Tie Resource. web site http://dankuchma.com/stm

CEB-FIP MC 90 (1993): Design of concrete structures. CEB-FIP-Model-Code 1990. Thomas Telford, 1993

CSA (1984): Design of Concrete Structures for Buildings. Canadian Standards Association (CAN3-A23.3-M84), 281, Rexdale, Ontario, 1984

Cook, W.D.; Mitchel, D. (1988): Studies of Disturbed Regions near Discontinuities in Reinforced Concrete Members. ACI Structural Journal V.85 (1988), No.2, 206-216

This document is the intellectual property of the fib – International Federation for Structural Concrete. All rights reserved.
This PDF of fib Bulletin 61 is intended for use and/or distribution solely within fib National Member Groups.

DIN 1045-1 (2001): Deutsche Norm: Tragwerke aus Beton, Stahlbeton und Spannbeton - Teil 1: Bemessung und Konstruktion. S. 1 - 148. (Concrete, reinforced and prestressed concrete structures - Part 1: Design). Normenausschuss Bauwesen (NABau) im DIN Deutsches Institut für Normung e.V. Beuth Verl. Berlin, Juli 2001

DIN 1045-1 (2008): Deutsche Norm: Tragwerke aus Beton, Stahlbeton und Spannbeton - Teil 1: Bemessung und Konstruktion. S. 1 - 183. (Concrete, reinforced and prestressed concrete structures - Part 1: Design). Normenausschuss Bauwesen (NABau) im DIN Deutsches Institut für Normung e.V. Beuth Verl. Berlin, August 2008

EC 2, Part 1-1 (2005): Eurocode 2: Design of concrete structures. Part 1.1: General rules and rules for buildings. 2005

Elia, G.; Palmisano, F.; Vitone, A.; Vitone, C. (2002): An interactive procedure to design strut-and-tie models in reinforced concrete structures using the "Evolutionary Structural Optimisation" method. Proceedings of the 4th ASMO-UK/ISSMO conference. Newcastle-upon-Tyne, UK July 2002

fib Bulletin 3 (1999): Structural concrete. Textbook on behaviour, design and performance - updated knowledge of the CEB/FIP Model Code 1990. Vol. 3: Durability - design for fire resistance -member design - assessment, maintenance and repair - practical aspects. *fib* Lausanne, December 1999.

fib Bulletin 16 (2002): Design Examples for the FIP Recommendations "Practical design of structural concrete". *fib*, Lausanne, January 2002

FIP Recommendations (1999): Practical Design of Structural Concrete. FIP-Commission 3 "Practical Design", Sept. 1996. Publ.: SETO, London, Sept. 1999. (Distributed by: *fib*, Lausanne. Web http://www.fib-international.org)

Hajdin, R. (1990): Computerunterstützte Bemessung von Stahlbetonscheiben mit Spannungsfeldern. Diss. Nr. 9167, ETH Zürich, Institut für Baustatik und Konstruktion. 1990

IABSE (1991): IABSE-Colloquium Stuttgart 1991: Structural Concrete - Summarizing statement. Publ. in: Structural Engineering International V.1 (1991), No.3, 52-54; Concrete International 13 (1991), No.10, Oct., 74-77; PCI-Journ. 36 (1991), Nov.-Dec., 60-63

Kostic, N. (2006): Computer-Based Development of Stress Fields. 6th International PhD Symposium in Civil Engineering, Zurich, August 23-26, 2006

Kuchma, D.A.; Tjhin (2000): Advances and Challenges to Design by the Strut-and-Tie Method. Open Paper Session at the ACI Fall Convention 2000 in Toronto, Canada, 2000

Leonhardt F.; Walther R. (1966): "Wandartiger Träger", DAfStb Heft 178. Wilhelm Ernst & Sohn, Berlin, 159 pp.

Lourenço, M. (2010): Adaptive Stress Field Models for Structural Concrete. PhD dissertation, IST, Lisbon, February 2010

MacGregor, J.G. (2002): Derivation of strut-and-tie models for the 2002 ACI Code. p. 7-40 in Reineck, K.-H. (Editor): Examples for the Design of Structural Concrete with Strut-and-Tie Models. ACI SP-208 (2002), ACI, Farmington Hills, MI

Marti, P. (1985 a): Basic Tools of Reinforced Concrete Beam Design. ACI Journ. V.82 (1985), No.1, 46-56. Discussion in: Vol.82 (1985), No.6, Nov.-Dec., 933-935

Marti, P. (1985 b): Truss Models in Detailing. Concrete International: Design and Construction, V 7 (1985), No.12, 66-73. Discussion in: V.8 (1986), No.10, 66-68

Mitchell, D.; Cook, W.D.; Uribe, C.M.; Alcocer, S.M. (2002): Experimental verification of strut-and-tie models. Part 3, 41-62 in: Reineck, K.-H. (Ed.): Examples for the Design of Structural Concrete with Strut-and-Tie Models. ACI SP-208 (2002), ACI, Farmington Hills, MI

Muttoni, A.; Schwartz, J.; Thürlimann, B. (1996): Design of concrete structures with stress fields. Birkhäuser, Basel, 1996

NS 3473 (1989): Design of Concrete Structures – Design and Detailing rules. 3rd ed., Norwegian Council for Building Standardisation

This document is the intellectual property of the fib – International Federation for Structural Concrete. All rights reserved.
This PDF of fib Bulletin 61 is intended for use and/or distribution solely within fib National Member Groups.

Reineck, K.-H. (2002): (Editor): Examples for the Design of Structural Concrete with Strut-and-Tie Models. ACI SP-208 (2002), ACI, Farmington Hills, MI

Reineck, K.-H. (2005): Modellierung der D-Bereiche von Fertigteilen (Modelling the D-regions of prefabricated members). Paper XI, 241 – 296 in: Betonkalender 94 (2005), Teil II. Ernst & Sohn, Berlin, 2005

Reineck, K.-H.; Novak, L.C. (2010) (Editors): Further Examples for the Design of Structural Concrete with Strut-and-Tie Models. ACI SP-273 (2010), ACI, Farmington Hills, MI

Rückert, K. (1991): Design and analysis with strut-and-tie models - computer-aided methods. IABSE Rep. V.62 (1991 a), 379-384

Rückert, K. (1993): Computer Aided Methods for the Design of Structural Concrete. IABSE Workshop, New Delhi, 1993

Rückert, K. (1994): Computer-unterstütztes Bemessen mit Stabwerkmodellen (Computer aided design with strut-and-tie models). BuStb 89 (1994), H.12, 319-325

Ruiz M.F., Muttoni A., Burdet O.L. (2007a): Computer-Aided Development of Stress Fields for the Analysis of Structural Concrete. ***fib*** Symp.Dubrovnik 2007, Croatia May 2007, 591-598

Ruiz M.F., Muttoni, A. (2007b): On Development of Suitable Stress Fields for Structural Concrete | 2007, ACI Structural Journal, V.104 (2007), No. 4, July-Aug., pp.495-502.

Salem, H.M. (2004): The Micro Truss Model: An Innovative Rational Design Approach for Reinforced Concrete. Journal of Advanced Concrete Technology Vol.2 (2004), No.1, February, 77-87

Schäfer, K. (1999): Deep beams and discontinuity regions.
Sect. 7.3, p. 141 – 184 in: *fib* Bulletin 3 (1999). *fib* Lausanne

Schlaich, J. (1984): Zur einheitlichen Bemessung von Stahlbetontragwerken. BuStb 79 (1984), H.4, 89-96

Schlaich, J.; Schäfer, K. (1984): Konstruieren im Stahlbetonbau (Detailing of Reinforced Concrete). Betonkalender 1984, Part 2, W. Ernst u. Sohn, Berlin, 1984, 787-1005

Schlaich, J.; Schäfer, K; Jennewein, M. (1987): Toward a consistent design for structural concrete. PCI-Journ. V.32 (1987), No.3, 75-150

Schlaich, J. (1991): The need for consistent and translucent models. p. 169-184 in: IABSE Colloquium Structural Concrete, Stuttgart April 1991. IABSE Rep. V.62, 1991

Schlaich, J.; Schäfer, K. (2001): Konstruieren im Stahlbetonbau. Betonkalender 90 (2001), Teil II, 311 - 492. Ernst & Sohn Verlag, Berlin 2001

Schlaich, M. (1989): Computerunterstützte Bemessung von Stahlbetonscheiben mit Fachwerkmodellen. Diss., ETH Zürich, Bericht 1, Professur für Informatik, Oktober 1989

Steinle, A.; Rostásy, F.S. (1974): Zum Tragverhalten ausgeklinkter Trägerenden. Betonwerk + Fertigteil - Technik 41 (1975), Nr. 6, 270 - 277 und Nr. 7, 337 - 341

Steinle, A.; Hahn, V. (1988): Bauen mit Betonfertigteilen im Hochbau. Überarb. Sonderdruck aus Beton Kalender 1988, 1-173, Fachvereinigung Deutscher Betonfertigteilbau e.V., 1991

Steinle, A.; Hahn, V. (1995): Bauen mit Betonfertigteilen im Hochbau. 459-629 in: Beton Kalender 84 (1995), T. II. Ernst & Sohn, Berlin

Sundermann, W., Mutscher P. (1991): Nonlinear Behaviour of Deep Beams. 385 - 390 in: IABSE Rep. V.62 (1991)

Sundermann, W. (1994): Tragfähigkeit und Tragverhalten von Stahlbeton-Scheibentragwerken. Diss., Institut für Tragwerksentwurf und -konstruktion, Univ. Stuttgart, 1994

Vitone A., Palmisano F., Vitone C. (2006): Load Path Method (LPM) in Detailing Design. Proceedings of the 2nd ***fib*** congress, Naples June 5-8, 2006

This document is the intellectual property of the fib – International Federation for Structural Concrete. All rights reserved.
This PDF of fib Bulletin 61 is intended for use and/or distribution solely within fib National Member Groups.

Author information

João F. Almeida received his Civil Engineering degree from Instituto Superior Técnico, Lisbon, in 1981, MSc in Structural Engineering in 1985 and PhD degree in Civil Engineering from Technical University of Lisbon in 1990. He is presently Associate Professor of Concrete Structures at Instituto Superior Técnico. Since 1990 he is partner and technical director of JSJ Consulting Ltd. He is member of ***fib*** Commission 1, *Structures,* and convenor of TG1.1, *Design Applications,* from 1998 to 2008.

Carlos J. Bajo Pavía received his degree of "Ingeniero de Caminos Canales y Puertos" from the Madrid High Technical School, in 1991. He has worked from 1990 until now at the Technical Offices of several construction companies. Since 1994 he has been working for the Bridge Design Department of Ferrovial. He has been involved in the design and construction of several types of bridges, including segmental cantilever bridges, composite and cable-stayed bridges, footbridges, etc. He is member of the ACHE society, and member of the *fib* Task Group 1.1 *Design Applications.*

Sebastián Dieste Ballestrino is a structural design engineer at FHECOR Consulting Engineers, Madrid, Spain. He received his Dipl.-Ing. from the University of La República, Montevideo, Uruguay. He is a PhD student at the Civil Engineering School of Madrid. He has a wide structural design experience, designing different kinds of structures at Fhecor Ingenieros Consultores.

Vladimír Benko received his CEng. degree 1983, PhD. degree 1990, Ass. Prof 1994 from Slovak University of Technology in Bratislava and Dipl.-Ing. 1997 from Vienna University of Technology. He works at Vienna University of Technology. His research covers analysis and design of buildings made of structural concrete, as well as the design of structures for earthquake resistance. He is member of National Austrian Standards Committee FNA 176, (Belastungsannahmen), FNA 176.02 (PG Erdbeben), FNA 014 (Brücken) AK1011 (Spiegelausschuss für Eurocodes).

Rui Bóia received his Civil Engineering degree from Instituto Superior Técnico, Lisbon in 2000. Since 2000 as joined the structural engineering company JSJ, Ltd. in Lisbon, Portugal working as a designer of bridges and buildings.

José N. Camara received his Civil Engineering degree from Instituto Superior Técnico, Lisbon, in 1977, MSc in Structural Engineering in 1983 and PhD degree in Civil Engineering from Technical University of Lisbon in 1988. He is presently Associate Professor of Concrete Structures at Instituto Superior Técnico. Since 1990 he is partner and technical director of JSJ Consulting Ltd.

Hugo Corres Peiretti received his Dipl.-Ing and Dr.-Ing from the Civil Engineering School of Madrid. In 2003 he received the Doctor Honoris Causa from Slovak University of Technology. He is the Head Professor of Structural Concrete at the Civil Engineering School of Madrid, where he is involved in research and teaching. He is member of the Permanent Comission of Concrete and was the chairman of the project team for the EHE, the Spanish Standard of Structural Concrete. He was a member of the project team for the Eurocode 2. He is a member of the Spanish Delegation of FIB and member of the Presidium. He has a wide structural design experience, designing different kinds of structures at Fhecor Ingenieros Consultores.

Ľudovít Fillo received his CEng. degree 1973 from Slovak University of Technology in Bratislava. PhD. degree 1978 from Slovak Academy of Sciences. University Professor 1997 from Slovak University of Technology in Bratislava, where he is involved in both research

This document is the intellectual property of the fib – International Federation for Structural Concrete. All rights reserved.
This PDF of fib Bulletin 61 is intended for use and/or distribution solely within fib National Member Groups.

and teaching at Department of Concrete Structures and Bridges. His research covers analysis and design of buildings and bridges made of structural concrete. He is representative of Slovak Republic in CEN TC 250-SC2 Concrete Structures, member of National Standard Committee 5 for structural concrete and member of the *fib* Task Group 1.1 "Design Applications".

Eduardo García Díaz received his Dipl.-Ing. from Alfonso X el Sabio University from Madrid. He is a PhD student at the Civil Engineering School of Madrid and works as a researcher for the Structural Concrete Group of this University.

Jaroslav Halvoník received his CEng. degree in 1988 from Slovak University of Technology in Bratislava. PhD. degree in 1993 from the same University. Associated Professor since 2000 at Slovak University of Technology in Bratislava, where he is involved in both research and teaching at Department of Concrete Structures and Bridges. He is representative of Slovak Republic in CEN TC 250-SC1 Actions and a chairman of National Standard Committee 5 for structural concrete.

Stein Atle Haugerud received his Dipl.-Ing. degree in Civil Engineering from the Technische Hochschule Darmstadt, Germany in 1990. He then joined the structural engineering company Dr.techn. Olav Olsen a.s in Oslo, Norway where he specialised as a designer of bridges and marine concrete structures. His professional experience spans from conceptual development to detail design, verification and 'special tasks'. Since 1998 member of the *fib* Task Group 1.1 *Practical Design*.

Daniel Kuchma is an Associate Professor at the University of Illinois at Urbana-Champaign. He received his PhD at the University of Toronto in 1996. He is chair of joint ACI/ASCE committee 445 "Shear and Torsion" and is active in ACI, PCI, *fib* and the Network for Earthquake Engineering Simulation.

Miguel S. Lourenço received his Civil Engineering degree from Instituto Superior Técnico, Lisbon in 1995, MSc in Structural Engineering in 2000 and PhD degree in 2010 at the same Technical Institute. Since 1995 as been working as a designer and joined the structural engineering company JSJ, Ltd. in Lisbon, Portugal, in 1998, where his professional experience extends over conceptual design to detailing, particularly, of bridges and buildings. Since 2004 he is partner and technical director of JSJ Consulting Ltd. He is member of the *fib* Task Group 1.1 since 2003.

Hannes Ludescher graduated as master in civil engineering (Dipl.Bauing.ETH) at the Swiss Federal Institute of Technology in Zurich in 1996. After three years of practical experience in civil and software engineering he joined the Swiss Federal Institute of Technology in Lausanne and defended his Ph.D. thesis on the dynamic traffic action on road bridges in 2003. Since 2004 he is working for Dr.techn. Olav Olsen a.s in the field of reinforced concrete offshore structures.

Duc Thanh Nguyen received his Dipl.-Ing. from Hanoi University of Communications and Transport in Bridge Engineering in 1987. He then worked as assistant researcher and lecturer at the division of structural engineering of the same university. From 1997 until 2002 he was an assistant researcher at the Institute for Structural design II, now the Institute for Lightweight Structures Conceptual and Structural Design (ILEK) of the University of Stuttgart, where he received the Dr.-Ing. in 2002. From 2002 to 2004 he worked as design engineer at Leonhardt, Andrä and Partner consulting engineers in Stuttgart, Germany before he continuing his career at his current employer, König und Heunisch Planungsgesellschaft mbH in Leipzig, Germany. His research fields cover the design and modeling of structural concrete and bridge design.

This document is the intellectual property of the fib – International Federation for Structural Concrete. All rights reserved.
This PDF of fib Bulletin 61 is intended for use and/or distribution solely within fib National Member Groups.

Santiago Pérez-Fadón received his degree of "Ingeniero de Caminos Canales y Puertos" (equivalent to a Master Civil Engineer) from the Madrid High Technical School, in 1971. He was from 1971 to 1981 in Euroestudios, Engineering Company and designed several highways. In 1981 he moved to Ferrovial Construction Company and from 1990 until now is the Technical Direction of the Company. He has designed many bridges, among them "los Tilos" arch (high strength concrete, 250 m span), several segmental cantilever bridges (up to 125 m span), Ricobayo arch (composite arch, 170 m span), Arosa bridge (travelling centering, 2000 m long, without joints), several stay cables bridges, etc. He is member of many scientific societies, like e.g. the Steering Committee of ACHE, the Spanish branch of *fib*, and *fib* Task Group 1.1 *Design Applications*. He has written many papers and given many talks on conferences and has received many Spanish awards for his design works.

Karl-Heinz Reineck received his Dipl.-Ing. and Dr.-Ing. degrees from the University of Stuttgart. He is retired Akad. Director at the Institute for Lightweight Structures Conceptual and Structural Design (ILEK) of the University of Stuttgart and is involved in both research and teaching. He is also Associate Professor at the University of Sarajevo. His research covers the design with strut-and-tie models and shear design of structural concrete including UHPC. He is member of the ASCE-ACI Committees 445 "Shear and Torsion" and chairs the subcommittees 445-A "Strut-and-tie models" and 445-F "Shear database". He is member of the DIN Committee for structural concrete and member of several subcommittees, and also a member of the *fib* Task Group 1.1 "Design Applications".

Karolin Reineck received her Dipl.-Ing. degree from the Technische Universität München, Germany in 1997. Since 1998 she has worked with the structural engineering company Dr.techn. Olav Olsen a.s, Norway, where she has been involved in the structural design of various types of structures. Her technical experience includes detail structural design in concrete and steel, with emphasis on multi-story buildings.

José Romo Martín received his Dipl.-Ing from the Civil Engineering School of Madrid. He is the Professor in charge of the Structural Analysis course at the Building School of Universidad Nacional de Educación a Distancia (UNED). He was adviser of the EHE the Spanish Standard of Structural Concrete. He is vice-chairman of the Spanish Group IABSE and member of the commission WC2 Steel and Composite Structures IABSE. He has a wide structural design experience, designing different kinds of structures at Fhecor Ingenieros Consultores.

Tjen Tjhin received his PhD from the University of Illinois at Urbana-Champaign in 2004, and is now working as a structural engineer for Buckland & Taylor Ltd., in North Vancouver, British Columbia, Canada.

Jean-Marc Voumard is retired Manager of the Technical Centre Europe (CH) of VSL (Switzerland) Ltd., Switzerland. He was a member of the *fib* Task Group 1.1 "Design Applications" until 2008.

Sukit Yindeesuk received his PhD from the University of Illinois at Urbana-Champaign in 2006 and is now working in the research division of the department of transportation in Bangkok, Thailand.

This document is the intellectual property of the fib – International Federation for Structural Concrete. All rights reserved.
This PDF of fib Bulletin 61 is intended for use and/or distribution solely within fib National Member Groups.

fib Bulletins published since 1998

N°	Title
1	Structural Concrete – Textbook on Behaviour, Design and Performance; Vol. 1: Introduction - Design Process – Materials Manual - textbook (244 pages, ISBN 978-2-88394-041-3, July 1999)
2	Structural Concrete – Textbook on Behaviour, Design and Performance Vol. 2: Basis of Design Manual - textbook (324 pages, ISBN 978-2-88394-042-0, July 1999)
3	Structural Concrete – Textbook on Behaviour, Design and Performance Vol. 3: Durability - Design for Fire Resistance - Member Design - Maintenance, Assessment and Repair - Practical aspects Manual - textbook (292 pages, ISBN 978-2-88394-043-7, December 1999)
4	Lightweight aggregate concrete: Extracts from codes and standards State-of-the-art report (46 pages, ISBN 978-2-88394-044-4, August 1999)
5	Protective systems against hazards: Nature and extent of the problem Technical report (64 pages, ISBN 978-2-88394-045-1, October 1999)
6	Special design considerations for precast prestressed hollow core floors Guide to good practice (180 pages, ISBN 978-2-88394-046-8, January 2000)
7	Corrugated plastic ducts for internal bonded post-tensioning Technical report (50 pages, ISBN 978-2-88394-047-5, January 2000)
8	Lightweight aggregate concrete: Part 1 (guide) – Recommended extensions to Model Code 90; Part 2 (technical report) – Identification of research needs; Part 3 (state-of-art report) – Application of lightweight aggregate concrete (118 pages, ISBN 978-2-88394-048-2, May 2000)
9	Guidance for good bridge design: Part 1 – Introduction, Part 2 – Design and construction aspects. Guide to good practice (190 pages, ISBN 978-2-88394-049-9, July 2000)
10	Bond of reinforcement in concrete State-of-art report (434 pages, ISBN 978-2-88394-050-5, August 2000)
11	Factory applied corrosion protection of prestressing steel State-of-art report (20 pages, ISBN 978-2-88394-051-2, January 2001)
12	Punching of structural concrete slabs Technical report (314 pages, ISBN 978-2-88394-052-9, August 2001)
13	Nuclear containments State-of-art report (130 pages, 1 CD, ISBN 978-2-88394-053-6, September 2001)
14	Externally bonded FRP reinforcement for RC structures Technical report (138 pages, ISBN 978-2-88394-054-3, October 2001)
15	Durability of post-tensioning tendons Technical report (284 pages, ISBN 978-2-88394-055-0, November 2001)
16	Design Examples for the 1996 FIP recommendations *Practical design of structural concrete* Technical report (198 pages, ISBN 978-2-88394-056-7, January 2002)

This document is the intellectual property of the fib – International Federation for Structural Concrete. All rights reserved.
This PDF of fib Bulletin 61 is intended for use and/or distribution solely within fib National Member Groups.

N°	Title
17	Management, maintenance and strengthening of concrete structures Technical report (180 pages, ISBN 978-2-88394-057-4, April 2002)
18	Recycling of offshore concrete structures State-of-art report (33 pages, ISBN 978-2-88394-058-1, April 2002)
19	Precast concrete in mixed construction State-of-art report (68 pages, ISBN 978-2-88394-059-8, April 2002)
20	Grouting of tendons in prestressed concrete Guide to good practice (52 pages, ISBN 978-2-88394-060-4, July 2002)
21	Environmental issues in prefabrication State-of-art report (56 pages, ISBN 978-2-88394-061-1, March 2003)
22	Monitoring and safety evaluation of existing concrete structures State-of-art report (304 pages, ISBN 978-2-88394-062-8, May 2003)
23	Environmental effects of concrete State-of-art report (68 pages, ISBN 978-2-88394-063-5, June 2003)
24	Seismic assessment and retrofit of reinforced concrete buildings State-of-art report (312 pages, ISBN 978-2-88394-064-2, August 2003)
25	Displacement-based seismic design of reinforced concrete buildings State-of-art report (196 pages, ISBN 978-2-88394-065-9, August 2003)
26	Influence of material and processing on stress corrosion cracking of prestressing steel – case studies. Technical report (44 pages, ISBN 978-2-88394-066-6, October 2003)
27	Seismic design of precast concrete building structures State-of-art report (262 pages, ISBN 978-2-88394-067-3, January 2004)
28	Environmental design State-of-art report (86 pages, ISBN 978-2-88394-068-0, February 2004)
29	Precast concrete bridges State-of-art report (83 pages, ISBN 978-2-88394-069-7, November 2004)
30	Acceptance of stay cable systems using prestressing steels Recommendation (80 pages, ISBN 978-2-88394-070-3, January 2005)
31	Post-tensioning in buildings Technical report (116 pages, ISBN 978-2-88394-071-0, February 2005)
32	Guidelines for the design of footbridges Guide to good practice (160 pages, ISBN 978-2-88394-072-7, November 2005)
33	Durability of post-tensioning tendons Recommendation (74 pages, ISBN 978-2-88394-073-4, December 2005)
34	Model Code for Service Life Design Model Code (116 pages, ISBN 978-2-88394-074-1, February 2006)
35	Retrofitting of concrete structures by externally bonded FRPs. Technical Report (224 pages, ISBN 978-2-88394-075-8, April 2006)

This document is the intellectual property of the fib – International Federation for Structural Concrete. All rights reserved.
This PDF of fib Bulletin 61 is intended for use and/or distribution solely within fib National Member Groups.

N°	Title
36	2006 *fib* Awards for Outstanding Concrete Structures Bulletin (40 pages, ISBN 978-2-88394-076-5, May 2006)
37	Precast concrete railway track systems State-of-art report (38 pages, ISBN 978-2-88394-077-2, September 2006)
38	Fire design of concrete structures – materials, structures and modelling State-of-art report (106 pages, ISBN 978-2-88394-078-9, April 2007)
39	Seismic bridge design and retrofit – structural solutions State-of-art report (300 pages, ISBN 978-2-88394-079-6, May 2007)
40	FRP reinforcement in RC structures Technical report (160 pages, ISBN 978-2-88394-080-2, September 2007)
41	Treatment of imperfections in precast structural elements State-of-art report (74 pages, ISBN 978-2-88394-081-9, November 2007)
42	Constitutive modelling of high strength / high performance concrete State-of-art report (130 pages, ISBN 978-2-88394-082-6, January 2008)
43	Structural connections for precast concrete buildings Guide to good practice (370 pages, ISBN 978-2-88394-083-3, February 2008)
44	Concrete structure management: Guide to ownership and good practice Guide to good practice (208 pages, ISBN 978-2-88394-084-0, February 2008)
45	Practitioners' guide to finite element modelling of reinforced concrete structures State-of-art report (344 pages, ISBN 978-2-88394-085-7, June 2008)
46	Fire design of concrete structures —structural behaviour and assessment State-of-art report (214 pages, ISBN 978-2-88394-086-4, July 2008)
47	Environmental design of concrete structures – general principles Technical report (48 pages, ISBN 978-2-88394-087-1, August 2008)
48	Formwork and falsework for heavy construction Guide to good practice (96 pages, ISBN 978-2-88394-088-8, January 2009)
49	Corrosion protection for reinforcing steels Technical report (122 pages, ISBN 978-2-88394-089-5, February 2009)
50	Concrete structures for oil and gas fields in hostile marine environments State-of-art report (36 pages, IBSN 978-2-88394-090-1, October 2009)
51	Structural Concrete – Textbook on behaviour, design and performance, vol. 1 Manual – textbook (304 pages, ISBN 978-2-88394-091-8, November 2009)
52	Structural Concrete – Textbook on behaviour, design and performance, vol. 2 Manual – textbook (350 pages, ISBN 978-2-88394-092-5, January 2010)
53	Structural Concrete – Textbook on behaviour, design and performance, vol. 3 Manual – textbook (390 pages, ISBN 978-2-88394-093-2, December 2009)
54	Structural Concrete – Textbook on behaviour, design and performance, vol. 4 Manual – textbook (196 pages, ISBN 978-2-88394-094-9, October 2010)
55	*fib* Model Code 2010, First complete draft – Volume 1 Draft Model Code (318 pages, ISBN 978-2-88394-095-6, March 2010)

This document is the intellectual property of the fib – International Federation for Structural Concrete. All rights reserved.
This PDF of fib Bulletin 61 is intended for use and/or distribution solely within fib National Member Groups.

N°	Title
56	*fib* Model Code 2010, First complete draft – Volume 2 Draft Model Code (312 pages, ISBN 978-2-88394-096-3, April 2010)
57	Shear and punching shear in RC and FRC elements. Workshop proceedings. Technical report (268 pages, ISBN 978-2-88394-097-0, October 2010)
58	Design of anchorages in concrete Guide to good practice (282 pages, ISBN 978-2-88394-098-7, July 2011)
59	Condition control and assessment of reinforced concrete structures exposed to corrosive environments (carbonation/chlorides) State-of-art report (80 pages, ISBN 978-2-88394-099-4, May 2011)
60	Prefabrication for affordable housing State-of-art report (132 pages, ISBN 978-2-88394-100-7, August 2011)
61	Design examples for strut-and-tie models Technical report (220 pages, ISBN 978-2-88394-101-4, September 2011)

Abstracts for *fib* Bulletins, lists of available CEB Bulletins and FIP Reports, and an order form are available on the *fib* website at www.fib-international.org/publications.